Presynaptic nicotinic modulation of neurotransmitter release in the central nervous system

Kaiser, Sergio

Award date:
1999

Awarding institution:
University of Bath

Presynaptic nicotinic modulation of neurotransmitter release in the Central Nervous System

Submitted by SERGIO KAISER

for the degree of PhD of the University of Bath, 1999

ProQuest LLC
789 East Eisenhower Parkway
P.O. Box 1346
Ann Arbor, MI 48106-1346

Summary

The general objective of my research project was to study *in vitro* neurotransmitter release from different brain areas, as a consequence of presynaptic nicotinic acetylcholine receptor (nAChR) activation. Chapter I in this thesis presents a general introduction to ligand gated ion channels and modulation of neurotransmitter release by presynaptic nAChR in the vertebrate Central Nervous System. The experimental core of this work (chapters 2 - 6) is divided into two main sections: section I (chapters 2 & 3) and section II (chapters 4 - 6) relate to the rat hippocampal and striatal brain areas, respectively. Finally, chapter 7 summarises the main achievements of the project and suggests possible research directions derived from the results presented.

In particular, **section I** of this thesis describes initial experimental attempts aimed to examine the involvement of rat α7 nAChR in nicotinic agonist-evoked glutamate release from hippocampus. Electrophysiological evidence relating presynaptic α-bungarotoxin-sensitive nAChR to glutamatergic transmission (McGehee *et al.*, 1995; Gray *et al.*, 1996) together with previous pharmacological / neurochemical studies carried out in rat hippocampal preparations in Dr. Wonnacotts' lab (Barrantes *et al.*, 1995a; 1995b; Wilkie *et al.*, 1996) supported the plan. The project initially involved the development of two topics:

1) the biochemical, pharmacological and functional characterisation of native and heterologously expressed rat α7 nAChR (this thesis chapter 2); and
2) the study of nicotinic-evoked glutamate release in rat hippocampus (this thesis chapter 3).

As a source of "wild type" hippocampal α7 nAChR, E18 neuronal cultures from foetal rat hippocampi (Barrantes *et al.*, 1995a) were established and assayed for surface expression of [^{125}I]-α-bungarotoxin binding sites (B_{max} = 97.0±14.0 fmol / mg protein). To heterologously express the rat α7 nAChR subunit, its cDNA was subcloned into the commercial vector pCDNA3, a plasmid previously used in studies involving protein expression in either *Xenopus* oocytes or mammalian cell lines. To test if pCDNA3α7 was capable of generating functional surface homomeric α7 nAChR, it was transiently expressed in *Xenopus* oocytes and assayed using the Two-electrode Voltage Clamp technique. The α-Bgt-sensitivity, fast desensitisation and inward rectifying properties of (-)-nicotine-evoked currents observed in *Xenopus* oocytes injected with pCDNA3 α7, demonstrated its viability as an expression vector. When the same plasmid was lipotransfected into α7-non-expressing- (HEK-293) and α7-expressing- (SH-SY5Y - B_{max} = 26.8±5.9 fmol [^{125}I]-α-bungarotoxin binding sites / mg protein) mammalian cell lines, it failed to increase basal levels of surface [^{125}I]-α-bungarotoxin binding sites, although rat α7 mRNA was detected. The discussion in chapter 2 reviews the scarcity of successful studies and possible explanations for the difficulties reported worldwide in heterologously expressing the α7 nAChR subunit in mammalian cell lines.

In chapter 3, two different experimental approaches were utilised to explore possible functional responses elicited in rat hippocampal synaptosomes when challenged with nicotinic agonists. [^{3}H]-glutamate release evoked by (-)-nicotine was studied using the superfusion technique, and (-)-nicotine-evoked Ca^{2+}-influx was examined by fluorimetry in rat hippocampal synaptosomes preloaded with fura-2/AM. Stimulation with the general depolarising agent KCl resulted in detectable responses, whereas (-)-nicotine failed to produce detectable signals. The discussion in chapter 3 analyses the negative results in terms of the functional properties/density of the putative nAChR proposed to be present and the limitations of the techniques applied in their study.

The facilitation of catecholamine release, particularly dopamine release, by nAChR is well documented, especially at the level of the terminal projections *in vitro* (Wonnacott, 1997). In **section II**, the superfusion technique was used to explore the following aspects of the nicotinic modulation of dopamine release in rat striatum:

1) identification of presynaptic and/or preterminal nAChR subtypes modulating striatal dopamine release (this thesis chapters 4 & 5)
2) functional crosstalk between striatal nerve terminals as a consequence of nAChR stimulation (this thesis chapter 5), and
3) second messenger mechanisms underlying nicotinic agonist-evoked striatal dopamine release (this thesis chapter 6)

In chapter 4, the novel *Conus* toxin α-conotoxin-MII, a potent and selective antagonist of α3β2-containing nAChR (Cartier *et al.*, 1996; Harvey *et al.*, 1997), was exploited to evaluate the contribution of the α3β2 subunit combination to the presynaptic modulation of striatal DA release. Moreover, the nicotinic agonist UB-165, a novel anatoxin-a/epibatidine hybrid (Wright *et al.*, 1997), was also assayed to evoke dopamine release from rat striatal synaptosomes. These studies primarily showed that:

1) a maximally effective concentration of α-conotoxin-MII (112 nM) inhibited mecamylamine-sensitive 1μM (±)-anatoxin-a-evoked [^{3}H]-dopamine release from striatal synaptosomes and slices by 56.0±5.5% (IC_{50}=24.3±2.9nM) and 28.4±4.1% (IC_{50}=17.3±0.1nM), respectively; and

2) UB-165 potently stimulated [^{3}H]-dopamine release from rat striatal synaptosomes (EC_{50}=88±18nM) but only elicited ~40% of the maximum release evoked by 1 μM (±)-anatoxin-a (EC_{50}=134±26nM). Moreover, this partial agonism of UB-165 was almost completely abolished by α-conotoxin-MII (112nM) but unaffected by MLA (50nM).

From these results it was concluded: 1) at least two populations of presynaptic nAChR (α-CTx-MII sensitive and α-CTx-MII insensitive) are involved in the direct modulation of dopamine release from rat striatal dopaminergic terminals; 2) the presynaptic α-CTx-MII sensitive nAChR comprises α3 and β2 nAChR subunits but additional subunits cannot be excluded; 3) nAChR on non-dopaminergic terminals may enhance DA release by releasing other neurotransmitters that in turn act on dopamine terminals; 4) α-CTx-MII sensitive nAChR

are not involved or play a minimum role in this indirect effect; and 5) UB-165 may selectively activate $\alpha 3\beta 2$ type nAChR on dopamine terminals.

The results in chapter 4 demonstrated that nAChR on dopaminergic nerve terminals are heterogeneous and those containing $\alpha 3\beta 2$ subunits have been identified. The aims of the studies performed in chapter 5 were: 1) to investigate in the striatum a possible indirect enhancement of nicotinic agonist-evoked dopamine release, via activation of nAChR on glutamatergic nerve terminals, and 2) to pharmacologically characterise the nAChR subtype/s involved.

In rat striatal slices, (±)-anatoxin-a-evoked [^{3}H]-dopamine release was biphasic with apparent EC_{50}s of 241.8±36.1nM and 5.1±0.3μM. Moreover, the second phase of the dose-response curve was almost completely suppressed in the presence of ionotropic glutamate receptor antagonists (kynurenic acid, DNQX) or $\alpha 7$-containing nAChR antagonists (α-bungarotoxin, α-conotoxin-lmI, methyllycaconitine). The observations presented in this chapter suggest for the very first time, and using a neurochemical approach, the involvement of presynaptic α-bungarotoxin-sensitive nAChR in striatal glutamate release that in turn enhances (±)-anatoxin-a-evoked DA release by acting on dopamine nerve terminal ionotropic glutamate receptors.

Finally, chapter 6 explores the involvement of second messenger cascades in the response evoked by nicotinic agonists acting on dopaminergic nerve terminal nAChR. This study presents preliminary functional (from superfusion experiments) and biochemical evidence (from immunoblot assays) for the involvement of Ca^{2+}/calmodulin kinase II and protein kinase C in (±)-AnTx-a-evoked DA release from rat striatal synaptosomes.

Acknowledgements

First, I would like to express my gratitude to Dr Susan Wonnacott for believing in me, giving me not only the opportunity to grow as a person and as a scientist, but also for her sincere and kind support when I really needed it. Thanks "Sue" from deep in my heart!

My heartfelt gratefulness to you Lev (Dr L.Soliakov): for your friendship, knowledge and for being close to me during hard times. I will always be indebted to you.

To my colleagues at the Nicotine Research Lab ... It is really difficult to put into words the emotions and memories that cross my heart and mind when I try to write these paragraphs. Just a: "thanks mates!!!" hardly could summarise my feelings. Thanks for " the nice piece of life " we have shared together. I will truly miss and always remember you: "Di" (Diana Ridley) and "Cookie" (Chris Sharples), "H. Andy" (Dr Andrew Davies), "Jolly R." (Dr Adrian Rogers), "Manya" (Federico Dajas-Bailador), Ian (Dr I.Jones) and Adrian (A.Mogg).

I would also like to take this opportunity to thank Professor George G. Lunt and Professor F.J. Barrantes who helped me to embark upon a PhD course at Bath University and follow my progress with enthusiasm and encouragement. My deepest gratitude to both of you.

Everyone at the Biochemistry Department has been very friendly and helpful, making from my stay in Bath a unique experience. In particular I would like to thank you Adrian (Dr A.Wolstenhome) and all the members of the "worm lab". My thanks are also extended to Lesley, Ewan and other members of the Animal House for their daily happiness and kindness.

The fact that I am able to achieve a thesis in a foreign country is owed to my parents, Martha and Bernd, who have always made every possible effort to support/understand what I wanted to become and do, encouraging me in the daily "fight against routines" and in my long-standing need to find out how things work the way they do. I also thank them and my beloved grandma Caly for teaching me, with the example, to choose with total freedom the way to survive with honesty in this, sometimes difficult, world. Gracias " (viejos) amigos "!

To my friend and wife for being so patient and comprehensive, but also for helping me to see further in life. Thanks dearest Mariel for your love and each day we are together.

To my brothers German and Rosana, for filling my life with happiness when Flopys' birth and because "attenuating" at home "the effects" of my long absence.

Ariel, Andrea, Alejandro, Mario, Sucho, Gori, Sil & Gus, Lía, Ana María, Eugenio, Dora, Silvia, Telma, Idi, Leticia, Hugo ... my argentinian friends. Thanks for your friendship and unconditional support.

This studentship was funded from an EC grant and an ORS award.

for Mariel, Caly,

Martha and Bernd

Publications and communications resulting from this work

In Refereed Journals

- Kaiser S.A., Soliakov L., Harvey S.C., Luetje C.W. and Wonnacott S. (1998). **Differential inhibition by α-conotoxin-MII of the nicotinic stimulation of [^{3}H]-dopamine release from rat striatal synaptosomes and slices.** Journal of Neurochemistry 70: 1069-1076.
- Kaiser S.A. and Wonnacott S. **(±)-Anatoxin-a indirectly enhances striatal dopaminergic transmission by evoking glutamate release** (IN PREPARATION).
- Sharples C.G.V., Kaiser S.A., Wright E., Gallagher T. and Wonnacott S. **UB-165: a novel nicotinic agonist with subtype selectivity in the modulation of dopamine release from rat striatal synaptosomes** (IN PREPARATION).

Communications

- Kaiser S.A., Soliakov L. and Wonnacott S. (1997). **Inhibition of the nicotinic stimulation of dopamine release from the rat striatum in vitro by α-conotoxin-MII, an antagonist selective for the alpha 3 beta 2 nicotinic receptor.** British Journal of Pharmacology 122: 165.
- Kaiser S.A., Soliakov L., Luetje C.W., Harvey S.C. and Wonnacott S. (1997). **Nicotinic receptor subtypes modulating glutamate-dopamine interactions in rat striatum.** Society for Neuroscience 27: 266.22.
- Kaiser S.A. and Wonnacott S. (1998). **Nicotinic acetylcholine receptors on glutamatergic nerve terminals can enhance dopamine release in rat striatal slices.** British Journal of Pharmacology 123: 11.
- Sharples C.G.V., Kaiser S.A., Mogg A.J., Wright E., Gallagher T. and Wonnacott S. (1998). **UB-165: A novel epibatidine - anatoxin-a hybrid that is a nicotinic agonist with subtype selectivity.** Society for Neuroscience 28: 39.15.
- Kaiser S.A. and Wonnacott S. (1998). **Indirect nicotinic modulation of dopaminergic transmission in rat striatum by (±)-anatoxin-a evoked glutamate and 5-HT release.** Society for Neuroscience 28: 39.16.

Invited reviews

- Kaiser S.A. and Wonnacott S. (1999). **Nicotinic Receptor Modulation of Neurotransmitter Release.** In: Neuronal Nicotinic Receptors: Pharmacology and Therapeutic Opportunities (Arneric S. and Brioni D., eds.), pp 141-159. New York: John Wiley and Sons.
- Kaiser S.A., Soliakov L. and Wonnacott S. (1999). **Presynaptic Neuronal Nicotinic Receptors - Pharmacology, Heterogeneity and Cellular Mechanisms.** In: Handbook of Experimental Pharmacology – Neuronal Nicotinic Receptors (Clementi F., Gotti C. and Fornasari D., eds.), Heidelberg: Springer-Verlag (IN PRESS).

Contents

Section I: The hippocampus

Abbreviations

4-AP	4-aminopyridine
α-Bgt	α-bungarotoxin
α-CTx-AuIB	α-conotoxin-AuIB
α-CTx-ImI	α-conotoxin-ImI
α-CTx-MII	α-conotoxin-MII
ACh	acetylcholine
ATP	adenosine 5'-triphosphate
AMPA	α-amino-3-hydroxy-5-methyl-4-isoxazole propionic acid
ANOVA	analysis of variance
AnTx-a	anatoxin-a
aq.	aqueous
B_{max}	maximal concentration of binding sites
bp	base pairs
BSA	bovine serum albumin
°C	Celcius degree
$[Ca^{2+}]_i$	intracellular free calcium
$[Ca^{2+}]_o$	extracellular free calcium
CaM	calmodulin
CaM-KII	calcium calmodulin kinase II
Cd^{2+}	cadmium ion
cDNA	copy DNA
cfu	colony forming unit
CIP	calf intestinal alkaline phosphatase
CNS	central nervous system
DA	dopamine
DAG	diacylglycerol
DAT	digital audio tape
DHβE	dihydro-β-erythroidine
DMEM	Dulbecco's Modified Eagle Medium
DMPP	dimethylpiperazine
DNQX	6,7-dinitroquinoxaline-2,3-dione
dTC	d-tubocurarine
E18	embryonic day 18
EC_{50}	agonist concentration which gives half-maximal response
EDTA	ethanediamino-N,N'-tetraacetic acid
EGTA	ethyleneglycol-bis-(β-aminoethylether)-N,N,N',N'-tetraacetic acid
EPSC	excitatory post-synaptic current
ERK2	extracellular signal-related kinase
FCS	fetal calf serum

Fura-2	1-[2-(5-carboxyoxazol-2-yl)-6-aminobenzofuran-5-oxy]-2-(2'-amino-5'methylphenoxy)ethane N,N,N',N'-tetraacetic acid
g	gram
GABA	γ-aminobutyric acid
GLB	gel loading buffer
Glu	L-glutamate
GP	globus pallidus
5-HT	5-hydroxytryptamine, serotonin
HEK	human embryonic kidney cell line
HEPES	N-[2-hydroxyethyl]piperazine-N'-[2-ethane sulfonic acid]
IC_{50}	ligand concentration which reduces radioligand binding or functional response to half-maximal
iGluR	ionotropic glutamate receptor
IP_3	inosytol triphosphate
IU	international unit
l	litre
K^+	potassium ion
Kd	equilibrium dissociation constant
kDa	kilodaltons
Ki	inhibition constant
KYNA	kynurenic acid
λ	wavelength
LB	Luria Bertani broth medium
LGIC	ligand gated ion channel
m	metre
M	molar
MΩ	megaohm
mAb	monoclonal antibody
mAChR	muscarinic acetylcholine receptor
MARCKS	myristoylated alanine-rich C-kinase substrate
mEPSC	miniature EPSC
min	minute
MLA	methyllycaconitine
mRNA	messenger ribose nucleic acid
MW	molecular weight
NA	noradrenaline, norepinephrine
nAChR	nicotinic acetylcholine receptor
n-Bgt	neuronal-bungarotoxin
n_H	Hill number
NMDA	N-methyl-D-aspartate
NMDA-R	N-methyl-D-aspartate receptor

NT	neurotransmitter
O.D.	optical density
6-OHDA	6-hydroxydopamine
PBS	phosphate buffer saline
PNC	peripheral nervous system
PCR	polymerase chain reaction
PEI	polyethylenimine
PKC	protein kinase C
PLC	phospholipase C
PMSF	phenylmethylsulphonyl fluoride
Rb^+	rubidium ion
rpm	revolutions per minute
RT-PCR	reverse transcriptase - polimerase chain reaction
s	second
SD	standard deviation
SDS	sodium dodecyl sulfate
SDS-PAGE	sodium dodecyl sulphate polyacrylamide gel electrophoresis
S.E.M.	standard error mean
SNc	substantia nigra pars compacta
SNr	substantia nigra pars reticulata
SOS	*Xenopus* oocyte buffer
Syn I	synapsin I
TBE	Tris.Cl Borax EDTA buffer
TE	Tris.Cl EDTA buffer
TEVC	two-electrode voltage clamp
Th	thalamus
TK	tyrosine kinase
TM	transfection medium
TRIS	Tris[hydroxymethyl]aminomethane
TTX	tetrodotoxin
UV	ultraviolet
V	volt
v/v	volume / volume
VOCC	voltage operated calcium channel
vol	volume
VTA	ventral tegmental area
w/v	weight / volume

1 General Introduction

The work carried out during the course of this project has been aimed at understanding some of the effects that chemical species capable of interacting with nicotinic acetylcholine receptors (nAChR) have on brain preparations, in particular on evoked-neurotransmitter release with relevance to brain function. In order to set this work in context, the General Introduction covers two areas:

1. The ionotropic acetylcholine receptor: a fast transducer of chemical signals with specificity for the alkaloid (-)-nicotine.
2. nAChR as presynaptic modulators of neurotransmitter release in Central Nervous System

1.1 Ligand Gated Ion Channels: the nicotinic acetylcholine receptor

1.1.1 "Receptive substances"

The existence of synaptic transmission and, indirectly, the presence of ligand-gated ion channels were first adequately reported by Claude Bernard in the 1850s on the basis of the blockage of the neuromuscular junction by curare (Bernard, 1857). In 1862, Kölliker (Kölliker, 1862) and Kühne (Kühne, 1862) first described it using oblique illumination at the microscope.

At the end of the nineteenth century, Paul Ehrlich (Ehrlich, 1865) from the field of the Immunology and John Langley (Langley, 1905; 1907; 1914) from that of Pharmacology, proposed that hormones and neurotransmitters are recognised by "receptive substances", now more commonly known as receptors. They introduced, for the very first time, the concept that these "receptive substances" combine with pharmacologically active compounds, drugs or toxins, and behave as their specific physiological targets. Langley went further and specified that "the muscle substance which combines with nicotine and curare is not identical to the substance that contracts" and that such a "receptive substance" or receptor is capable of "receiving the stimulus" and "transmitting" it, thus formulating the concepts of receptor and signal transduction in his present day terms. For many years Langleys' receptive substance was considered "mythical".

In 1914 Sir Henry Dale first differentiated receptor subtypes when he noted that the action of acetylcholine (ACh) at the neuromuscular junction could be selectively mimicked by nicotine but that its action in the autonomic nervous system was mimicked by another alkaloid: muscarine. He postulated that the different actions of muscarine and nicotine were caused by two distinct cholinergic receptors with different specificities. The observation that each receptor also responded selectively to different competitive antagonists supported this distinction: curare selectively blocked nicotinic receptors and atropine blocked muscarinic receptors. But, despite of all these observations, he was reticent to use the term receptor.

Present in very small quantities, this protein seemed to defy chemical identification. Two convergent strategies led to success.

First, one had to find an organ containing much greater quantities of receptor than the striated muscle. The electric organ of the teleost fish *Torpedo* or the elasmobranch *Electrophorus* (electric eel) satisfied this condition (Nachmanson, 1959). The other point was to specifically isolate this protein from the other components of the electroplax to identify its chemical structure. Once again, the answer came from the animal world. Certain cobra (i.e. *Naja Naja*) or krait (i.e. *Bungarus multicinctus*) venoms cause death by paralysing the respiratory muscles when injected into the bloodstream. The paralysing substance in the venoms of these snakes are small proteins (MW 7000-8000) called alpha-toxins (Lee and Chang, 1966). These α-toxins, notably α-bungarotoxin (α-Bgt), bind pseudo-irreversibly and very selectively to the synaptic site where acetylcholine binds. Even if the *Torpedo* fish and the *Bungarus* snake have little chance of meeting naturally, their encounter in the test tube finally resulted in the isolation of the muscle embryonic nicotinic acetylcholine receptor (Changeux *et al.*, 1970). These natural advantages, as well as advances in experimental techniques applicable to studying the end-plate region of the neuromuscular junction have secured the nAChR its position as one as the most studied of all receptors.

1.1.2 nAChR as members of a superfamily of ligand gated ion channels

The nicotinic acetylcholine receptors are members of a gene superfamily of ligand-gated ion channels (LGIC) which includes the inhibitory receptors gated by glycine (Betz, 1992) and γ-amino butyric acid ($GABA_A$ receptors; review: McKernan and Whiting, 1996) which contain a chloride selective ion channel; and the excitatory receptors gated by acetylcholine (nAChR), serotonin ($5\text{-}HT_3$ type) and glutamate (forming a related group; review: Seeburg, 1993; Galzi and Changeux, 1995). These LGIC are involved in fast transmission of "information" between nerve cells and sensory or effector cells, where they transduce a chemical signal released by the nerve into an electrical one. Moreover, all these membrane intrinsic proteins share the common function of regulated opening (upon ligand binding to a specific binding site) and closing of an ion channel (Figure 1.1).

Hydropathy analysis of cloned and sequenced LGIC subunits have revealed the presence of a common four hydrophobic segment motif (designated M1-M4 - Figure 1.2), first interpreted for *Torpedo* nAChR subunits to be membrane spanning regions (Popot and Changeux, 1984). Although the subunits of nAChR, $5HT_3$, $GABA_A$ and glycine receptors are homologous, particularly in their predicted transmembrane segments, this subfamily shares no overall homology with the glutamate-gated family which consists of AMPA- (α-amino-3-hydroxy-5-methyl-4-isoxazole propionic acid), NMDA- (N-methyl-D-aspartate) and kainate-sensitive receptors.

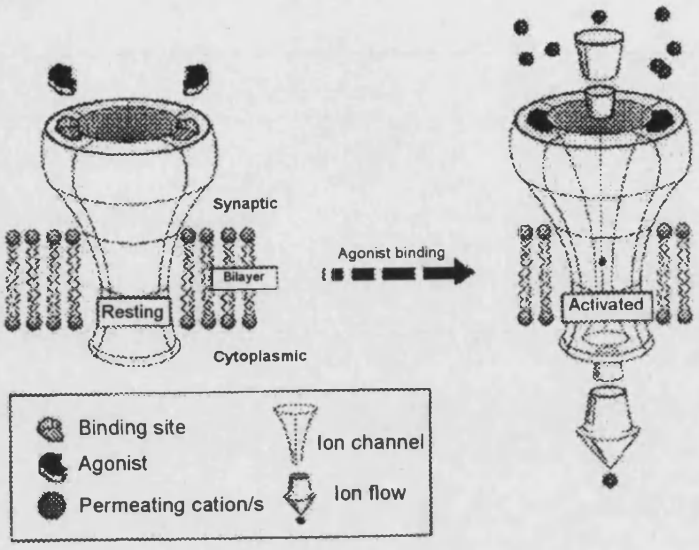

Figure 1.1 The ligand gated ion channel (LGIC). Stylised representation of a receptor inserted in the membrane of an excitable cell. Upon the binding of an agonist molecule, conformational changes in the protein structure occur, the channel opens and ions flow through the pore following their electrochemical driving forces (adapted from Thomas, 1995).

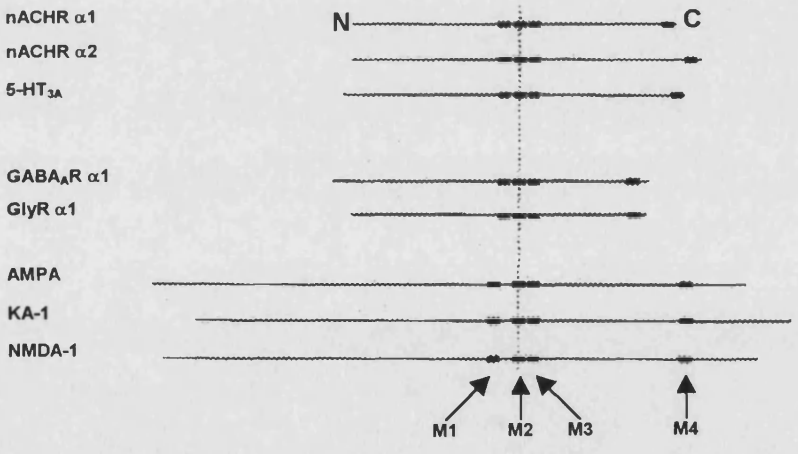

Figure 1.2 Subunits of the LGIC superfamily members. Represented are the "nAChR-type" (first 5 subunits) and the "Glutamate-type" (remainder) LGIC families, aligned at the predicted pore forming M2 region. Lengths correspond directly to amino acid numbers. Predicted membrane-spanning regions common to all subunits are shown (M1-M4). These similarities may be misleading as several lines of evidence show that the structure and topology of ionotropic glutamate LGIC receptor subunits differ from the others ("nAChR-type" family, see text below) (adapted from Thomas, 1995).

Homology between the subunits of different members of the LGIC superfamily is between 20% and 40% whereas in the different subunits which create the individual receptors of each family, homology is generally at least 40%. In addition all members of the "nAChR-like" family share certain motifs which are absent or substantially different in ionotropic glutamate receptor subunits:

1. An extracellular N-terminal domain of approximately 200 amino acids containing the agonist binding site. The corresponding domain in glutamatergic LGIC receptor subunits is typically at least twice as long (Unwin, 1993). In addition, sequence comparisons with metabotropic glutamate receptors and bacterial periplasmic amino-acid binding proteins suggest that the portion of sequence between M3 and M4 contributes to binding in this receptors (O'Hara *et al.*, 1993). This has been confirmed by the creation of chimeric constructs (Stern-Bach *et al.*, 1994).
2. A 15 residue cys-loop in the N-terminal domain (Ortells and Lunt, 1995) which is absent in glutamatergic subunits (Hollman *et al.*, 1994).
3. Conserved residues in the M2 transmembrane segment, proposed to form a primarily α-helical structure lining the ion channel and gating ion-flow (Akabas *et al.*, 1994; Ortells and Lunt, 1995; Unwin *et al.*, 1995). Evidence gained using N-glycosilation site tagging (Hollman *et al.*, 1994) and prolactin reporter epitopes (Bennett and Dingledine, 1995) suggests that the "M2" sequence identified in glutamatergic subunits does not traverse the cell membrane at all, instead forming a re-entrant loop similar to that seen in, e.g. K^+ channels. As a consequence the large M3-M4 loop is extracellular and appears to form part of the ligand binding site. In these receptors, the C-terminus is cytoplasmic.

This evidence suggests that LGIC receptor subunits may be divided into two-families ("nAChR-type" and "glutamate-type"), with different binding site structures, transmembrane topologies and channel lining structures.

1.1.3 nAChR classification and general structural architecture

A rational description of this receptor family can be based on sequence comparisons, but this lacks the functional significance, as knowledge of the contribution of particular subunits to specific nAChR is lacking. Alternatively, an anatomical-pharmacological approach can be adopted (Lindstrom, 1996), which serves as a useful, but not totally adequate, classification. The latter approach, adopted here, divides the nAChR family into three main branches: (1) peripheral, muscle or end-plate nAChR, (2) central and autonomic nAChR that, unlike those of muscle, do not bind α-Bgt, and (3) central an autonomic nAChR that do bind α-Bgt. All are presumed to be pentameric ACh-gated cation channels (Cooper *et al.*, 1991; Anand *et al.*, 1991; Unwin, 1993; Palma *et al.*, 1996) formed by one to four homologous subunit types. These are thought to be organised like barrel staves around a central cation channel (Figure 1.3). As mentioned in 1.1.2, the nAChR subunit genes encode proteins that

have a relatively hydrophilic amino terminal portion, constituting a major extracellular domain of the receptor protein where ACh binds, followed by putative three hydrophobic transmembrane domains (M1-M3), a large intracellular loop, and a fourth hydrophobic transmembrane domain (M4). The hydrophobic segments are thought to stack in the membrane with the amphiphilic M2 helix orientated towards the channel lumen to form an ion permeant pathway (Karlin,1993). At least in the nAChR, a kink in this helix projects a hydrophobic leucine residue into the pore in the closed configuration (Unwin, 1993). The predicted M2 region forms a rather non-selective channel, largely by virtue of hydroxylated serine and threonine residues which line the internal face and is identical or highly homologous in excitatory (cation channels) and inhibitory (anion channels) receptors (Imoto *et al.*, 1991; Konno *et al.*, 1991; Villarroel and Sakmann, 1992; Bertrand *et al.*, 1993). Ionic selectivity appears to be conferred by rings of fully charged amino acids just outside the bilayer plane which may attract permeant counterions to each end of the pore (Imoto *et al.*, 1988).

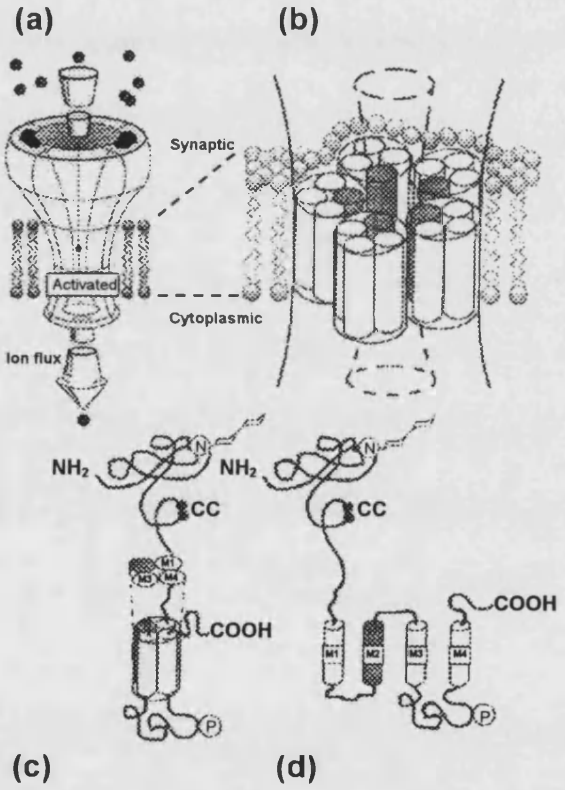

Figure 1.3 Model of transmembrane topology and organisation of the nAChR subunits. Possible arrangement of the five subunits about the axis of pseudosymmetry of the receptor (a) in the creation of the ion pore (b). Models of the subunit topology, largely based on hydrophobicity profiles of the amino acid sequence and antibodies studies, reveal the presence of four transmembrane regions (M1-M4) per subunit which associate non-covalently as they cross the membrane with the M2 portion (dark gray) facing the channel lumen (b). Each subunit (c) and (d) is characterised by a large extracellulary located N-terminal domain bearing glycosilation sites (N) and, in α subunits, a pair of conserved cysteines (CC - Karlin, 1993). Between M3 and M4 is an intracellular loop containing potential phosphorylation sites through which receptor function can be modulated (from Thomas, 1995).

Nicotinic acetylcholine receptors are the predominant excitatory receptors in the mammalian peripheral nervous system (PNS), whereas glutamate receptors are the predominant excitatory receptors in central nervous system (CNS). In the peripheral nervous system nAChR are critical for controlling skeletal muscles and consequently, as mentioned above, are the target of toxins such as snake venom toxins like α-Bgt, and muscle nAChR are the target of an antibody-mediated autoimmune response in myasthenia gravis. Although outnumbered by glutamate receptors in the vertebrate central nervous system, neuronal nAChR are widespread.

1.1.4 Neuronal nAChR

The synthesis, structure, and function of muscle-type nAChR are known in relatively great detail, whereas the more diverse structures, functional properties, and functional roles of neuronal nAChR are much less well characterised. The functional properties of various combinations of neuronal nAChR subunits expressed in *Xenopus* oocytes have been better characterised than have the functional properties of diverse neuronal nAChR subtypes *in vivo.* ("native" nAChR). However, the actual functional roles in the nervous system of many of the real and potential subtypes of neuronal nAChR still remain to be determined. Despite this, they have been implicated in learning and memory, and it has been observed that their number is decreased in Parkinsons' syndrome and Alzheimer's disease. One measure of their scientific and commercial significance is that through nicotine they mediate the addiction to tobacco (Dani and Heinemann, 1996). The idea that neuronal nAChR have the same direct and linking role that has the muscle endplate type receptor in neurotransmission, is changing. Now, these receptors are viewed like putative modulators / regulators of conventional mechanisms of neurotransmission (Role and Berg, 1996; Wonnacott, 1997).

During the past decade, diverse nAChR subunits have been identified in the central nervous system. To date, 11 gene products (α2-α9; β2-β4 in rat or nα1-nα3 in chick) have been isolated from avian, rodent or human tissues (reviewed in: Role and Berg, 1996; Lindstrom, 1996). Unlike the α2-α6 subunits that require the presence of at least a β subunit to form a functional receptor (Luetje and Patrick, 1991; Role, 1992; Conroy and Berg, 1995; McGehee and Role, 1995; Lindstrom 1996; Forsayeth and Kobrin, 1997), the α7-α9 subunits are capable of forming functional ion channels when expressed as homo-oligomers in *Xenopus* oocytes (Couturier *et al.*, 1990; Bertrand *et al.*, 1992; Séguéla *et al.*, 1993; Elgoyhen *et al.*, 1994; this study chapter 2). As mentioned before, the receptor macromolecules are composed most likely of five subunits. With the presence of such variety of nAChR gene products, there is much scope for diversity of nAChR, through the formation of hetero-oligomeric assemblies. Expression of brain nAChR subunits in *Xenopus* oocytes have shown that only one or two different subunits are needed to form functional channels (α or ACh binding subunit and β or structural subunit) (e.g. Deneris *et al.*, 1991). One of the key questions in the field involves the determination of all the possible neuronal nAChR subunit combinations actually present in the brain and their distribution. Based on autoradiography / radiolabelled ligand binding (e.g. Clarke *et al.*, 1985;

Wonnacott, 1990), lesion studies (e.g. Schwartz *et al.*, 1984; Clarke and Pert, 1985), immunohistochemistry (e.g. Dominguez del Toro; 1994), *in situ* hybridisation (Wada *et al.*, 1989; Séguéla *et al.*, 1993) and knock-out suppression of particular neuronal nAChR subunits (β2 - Zoli *et al.*, 1998; α7 - Orr-Urtreger *et al.*, 1997), evidence for discrete anatomical and cellular expression of subunits is beginning to emerge.

Three pharmacological classes of native neuronal nAChR have been identified

By definition, all nAChR bind (-)-nicotine. However in order for binding by a tritiated ligand to be detectable in binding assays, it must be of relatively high affinity (K_D measurable in nM or lower; see Wonnacott, 1987). As early as 1985 (Clarke *et al.*, 1985), autoradiographic analysis of rat brain sections labelled with [^{3}H]-(-)-nicotine and [^{3}H]-ACh revealed an identical pattern of distribution of these ligands. The strongest presence was revealed in the interpeduncular nucleus, superior colliculus, medial habenula, some thalamic nuclei, layers I and III/IV of the cerebral cortex, substantia nigra pars compacta and ventral tegmental area. [^{3}H]-Cytisine and [^{3}H]-methylcarbamylcholine also bound to the same site with high affinity (Anderson and Arneric, 1994). α-Bgt (see below) interacts with the high affinity [^{3}H]-(-)-nicotine binding site very weakly if at all (no displacement of binding is seen even at high micromolar concentrations). Immunoprecipitation studies have uncovered the composition of the main high affinity [^{3}H]-(-)-nicotine binding sites in mammalian and avian brain. In rodent brain, experiments with mAb270 (an antibody raised against the chick β2 nAChR subunit) have shown the mammalian high affinity [^{3}H]-(-)-nicotine binding site to be composed of α4 and β2 subunits alone (Whiting and Lindstrom, 1986). In chick brain, more than 90% of high affinity [^{3}H]-(-)-nicotine binding immunoprecipitated using mAb270, appeared to be composed of α4β2 and α2β2 receptors with trace contributions by α3. In the light of the finding that α5 can coassemble with α4 subunits in chicken brain (Conroy *et al.*, 1992), it is possible that some α4α5β2 sites may also be present. Flores *et al.* (1992) used antisera to α4 and β2 fusion proteins to show that immunoprecipitation of either subunit from rat brain also removes virtually all of the other, and that this results in the removal of >90% of high affinity [^{3}H]-cytisine binding sites from rat brain extracts. Moreover, loss of high affinity-agonist binding sites in β2 null mice has been recently reported by Picciotto *et al.* (1995). Thus, in mammalian brain, the great majority of high affinity [^{3}H]-(-)-nicotine binding sites are α4β2 receptors.

As mentioned before, α-Bgt displaces high affinity [^{3}H]-(-)-nicotine binding weakly (if at all), despite [^{125}I]-α-Bgts' ability to bind with extremely high affinity (K_D in the pM-nM range) to many neuronal preparations (Wonnacott, 1990). Clarke *et al.* (1985) showed in rat brain that the distribution of [^{3}H]-(-)-nicotine binding was significantly different from that observed for [^{125}I]-α-Bgt which was high in distinct layers of cerebral and cerebelar cortices, hypothalamus, hippocampus, inferior and superior colliculus and some regions of the brain stem. The only brain regions showing significant overlap between tritiated agonist and iodinated antagonist binding were the superior colliculus and layer I of the cortex. This indicated that this two labelled ligands could not be labelling the same receptor. nAChR immunoprecipitated using

α7 and α8 antisera have been characterised pharmacologically and biophysically (Anand *et al.*, 1993; Gotti *et al.*, 1994; Gerzanich *et al.*, 1994). These investigations have confirmed that these receptors have high affinities for [^{125}I]-α-Bgt (higher for α7-containing receptors) and generally low affinities for nicotinic agonists (although α8-containing receptors generally have higher affinities for this type of ligand than those containing α7 alone). Extensive immunocytochemical studies have shown that the distribution of α7 subunits in rat brain (α8 has not been found in rat) is well correlated with that of α-Bgt binding (Dominguez del Toro *et al.*, 1994). Moreover, the distribution of the α7 gene transcript in rat brain (Séguéla *et al.*, 1993) and loss of [^{125}I]-α-Bgt binding sites in α7 null mouse brain (Orr-Urtreger *et al.*, 1997) overlapped the pattern of [^{125}I]-α-Bgt binding sites (Clarke *et al.*, 1985). The recently cloned α9 subunit (Elgoyhen *et al.*, 1994) has also been found to interact with α-Bgt with high affinity, and preliminary *in situ* hybridisation studies in rat and chicken have shown it to have an unsually restricted pattern of expression (consistent with a role in the auditory system where α-Bgt is known to block auditory gating in rat and chicken).

The venom of *Bungarus multicinctus* contains a mixture of related α-toxins (Ravdin and Berg, 1979), including α-Bgt and a minor component which has by consensus been named neuronal bungarotoxin (n-Bgt; other names previously used include toxin F, κ-Bgt and toxin 3.1). It is capable of blocking the ACh-induced currents in the *Xenopus* oocyte expressed rat α3β2 subtype and partially blocking the α4β2 subtype, but is incapable of blocking the α2β2 and α3β4 subtypes (Luetje *et al.*, 1990; 1993; Luetje and Patrick, 1991). More recent studies have shown the interaction of n-Bgt with nAChR subtypes to be more complex, with the β-subunit dictating the kinetics of binding (Papke *et al.*, 1993). Hence interpretation of results with this toxin may be difficult. α-Bgt insensitive binding of this toxin has been reported in the rat CNS (reviewed by Sargent, 1993) and it has been reported to partially (Wonnacott and Drasdo, 1991) or completely (Schulz and Zigmond, 1989; Grady *et al.*, 1992) block nAChR-mediated [^{3}H]-dopamine release from striatal preparations. A partial decrease of striatal [^{3}H]-dopamine release would be consistent with the evidence for heterogeneity of nAChR, including α3β2-containing nAChR (see chapter 4; Kulak *et al.*, 1997; Kaiser *et al.*, 1998).

In summary, the mammalian brain expresses three predominant and pharmacologically distinguishable classes of nAChR: those labelled with high affinity by [^{3}H]-(-)-nicotine and [^{3}H]-ACh (~90% α4β2 nAChR - Whiting and Lindstrom, 1986), those labelled with high affinity by [^{125}I]-α-Bgt (α7-containing nAChR - Clarke *et al.*, 1985; Dominguez del Toro, 1994) and those labelled with high affinity by [^{125}I]-n-Bgt (α3-containing nAChR - Schulz *et al.*, 1991). Recently, Zoli *et al.* (1998) used [^{3}H]-epibatidine for nAChR autoradiography studies, and demonstrated that this tritiated ligand labels more than one nAChR subtype (type 2 (α4β2-containing receptor in most brain regions), type 3 (α3β4-containing receptor) and type 4 (α2β4- and/or α4β4-containing receptor) nAChR).

nAChR subunit mRNA expression

The distribution of nAChR subunit mRNAs within the rat CNS has been characterised using *in situ* hybridisation techniques (Wada *et al.*, 1989; Séguéla *et al.*, 1993). These studies have shown that expression of nAChR subunit mRNAs within the brain is widespread, with most regions of the brain expressing significant quantities of at least one example. However, the pattern of expression differ between subunits, and some subunits are much less common than others. For example, high concentrations of α2 transcripts were only found in the interpeduncular area of the rat, with small amounts detected at a limited number of other sites, while α4 mRNAs were strongly expressed in a large number of locations. The extent of α3 gene expression was shown to be intermediate between those of the α2 and α4 subunits (Wada *et al.*, 1989). Extensive expression of α6 mRNA was found in catecholaminergic nuclei of the brain: i.e. locus coeruleus, ventral tegmental area and substantia nigra (LeNovere *et al.*, 1996). Similarly, among the β-subunits, β2 mRNA was almost found in all parts of the brain (Wada *et al.*, 1989), while β4 mRNA was initially found only in the medial habenula (Duvoisin *et al.*, 1989) with low levels of expression at other loci identified later by Dineley-Miller and Patrick (1992). β3 has been shown to colocalise with α6 in catecholaminergic nuclei (LeNovere *et al.*, 1996). However, β3 is less commonly expressed than β2, but is more widely expressed than the β4 subunit (Deneris *et al.*, 1989). α7 mRNA is found in most regions of the brain, but particularly high levels are found in the amygdala, olfactory regions, and distinct layers of the hippocampus and cerebral cortex (Séguéla *et al.*, 1993). In some (but not most) weakly expressing regions, a small subset of cells may be strongly labelled. For example, a small percentage of Purkinje cells in the cerebellum transcribe large amounts of α2 mRNA, but overall α2 expression in this region is rather weak (Wada *et al.*, 1989).

From the brief account above, it can be concluded that every brain region expresses mRNAs for a plethora of nAChR subunits (Wada et al., 1989, see Wonnacott 1997). Although this approach cannot provide definitive answers, it can exclude the presence of certain subunits and can provide supporting evidence for subunit combinations suggested on the basis of other techniques.

Summary

It is evident that a variety of nAChR subtypes are present in different neuronal tissues, and even within individual neurones (e.g. Alkondon *et al.*, 1993). As a consequence of this diversity, particular nAChR subunit combinations exhibit distinct 1) pharmacological and biophysical properties (e.g. Alkondon *et al.*, 1993), 2) Ca^{2+} conductances (e.g. reviewed in Lindstrom, 1996), 3) expression patterns during development (e.g. Blumenthal *et al.*, 1999), 4) regulatory mechanisms e.g. through nAChR phosphorylation (e.g. Gopalakrishnan *et al.*, 1997) and 5) subcellular targeting (e.g. Shoop *et al.*, 1999).

The next section will primarily discuss how neuronal nAChR activation contributes to neurotransmitter release at the level of the nerve terminal. The local integration of neuronal elements and the contribution of presynaptic nAChR to synaptic transmission in a broader physiological context will also be discussed.

1.2 Presynaptic Neuronal Nicotinic Receptors: Pharmacology, Heterogeneity and Cellular Mechanisms

1.2.1 Presynaptic receptors

Despite the widespread distribution and extensive heterogeneity of nAChR subunits in the CNS (see 1.1.4), the physiological significance of nAChR remains more or less obscure. The paucity of evidence of nicotinic synaptic transmission in the CNS prompted speculation that the purpose of nAChR is to modulate, rather than mediate, neurotransmission (Role and Berg, 1996). The presynaptic localisation of nAChR is compatible with such a role (Wonnacott, 1997).

In 1961, Koelle proposed that ACh can facilitate its own release from preganglionic sympathetic neurones, in addition to its postsynaptic action. Subsequently, receptors that could modulate the release of other neurotransmitters from their respective nerve endings were demonstrated, and the term "presynaptic receptor" was coined (see Langer, 1997). The initial reports described autoreceptors, where the presynaptic receptor was stimulated by the endogenous transmitter of that neurone, presumably serving a feedback loop through which the transmitter could regulate its own release. In addition to the case described by Koelle (1961), there are a number of examples of nicotinic autoreceptors modulating ACh release (see 1.2.2.1). Presynaptic nAChR also reside on terminals releasing transmitter(s) other than ACh. Such heteroreceptors are assumed to reflect an opportunity for crosstalk between different nerve terminals. A further distinction is sometimes made between presynaptic and preterminal receptors (see Wonnacott, 1997). The latter are considered to reside on axons, rather than terminal boutons, and to elicit neurotransmitter release via a tetrodotoxin (TTX)-sensitive mechanism (Wessler, 1992; see 1.2.3.2). Thus, TTX-sensitivity has been taken to define a preterminal localisation. While this may be a reasonable assumption for the motor nerve terminals originally studied (Wessler, 1992), it may not be valid to extend this distinction to the CNS where the configuration of synaptic specialisations can vary enormously, from small synaptic boutons to glomerular terminals and varicosities (Walmsley *et al.*, 1998). TTX-sensitivity is likely to reflect the relative proximities of nAChR to voltage dependent Na^+ channels, voltage operated Ca^{2+} channels (VOCC) and the active zone for release, as well as factors such as the local membrane potential etc. which may be perturbed by the experimental conditions.

The occurrence of heteroreceptors raises a fundamental (and largely unanswered) question about the endogenous source of agonist. Not only is the precise location of nAChR on the nerve terminal unknown but there is little knowledge about the precise topographical relationship between nicotinic heteroreceptors and cholinergic terminals. For example, in the rat striatum where the association of nAChR with dopamine terminals is well documented (see 1.2.2.2), cholinergic interneurones form symmetrical synapses with shafts and spines of the medium spiny projection neurones that are GABAergic (Smith and Bolam, 1990). Rather than a brief pulse of a high concentration (mM) of ACh delivered across the synaptic cleft, ACh may be required to diffuse to adjacent terminals, achieving a lower concentration (μM-nM) but for a

longer duration. This assumes that sufficient ACh will escape hydrolysis by acetylcholinesterase: the sensitivity of particular nAChR subtypes to ACh, and their propensity to desensitise may become important factors in shaping their responsiveness. The recent demonstration that choline is an agonist at α7-type nAChR (Alkondon *et al.*, 1997) offers an alternative candidate for activation (and / or desensitisation) of nAChR. Ultrastructural and / or electrophysiological approaches will be necessary to determine the relationship between nAChR and the source of endogenous agonist, before we can appreciate the physiological potential of presynaptic nAChR. Despite this caution, presynaptic nAChR are valid therapeutic targets for pharmaceutical products, and have been employed as screens for the evaluation of novel drugs (see Holladay *et al.*, 1997).

1.2.2 Pharmacology and heterogeneity of presynaptic nAChR

There is considerable evidence for presynaptic nAChR, but in no case has the complete subunit composition of any presynaptic nAChR been unequivocally assigned. The ability to define their subunit composition is constrained not only by methodological limitations (see Kaiser and Wonnacott, 1999), but also by a lack of definitive subtype-selective antagonists or agonists. The following review of the literature, grouped by neurotransmitter released, attempts to summarise the current knowledge of some of the better characterised examples.

1.2.2.1 Acetylcholine (ACh)

Nicotinic autoreceptors on cholinergic terminals represent the most straightforward example of presynaptic nAChR and, as already noted, were the first to be recognised (Koelle, 1961). More recently, the pharmacology of the positive feedback modulation via nAChR of [^{3}H]-ACh release from acutely isolated rat superior cervical ganglia was studied (Liang and Vizi, 1997). Inhibition by α-Bgt suggests an involvement of the α7 subunit. This corroborates the findings of McGehee *et al.* (1995) who used an antisense approach to implicate α7-containing nAChR (α-Bgt-sensitive) in the release of ACh from chick sympathetic neurones in culture. Both electrophysiological and neurochemical techniques have demonstrated that nAChR have a modulatory role at motor nerve terminals (Bowman *et al.* 1990; see Wonnacott, 1997). These presynaptic nAChR may be heterogeneous, with co-expression of both positive and negative feedback mechanisms requiring different stimulation frequencies and having different drug specificities (Bowman *et al.* 1990; Tian *et al.* 1994). The facilitatory nicotinic effect is blocked by hexamethonium and d-tubocurarine (dTC) but is insensitive to α-Bgt and n-Bgt (Wessler, 1989; Vizi and Somogyi, 1989; Bowman *et al.* 1990). An inhibitory nicotinic action, observed at low frequency stimulation, has been attributed to prejunctional (preterminal) nAChR (Tian *et al.*, 1994). The relative insensitivity to methyllycaconitine (MLA) would seem to exclude the α7 subunit (Tian *et al.* 1997), although α-Bgt has been claimed to block this negative feedback (Domet *et al.* 1995). A α7-type presynaptic nAChR has recently been implicated in the development of neuromuscular synapses, studied in cocultures of *Xenopus laevis* embryos

(Fu and Liu, 1997). Cholinergic autoreceptors also serve a feedback role in the regulation of ACh release from cholinergic fibres innervating the guinea pig ileum. Pharmacological evidence for both inhibitory muscarinic receptors and facilitatory nAChR was derived using synaptosomes from the myenteric plexus (Briggs and Cooper, 1982), and DMPP was shown to stimulate [^{3}H]-ACh release from perfused myenteric plexus (Takahashi *et al.*, 1992).

In the CNS, the superfusion technique has been used to demonstrate the nicotinic stimulation of ACh release from rat hippocampal synaptosomes and slices (Araujo *et al.*, 1988; Wilkie *et al.*, 1996) and cortical synaptosomes and slices (Rowell and Winkler, 1984; Ochoa and O'Shea, 1994; Marchi and Raiteri, 1996). nAChR comprised of α4 and β2 subunits are a candidate for the autoreceptors in hippocampus (Wilkie *et al.*, 1996), based on pharmacology (sensitivity to mecamylamine, dTC and dihydroβerythroidine (DHβE), but not to methyllycaconitine (MLA) or α-Bgt) and agonist dose-response profiles, compared with rat α4β2 nAChR expressed in *Xenopus* oocytes, although cytisine appeared to be a full agonist in evoking ACh release. α4β2 nAChR are consistent with the loss of [^{3}H]-nicotine binding sites in the hippocampus, following degeneration of the septo-hippocampal projection in Alzheimer's disease. In contrast to these examples, attempts to demonstrate the nicotinic stimulation of ACh release in rat striatum have proved negative (Lapchak *et al.*, 1989; Rao *et al.*, 1997).

1.2.2.2 Dopamine

The nicotinic stimulation of dopamine (DA) release has been the most documented example of presynaptic nicotinic modulation in the CNS and its pharmacological profile has been examined with respect to both conventional and novel ligands (see Holladay *et al.*, 1997). The superfusion technique has been widely used in this respect, to characterise the nicotinic stimulation of DA release from striatal synaptosomes (e.g. Rapier *et al*, 1990; Grady *et al*, 1992; El-Bizri and Clarke, 1994, Kulak *et al.*, 1997) and slices (e.g. Giorguieff-Chesselet *et al.*, 1979; Sacaan *et al.*, 1995; Kaiser *et al.* 1998), as well as from nucleus accumbens minces (Rowell *et al.*, 1987) and frontal cortex synaptosomes (Whiteaker *et al.*, 1995). In striatal synaptosomes, the nicotinic stimulation of DA release is blocked by mecamylamine, DHβE and n-Bgt but is insensitive to α-Bgt, α-conotoxin-Iml (α-CTx-Iml) and low concentrations of MLA. The sensitivity of (-)-nicotine-evoked [^{3}H]-DA release to n-Bgt has been interpreted in favour of α3-type nAChR (Schulz and Zigmond, 1989; Grady et al., 1992). However, loss of [^{3}H]-(-)-nicotine binding sites following lesion of the nigrostriatal tract (Clarke and Pert, 1985) favours presynaptic nAChR composed of α4 and β2 subunits on dopamine terminals in the striatum. This paradox can be explained in the light of recent reports that used the α3β2-selective antagonist α-conotoxin-MII (α-CTx-MII - Kulak *et al.*, 1997; Kaiser *et al.*, 1998 - chapter 4). Low nanomolar concentrations of α-CTx-MII dose-dependently inhibited [^{3}H]-DA release from striatal synaptosomes, elicited by (-)-nicotine (Kulak *et al.*, 1997) or (±)-anatoxin-a ((±)-AnTx-a; Kaiser *et al.*, 1998 - chapter4). The IC_{50} value for this inhibition is close to that for blockade of α3β2 nAChR in

Xenopus oocytes. However, the maximum inhibition achieved was only 40-60% of the evoked release, compared with antagonism by the non-selective nicotinic antagonist, mecamylamine, of greater than 80%. This suggests the presence of a heterogeneous population of presynaptic nAChR, with a proportion containing α3 and β2 subunits (possibly in association with other, additional subunits) having sensitivity to nanomolar concentrations of α-CTx-MII, and a proportion lacking one or both of these subunits and insensitive to α-CTx-MII (chapter 4).

Nicotinic agonists evoke dopamine release with different potencies and efficacies (see chapter 4 and Holladay *et al.*, 1997). For example, the novel agonist UB-165 that is a hybrid of (+)-AnTx-a and (-)-epibatidine (Wright *et al.*, 1997) elicits only ~40% of the maximum [^{3}H]-DA release evoked by (±)-AnTx-a from striatal synaptosomes (chapter 4). This partial effect of UB-165 is totally blocked by α-CTx-MII, suggesting that UB-165 only activates the α3β2-containing nAChR on striatal dopamine terminals (chapter 4).

1.2.2.3 Noradrenaline

Presynaptic nAChR on noradrenergic afferents were postulated to be responsible for (-)-nicotine-evoked noradrenaline release in hypothalamus, cortex and cerebellum (Westfall, 1974). Subsequently, presynaptic nAChR modulating noradrenaline release from hippocampal slices (Sacaan *et al.*, 1995, 1996; Sershen *et al.*, 1997) and synaptosomes (Clarke and Reuben, 1996), and in the dorsal raphe nucleus (Li *et al.*, 1998) have been characterised. In the peripheral nervous system, presynaptic nAChR can induce the release of noradrenaline from sympathetic neurones (Dolezal *et al.*, 1996). nAChR in vas deferens are located on noradrenaline terminals. Stimulation of these nAChR induces the release of noradrenaline and ATP, which in turn induce contraction of the smooth muscle cells (Carneiro and Markus, 1990; Todorov *et al.*, 1991). ACh has no direct effect on the muscle cells in this preparation, and it is interesting to consider that the sole purpose of the cholinergic innervation of the tissue may be to exert this presynaptic modulation. The nicotinic enhancement exhibits a diurnal variation (Markus *et al.*, 1996), attributed to the appearance of a second population of low affinity nicotinic binding sites in response to melatonin.

To gain an insight into the subtypes of nAChR that modulate noradrenaline release, the pharmacological profile of the presynaptic response can be compared with that of heterologously expressed nAChR (although in most cases the latter comprise pairwise combinations of subunits, whereas evidence is accumulating that native nAChR may be more complex, Ramirez-Latorre *et al.*, 1996). Such a comparison led Clarke and Reuben (1996) to propose that the presynaptic nAChR mediating noradrenaline release from hippocampal synaptosomes most closely resembles α3β4 nAChR. The lower potency of nicotinic agonists in eliciting noradrenaline release, and the lower sensitivity of (-)-nicotine-evoked noradrenaline release to DHβE and MLA was distinctly different from striatal dopamine release measured in parallel. Noradrenaline release from hippocampal and thalamic slices (Sacaan *et al.*, 1995;

1996) has been described with similar properties to those seen in synaptosome preparations. Sensitivity to n-Bgt, together with insensitivity to the α7-selective antagonists α-Bgt and α-CTx-Iml (Sershen *et al.*, 1997), reinforces the idea of a nAChR containing the α3 subunit. Furthermore, a nAChR with an α3β2 interface can be excluded, since Kulak *et al.* (1997) showed that (-)-nicotine-evoked noradrenaline release from hippocampal synaptosomes is not blocked by α-CTx-MII. A novel *Conus* toxin, α-conotoxin-AulB (α-CTx-AulB), with specificity for α3β4 subunit combinations, has just been used to confirm that these subunits contribute to the presynaptic nAChR that modulates noradrenaline release from hippocampal synaptosomes (Luo *et al.*, 1998). This finding validates the conclusion arrived at by Clarke and Reuben (1996) that presynaptic nAChR mediating noradrenaline release are pharmacologically and structurally distinct from those involved in the regulation of dopamine release in striatum.

In contrast, the DMPP-evoked depolarisation of dorsal raphe neurones, attributed to the nicotinic stimulation of noradrenaline release, was selectively blocked by MLA (0.1 and 1 μM), and a α7-containing nAChR has been invoked (Li *et al.*, 1998). This result suggests that different subtypes of presynaptic nAChR may regulate noradrenaline release in different brain regions, although more data are required to confirm or refute this assertion.

1.2.2.4 5-Hydroxytryptamine (5-HT)

Nicotine is reported to increase arousal and attention and to elevate mood, effects that are associated with monoaminergic systems. It is perhaps surprising that there are few reports of a direct presynaptic nicotinic modulation of 5HT release. (-)-Nicotine can release [^{3}H]-5-HT from striatal slices (Westfall *et al.*, 1982; Yu and Wecker, 1994). Moreover, a recent *in vivo* study (Takahashi *et al.*, 1998) demonstrated that (-)-nicotine induces striatal 5-HT release upon stress application by stimulating presynaptic nAChR. DMPP (but not (-)-nicotine or cytisine) is reported to stimulate [^{3}H]-5-HT release from hippocampal slices and this response was blocked by mecamylamine (but not by DHβE) but was Ca^{2+}-independent (Lendvai *et al.*, 1996). This differs from the Ca^{2+}-dependent nicotinic modulation of other transmitters. A recent report (Li *et al.*, 1998) documents the nicotinic facilitation of 5-HT release in the dorsal raphe via a MLA-insensitive mechanism, in contrast to the nicotinic stimulation of noradrenaline release from the same preparation (see 1.2.2.3). The nicotinic modulation of 5-HT release deserves more attention, especially in the light of increasing evidence that 5-HT can modulate the activity of neural reward pathways (Parsons *et al.*, 1996).

1.2.2.5 γ-Aminobutyric acid (GABA)

Neurochemical and electrophysiological studies have provided evidence for presynaptic nAChR modulating GABA release in both avian and mammalian brain. Chiappinelli and colleagues have used whole cell patch clamp recording in the chick lateral spiriform (McMahon *et al.*, 1994a) and ventral lateral geniculate nuclei (McMahon *et al.*, 1994b; Guo *et al.*, 1998) to disclose a nicotinic facilitation of GABA release. Responses were insensitive to α-Bgt and MLA, disqualifying α7-type nAChR as likely

contenders. Responses from the lateral spiriform nucleus were also insensitive to n-Bgt, making the α3β2 subunit combination unlikely.

(-)-Nicotine-induced inhibition in rat medial septum, studied using extracellular, single unit recording *in vivo*, was attributed to presynaptic nAChR on GABA terminals (Yang *et al.*, 1996). This response was blocked by DHβE but subtypes were not characterised further. Presynaptic ("preterminal") nAChR are present on GABAergic terminals in the rat interpeduncular nucleus and facilitate GABA release in a TTX- and DHβE-sensitive manner (Lena *et al.*, 1993). In the mouse thalamus, nicotinic agonists increased the frequency of miniature GABAergic synaptic currents in the presence of TTX, consistent with presynaptic nAChR on the GABA terminals (Lena and Changeux, 1997). The absence of this facilitation in transgenic mice lacking the β2 subunit provides compelling evidence for the participation of this subunit in the presynaptic nAChR in question. This view is supported and extended in a comprehensive neurochemical study of the stimulation by nicotinic agonists of [^{3}H]-GABA release from mouse synaptosomes (Lu *et al.*, 1998). Nicotine stimulated [^{3}H]-GABA release in all crudely dissected brain regions examined, and was highest in striatum and thalamus. The magnitude of nicotine-evoked [^{3}H]-GABA release was highly correlated with the level of [^{3}H]-nicotine binding sites and with the magnitude of nicotine-evoked Rb^+ flux in each region, measures which are proposed to reflect α4β2 nAChR. Nicotine-stimulated release was absent in tissues prepared from β2 knockout mice, with an intermediate level of responsiveness in heterozygotes. Thus there is a consistent picture from these mammalian studies of presynaptic nAChR containing the β2 subunit (possibly in combination with α4).

1.2.2.6 Glutamate

Sensitive electrophysiological recording has disclosed a α-Bgt- and MLA-sensitive modulation of glutamate transmission in rat hippocampus (Gray *et al.*, 1996; Radcliffe and Dani, 1998) and olfactory bulb (Alkondon *et al.*, 1996). In cocultures of chick interpeduncular nucleus and medial habenula, antisense ablation of the α7 subunit abolished the α-Bgt-sensitivity of the enhancement by nicotine of EPSC frequency (McGehee *et al.*, 1996). Interestingly, (-)-nicotine continued to modulate glutamate transmission after antisense treatment, suggesting plasticity in the assembly of subunits to create nAChR. Recently, Guo and colleagues (1998) reported that carbachol and other nicotinic agonists produced marked increases in the frequency of glutamatergic spontaneous postsynaptic currents in chick ventral lateral geniculate nucleus. While sensitivity to α-Bgt implies the involvement of a α7-type nAChR, the pharmacology is unusual in the lack of sensitivity to MLA and strychnine (other antagonists of α7-containing nAChR).

Attempts to directly demonstrate the nicotinic modulation of glutamate release using neurochemical approaches have been negative (e.g. Wonnacott *et al.*, 1995 - chapter 3). This may reflect the rapid desensitisation of α7-type nAChR which will require more sensitive methods with better time resolution in order to detect their direct effects. However, our lab has

recently acquired indirect evidence for the nicotinic modulation of glutamate release from rat striatal slices; again this effect appears to mediated by a α7-type nAChR (Kaiser *et al.*, 1998 - chapter 5). In this preparation, [^{3}H]-DA release elicited by nicotinic agonists includes a component that is blocked by α-Bgt, α-CTx-IMI, MLA and ionotropic glutamate receptor antagonists. It has been hypothesised that this derives from the nicotinic stimulation of glutamate release via a α7-type nAChR on cortico-striatal afferents; the glutamate released in turn promotes [^{3}H]-DA release which is measured (chapter 5).

1.2.2.7 ATP

ATP is co-released with classical transmitters with which it is co-stored in synaptic vesicles. Therefore, presynaptic nAChR that modulate the release of such classical transmitters (e.g. ACh, noradrenaline) will be expected to also elevate extracellular levels of ATP. There is direct evidence for (-)-nicotine-stimulated ATP release from myenteric plexus synaptosomes (White and Al-Hummayyd, 1983).

1.2.2.8 Summary

It is evident that presynaptic nAChR are widespread, and are associated with many different transmitters. The pharmacological characteristics of nAChR in different preparations vary, consistent with various nAChR subtypes fulfilling a presynaptic role. While the evidence to date associates the α7 subtype with glutamate terminals and the α4β2 subtype with GABA terminals, nAChR found on dopamine terminals are heterogeneous. There are insufficient data to draw any firm conclusions about the patterns of distribution. Moreover, despite the wealth of information, we are still far from understanding the contribution of presynaptic nAChR to synaptic transmission and brain function.

1.2.3 Molecular and cellular mechanisms underlying the nicotinic modulation of transmitter release

1.2.3.1 Current views of exocytosis

The coupling between presynaptic nerve terminal depolarisation (e.g. by an incoming action potential) and transmitter release has been the subject of a large number of studies over several decades (e.g. Katz, 1969; Südhof, 1995). In the nerve terminal, different compartments are assumed for storage (reserve pool of vesicles or vesicles tethered to the cytoskeleton) and for docking and release (readily releasable vesicle pool). It is clear that nerve terminal depolarisation causes the opening of voltage-operated calcium channels (VOCC), entry of Ca^{2+} into the nerve terminal, and Ca^{2+}-dependent release of neurotransmitters. Moreover, Ca^{2+} influx following nerve terminal depolarisation has also been shown to increase the phosphorylation state of a number of proteins, including synapsin I. This protein binds synaptic vesicles to cytoskeletal elements and after phosphorylation by CaM kinase II (Ca^{2+}-dependent) liberates vesicles from these attachments (Llinás *et al.*, 1991).

The docking of vesicles at specialised areas of the presynaptic plasma membrane called active zones, fusion and release of transmitter involve interactions between vesicle (VSNARES) proteins and proteins of the nerve terminal plasma membrane (TSNARES): the VAMPs (synaptobrevins) and synaptotagmin (P65) on the vesicle membrane and syntaxins and neurexins on the nerve terminal membrane (reviewed by Südhof, 1995). It is interesting to highlight the close topological association that exists between nerve terminal VOCC and the exocytotic machinery. The colocalisation of N-type VOCC and syntaxin have been reported (Sheng *et al.*, 1994). After docking, synaptic vesicles go through a maturation or "priming" process that makes them competent for Ca^{2+}-triggered membrane fusion. Then, primed synaptic vesicles are stimulated for rapid fusion / exocytosis by a transient and local increase in the intraterminal Ca^{2+} concentration, e.g. during an action potential. The identity of the vesicle and plasma membrane proteins that constitute the fusion pore remains unclear, but synaptophysin is thought to form the vesicle contribution to the fusion pore while physophilin may constitute the plasma membrane contribution to the pore protein.

1.2.3.2 Na^+ dependence and TTX sensitivity

In the few instances where it has been examined, the nicotinic stimulation of transmitter release is Na^+-dependent: replacement of extracellular Na^+ with N-methyl-D-glucamine abolished (±)-antx-a-evoked dopamine release from striatal synaptosomes (Soliakov and Wonnacott, 1996). This is in agreement with the earlier demonstration that the (-)-nicotine-induced depolarisation of cortical synaptosomes is Na^+-dependent (Hillard, 1992). More controversial is whether the Na^+ current through nicotinic channels alone accounts for the nerve terminal depolarisation and is sufficient for stimulating transmitter release, or if it is augmented by the opening of voltage gated Na^+ channels. Sensitivity to TTX has been used to assess the contribution of voltage gated Na^+ channels, and various degrees of inhibition of nAChR-evoked transmitter release have been reported. For example, in striatal synaptosome preparations [^{3}H]-DA release elicited by nicotinic agonists has been found to be insensitive to TTX (Rapier *et al.*, 1988; Prince *et al.*, 1996) or partially blocked by TTX (Soliakov and Wonnacott, 1996 - chapter 4), whereas [^{3}H]-DA release from striatal slices may be partially (Sacaan *et al.*, 1995) or totally blocked by TTX (Marshall *et al.*, 1996). Examination of (-)-nicotine-stimulated efflux of $^{86}Rb^+$ from mouse brain synaptosomes, a direct measure of ion flux arising from nAChR activation, found a partial (40%) inhibition by TTX (Marks *et al.*, 1995). TTX was shown to decrease the rate of $^{86}Rb^+$ flux without affecting the EC_{50} for (-)-nicotine, consistent with a block of voltage gated Na^+ channels that augment the response to (-)-nicotine. This conclusion, together with the varying degrees of TTX sensitivity reported in the literature, makes the use of TTX-insensitivity to define functional presynaptic nAChR problematic. Rather, the failure of TTX to inhibit a nAChR-mediated enhancement of transmitter release is likely to reflect the location of receptors close to the release sites (Guo *et al.*, 1998).

1.2.3.3 Ca^{2+} dependence and involvement of VOCC

The high relative permeability to Ca^{2+} of neuronal nAChR raises the possibility that they might interface directly with the exocytotic machinery to promote transmitter release. Alternatively, the Na^{+} current and ensuing depolarisation might activate VOCC (Figure 1.4). In most cases examined, a partial (Lena and Changeux, 1997) or total (Soliakov and Wonnacott, 1996; Sershen *et al.*, 1997) inhibition of nicotinic responses by non-selective blockers of VOCC such as Cd^{2+} has been observed, consistent with the participation of such channels. Selective inhibitors of subtypes of VOCC have implicated N-type channels as the principle mediator of the nicotinic stimulation of neurotransmitter release (Harsing *et al.*, 1992; Soliakov and Wonnacott, 1996; Sershen *et al.*, 1997). Then, it could be suggested that in the case of TTX-insensitive nicotinic stimulation of transmitter release, Na^{+} influx though the nicotinic channel produces sufficient local depolarisation to activate e.g. N-type VOCC. As these channels colocalise with syntaxin (Sheng et al., 1994), presynaptic nAChR may reside in close proximity at the active zone. A similar situation is observed in the presynaptic nAChR modulation of transmitter release in the peripheral nervous system: DMPP-evoked release of [^{3}H]-ACh from guinea pig myenteric plexus is coupled to Ca^{2+} influx via N-type channels (Takahashi *et al.*, 1992). In CNS preparations, ω-Agatoxin IVA, a blocker of P-type VOCC, has a small (Prince *et al.*, 1996) or negligible effect (Soliakov and Wonnacott, 1996) on release evoked by nicotinic agonists, and inhibitors of T-type channels have no effect (Harsing *et* al., 1992). L-type channel blockers (e.g dihydropyridines such as nifedipine) exert nonspecific actions on the nicotinic stimulation of transmitter release, attributed to a direct interaction with nAChR (Prince *et al.*, 1996; Soliakov and Wonnacott, 1996).

Evidence that in some cases the Ca^{2+} flux through the nicotinic channel itself is sufficient for transmitter release comes from electrophysiological studies, coupled with the use of fluorescent indicators to demonstrate an increase in presynaptic intracellular Ca^{2+} in the presence of TTX and Cd^{2+} (Gray *et al.*, 1996). The fact that the α7-type nAChR is responsible in this case may be relevant as it has the highest Ca^{2+} permeability of any neuronal nAChR: indeed the Ca^{2+} signal attributed to influx via the α7 nAChR is equivalent to that generated by an action potential. As experiments were not carried out in the absence of Cd^{2+} it is not certain that VOCC would not enhance the response. At GABAergic terminals in the medial habenula, presynaptic nicotinic enhancement of postsynaptic currents was insensitive to Cd^{2+} at some synapses but not others (Lena and Changeux, 1997); the α7 subunit has not been implicated in this response (see 1.2.2.5). In the presence of TTX, DMPP-evoked [^{3}H]-noradrenaline release from chick sympathetic neurones in culture was not blocked by inhibitors of VOCC (Dolezal *et al.*, 1996). The relative proximity of presynaptic nAChR to the exocytotic machinery and/or VOCC is likely to be the determining factor.

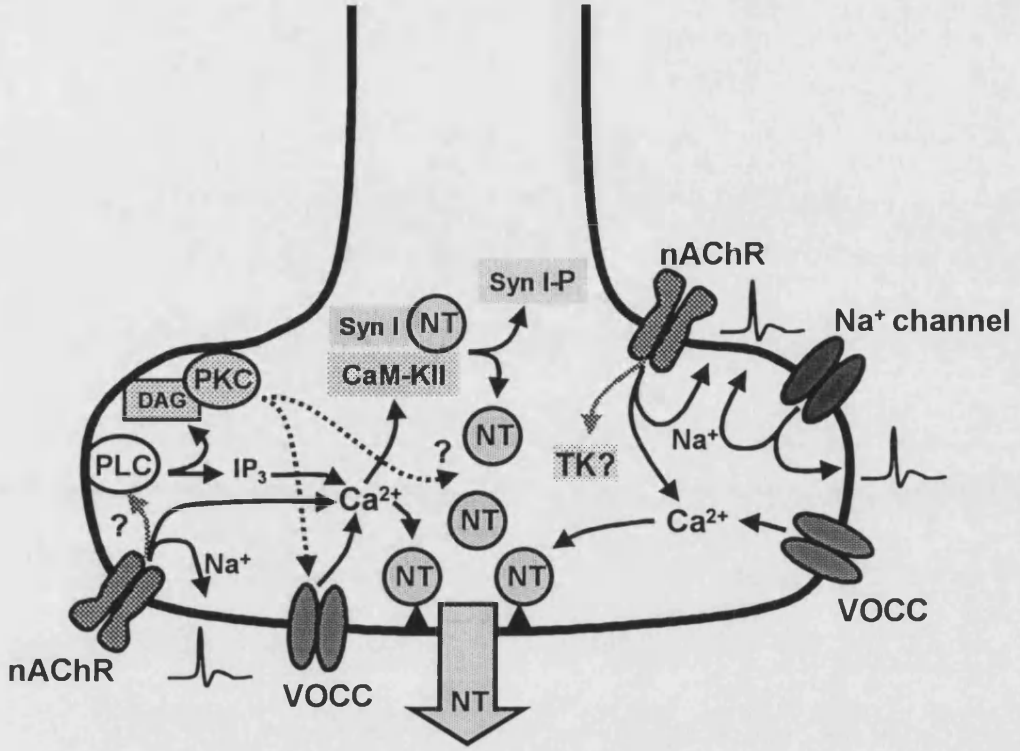

Figure 1.4 Proposed model for the nAChR-mediated facilitation of neurotransmitter release from nerve terminals. Stimulation of nAChR with agonist initiates Na^+ and Ca^{2+} influx through the receptor channel. The increase in intracellular Na^+ results in depolarisation of the synaptic membrane and, depending on their relative proximities, may lead to opening of Na^+ channels and / or voltage operated Ca^{2+} channels (VOCC). Alternatively, Ca^{2+} entering via the nicotinic channel may itself be sufficient to provoke neurotransmitter (NT) release. In parallel, activation of nAChR may lead to a number of intracellular events. **(i)** Phospholipase C (PLC) localised close to the nAChR may be activated (possibly by a Ca^{2+}-dependent mechanism), leading to the generation of inositol triphosphate (IP_3) and diacylglycerol (DAG). The latter, in concert with Ca^{2+}, can lead to concomitant activation of protein kinase C (PKC). In turn, PKC could modulate the efficacy of neurotransmitter release by regulating ion-channel function or by enhancement of the readily releasable pool of synaptic vesicles, or both. **(ii)** The increase in intracellular Ca^{2+} may activate the synaptic vesicle-associated Ca^{2+} / calmodulin-dependent protein kinase II (CaM-KII), resulting in the phosphorylation of synapsin I. In its unphosphorylated state, synapsin I anchors synaptic vesicles to the actin cytoskeleton, whereas phosphorylation releases them from this reserve position, increasing the readily releasable pool of synaptic vesicles near the active zone. **(iii)** Further regulation of presynaptic mechanisms may be achieved through tyrosine kinase (TK) pathways that may be linked to nAChR activation by a route that is presently unknown.

1.2.3.4 The involvement of second messengers in the nicotinic modulation of neurotransmission

Presynaptic nAChR may have more subtle modulatory functions than simply provoking transmitter release: they are proposed to increase the probability of release (Gray *et al.*, 1996) or to sustain release through mobilisation of a reserve pool of transmitter (Bowman *et al.*, 1990). Such actions are likely to be mediated by second messengers, and phosphorylation / dephosphorylation events offer a plausible regulatory mechanism. The high relative permeability to Ca^{2+} of neuronal nAChR advocates the potential involvement of Ca^{2+}-dependent kinases (such as protein kinase C (PKC) and calcium-calmodulin dependent kinase II (CaM kinase II)) and Ca^{2+}-activatable phosphatases (see Figure 1.4).

1.2.3.4.1 PKC

PKC is implicated in the modulation of exocytosis and PKC activators such as phorbol esters enhance neurotransmitter release evoked by electrical stimulation or KCl depolarisation (Dekker *et al.*, 1991). Evidence for a PKC enhancement of the nicotinic stimulation of transmitter release comes from chromaffin cells (Terbush *et al.*, 1988; Cox and Parsons, 1997). Here the (-)-nicotine-induced secretion of catecholamines is associated with entry of extracellular Ca^{2+} (Wakade *et al.*, 1986), rapid translocation of PKC from cytosol to membrane (Terbush *et al.*, 1988) and concomitant activation of PKC (Brocklehurst *et al.*, 1985). There has been little work published on any interaction between nAChR and PKC in neurones. Chéramy and colleagues (1996) reported that the synergism between (-)-nicotine and NMDA in stimulating [^{3}H]-dopamine release from striatal synaptosomes (attributed to the nicotinic depolarisation relieving the Mg^{2+} block of NMDA receptors) was sensitive to blockade by the PKC inhibitors staurosporine and chelerythrine.

Dr Wonnacott's lab has examined the potential interaction between presynaptic nAChR and PKC in striatal terminals in more detail (Soliakov and Wonnacott, 1998). They observed that two potent and specific PKC inhibitors, Ro 31-8220 and D-*erythro*-sphingosine (but not the inactive analogue bisindolylmaleimide V) significantly inhibited the release of [^{3}H]-dopamine evoked by the nicotinic agonist anatoxin-a. Moreover, two phorbol esters that activate PKC, phorbol-12,13-dibutyrate and phorbol-12-myristate-13-acetate (but not the inactive phorbol ester 4α-phorbol-12,13-didecanoate) potentiated anatoxin-a-evoked [^{3}H]-dopamine release. This potentiation was Ca^{2+}-dependent and blocked by PKC inhibitors. Identification of particular PKC subtypes involved has proved to be less tractable, not least because a large proportion of the majority of subtypes is already membrane bound in the brain under resting conditions, so that translocation to the membrane fraction is not an absolute prerequisite for activation if other necessary conditions (e.g. Ca^{2+} and diacylglycerol) prevail (Chakracarthy *et al.*, 1994). The source of diacylglycerol following nAChR stimulation is not clear. There is considerable documentation that depolarising conditions elicit the generation of inositol phosphates (presumably in concert with the formation of diacylglycerol; see Dekker *et al.*, 1991), and nicotinic stimulation may fall into this category.

Indeed, in chromaffin cells KCl depolarisation or nAChR stimulation by DMPP increased the accumulation of inositol phosphates (Eberhard and Holz, 1987), and a mechanism based on the activation of PLC_γ by the increase in intracellular Ca^{2+} was advocated. There is also scope for interplay between nicotinic and muscarinic receptors (or with other metabotropic receptors coupled to phosphoinositide turnover). Both nicotinic and muscarinic stimulation of PC12 cells results in the translocation of PKC to the plasma membrane (Messing *et al.*, 1989).

PKC can influence transmitter release by phosphorylating ion channels (Smart, 1997) or acting on proteins that participate in vesicle docking and fusion events (Gillis *et al.*, 1996). The presynaptic nAChR may itself be a target for PKC: phosphorylation of the $\alpha4$ subunit by PKC has been hypothesised to be necessary for maintaining the $\alpha4\beta2$ nAChR in an activatable state (Eilers *et al.*, 1997), although phosphorylation of muscle and ganglionic nAChR has been found to enhance desensitisation (Downing and Role, 1987; Hoffman *et al.*, 1994). Transmitter release or $^{86}Rb^+$ efflux stimulated by presynaptic nAChR is subject to short term (desensitisation) and long term (functional inactivation) reduction, in response to sub-stimulating and stimulatory agonist concentrations, respectively (Marks *et al.*, 1996; Rowell and Hillebrand, 1994). Any contribution of kinase or phosphatase activities in mediating these responses is not known, but such mechanisms are very plausible.

1.2.3.4.2 CaM kinase II

Another link between presynaptic nAChR stimulation, protein kinase activation and transmitter release, relevant to the mobilisation of a reserve pool of transmitter, comes from the study of Ochoa and O'Shea (1994). These authors reported that the nicotinic stimulation of ACh release from cortical synaptosomes was accompanied by a Ca^{2+}-dependent increase in the phosphorylation of an 80 KDa band, proposed to correspond to synapsin I. This synaptic vesicle-associated protein regulates the availability of vesicles for release via its phosphorylated status (Greengard *et al.*, 1993). Further analysis indicated that nicotine (50 μM) results in phosphorylation of site 3 on the synapsin I molecule (Ochoa an O'Shea, 1994). This site is known to be phosphorylated by vesicle-associated CaM kinase II (Benfenati *et al.*, 1992), and Ca^{2+} entry accompanying nAChR activation might provide the stimulus.

Recently, an increase in the level of site 3-phospho-synapsin I, together with an increase in CaM kinase II activity, has been proposed to play a role in the enhancement of dopamine release from striatal synaptosomes provoked by amphetamine (Iwata *et al.*, 1997). Our preliminary data (Soliakov and Kaiser, unpublished data - see chapter 6) also support synapsin I phosphorylation in response to the stimulation of nAChR in striatal nerve terminals: this response shows a critical, biphasic time dependence similar to that observed in response to KCl depolarisation (Sihra *et al.*, 1989).

1.2.3.4.3 Tyrosine kinase signalling pathways

Tyrosine kinases are increasingly recognised as important mediators and regulators of intracellular events, as well as intercellular communication. Although there is no evidence for the participation of tyrosine kinases in the nicotinic modulation of transmitter release in the brain, some support for such a link comes from chromaffin cells (Ely *et al.*, 1990). Stimulation with either nicotine or KCl resulted in rapid tyrosine phosphorylation of the extracellular signal-related kinase (ERK2), and this was correlated with the Ca^{2+}-dependent release of catecholamines provoked by the same depolarising agents. An involvement of tyrosine kinase is supported by the blockade of both nicotine-induced protein tyrosine phosphorylation and noradrenaline exocytosis in chromaffin cells by two different tyrosine kinase inhibitors, genistein and tyrphostin 23 (Cox *et al.*, 1996).

In chromaffin cells, the tyrosine kinase Fyn, a member of the Src family, resides predominantly in the plasma membrane fraction and undergoes nicotine-induced activation in a Ca^{2+}-dependent manner; this activation is abolished by mecamylamine (Allen *et al.*, 1996). In the brain, Fyn is widely expressed and involved in a variety of neuronal events (Umemori *et al.*, 1992). Consensus sequences for tyrosine kinases have been identified in the intracellular loops of several subunits of neuronal nAChR (Gurd, 1997) so modulation of the receptor via such pathways is also plausible.

1.2.4 Concluding remarks

This section has attempted to summarise the evidence for presynaptic nAChR on central and peripheral nerve terminals. It is evident that presynaptic nAChR are widespread, they are associated with all of the classical transmitters. However, presynaptic nAChR are not ubiquitous with respect to all nerve terminals and the release of some neurotransmitters in certain brain areas does not appear to be modulated by nicotinic agonists. In addition to this gross anatomical heterogeneity in their distribution, differences in the susceptibility to TTX and VOCC blockers suggests that there is local heterogeneity with respect to the localisation of presynaptic nAChR on nerve terminals, in relation to release sites. The subunit composition of presynaptic nAChR is also heterogeneous. So far, α7-type nAChR appear to modulate glutamate release, the β2 subunit is associated with GABA release, and multiple subtypes may influence dopamine release. More extensive information is required before generalisations can be made with any confidence. For the widespread occurrence of presynaptic nAChR to have physiological relevance, a similarly widely distributed source of ACh is required. Although cholinergic innervation is extensive in the brain, lack of evidence for axo-axonic synapses may favour a diffuse action of ACh (Descarries *et al.*, 1997).

In this section, several ways in which presynaptic nAChR might interface with signalling pathways to modulate transmitter availability and its release, were also briefly considered. Such studies are in their infancy but can be predicted to constitute a major research initiative in the near future. Signalling cascades provide a route for receptor crosstalk, well documented for metabotropic receptors but applicable also to ligand gated ion channels. Knowledge of this interface will illuminate the mechanisms of local regulation of nerve terminal functioning, that will extend beyond the simple enhancement of transmitter release.

1.3 Project aims

The general aim of this work was to study *in vitro* the modulation of neurotransmitter release by presynaptic nAChR in the vertebrate CNS. In this respect, two rat brain areas were examined: the **hippocampus** (section I) and the **striatum** (section II).

Section I of this thesis presents initial experimental attempts aimed at examining the involvement of presynaptic α7 nAChR in nicotinic agonist-evoked glutamate release from hippocampal preparations. The project initially involved the development of two topics:

1) the biochemical, pharmacological and functional characterisation of native and heterologously expressed rat α7 nAChR (this thesis next chapter), and the application of the potential results to
2) the study of nicotinic agonist-evoked glutamate release in rat hippocampus (this thesis chapter 3).

These studies were largely unsuccessful. Consequently, the modulation of striatal dopamine release as a consequence of presynaptic nAChR activation became the main focus of this thesis. In **section II**, the superfusion technique was used to explore the following aspects of the nicotinic modulation of dopamine release in striatum:

1) identification of presynaptic and/or preterminal nAChR modulating striatal dopamine release (this thesis chapters 4 & 5)
2) functional crosstalk between striatal nerve terminals as a consequence of nAChR stimulation (this thesis chapter 5), and
3) second messenger mechanisms underlying nicotinic agonist-evoked striatal dopamine release (this thesis chapter 6)

Section I: The hippocampus

Learning and memory have since long been considered to be related to changes in synaptic efficacy, and long-term potentiation is a major candidate for such a role. In the last few years there has been a rapid advance in the understanding of long-term potentiation, especially with regard to its induction mechanisms. This advance has been based mainly on work performed on pathways in the hippocampal formation but similar induction mechanisms for long-term synaptic potentiation might operate for neocortical synapses as well.

The hippocampus is necessary for early stages of memory formation

Enduring memories are stored in a stable form that survives seizures, most injuries to the brain and coma. Such memories appear to be stored, at least in part, as structural changes at specific synapses within neuronal networks that encode and connect the sensory impressions associated with each memory. These structural changes are thought to occur in the neocortex. Loss of neurones in a particular area of cortex never erases one particular set of memories but can degrade specific aspects of many memories. Thus, memories seem to be stored in a highly distributed fashion throughout many neocortical areas.

Some of the processes underlying the early stages if memory formation are more localised. For example a set of cortical structures including the entorhinal cortex, the subicullum, and the hippocampus are necessary to transform short-term declarative memories (e.g. memories of persons, places, things) into a more permanent form. The role of the hippocampus, a brain structure that lies beneath the caudal edge of the neocortex, has been thoroughly examined. Clinical studies have demonstrated that destruction of parts of the hippocampus, e.g. by ischemia, is sufficient to cause severe anterograde amnesia, an inability to form new memories.

Neuroanatomy of the hippocampus

The hippocampal formation is composed of two sheets of neurones that are highly interconnected with each other. The first sheet consists of three contiguous areas of cortex called CA fields (cornu Ammonis or Ammons' horn), the subicular complex, and the entorhinal cortex, which is continuous with the neocortex (see Figure Ia). The CA fields are often referred to as the hippocampus proper. They form a large flap of tightly packed pyramid-shaped neurones that is folded and tucked under the edge of the neocortex. The second sheet of neurones in the hippocampal formation is the dentate gyrus, which contains round, tightly packed neurones called granule cells.

In primates, the axons of pyramidal neurones from many neocortical association areas project into the entorhinal cortex. Information from these areas is relayed via a fan of axons called the perforant pathway through the subicullum and into the dentate gyrus. This cortical information is processed in the hippocampus through a network of synaptic connections that is not yet completely understood. One major part of the network, called the trisynaptic loop, has been

extensively studied *in vitro* because it is preserved in coronal thin slices of hippocampus (Figure Ia). The first segment of this loop is formed by the synapses from perforant path axons onto dentate granule cells. Axons of the granule cells, called mossy fibres, leave the dentate gyrus and make the second set of synapses on dendrites of pyramidal cells in area CA3 in the hippocampus proper. The pyramidal cells of area CA3 produce branched axons. One branch leaves the hippocampus; the other makes a loop to form synapses with dendrites of pyramidal cells in area CA1. This third projection in the trisynaptic loop is called the Schaeffer collateral pathway. Axons of the CA1 neurones project to dendrites of neurones in the subicullar complex and, to complete the circuit, these neurones send axons to the entorhinal cortex. All areas of the hippocampal formation except the dentate gyrus contain neurones that project to various other parts of the brain. The apparent flow of information from neocortical association areas, through the hippocampal formation, and back out to the rest of the brain suggests that a function of the hippocampus may be to act "linking" activity from areas of the brain encoding information from many different sensory modalities into a record of a specific object or event. Such widespread temporary associations may constitute a short-term memory, which can be slowly transformed into a permanent memory encoded in the neocortex.

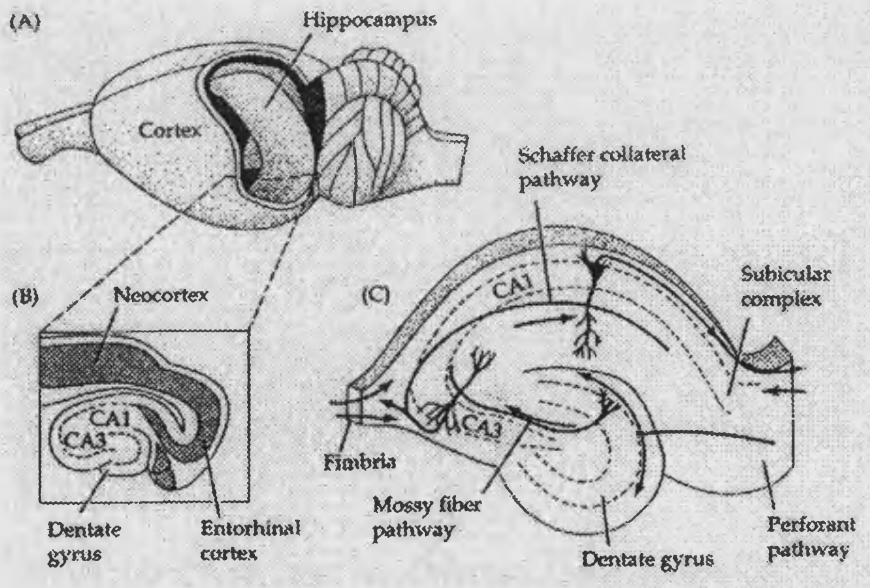

Figure Ia The hippocampal formation and the trisynaptic loop in the rat. (A) Schematic diagram of the rat brain showing the position of the hippocampal formation. The dashed line shows the position of the horizontal section shown in (B). (B) Schematic diagram of a horizontal section through the hippocampal formation and overlying neocortex. Dashed lines and shaded areas represent layers of neuronal cell bodies. In the CA fields and dentate gyrus, cell bodies are packed into narrow layers. CA1 and CA3 are areas of the hippocampus. (C) Schematic diagram of the trisynaptic circuit in a hippocampal slice. Dashed lines represent outlines of tightly packed layers of neuronal cell bodies. Areas outside the dashed lines contain axons, dendrites, and numerous synaptic contacts. Additional axons enter the hippocampus through the fimbria or through the subicular complex and entorhinal cortex (A & B from Kennedy, 1989; C from Amaral, 1987).

Afferent projections to the hippocampus include those containing acetylcholine (from the medial septum nucleus and diagonal band of Broca), noradrenaline (from nuclei in brain areas: A6 (locus coeruleus), A1, A5 & A7) 5-hydroxytryptamine (from dorsal (B7) and medial (B8) raphe nuclei), glutamate (perforant pathways, mossy fibre input, Schaffer collateral), aspartate (commisural pathway i.e. from contralateral entorhinal cortex), dopamine (from midbrain) and histamine (mainly from hypothalamus). Inhibitory GABA-containing innervation is also present (e.g. basket cells and GABAergic interneurones in CA1).

Synapses in the trisynaptic loop display LTP

A brief high-frequency train of stimuli to one of the segments of the trisynaptic loop, increases the excitatory postsynaptic potentials in the target hippocampal neurones, an increase that can last for hours *in vitro*, and *in vivo* for days and even weeks. This facilitation is called long-term potentiation (LTP). However, LTP is not produced in the same way in all three of these pathways. At glutamatergic synapses from the mossy fibres onto pyramidal neurones in area CA3, LTP can be induced only by high-frequency stimulation of presynaptic terminals. The strength of stimulation is not influenced by depolarisation of the postsynaptic membrane. This type of LTP is called homosynaptic or nonassociative, because is independent of events occurring at other, neighbouring synapses.

A second type of LTP occurs at the first and third synapses of the trisynaptic loop. In these two synapses, LTP is induced by strong, high-frequency presynaptic stimulation and also by weak stimulation that occurs at the same time that the postsynaptic membrane is depolarised, either by injection of currents or by stimulation of nearby excitatory synapses. This form of LTP is called heterosynaptic or associative LTP because stimulation of one set of synapses increases the probability that other synapses on the same neurone will be potentiated if the synapses are activated at the same time or a few milliseconds later. In brief, when glutamate is released from presynaptic terminals, as occurs during a high-frequency tetanus that induces LTP, it acts on non-NMDA ionotropic glutamate receptors depolarising the postsynaptic membrane, relieving NMDA receptors from their Mg^{2+} blockade and allowing Na^{+}, K^{+} and Ca^{2+} to flow through the NMDA channels. The resulting rise in Ca^{2+} in the dendritic spine triggers calcium-dependent kinases (calcium/calmodulin kinase and kinase C) that induce LTP. Once LTP is induced, the postsynaptic cell releases a retrograde messenger (in ways that are still not understood) that is thought to act on kinases in the presynaptic terminal to produce the sustained enhancement of transmitter release that contributes to the persistence of LTP. This second form of LTP provides a possible cellular mechanism for encoding associations between different events or sensations that happen at the same time, as is seen during formation of memories.

Hippocampal nAChR and glutamate release

For many years, the lack of specific agonists and antagonists for particular neuronal nAChR subtypes and the fast kinetics of inactivation of some of them (see Sargent, 1993; Lindstrom, 1996; Albuquerque *et al.*, 1997), limited the identification of functional nAChR in various brain areas. With the development of systems that allow fast application and removal of agonists (e.g. Radcliffe and Dani, 1998), and with the discovery of new pharmacological tools, it became possible to identify various subtypes of functional nAChR present on neurones from different brain areas, including the hippocampus (Alkondon and Albuquerque, 1993). Electrophysiological studies (Alkondon and Albuquerque, 1993) have shown that rapid exposure of ~85% of cultured hippocampal neurones to nicotinic agonists result in activation of fast-decaying currents that were named type IA currents. Type IA currents 1) are sensitive to blockade by α-Bgt, MLA or α-conotoxin-Iml, 2) show an inward rectification that depends on the intracellular level of Mg^{2+}, 3) display a rundown that can be prevented by the presence of ATP-regenerating compounds in the intracellular solution and 4) are sensitive to modulation by extracellular concentration of Ca^{2+}. Only 10% of the cultured hippocampal neurones respond to nicotinic agonists with slowly decaying currents that are sensitive to blockade by DHβE and are referred as type II, and no more than 2% of the neurones respond to such agonists with slowly decaying currents that are sensitive to blockade by mecamylamine and are referred to as type III (Alkondon and Albuquerque, 1993). The pharmacological and kinetic characteristics of type IA, type II and type III, when compared with the properties of nAChR subunit combinations ectopically expressed in *Xenopus* oocytes, suggest that they are subserved by α7 nAChR, α4β2 nAChR and α3β4 nAChR respectively (Alkondon and Albuquerque, 1993). The original classification of the nicotinic responses recorded from cultured hippocampal neurones has been recently expanded (Zoli *et al.*, 1998).

Many of the biological roles identified to date for neuronal nAChR have been associated with receptor mediated-changes in intracellular calcium (e.g. modulation of neurotransmitter release - see 1.2.2). Moreover, increasing evidence suggests that CNS nAChR are involved in cognitive processes such as learning and memory. In fact, it seems that the brain cholinergic system (Aigner and Mishkin, 1986; Dunnet and Fibiger, 1993) and the hippocampus (Squire, 1992; Bunsey and Eichenbaum, 1996 - see above) are vital "pieces" for memory processing in the mammalian CNS. Not only are nicotinic agonists able to improve cognition in experimental animals (reviewed by Stolerman *et al.*, 1995), but also the number of neuronal nAChR is markedly decreased in the cortex and hippocampus of patients with Alzheimers' disease, a pathological condition characterised by progressive neurodegeneration and cognitive impairment (reviewed by Kellar and Wonnacott, 1990; Schröder *et al.*, 1991; Maelicke and Albuquerque, 1996).

At hippocampal glutamatergic synapses, low concentrations of (-)-nicotine were found to increase the frequency of mEPSCs (Gray *et al.*, 1996; Radcliffe and Dani, 1998 - also see 1.2.2.6). In those cases, presynaptic α7-containing nAChR were capable of directly mediating a Ca^{2+} influx that initiated the enhanced glutamate release. Moreover, Radcliffe and Dani (1998) went further and demonstrated in cultured hippocampal neurones that the same information arriving along the same glutamatergic afferents is processed differently when properly timed nicotinic activity converges onto the glutamatergic presynaptic terminals. These results suggest that influencing information processing at glutamatergic synapses may be one way in which nicotinic cholinergic activity influences cognitive processes and that disruption of these nicotinic cholinergic mechanisms may contribute to deficits associated with the degeneration of cholinergic functions during e.g. Alzheimers' disease.

Section I of this thesis describes initial experimental attempts aimed to examine the involvement of rat α7 nAChR in nicotinic agonist-evoked glutamate release from hippocampus. The aim of chapter 2 was the biochemical, pharmacological and functional characterisation of native and heterologously expressed rat α7 nAChR whereas chapter 3 attempted the study of nicotinic-evoked glutamate release in rat hippocampus.

2 Heterologous expression of rat α7 nAChR

2.1 Introduction

2.1.1 Ectopic expression of nAChR subtypes

The coexistence in the same brain area (and even in the same neurone) of different nAChR subtypes makes the *in vivo* study of the properties of individual nAChR subtypes extremely difficult. That is why heterologous expression of nAChR has been extensively used, and provided much of our knowledge concerning the electrophysiological and pharmacological properties of the subtypes. Although the results from these studies may not fully represent the situation in the vertebrate brain, they at least indicate that some subunit combinations are functional whereas others are not. Such studies have been carried out in *Xenopus* oocytes and mammalian transfected cell lines.

2.1.1.1 *Xenopus* oocytes

Electrophysiological studies have demonstrated that various functional nAChR can be generated by injecting neuronal mRNAs or cDNAs encoding α2, α3 or α4 subunits in pairwise combinations with β2 or β4 subunits. The resulting nAChR subtypes have different biophysical and pharmacological properties, some of which may match those of native nAChR. When the same subunits are expressed alone, they are not capable of forming functional receptors, thus suggesting that this class of receptors can only form heteromeric receptors (reviewed by Sargent, 1993; McGehee and Role, 1995).

These heterologous studies have demonstrated that both α and β subunits determine the pharmacological and functional properties of the expressed subtype. For example the channels formed when the β2 subunit is expressed in combination with either α2, α3 or α4 subunits, differ in their average open times, single channel conductances and antagonist sensitivity. The β subunit apparently regulates the rate at which the agonists and antagonist dissociate from the subtypes, as well as the rate at which agonist-subtypes open (Papke, 1993; Papke and Heinemann, 1991; 1994).

A further complexity of the structure of nAChR is contributed by the α5 subunit. When expressed alone or with any other β subunit, α5 fails to generate functional channels. It only gives rise to a functional receptor when coexpressed with α4 and β2 subunits (chick α5 - Ramirez-Latorre *et al.*, 1996), with α3 and β2 or with α3 and β4 subunits (human α5 - Wang *et al.*, 1996; Gerzanich *et al.*, 1998). Moreover, it has been reported that α3, β2 and β4 cDNAs form heterotrimeric neuronal nAChR when coinjected into *Xenopus* oocytes. Recently, Gerzanich *et al.* (1997) showed that chicken α6 only generates detectable functional nAChR when coexpressed with the human β4 nAChR subunit.

Unlike the heteromeric nAChR expressed in oocytes, the injection of α7, α8 or α9 cDNA alone produces homomeric receptors that are activated by ACh and blocked by nanomolar concentrations of α-Bgt (Gerzanich *et al.*, 1994; Elgoyhen *et al.*, 1994).

These expression studies have demonstrated that both homomeric and heteromeric receptors share two pivotal properties: 1) they are not only permeable to monovalent cations but also to Ca^{2+} and 2) they are modulated by changes in extracellular Ca^{2+} regardless of any increase in intracellular Ca^{2+}, suggesting that neuronal nAChR play a relevant role in Ca^{2+} signalling.

2.1.1.2 Mammalian cell lines

A number of transiently and stably transfected cell lines expressing different combinations of nAChR subunits have been recently created and used to characterise the pharmacology and functional properties of the possible subtypes present in neurones. The chick and rat α4β2 nAChR subtype have been stably transfected in M10 (Whiting *et al.*, 1991) and HEK-293 cells (Gopalakrishnan *et al.*, 1996). The rat α3β4 subunit combination, which is thought to represent a ganglionic subtype, have been transiently (Wong *et al.*, 1995) and stably (Stetzer *et al.*, 1996) transfected in HEK-293 cells. Moreover, Eusebi and colleagues have successfully used the human cell line BOSC 23 to transiently express an interesting variety of subunit combinations: human and rat α3β4, chick α3β2, α4β2, α4β4, α7, α8, α3β4α5, α6β2, α6β4 and α3β4α6 (Ragozzino *et al.*, 1997; Fucile *et al.*, 1997; 1998). Recently, Forsayeth and Kobrin (1997) reported the assembly of β3 into a functional receptor of probable stoichiometry $(\alpha4)_2\beta2\beta3\beta4$ upon transfection in COS cells. The α7 nAChR subunit has been stably expressed in the following mammalian cell lines: SH-SY5Y (Puchacz *et al.*, 1994), HEK-293 (Gopalakrishnan *et al.*, 1995); GH_4C_1 (Quick *et al.*, 1996) and QT6 (Kassner and Berg, 1997).

2.1.2 A neuronal LGIC that binds α-Bgt: the α7 nAChR.

Studies performed in 1985 by Raftery and colleagues with α-Bgt binding proteins affinity-purified from chick brain, generated four partial amino-acid sequences. Only the N-terminal region of one of them revealed homology to nAChR (Conti-Tronconi *et al.*, 1985). Using an oligonucleotide probe corresponding to this N-terminal protein sequence (Conti-Tronconi *et al.*, 1985), Lindstom and colleagues identified a cDNA for a subunit that they originally named α-Bgt binding protein α1 (Schoepfer *et al.*, 1990 - subsequently named the α7 subunit by Couturier *et al.*, 1990). This cDNA sequence was in turn used to identify another cDNA from chicken brain that exhibited a very similar sequence (82% similarity as determined by Schoepfer *et al.*, 1990) and encoded the α-Bgt binding protein α2, later renamed as the α8 nAChR subunit. Since then, α7 has also been cloned from rat (Séguéla *et al.*, 1993), human (Doucette-Stamm, 1993; Peng *et al.*, 1994; Chini *et al.*, 1994)

and mouse (Orr-Urtreger *et al.*, 1995). The α7 and α8 subunits are homologous in sequence to, but about equally distinct from, muscle α1 and neuronal α2-α6 (Schoepfer *et al.*, 1990). The α8 protein has not yet been found in other species, but while searching for it in rats, α9 was discovered (Elgoyhen *et al.*, 1994). In 1990, Ballivet and coworkers first reported that α7, when expressed in *Xenopus* oocytes, was capable of forming functional homomeric nAChR which were blocked by α-Bgt (IC_{50}= 0.7 nM - Couturier *et al.*, 1990; Eiselé *et al.*, 1993).

2.1.3 Is the wild type α7 nAChR an homomer?

There is no doubt that the α-Bgt sensitivity of (-)-nicotine-evoked responses in *Xenopus* oocytes injected with α7 (this study Figure), are of the purely homomeric rat α7 nAChR. In the initial instance, when the chicken α7 subunit gene was cloned and expressed (Couturier *et al.*, 1990), control studies were performed to evaluate a possible interference of nAChR α-like subunits that might be endogenously expressed in the oocytes (Buller and White, 1990; Hartman and Claudio, 1990). To check this possibility, oocytes were injected with equimolar mixtures of muscle β, γ and δ cDNAs or with β2, β3, or β4 cDNAs. All such oocytes failed to respond to ACh (100 µM), conversely α1β1γδ and α4β2 combinations were responsive when challenged with 1 µM ACh. Similarly, expression of the α7 cDNA coinjected with other neuronal nicotinic subunits known to be expressed in PC12 cells (α3, α5, β2 or β4), did not lead to the formation of receptors pharmacologically distinct from α7 alone (Séguéla *et al*, 1993). Supporting this view, it was also found that the current recorded was only proportional to the amount of α7 mRNA or cDNA injected and was not proportional to the total amount of message injected (Séguéla *et al.*, 1993).

Anand *et al.* (1993) used sucrose gradient sedimentation analysis to compare chicken α7 protein expressed in *Xenopus* oocytes and native detergent-solubilised brain α7 nAChR. All the [^{125}I]-α-Bgt labelled receptors cosedimented at ~10S implying a common size and "shape". By immunoisolating [^{35}S]-methionine labeled α7 subunits it was also demonstrated that the α7 subunits do not appear to assemble with endogenous *Xenopus* nAChR subunits (assuming that the oocyte does not express subunits (known or unknown) with the size and "shape" of α7). The same study revealed subtle pharmacological differences between native chick brain nAChR containing the α7 gene product and those resulting from heterologous expression of the chick α7 gene in *Xenopus* oocytes, and the differences were cited as evidence that the native receptors are heteromeric (Anand *et al.*, 1993). A study by Keyser *et al.* (1993) supported this observation. They immunoprecipitated three subtypes of α-Bgt-binding nAChR from extracts of chick brain and retina: 1) homomeric α7 nAChR (predominant in chick brain), 2) homomeric α8 nAChR (predominant in chick retina) and 3) α7α8 nAChR, a minor subtype in both brain and retina.

The first report of heterologous expression of α7-containing heteromeric nAChR was published by Helekar *et al.* (1994). They demonstrated that the rat α7 is capable of coassembling with muscle nAChR subunits under certain particular conditions when coexpressed in *Xenopus* oocytes. Recently, and using an approach similar to that used by Anand (Anand *et al.*, 1993), Marika Quik *et al.* (1996) compared the properties of rat α-Bgt-binding sites stably expressed in the pituitary cell line GH_4C_1 with those present in rat brain membranes. Their studies showed that the pharmacological properties, molecular size and regulation of stably expressed rat brain α-Bgt binding sites in α7-GH_4C_1 cells, closely resemble those of native rat brain receptors. Finally, they suggested that rat brain α-Bgt receptors are homomeric or, if these receptors are heteromeric, that at least the α7 subunit is a key element in determining this receptor properties.

However, the first studies reporting native α7 heteromeric nAChR came from Lorna Role's lab (Yu and Role, 1998a; 1998b). They presented evidence that in embryonic chick sympathetic neurones, the α7 subunit contributes to the function of at least three subtypes of native nAChR that differ from each other in their sensitivity to block by α-Bgt and MLA. Also in Cuevas and Berg (1998) it is suggested that the particular features (e.g. slow desensitisation and reversible α-Bgt blockade) of a α7-containing nAChR found in intracardiac ganglia could be due to the presence of non-α7 subunits in the pentamer.

2.1.4 Channel properties of the α7 nAChR

The ion channel properties of the α7 nAChR could be summarised by 1) high permeability to Ca^{2+}, 2) rapid desensitisation and 3) strong inward rectification. The α7 nAChR has an unusual high permeability to calcium compared to other nAChR subtypes (Vijayaraghavan *et al.*, 1992; Rathouz *et al.*, 1996; Delbono *et al.*, 1997) and they are at least as selective for Ca^{2+} as are NMDA channels (Séguéla *et al.*, 1993). By replacing all extracellular cations with 200 mM sucrose and leaving 1.8 mM $CaCl_2$ in the bathing solution, Lindstrom (1995) showed that the fraction of current carried by Ca^{2+} for α7, α4β2 and muscle nAChR expressed in oocytes is: 11%, 3% and 1%, respectively. The kinetic behaviour of neuronal nAChR is also modulated by external Ca^{2+} (Vernino *et al.*, 1992). In contrast to the muscle receptor where external Ca^{2+} decreases the current carried by monovalent cations, in neuronal nAChR ACh-induced currents increase as the extracellular Ca^{2+} concentration increases (Vernino *et al.*, 1992). Recently, the α7 nAChR in particular has been shown to be sensitive to changes in the $[Ca^{2+}]_o$. Extracellular Ca^{2+} modulates the affinity of the α7 nAChR for ACh, the cooperativity between ACh-binding sites, as well as the inward rectification and the decay and rundown of α7 nAChR mediated type IA currents (Bonfante-Cabarcas *et al.*, 1996; Albuquerque *et al.*, 1997). Both the rapid desensitisation and the inward rectification combine to minimise sustained influx

through these nAChR. These self-limiting features are specially interesting when considering the possible functional roles of such nAChR.

2.1.5 Functional role of α-Bgt-sensitive nAChR

The α7 nAChR have been histologically localised by binding of labelled α-Bgt (Clarke *et al.*, 1985), mAbs (Britto *et al.*, 1992; Keyser *et al.*, 1993; Dominguez del Toro *et al.*, 1994) and *in situ* hybridisation (Séguéla *et al.*, 1993). In rat brain, α7-containing nAChR, or [^{125}I]-α-Bgt binding sites, have been found at relatively moderate to high density in many regions, including olfactory regions, the hippocampus, the amygdala, the hipothalamus and the cerebral cortex (Clarke *et al.*, 1985; Séguéla *et al.*, 1993; Alkondon *et al.*, 1996).

Despite morphological, biochemical, and electrophysiological analysis, the functions of neuronal α-Bgt binding sites and nAChR in the mammalian brain remain largely unknown. Various neuronal nAChR are involved in nicotine addiction (Dani and Heinemann, 1996), and there is evidence that nicotine can improve attention, rapid information processing and working memory (Levin, 1992; Ohno *et al.*, 1993; Piccioto *et al.*, 1995; McGehee and Role, 1996). Cholinergic mechanisms may be involved in neurobehavioural disorders including seizures and schizophrenia (Steinlein *et al.*, 1995; Freedman *et al.*, 1997). A locus for juvenile myoclonic epilepsy is mapped near the α7 gene in humans (Elmslie *et al.*, 1997). Some functions attributed to the α-Bgt sites and/or the α7 subunit include synapse formation/modulation of neurite outgrowth (Fuchs, 1989, Pugh and Berg, 1994; Broide *et al.*, 1995), mediation of (-)-nicotine-induced seizures (Miner and Collins, 1989; Stitzel *et al.*, 1997), control of synthesis and/or release of neurotrophins, regulation of early genes (e.g c-fos) transcript levels (Greenberg *et al.*, 1986), activation of second messengers (e.g. Vijayaraghavan *et al.*, 1995), presynaptic modulation of neurotransmitter release (e.g. McGehee *et al.*, 1995; Gray *et al.*, 1996; Radcliffe and Dani, 1998) as well as mediation of synaptic transmission (e.g. Alkondon *et al.*, 1997; Frazier *et al.*, 1998a).

The main objective of chapter 2 was to compare the pharmacological and functional properties of homomeric rat α7 nAChR heterologously expressed in mammalian cell lines with those of native α-Bgt-sensitive nAChR. This chapter presents these attempts to heterologously express the rat α7 nAChR in a non-neuronal mammalian cell line.

2.2 Experimental procedures

2.2.1 Molecular biology: subcloning the rat α7 cDNA into the pCDNA3 plasmid

2.2.1.1 Source of the rat α7 nAChR gene

The rat α7 nAChR cDNA, cloned by Séguéla *et al.* (1993), was generously provided in the pSM vector by Dr Jim Patrick (Baylor College of Medicine - Houston, TX USA).

2.2.1.2 Preparation and transformation of competent *Escherichia coli*

A single *E.coli* (strain XL1-Blue) colony forming unit (cfu) was picked from an agar plate (15 g bacto-agar (Sigma - Poole, Dorset UK) / l Luria-Bertani broth (LB: 10 g NaCl, 5 g yeast extract (Sigma), 10 g tryptone (Sigma) in 1 l sterile water, pH 7.5)) freshly grown overnight at 37°C and transferred into 100 ml LB. The culture was incubated for 3 h at 37°C with vigorous shaking (300 cycles / min in a rotary shaker). Under sterile conditions, the cells were transferred to ice-cold 50 ml polypropylene tubes and kept on ice for 10 min. Cells were pelleted by centrifugation at 4000 rpm for 10 min at 4°C and the supernatant fraction was discarded. Each pellet was washed with 10 ml ice-cold 0.1 M $CaCl_2$ (in sterile water, pH 8.0) and resuspended in 2 ml ice-cold 0.1 M $CaCl_2$ for each 50 ml of original culture. The cell suspension was retained on ice for at least 1 h. Then competent cells, 200 µl of each suspension, were transferred to sterile 1.5 ml E-cups. The pSMα7 plasmid incorporating the rat α7 cDNA (in sterile water) was mixed (~10 ng / µl) with this solution of permeabilised cells (4°C, 30 min). The reaction mixture was then placed in a 42°C water bath for 3 min. Immediately after, LB (1 ml) was added and the E-cups incubated on ice for 2 min. Cells were then maintained at 37°C for 1 h with occasional gentle mixing.

Successful transformants were selected by their resistance to ampicillin (Sigma). The ampicillin-resistance gene is included in the pSM plasmid. Bacterial cells treated as above were spread on selective agar plates media (containing 100 µg ampicillin / ml), inverted and maintained at 37°C (12-16 h). Plates were stored at 4°C. Resistant cfu were picked and inoculated into ampicillin-containing LB (one cfu per vial containing 3 ml LB + 100 µg ampicillin / ml) and these bacterial suspensions incubated overnight in a shaker at 37°C.

2.2.1.3 Preparation of bacteria glycerol stocks

Bacteria (transformed or not) were stored at for up to 1 year in cultures containing glycerol. Bacteria glycerol stocks were prepared by adding to 0.50 ml of bacterial culture 0.50 ml of sterile glycerol (Sigma - Poole, Dorset UK). After vortexing the tube to ensure that the glycerol was evenly dispersed, the culture was frozen in ethanol-dry ice and transferred to -80°C for long term storage.

2.2.1.4 Alkaline lysis miniprep

Transformed cells from a single bacterial colony were inoculated into 5 ml ampicillin-containing LB (100 µg antibiotic / ml LB) and grown to saturation at 37°C with vigorous shaking (overnight). The bacterial suspension (1.5 ml) was harvested by centrifugation at 8000 rpm for 5 min at 4°C. The supernatant was discarded. The pellet was resuspended in 100 µl TE (10 mM Tris.Cl (Sigma - Poole, Dorset UK), 1 mM EDTA (Sigma), pH 7.8), and kept at room temperature for ~5 min. Then, 200 µl NaOH / SDS solution (0.2 M NaOH, 1 % (w/v) SDS (Sigma)) was added, the tube content gently mixed and kept on ice for 5 min. Addition of 150 µl ice-cold 5M potassium acetate (pH 4.8 in 3M acetic acid) and thorough inversion precipitated the larger cell remnants (4°C, 10 min).

Chromosomal DNA and cell debris were spun down at high speed (13000 rpm, 4°C, 20 min) leaving the plasmid DNA in the supernatant. Plasmid DNA was recovered by precipitation with absolute ethanol (2 vol, -70°C for 20 min), spun down (13000 rpm, 4°C, 60 min) and the pellet washed with ice-cold 70 % ethanol (aq.) before eventually being dried and redissolved in 50 µl sterile water.

A commercially available kit (Promega's Wizard Miniprep DNA purification system - Madison, WI USA) was also used to perform small-scale plasmid DNA purifications (LB culture volume: 1-3 ml - Expected DNA yield: 1 - 10 µg).

2.2.1.5 DNA digestion with restriction enzymes

The rat α7 sequence was originally inserted into the EcoRI restriction site of the multiple cloning site of the pSM plasmid (Baylor College of Medicine - Houston TX USA). Digestion with this enzyme should yield two fragments of lengths ~1.9 Kb and ~3.0 Kb corresponding to the rat α7 cDNA and the pSM plasmid, respectively. pSMα7 DNA (5 µl: 4 µg DNA) was mixed with EcoRI restriction enzyme (1µl (10 units) - Promega, Madison, WI USA), the appropriate buffer (2µl 10X buffer H - Promega) and made up to 20 µl with sterile water. The reaction was incubated at 37°C for 2 h and stopped by heating it at 70°C for 20 min. Fragmented DNA was extracted with phenol : chloroform : isoamyl alcohol. In brief, an equal volume of phenol : chloroform : isoamyl alcohol (25:24:1) was added to the nucleic acid sample. To separate the organic and the aqueous phases, the mixture was centrifuged at 13000 rpm for 1 min. The aqueous phase was transferred to a fresh tube. An equal volume of chloroform was added and the aqueous phase recovered after centrifugation (13000 rpm for 1 min). Nuclei acids were precipitated by adding 3 M sodium acetate pH 5.4 (0.1 vol), cold absolute ethanol (2.0 vol) and further cooling at -70°C for 20 min. Precipitate was centrifuged (13000 rpm, 4°C, 60 min) and the pellet washed in ice-cold 70 % ethanol (aq.) before being dried and redissolved in sterile water (50 µl).

2.2.1.6 Agarose gel electrophoresis

Digested DNA (5µl) was added to 1 µl Gel Loading Buffer (GLB: 30 % glycerol (v/v) (Sigma - Poole, Dorset UK), 0.25 % xylene cyanol (v/v) (Sigma), 0.25 % bromophenol blue (v/v) (Sigma)) and run on a 1 % agarose (Sigma), gel along with 1 Kb DNA ladder (Gibco BRL Life Technologies - Paisley, Scotland) at 15 V / cm for 30 min. Gel running buffer, TBE (89 mM Tris.Cl (Sigma), 89 mM borax (Sigma), 2 mM EDTA (Sigma)), included ethidium bromide (0.5 µg / ml - Sigma). Bands were visualised using a UV transilluminator and results documented on Polaroid film Type 667 (Sigma).

2.2.1.7 Large-scale plasmid DNA purification: maxi preps

A commercially available system, QIAfilter Plasmid Maxi Kit (Qiagen - Dorking, Surrey UK), was used to perform large-scale plasmid DNA purifications (LB culture volume: 100 ml - Expected DNA yield: 300-500 µg).

2.2.1.8 Dephosphorylation of linearised pCDNA3 plasmid DNA

The pCDNA3 plasmid (Invitrogen - San Diego, CA USA) was linearized (~5.4 Kb) with EcoRI (Promega - Madison, WI USA). The entire coding sequence for the rat α7 nAChR subunit (~1.9 Kb) was excised from the plasmid pSMα7 (~4.9 Kb) with the same restriction enzyme (see 2.2.1.5). The α7 sequence (~2.3 µg DNA) was extracted from a preparative agarose gel (0.8 %, TBE) with the Sephaglas Bandprep Kit (Pharmacia Biotech - Uppsala, Sweden) and resuspended in 60 µl TE buffer.

Calf intestinal alkaline phosphatase (CIP) was used to remove 5'-phosphate groups from linear pCDNA3. After addition of 4.5 µl CIP dephosphorylation buffer (10X) and 1 µl CIP (1 U - Boehringer Mannheim - Lewes, East Sussex UK) to 40 µl (~1.5 µg) linear pCDNA3, the mixture was incubated for 30 min at 37°C. At the end of the incubation period, the CIP was inactivated by heating to 75°C for 10 min in the presence of 5 mM EDTA (pH 8.0 - Sigma - Poole, Dorset UK).

Dephosphorylated pCDNA3 was purified by extraction with phenol : chloroform : isoamyl alcohol followed be ethanol precipitation (see 2.2.1.5). DNA was finally redissolved in 10 µl sterile water.

2.2.1.9 Ligation

Rat α7 DNA was mixed with dephosphorylated linear pCDNA3 to a final molar ratio of 1.9. After addition of bacteriophage T4 DNA ligase buffer (10X - Promega - Madison, WI USA), bacteriophage T4 DNA ligase (0.1 Weiss unit - Promega) and sterile water to a final volume of 20 µl, the reaction mixture was incubated at 16°C overnight. The reaction product (1-2 µl) was used to transform competent *E.coli* as described in 2.2.1.2. Two control reactions containing only 1) the vector or 2) α7, were also set up.

2.2.1.10 Spectrophotometric determination of nucleic acid concentration and purity

DNA concentration and purity was determined using an Unicam Helios Gamma spectrophotometer (Unicam Ltd. - Cambridge, UK). The optical density (OD) at wavelength (λ) = 260 nm and λ = 280 nm was measured for dilutions of the plasmid DNA solution following standardisation with sterile water. A complete scan was performed between λ = 240 -320 nm. The OD_{260} / OD_{280} ratio was used to determine the purity of the DNA product. Pure preparations of DNA had a ratio between 1.8 and 2.0, contaminants significantly reduced this value. An OD of 1.0 at λ = 260 nm corresponds to ~50 µg / ml for double-stranded DNA.

2.2.2 Electrophysiology of the homomeric rat α7 nAChR expressed in *Xenopus* oocytes

Preparation of *Xenopus laevis* oocytes, injection with receptor cDNA, and measurement of α7 nAChR responses using two-electrode voltage-clamp have been previously described (Bertrand *et al.*, 1992; Séguéla *et al.*, 1993).

2.2.2.1 *Xenopus* oocyte preparation

2.2.2.1.1 Animals and removal of oocytes

Adult *Xenopus laevis.* females (*Xenopus* Ltd. - Nutfield Ridge, Surrey UK) were kept in groups of up to eight animals for at least 3 months in a 12 h light : dark cycle at 18°C with access to diced heart or liver on alternate days. Removal of oocytes was carried out under Home Office Project License PPL 30/1551 by Mr Ewan Basterfield who holds a Personal License PIL 30/69 covering this procedure. Briefly, on the day of use, a frog was anesthesized by immersion in a 0.15 % tricaine solution (w/v - Sigma - Poole, Dorset UK) at room temperature for 60 min. Successful anesthesia was indicated by lack of response to an abdominal pinch. The anesthesized frog was then placed ventral side up on an ice bed and a small incision (0.5-1.0cm) was made in the lower abdomen. An ovarian lobe was pulled out through the incision, sutured to prevent internal bleeding and removed into SOS (100 mM NaCl, 2 mM KCl, 1.8 mM $CaCl_2$, 1 mM $MgCl_2$, 5 mM Hepes (Sigma), pH 7.6) at room temperature. Then the frog was sutured and returned to fresh water. After several weeks the frogs were fully recovered and were reused once and killed by a Schedule 1 method. All procedures were carried out under sterile conditions.

2.2.2.1.2 Oocyte isolation

Removal of the follicular layer was performed by incubation with collagenase type IA (Sigma - Poole, Dorset UK) followed by manual removal of the partially degraded tissue. The ovarian lobe was divided into clumps of 10-20 oocytes, transferred to a solution of collagenase (2 mg/ml) in SOS and incubated at 18°C until the follicular layer was completely removed (90 - 120 min). Oocytes used were at stage V or VI of development, characterised by a distinctive boundary between animal and vegetal poles, uniform coloration within each pole, and were ~1mm in diameter, spherical with intact membranes. Oocytes dissected in this way were generally washed at least five times in SOS and left overnight at 18°C to identified damaged eggs which were apparent as ruptured cells by the following morning. Approximately three times the number of cells to be injected were routinely isolated in order to compensate for such loses and to provide sufficient controls.

2.2.2.2 Oocytes: nuclear injection of α7 cDNA

The rat α7 subcloning procedure into the pCDNA3 plasmid was detailed in 2.2.1. Samples of pCDNA3α7 were stored at -20°C and thawed on the day of use before dilution in sterile water to a final concentration of 250 ng / µl. Injection needles were pulled on a 763 programmable micropipette puller (Campden Instruments - Loughborough, UK) using 3.5" borosilicate capillaries (10 µl - Drummond Sci.Co. - Broomall, PA USA). Tip diameters were typically <10µm. Needles were sealed with mineral oil and cDNA (total volume ~2µl) was drawn slowly into the needle using a "Nanoject variable" automatic injector (Drummond) secured to a micromanipulator. Approximately 14 nl (c. 10^8 copies of plasmid DNA) were injected into the oocyte nucleus under binocular magnification.

2.2.2.3 Oocyte incubation

Injected oocytes were transferred to 96 well titre plates, 1 oocyte per well containing 250 µl Incubation SOS (SOS containing 50 IU penicillin / ml - 50 µg streptomycin / ml (Gibco BRL Life Technologies Ltd. - Paisley, Scotland) and 50 µg gentamicin (Sigma - Poole, Dorset UK) / ml; 2.5 mM pyruvic acid (Sigma)) and incubated at 18°C under sterile conditions. Functional receptors (as judged by (-)-nicotine-induced responses) appeared in the oocyte membrane about two days after nuclear injection of cDNA. Incubation medium was replaced every 2-3 days.

2.2.2.4 Whole cell electrophysiology of injected oocytes

2.2.2.4.1 Perfusion chamber

A small volume chamber was used for the application of (-)-nicotine (Sigma - Poole, Dorset UK) during electrophysiological recording of α7 responses. In this setup, the bath volume was 300 µl and the chamber consisted of a plastic groove with a small recess in which the oocyte was placed (Figure 2.**Error! Unknown switch argument.**). Rapid solution exchange was achieved through the close proximity of perfusion inlet and outlet to the oocyte.
The superfusion was based on gravity flow. Drug solutions and perfusion medium (SOS containing 0.5 µM atropine (Sigma), 100 µM fluflenamic acid (Sigma) and 100 µM niflumic acid (Sigma)) were placed above the level of the recording chamber. They were connected to the chamber via continuous siliconized rubber tubing. Switching between reservoirs of the drugs and perfusion solution was achieved using a manually operated pinch-valve system. The dead volume between reservoirs and chamber was kept to a minimum and no mixing between solutions was possible. The outlet from the chamber was a polyethylene tube leading to a trap connected to a vacuum pump.

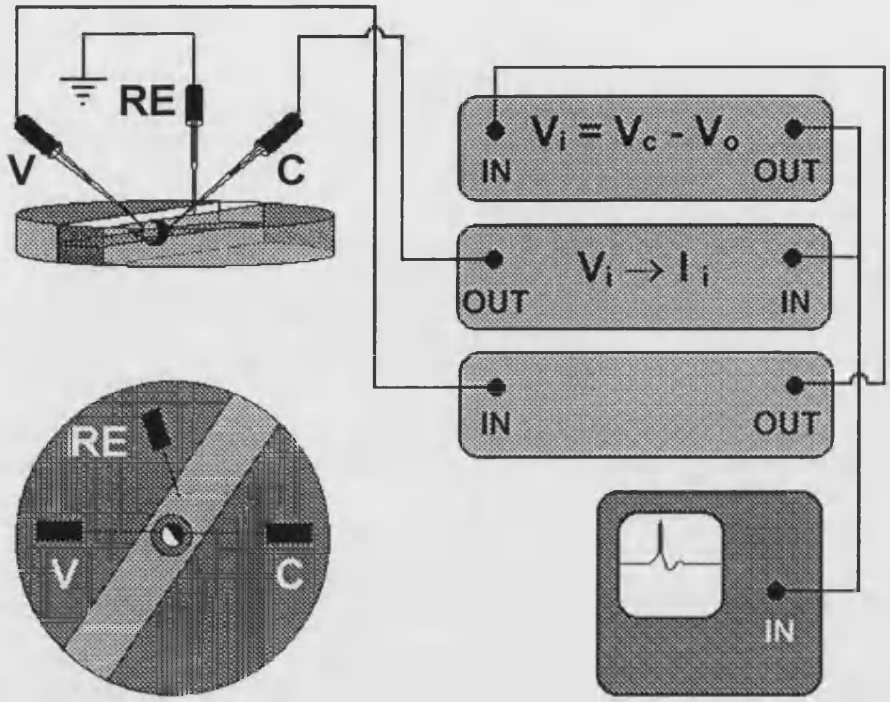

Figure 2. Error! Unknown switch argument.. **Schematic diagram of a voltage-clamp recording apparatus.** In a voltage clamp experiment one controls the membrane potential and measures the transmembrane current required to maintain that voltage. The oocyte membrane potential is monitored by the recording electrode (**V**). A reference electrode (**RE**) is also connected to a subtractor amplifier (not shown) where the value of the reference electrode is subtracted from that of the recording one ($\mathbf{V_o = V - R}$). The subtractor amplifier is connected to the VF-102 amplifier (Biologic). The output of this device is fed into the CA-100 clamping amplifier (Biologic) which compares V_o to the command voltage (V_c). The difference between these two values ($\mathbf{V_i = V_c - V_o}$) is then converted by the VF-180 amplifier into a current ($\mathbf{V_i \rightarrow I_i}$) that is fed to the current-injecting electrode (**C**). V_i is monitored on an oscilloscope.

2.2.2.4.2 Dual electrode voltage-clamp electrophysiology

Current, voltage and reference electrodes were pulled on a 763 programmable micropipette puller (Camden Instruments - Loughborough, UK) using borosilicate glass capillaries with inner filament (Clark Electromedical Instruments - Reading, UK) and filled with 3M KCl. Electrical connection to the recording equipment was established through silver chloride wire insulated with Teflon. Typical electrode tip resistances were 2-3 MΩ, i.e. small enough to inject current effectively and minimize damage to the oocyte.

Ligand-induced currents were measured using conventional two-electrode voltage-clamp (Figure 2.1). The resting potential of the cell was measured using a recording (Voltage: V) electrode connected to the input of a VF-102 dual microelectrode amplifier (Biologic - Claix France). A second (Reference: RE) electrode was connected to a subtractor

amplifier where the value of the reference was subtracted from that of the Voltage. This signal was fed into a CA-100 clamping amplifier (Biologic) and was used to set the required current to be injected into the oocyte to attain the desired holding potential. The output of the CA-100 amplifier was the input of the VF-180 microelectrode amplifier (Biologic) to which a third (Current: C) electrode was connected. The CA-100 amplifier output was monitored on an oscilloscope and also captured and stored on a DTR-1200 analogue-to-digital DAT recorder (Biologic) and on chart paper.

For data acquisition, recordings were selected from the DAT tape and fed into an AT486 IBM compatible PC. They were acquired using an AT-MIO-16DL adapter board (National Instruments Corp. - Austin, TX USA) controlled through the application programming interface "NI-DAQ software" version 4.4 (National Instruments Corp. - Austin, TX USA). The resulting 12-bit binary files were then plotted and analysed using Sigma Plot for Windows version 2.0 (Jandel Scientific - Germany).

2.2.2.4.3 Drugs and their application

All the solutions were prepared on day of use. To allow nAChR recovery from desensitisation, oocytes expressing the α7 nAChR were washed in SOS for a minimum of 5 min between agonist applications (3 s 200 μM (-)-nicotine – Figure 2.6). For inhibition studies with α-bungarotoxin (40 nM - Sigma), the antagonist was incubated with the oocyte in the chamber for a period of 30 min before stimulation with (-)-nicotine. In order that antagonist would not be washed off during agonist perfusion, the same concentration of the antagonist was included in the agonist solution pulse (3 s).

2.2.2.4.4 Current-voltage (I-V) relationships

The I-V characteristics for currents evoked by (-)-nicotine (200 μM - Sigma - Poole, Dorset UK) were determined by holding the membrane potential at a constant voltage and perfusing agonist to evoke a response. The holding membrane potential was then stepped to new values and the drug applied to each step. A wash period of 10 min was allowed between each 3 s (-)-nicotine pulse. The I-V curve was obtained by plotting the amplitude of the ligand-evoked currents as a function of the holding potential.

2.2.2.4.5 Data handling

The rat α7 I-V curve was constructed by normalising currents from an specific oocyte to the largest current evoked by (-)-nicotine (200 μM - Sigma - Poole, Dorset UK). The amplitude of the currents was determined by comparison with the amplitude of control pulses (1 μA/V) injected into the CA-100 amplifier using a Digitimer Isolated Stimulator DS2A (Digitimer Ltd. - Hertfordshire UK).

2.2.3 Primary culture of E18 hippocampal neurones

High-density hippocampal neuronal cultures were prepared from E18 Sprague-Dawley rat foetuses (University of Bath Animal House) as previously described (Goslin *et al.*, 1991; Barrantes *et al.*, 1995). Hippocampi were dissociated and plated in polyethylenimine (PEI)-coated dishes (50 μg PEI (Sigma - Poole, Dorset UK) / ml borate buffer pH 8.3) at a plating density of ~1.5 x 10^5 cells / cm^2 in 10 % foetal calf serum supplemented chemically defined medium (Dulbecco's Modification Eagle's Medium : Ham's F12 medium = 3 : 1 (ICN Biomedicals Inc. - Costa Mesa, CA USA), supplemented with: 100 μg / ml human transferrin (Sigma); 100 μM putrescine (Sigma); 5 μg insulin (Sigma) / ml; 20 nM progesterone (Sigma); 30 nM sodium selenite (Sigma); 2 mM L-glutamine (Gibco BRL Life Technologies Ltd. - Paisley, Scotland); 100 IU penicillin / ml and 100 μg streptomycin / ml (Gibco BRL Life Technologies Ltd.)). After two hours to allow cell attachment, the original medium was replaced with serum free chemically defined medium. This two step procedure resulted in viable cultures of neurons with low glial contamination (Barrantes *et al.*, 1995).

2.2.4 Heterologous expression of rat α7 in mammalian cell lines

2.2.4.1 Cell culture of mammalian cell lines

Human embryonic kidney 293 cells (ECACC No. 85120602 - Salisbury, Wiltshire UK) were grown in Dulbecco's modified Eagle's medium (ICN Biomedicals Inc. - Costa Mesa, CA USA) supplemented with 10 % foetal bovine serum (Gibco BRL Life Technologies Ltd. - Paisley, Scotland), 2 mM L-glutamine (Gibco BRL Life Technologies Ltd.), 1x non essential amino acids (ICN Biomedicals Inc.), 100 units penicillin / ml and 100 μg streptomycin / ml (Gibco BRL Life Technologies Ltd.) in a humidified atmosphere containing 5 % CO_2 at 37°C.

SH-SY5Y cells (ECACC No. 94030304 - Salisbury, Wiltshire UK) were grown in a 1:1 mixture of Ham's F12 medium (ICN Biomedicals Inc.) and Dulbecco's Modified Eagle's Medium supplemented with 15 % foetal bovine serum, 2 mM L-glutamine, 1x non essential amino acids, 100 units penicillin / ml and 100 μg streptomycin / ml, in a humidified atmosphere containing 5 % CO_2 at 37°C.

2.2.4.2 Lipotransfection of mammalian cell lines with pCDNA3α7

In brief, the entire coding sequence was excised from the plasmid pSMα7 with EcoRI (Promega - Madison, WI USA) and ligated into the EcoRI site of the expression vector pCDNA3 (Invitrogen - San Diego, CA USA) containing the constitutive human cytomegalovirus promoter to obtain the plasmid pCDNA3α7 (see 2.2.1).

HEK-293 (Harrison *et al.*, 1977; Graham *et al.*, 1977) and SH-SY5Y (Biedler *et al.*, 1973; Ross *et al.*, 1983) cells were transfected using the lipofectAMINE reagent (Gibco BRL Life Technologies Ltd. - Paisley, Scotland) as previously described by Gopalakrishnan *et al.* (1995), with some modifications that bore in mind the manufacturer's suggested protocol. The transfection conditions for the HEK-293 cell line were optimised (ratio pCDNA3α7 (μg) : lipofectAMINE reagent (μg); time of complex DNA-lipid formation; hours of incubation (cells + complex DNA-lipid); cell confluency; days of expression; presence of d-tubocurarine (dTC - Sigma - Poole, Dorset UK) in the medium).

Briefly, pCDNA3α7 (1.5 μg) was mixed with 20 μg of lipofectAMINE in serum free medium (transfection medium) at room temperature (30 min) to allow complex DNA - lipid formation. This complex was used to transfect cells previously grown to e.g. 30 - 40 % confluency. After 6 hours of incubation with this suspension, 20 % serum supplemented medium was added. Control HEK-293 cells (geneticin sensitive) were prepared by incubation with lipofectAMINE only. Twenty-four hours later, the cells were split 1:5. The basic transfection procedures are shown in Figure 2.2.

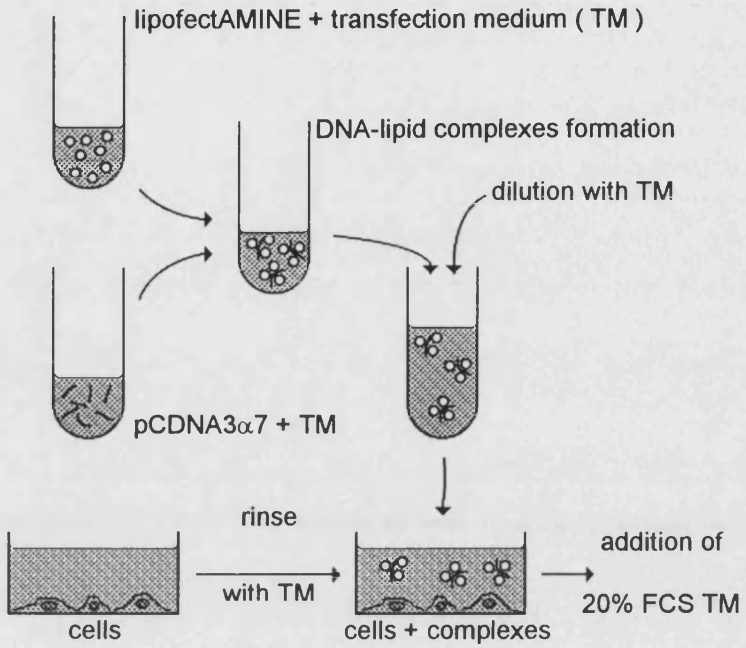

Figure 2.2 Diagram of lipotransfection procedure. For transient expression of DNA in the nucleus, plasmid DNA (e.g. pCDNA3α7) is complexed with a liposome suspension (e.g. lipofectAMINE) in serum-free medium (transfection medium: TM). These DNA-liposome complexes are added directly to cells grown in tissue culture plates and after 4-6 hours incubation period, fresh medium containing serum (20% FCS TM) is added. The cells are incubated to allow expression of the rat α7 gene and assayed. Stable transformation of mammalian cells using liposome-mediated transfection is similar to the protocol for transient expression except that after recovery from transfection, the cells are grown in selection medium (+ antibiotic) for expression of the desired marker (e.g. geneticin-resistance gene).

Transient and stable transfections were carried out. In transient transfections, 2+ days after treating the cells with the DNA - lipid complex, the cells were assayed for [^{125}I]-α-Bgt binding. In stable transfections, the transfected cells were cultured in selection medium (containing 500 μg geneticin (Sigma) / ml) to select for resistant clones. The purpose of this selection was to isolate those cells that had incorporated the genes (protein gene and resistance gene, or at least the latter) into their genomes. In several experiments, the medium was also supplemented with 10 μM d-tubocurarine (dTC). After 2-3 weeks, control HEK-293 cells were dead and geneticin-resistant clones were picked at random using the dilution or cloning-ring technique. When confluent, geneticin-resistant cells were assayed for rat α7 mRNA and α-Bgt binding sites.

2.2.4.3 RT-PCR: detection of α7 mRNA

Total cellular RNA was isolated from untransfected and transfected cells using a commercially available kit: Rneasy (Qiagen - Dorking, Surrey UK). The yield of total RNA was determined spectrophotometrically at λ = 260 nm (1 OD_{260} = 40 µg single-stranded RNA / ml). Pure RNA exhibited OD_{260} / OD_{280} ratios of or close to 2.0. The integrity of the purified RNA was tested by denaturing agarose gel electrophoresis (0.66M formaldehyde 0.8% agarose, 0.24 - 9.46 Kb RNA ladder (Gibco BRL Life Technologies Ltd. - Paisley, Scotland)). When resolved by this electrophoretic method, the 28S and 18S eukaryotic ribosomal RNAs exhibited a near 2:1 ratio of ethidium bromide staining, indicating that no significant degradation of RNA had occurred.

RT-PCR reactions (Titan RT-PCR System - Boehringer Mannheim - Lewes, South Sussex UK) were performed using as a template 0.6 - 0.8 µg total RNA / reaction and 11.2 picomoles / reaction of rat α7 forward (α7F) and α7 reverse (α7R) primers. The reaction mixture was cycled once at 50°C for 30 min and then 30 times at 94°C for 60 s, 54°C for 60 s and 68°C for 90 s in a PT-100 Programmable Thermal Cycler (MJ Research Inc. - Watertown, MA USA). After amplification, DNA products were analysed by agarose gel electrophoresis (see 2.2.1.6). The oligonucleotide primers derived from a published rat α7 nAChR subunit sequence (Entrez DNA S53987) and were designed using Vector NTI software version 4.0 (Informax - Gaithersburg, MD USA).). Numbering of nucleotides (bp) and amino acids (aa) begin with the first ATG codon (methyonine) of the α7 subunit sequence longest open reading frame (Séguéla *et al.*, 1993). The sequences of the specific primers used were: **α7F** 5'-TGCTGCACGTGTCCTGC-3' (bp47 (aa17) - bp64 (aa22)), and **α7R** 5'-GTGTCCTACGGCGCATGG-3' (bp674 (aa225) - bp691 (231)). The RT-PCR product (645 bp) encodes for the last 6 amino acids of the predicted signal peptide (22 amino acids) and the whole predicted amino terminal extracelullar domain (208 amino acids). To ensure that the obtained RT-PCR product was not the result of DNA amplification, total RNA samples were previously treated with DNAseI (1 Unit / µl reaction - 37°C for 15 min - Boehringer Mannheim). The identity of the RT-PCR product (645 bp) was confirmed by digestion with the restriction enzyme PstI (Promega - Madison, WI USA). This digestion yielded, as predicted by sequence analysis using the Vector NTI software, two fragments of ~509 bp and ~131 bp, respectively.

2.2.4.4 [^{125}I]-α-bungarotoxin binding assays: detection of the α7 nAChR

2.2.4.4.1 Iodination of α-bungarotoxin

α-Bungarotoxin (Sigma - Poole, Dorset UK) was iodinated by the chloramine T method (McConahey and Dixon, 1980) to a specific activity of 700 Ci / mmol, and stored in 10 mM potassium phosphate, pH 7.5, at 4°C for up to 4 weeks (Wonnacott *et al.*, 1980). Na[^{125}I] was purchased from Amersham International (Amersham - Buckinghamshire UK).

2.2.4.4.2 [^{125}I]-α-Bungarotoxin binding assay with cells attached to a substrate

[^{125}I]-α-Bungarotoxin binding assays were performed on E18 hippocampal neurones (grown for 7 days - see 2.2.3) and transfected HEK-293 cells cultured in different cell culture plasticware treated and not treated with attachment factors (poly-L-lysine MW 70000-150000 (Sigma - Poole, Dorset UK); fibronectin (Sigma); polyethylenimine (Sigma)).

The cultures were washed three times in medium prior to assay. For [^{125}I]-α-Bgt binding, triplicate cultures (on average) were incubated with 10 nM [^{125}I]-α-Bgt (20 nM for untrasfected and transfected mammalian cell lines). Non-specific binding was determined in presence of 1 μM α-Bgt (2 μM for mammalian cell lines). After 120 min at 37°C, the cultures were rapidly washed three times with PBS (10 mM phosphate, 0.18 M NaCl, pH 7.4). The cells were solubilised overnight in Markwell A solution (2 % (w/v) Na_2CO_3, 0.4 % (w/v) NaOH, 0.16 % (w/v) Na^+/K^+ tartrate (Sigma), 1 % SDS (Sigma)) and counted for γ radioactivity (Packard - COBRA II - Auto gamma counter). The protein concentration in each sample was determined by the method of Markwell *et al.* (1978).

2.2.4.4.3 [^{125}I]-α-Bungarotoxin binding assay with cells in suspension

Confluent transfected HEK-293 cells were washed with PBS and detached from the flask using 5 mM EDTA PBS. To pellet the cells, the cell suspension was centrifuged at 1000 rpm for 10 min. After that, the cells were resuspended in 0.1 % BSA (Sigma - Poole, Dorset UK) K^+-Ringer (140 mM KCl, 5.4 mM NaCl, 1.8 mM $CaCl_2.2H_2O$, 1.7 mM $MgSO_4.7H_2O$, 25 mM Hepes, pH 7.4) and divided into aliquots. One aliquot was reserved for protein determination (Markwell *et al.*, 1978).

The cell suspensions were incubated in a final volume of 150 μl with 10 nM [^{125}I]-α-Bgt for 120 min at 37°C. Specific binding was defined by the addition of 1 μM unlabeled α-Bgt (Sigma) to a duplicate set of tubes. After the incubation, cells were pelleted by centrifugation and washed four times with K^+-Ringer. Then, the pellets were counted for γ radioactivity.

2.2.4.4.4 Membrane preparation and [^{125}I]-α-bungarotoxin binding assay

Confluent transfected HEK-293 or SH-SY5Y cells were washed with ice-cold binding buffer (50 mM KH_2PO_4, 1 mM EDTA, 0.1 mM PMSF (Sigma - Poole, Dorset UK), pH 7.4 at room temperature), mechanically disaggregated and homogenised using a polytron for 10 s. The homogenate was centrifuged at 45000 x g for 30 min at 4°C and the pellet resuspended in ice-cold buffer at a concentration of 50 - 80 μg protein / sample.

Membranes were incubated in a final volume of 250 μl with 20 nM radioligand for 120 min at 37°C. Non-specific binding was determined by addition of 2 μM α-Bgt (Sigma) to duplicate set of samples. Incubations were terminated by rapid vacuum filtration through GF/C glass fibre filters presoaked in 0.5 % polyethylenimine, and filters washed four times with 5 ml of ice-cold buffer (Gopalakrishnan *et al.*, 1995). Bound radioactivity was quantitated by γ counting and protein determined using BSA (Sigma) as a standard (Markwell *et al.*, 1978).

2.3 Results

2.3.1 Subcloning rat α7 cDNA into pCDNA3

The first step in the project was to subclone the rat α7 cDNA into a vector capable of being used for heterologous protein expression both in *Xenopus* oocytes and mammalian cell lines. The plasmid chosen was the commercial vector pCDNA3 (Invitrogen) because previous studies demonstrated its successful use with the expression systems mentioned above (Séguéla *et al.*, 1993; Gopalakrishnan *et al.*, 1995, 1996; Stetzer *et al.*, 1996).

The entire coding sequence for the rat α7 subunit was excised from the plasmid pSMα7 with the EcoRI restriction enzyme and ligated into the same restriction site of the expression vector pCDNA3 . To ligate only one copy of the α7 gene with one copy of pCDNA3, an optimal ratio 2:1 for α7:pCDNA3 during the ligation step was determined. The correct orientation of the insert was tested by digestion of correct sized ligation products (~7.3Kb pCDNA3α7) with the Eco RV restriction enzyme (☺ correct orientation ☹ incorrect orientation – Figure 2.3 and Figure 2.4). To check the length of pSMα7, pCDNA3 and pCDNA3α7; these plasmids were linearised by digestion with the Xbal restriction enzyme (Figure 2.3 and Figure 2.5).

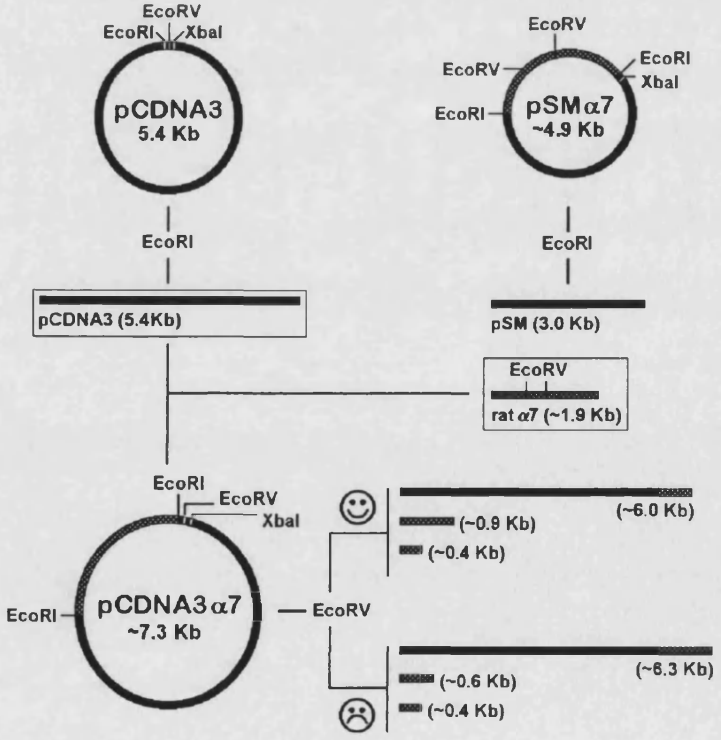

Figure 2.3 Flow diagram representing the subcloning of the rat α7 nAChR subunit cDNA into the pCDNA3 vector.

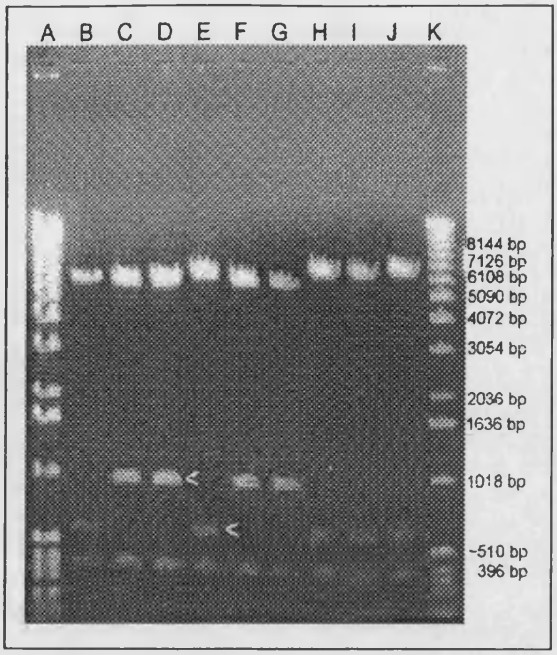

Figure 2.4 α7-insert orientation (0.7% agarose gel). Lanes **A & K**) 1 Kb DNA ladder Lanes **C → H**) pCDNA3α7 digested with Eco RV to test orientation of the insert. Lanes B, E, H, I & J: ~ 6.3Kb band, ~0.6 Kb band (<) and ~ 0.4 Kb band (☹ incorrect orientation of the insert). Lanes C, D, F & G: ~6.0 Kb band, ~0.9 Kb band (<) and ~0.4 Kb band (☺ correct orientation of the insert) (see **Error! Unknown switch argument.**).

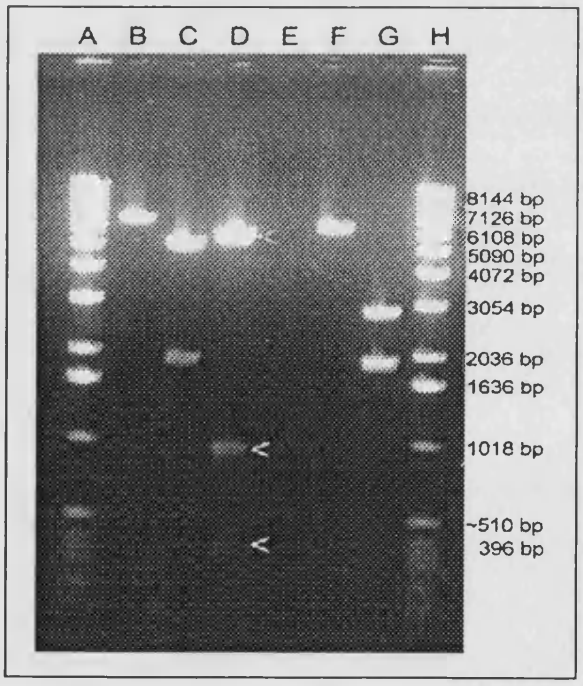

Figure 2.5 Rat α7 subcloning: summary (0.7% agarose gel). Lanes **A & H**) 1 Kb DNA ladder Lane **B**) pCDNA3α7 digested with Xba I: ~7.3 Kb band Lane **C**) pCDNA3α7 digested with Eco RI: ~5.4 Kb band (pCDNA3) and ~1.9 Kb band (α7 insert) Lane **D**) pCDNA3α7 digested with Eco RV: ~6.0 Kb band (<), ~0.9 Kb band (<) and ~0.4 Kb band (<) showing the correct orientation ☺ of the insert Lane **F**) pSMα7 digested with Xba I: ~6.8 Kb (~3.0 Kb of pSM + ~3.8 Kb (2 copies of α7 insert) Lane **G**) pSMα7 digested with Eco RI: ~3.0 Kb band (pSM) and ~1.9 Kb band (α7 insert) (see **Error! Unknown switch argument.**).

2.3.2 Two electrode voltage clamp recording

The suitability of the pCDNA3α7 construct was ascertained by examining its expression in *Xenopus* oocytes using the two electrode voltage clamp (TEVC) technique. Following nuclear injection of pCDNA3α7 into *Xenopus* oocytes, responses to (-)-nicotine could be recorded from ~40% of eggs after 2+ days (usually, experiments were carried out on the third day after nuclear injection of rat α7 cDNA). To prevent secondary activation of Ca^{2+}-dependent Cl^- currents (Séguéla *et al.*, 1993), all experiments were performed in the presence of 100 μM fluflenamic acid and 100 μM niflumic acid. The buffer also contained 0.5 μM atropine to inhibit muscarinic acetylcholine receptors (Kusano *et al.*, 1977). Typically, the oocytes had resting potentials of -44±13 mV (n=67). Currents (0.1μA-0.5μA) were recorded on application of saturating doses (high micromolar concentrations e.g. 200 μM) of (-)-nicotine to cells held at -70 mV. This holding potential was sufficiently far from the reversal potential to ensure reproducible currents evoked by (-)-nicotine stimulation (Figure 2.6). This holding potential also ensured the physiological stability and survival of the oocyte during prolonged periods of examination (e.g. during the construction of the I-V curve). Eggs injected with sterile water were insensitive to (-)-nicotine (n = 7 - data not shown). Receptor activation at high concentrations of (-)-nicotine was fast and displayed rapid desensitisation within the 3 s application time (Figure 2.6), according to published results for the same reconstituted homomeric receptor (Séguéla *et al.*, 1993).

Functional characterisation of α7 nAChR has relied for a long time on α-Bgt for its discrimination (Couturier *et al.*, 1990; Séguéla *et al.*, 1993). Currents evoked by (-)-nicotine (200 μM) were completely abolished after incubation (30 min at room temperature) of the α7-injected oocytes with the pseudo-irreversible antagonist α-Bgt (40 nM – Figure 2.6).

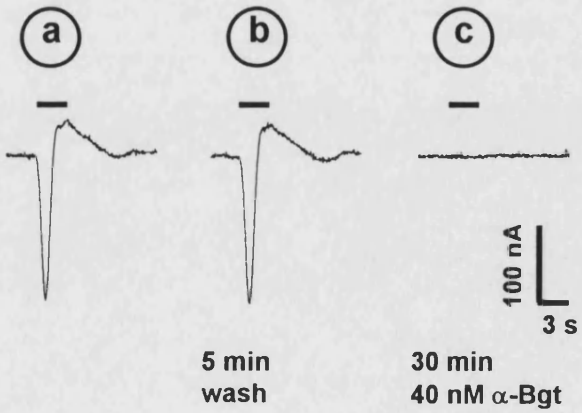

Figure 2.6 Nicotinic activation of the α7 nAChR expressed in *Xenopus* oocytes. (-)-Nicotine (200 μM) was given as a 3 s pulse (bar). This evoked an inward current (**a**) that could be reproduced by a second agonist application after 5 min wash with buffer to allow full nAChR recovery from desensitisation (**b**). The response was abolished by 30 min incubation at room temperature with 40 nM α-Bgt (**c**).

The relationship between holding potential (V_H) and the extent of the agonist evoked current (I) was determined as described in 2.2.2.4.4. (-)-Nicotine (200 µM) was applied as the membrane potential was stepped between -110 mV and +10 mV, in 20 mV increments (Figure 2.7). The rat α7 nAChR showed a strong linear dependence of current responses with membrane potentials between -110 mV and about -30 mV. α7 nAChR are strongly voltage sensitive at depolarised potentials: above -20 mV the current-voltage curve rectifies so thoroughly that no reversal potential is detectable.

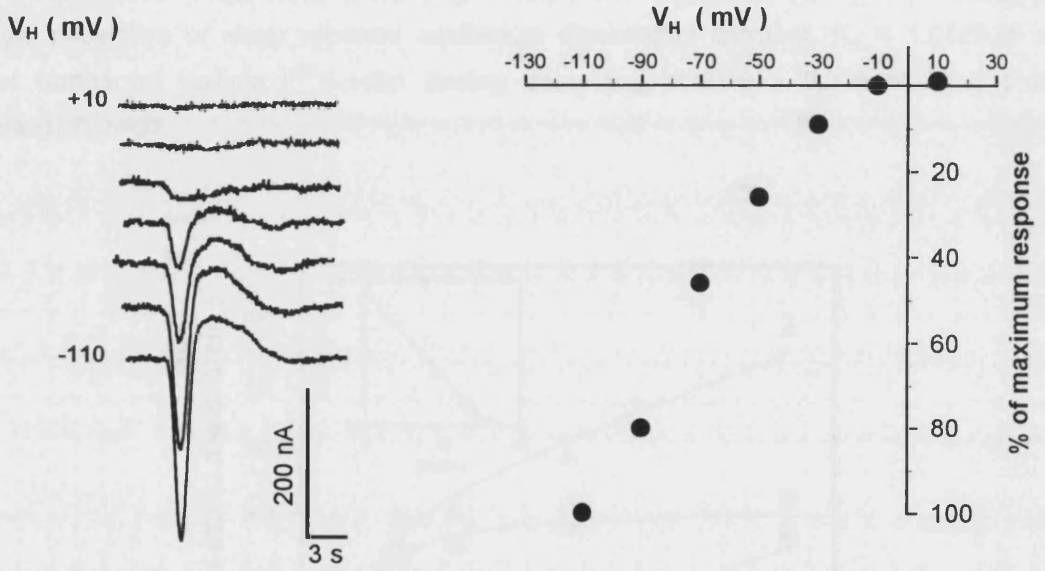

Figure 2.7 Voltage dependence of (-)-nicotine-induced currents in α7 channels. Left) Individual α7 currents in a single oocyte challenged with 200 µM (-)-nicotine between -110 mV and +10 mV. **Right)** Current-voltage values were obtained by consecutive 200 µM (-)-nicotine applications at increasingly depolarised voltages. Currents were normalised at -110 mV.

2.3.3 Endogenous expression of α7 nAChR

Ligand binding (rather than electrophysiology as in *Xenopus* oocytes) is a convenient way of screening transfected cells. The ligand binding approach for α7 nAChR was verified assaying cells that endogenously express surface α-Bgt-binding sites: the human neuroblastoma SHSY5Y cell line and rat E18 hippocampal neurones.

2.3.3.1 SH-SY5Y cell line: human α7 nAChR.

The equilibrium binding of [^{125}I]-α-Bgt to human neuroblastoma cells (SH-SY5Y cell line - passages 7 & 8) was studied. Specific binding of [^{125}I]-α-Bgt to cells *in situ* was saturable over the concentration range 0.1-20.0 nM (Figure 2.8). The data are consistent with binding to a single population of sites: apparent equilibrium dissociation constant, K_d = 1.04±0.25 nM; total number of surface [^{125}I]-α-Bgt binding sites, B_{max} = 31.9 ± 0.2 fmol / mg protein (mean±SD, n=2).

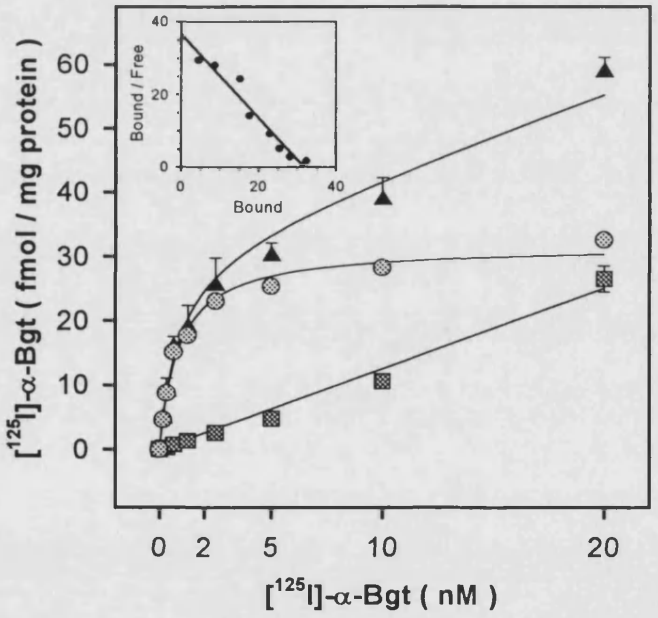

Figure 2.8 [^{125}I]-α-Bgt binding to SH-SY5Y cells. A representative saturation binding experiment for [^{125}I]-α-Bgt binding to human neuroblastoma cells ((triangles) total binding; (circles) specific binding; (squares) non-specific binding). The binding parameters determined by curve fitting to a rectangular hyperbola are B_{max} = 31.7 fmol / mg protein, K_d = 0.86 nM. Insert: Scatchard analysis of these data. Each point is mean±S.D. of triplicate determinations.

2.3.3.2 Rat α7 nAChR expression in E18 hippocampal neurones

High density (150000 cells / cm^2) hippocampal neuronal cultures were plated on polyethylenimine-coated dishes in serum supplemented medium and maintained in serum-free chemically defined medium for a week (Barrantes *et al.*, 1995). Cells strongly attached to pretreated surfaces and were assayed for surface expression of α-Bgt binding sites. For maximum [^{125}I]-α-Bgt binding, cultures were incubated with 10 nM [^{125}I]-α-Bgt (final concentration) for 120 min at 37°C. Non-specific binding was determined in the presence of 1 μM α-Bgt and accounted for 50% of total binding. The total number of specific [^{125}I]-α-Bgt binding sites was 97±14 fmol / mg protein (mean±S.D., n=4).

2.3.4 Heterologous expression of α7 in mammalian cell lines

2.3.4.1 The HEK-293 cell line

2.3.4.1.1 Culture of HEK-293 cells

HEK-293 cells, as described in Graham *et al.* (1977), had a general epithelial morphology, with a tendency to continue dividing after reaching confluency and grow in islands or clumps. They also showed a wide variation in cell size. One relevant feature to point out, because of its effect in the radioligand binding assays performed, was the poor attachment of these cells to substrates (in opposite to SHSY5Y cells and rat E18 hippocampal neurones).

HEK-293 cells were routinely maintained on standard cell culture-treated polystyrene surfaces. However, to perform [^{125}I]-α-Bgt binding assays, which involve several washing steps, the surfaces were pretreated with attachment factors (Table 2.1). HEK-293 cells were also grown on a commercially modified polystyrene surface: PRIMARIA surface (Falcon - Becton Dickinson Labware - Lincoln Park, NJ USA). This surface has a chemistry similar to those coated with poly-L-lysine, collagen I + IV and extracellular matrix. The different attachment conditions were tested and compared by naked eye visual inspection or under a visible light microscope.

When cells were plated on pretreated or PRIMARIA surfaces, 90+% of these cells settled and attached to the bottom of the dish within 20-30 min. When standard surfaces were used, up to 3 h had to be allowed to get the same cell adhesion percentage. The best results were achieved by treating the surfaces overnight with either 10 μg fibronectin / ml or 100 μg poly-L-lysine (MW 70000-150000) / ml. It was decided to treat the surfaces with the latter for economic reasons. Although there was a significant improvement in cell adhesion (rate and strength) to pretreated surfaces when compared to nontreated ones, did not prevent cell detachment during washing steps.

Attachment factor	Surface treatment (h)
500 μg polyethylenimine / ml	2, 6 & 14 (overnight)
10 & 100 μg poly-L-lysine (MW 70000 -150000) / ml	2 & 14 (overnight)
10 μg fibronectin / ml	14 (overnight)

Table 2.1 Attachment conditions tested to improve HEK-293 cells adherence to substrate. Attachment factors were prepared in borate buffer (150 mM borax, pH 8.3). Surfaces were washed 5 times (5 min each, at room temperature) with sterile water before plating the cells.

2.3.4.1.2 HEK-293 lipotransfection with pCDNA3α7

Transient transfection

Thirteen transient transfections of HEK-293 cells (internal passage <14) with pCDNA3α7 were performed. Cells were grown, as described in 2.2.4.1, in 24 well plates pre-treated with 100 μg poly-L-lysine / ml borate buffer (overnight). To test the transfected cells for surface expression of α-Bgt binding sites, [^{125}I]-α-Bgt binding assays on attached cells (see 2.2.4.4.2) or cells in suspension (see 2.2.4.4.3) were performed. Expression levels lower than 10 fmol α-Bgt binding sites / mg protein were considered non-significant. Untransfected HEK-293 cell did not show any specific [^{125}I]-α-Bgt binding (total cpm = non-specific cpm, $p>0.05$ one way ANOVA - n=2). For maximum [^{125}I]-α-Bgt binding, cultures were incubated with 20 nM [^{125}I]-α-Bgt (final concentration) for 120 min at 37°C. Non-specific binding was determined in the presence of 2 μM α-Bgt. The transfection conditions were optimized for the highest expression of surface α-Bgt binding sites and lower reagents' toxicity. The conditions optimised included DNA and lipid concentrations, time for DNA-lipid complexes formation, cell confluency, time of exposure of cells to DNA-liposome complexes, dTC addition to the medium, days between the transfection procedure and binding assays (Table 2.2).

Parameter	Tested
μg DNA / ml transfection suspension	0.5, 1.0, 2.5, 5.0 or 10.0
μg lipofectAMINE / ml transfection suspension	6, 12, 24 or 48
DNA-lipid complexes formation (min)	30, 40 or 50
Cells confluency (%)	(20-30), (50-60) or (90+)
Cells exposure to DNA-lipid complexes (h)	4 or 6
Cell culture medium	with or without 10 μM dTC
Expression time after transfection (days)	2 , 3 or 5

Table 2.2 Optimisation parameters tested for liposome-mediated transient transfections.

Expression of surface α-Bgt binding sites, after transient transfection of HEK-293 cells with pCDNA3α7, was largely (10/11) unsuccessful (total binding = non-specific binding, $p>0.05$ one way ANOVA). From these observations it can be concluded that:

a) up to 6 h exposure to DNA-lipid complexes (any ratio tested), in the absence of serum, was not toxic for HEK-293 cells.

b) the addition of dTC (10 μM) to the culture medium did not improve α7-surface expression, neither by protecting α7-expressing cells from putative expression-cytotoxic effects nor by up-regulating possible α-Bgt binding sites.

Only in one experiment an increase in specific surface expression of α-Bgt binding sites was observed. Figure 2.9 shows the highest expression level achieved in transient transfections of HEK-293 cells with pCDNA3α7: 12.3 fmol [^{125}I]-α-Bgt binding sites / mg protein. Reproducing these results under exactly the same conditions was completely unsuccessful (n=3).

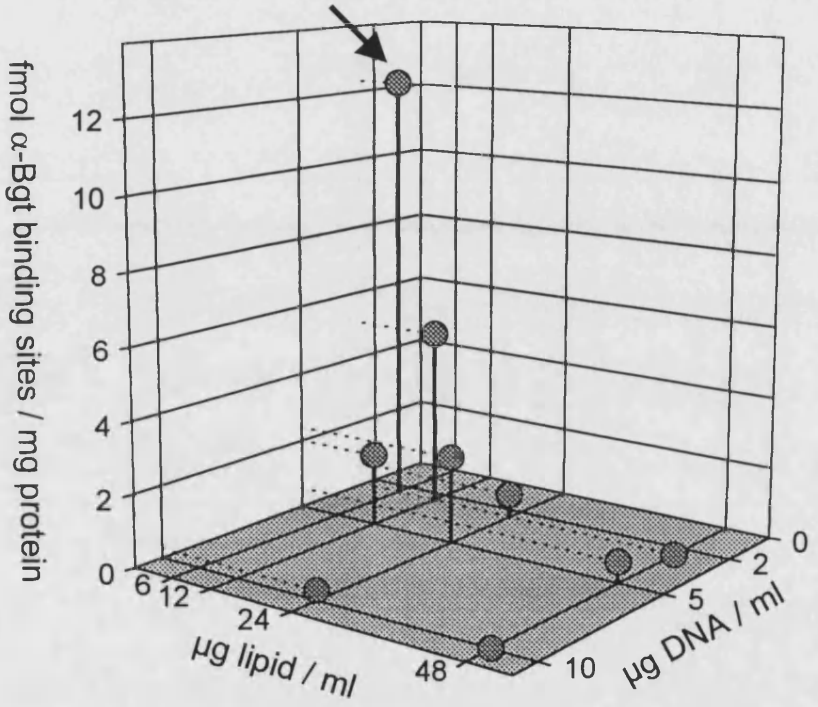

Figure 2.9 Effects of pCDNA3α7 concentration and lipofectAMINE:pCDNA3α7 ratio on transient surface expression of α-Bgt binding sites in HEK-293 cells. This 3D-graph presents the results of the only successful assay in which specific surface binding of [^{125}I]-α-Bgt was detected. The highest expression level (arrow: 12.3 fmol α-Bgt binding sites / mg protein) was obtained using 2.5 µg pCDNA3α7 / ml transfection medium and a ratio lipid:DNA of 2.4. Higher DNA concentrations or lipid:DNA ratios decreased expression. DNA-lipid complexes were allowed to form for 40 min. Cells (90% confluent) were incubated with the DNA-lipid complexes for 6 hours. Attached transfected cells were assayed two days after transfection for surface [^{125}I]-α-Bgt binding.

Stable transfection

At the same time as transient transfections were being carried out, stable transfection was also investigated. Four stable transfections of HEK-293 cells (internal passage <20) with pCDNA3α7 were performed. HEK-293 cells were grown as for transient transfections. To test the transfected cells for expression of α-Bgt binding sites, we performed [^{125}I]-α-Bgt binding assays on attached cells (see 2.2.4.4.2) or membrane preparations (see 2.2.4.4.3). Expression levels lower than 3 fmol α-Bgt binding sites / mg protein were considered non-significant. For maximum [^{125}I]-α-Bgt binding, cultures or cell membranes were incubated with 20 nM [^{125}I]-α-Bgt for 20 min at 37°C. Non-specific binding was determined in the presence of 2 μM α-Bgt.

To achieve the high expression levels in HEK-293 cells reported with the human α7 subunit (Gopalakrishnan *et al.*, 1995), their transfection conditions were reproduced (Table 2.3 in bold).

Parameter	Tested
μg DNA / ml transfection suspension	**1.5**
μg lipofectAMINE / ml transfection suspension	10 or **20**
DNA-lipid complexes formation (min)	40
cells confluency (%)	(20-30), (**50-60**) or (90+)
cells exposure to DNA-lipid complexes (h)	**5** or 10
cell culture medium	With or **without** 10 μM dTC

Table 2.3 Optimisation parameters for HEK-293 liposome-mediated stable transfections.

Transfected cells were selected in medium containing 0.5 mg geneticin (G418) / ml. Transfected G418-resistant cells did not lose the resistance to G418 for as long they were cultured (up to three months). Control HEK-293 cells (see2.2.4.2), when cultured in medium containing G418, died within 4-7 days. Between 6 and 10 clones were isolated and assayed for each condition (number of conditions tested: 24 (see Table 2.3)). Rat α7-mRNA expression was detected by RT-PCR in HEK-293 clones stably transfected with pCDNA3α7 (Figure 2.10).

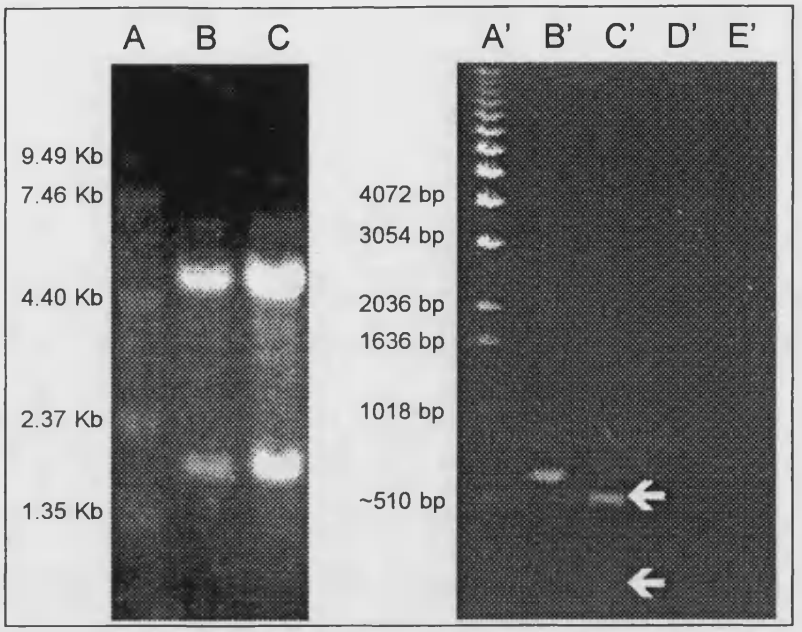

Figure 2.10 α7-mRNA expression in stably transfected HEK-293 cells. Left) Denaturing gel (0.66M formaldehyde 0.8% agarose) showing the 28S and 18S eukaryotic ribosomal RNAs from: Lane **B**) G418-resistant cells, and Lane **C**) untransfected HEK-293 cells. Lane **A**) 0.24 - 9.49 Kb RNA Ladder. **Right)** Electrophoresis of RT-PCR products (0.8% agarose gel) - Lane **A'**) 1 Kb DNA Ladder - Lane **B'**) Expected RT-PCR product (645 bp) using as a template total RNA showed in Lane A - Lane **C'**) Fragments (arrows: 509 bp & 131 bp) after digestion with PstI of the fragment showed in Lane B' - Lanes **D' & E'**) Same as Lanes B' & C' but using as a template total RNA isolated from untransfected HEK-293 cells (Lane C).

Although the isolated clones evidently incorporated the G418-resistance gene into their genomes and expressed rat α7-mRNA, it was not possible to detect clones expressing significant levels of α-Bgt binding sites either on intact cells or cell membrane preparations (total binding = non-specific binding, $p>0.05$ one way ANOVA).

2.3.4.2 The SH-SY5Y cell line

Two stable transfections of SH-SY5Y cells (passages 11 & 16) with pCDNA3α7 were performed following report by Gopalakrishnan *et al.* (1995). SH-SY5Y cells were grown as described in 2.2.4.1. To test SH-SY5Y cells for expression of α-Bgt binding sites, [^{125}I]-α-Bgt binding assays on transfected and untransfected attached cells were performed (see 2.2.4.4.2). For maximum [^{125}I]-α-Bgt binding, cultures were incubated with 20 nM [^{125}I]-α-Bgt for 120 min at 37°C. Non-specific binding was determined in the presence of 2 μM α-Bgt. The transfection conditions tested are shown in Table 2.4.

Parameter	Tested
μg DNA / ml transfection suspension	1, 10 or 20
μg lipofectAMINE / ml transfection suspension	2.4, 24.0 or 48.0
DNA / lipid ratio	2.4
DNA-lipid complexes formation (min)	40
cells confluency (%)	(50-60)
cells exposure to DNA-lipid complexes (h)	5

Table 2.4 Optimisation conditions tested for SH-SY5Y liposome-mediated stable transfections.

Transfected cells were selected in medium containing 0.5 mg geneticin (G418) / ml. G418-resistant cells did not lose the resistance to this antibiotic for as long they were cultured (up to nine weeks). Control (untransfected) SH-SY5Y cells, when cultured in medium containing G418, died within 4-7 days. Transfection efficiency (number of G418-resistant clones per plate) was proportional to the concentration of DNA used in the transfection. G418-resistant clones (6 per condition) were isolated and assayed for surface [^{125}I]-α-Bgt-binding (number of conditions tested: 3 (see Table 2.4)).

Although the isolated clones were resistant to 0.5 mg G418 / ml medium, it was no possible to detect increased levels of surface α-Bgt binding sites when compared with untransfected controls (26.8±5.9 fmol [^{125}I]-α-Bgt binding sites / mg protein - mean±S.D. n=4).

2.4 Discussion

This chapter presents attempts to heterologously express the rat α7 nAChR in mammalian cell lines. The ultimate purpose of constructing such α7 expression systems, was to compare the pharmacological and functional properties of native (i.e. α-Bgt binding sites expressed on the surface of rat E18 hippocampal neurones) and heterologously expressed rat α7 nAChR. The results emerging from these comparisons would have been applied to the study of presynaptic nAChR mediating glutamate release from rat hippocampal synaptosomes (chapter 3). At the time that these studies were initiated (1996), there was electrophysiological evidence (McGehee *et al.*, 1995; Gray *et al.*, 1996) for the involvement of α-Bgt-sensitive receptors in the presynaptic modulation of glutamate release. In this chapter, the construction of the expression vector pCDNA3α7 was described (2.3.1). This was shown to be functional in *Xenopus* oocytes (2.3.2) but failed to result in expression of surface receptors (as defined by [^{125}I]-α-Bgt binding) in mammalian cell lines, although α7 mRNA was detected (2.3.4).

2.4.1 Heterologous expression of nAChR in *Xenopus* oocytes

The expression of pCDNA3α7 plasmid in *Xenopus* oocytes was carried out to verify its suitability as a functional expression vector. From the pharmacological point of view, the homomeric rat α7 nAChR expressed in *Xenopus* oocytes is moderately sensitive to ACh and displays the following order of agonist potency: (-)-nicotine > cytisine > DMPP > ACh (Séguéla *et al.*, 1993). Moreover, (-)-nicotine is a full agonist on α7-homomers expressed in *Xenopus* oocytes with EC_{50}s of ~10 μM and ~40 μM for chick and human α7 homomers, respectively (Galzi *et al.*, 1991; Eiselé *et al.*, 1993; Gerzanich *et al.*, 1994; Peng *et al.*, 1994). Therefore 200 μM (-)-nicotine was selected, as it should give maximal responses. Oocytes injected with pCDNA3α7 responded with fast, desensitising responses characteristic of α7-containing nAChR. Consistent with previous observations (e.g. Couturier *et al.*, 1990), currents evoked by 200 μM (-)-nicotine were abolished by incubating pCDNA3α7-injected oocytes with 40 nM α-Bgt (30 min at room temperature). These results demonstrated that the pCDNA3α7 construct (2.3.1), when injected in *Xenopus* oocyte nuclei, was transcribed, translated and was also capable of forming surface functional rat α7 nAChR (2.3.2).

Xenopus oocytes are known to express Ca^{2+}-activated Cl^- conductances (Miledi, 1982; Barish *et al.*, 1983) and these channels have been previously used to demonstrate qualitatively that neuronal nAChR are permeable to Ca^{2+} (e.g. Vernino *et al.*, 1992). Because the reversal potential of the Ca^{2+}-activated Cl^- current in the oocyte is about -25 mV (Miledi and Parker, 1984), currents through both the α7-channel and the Cl^- channel would appear as inward cationic currents at potentials below -25 mV. Then, these two currents would

add at the holding potential of -70 mV used in Figure 2.6. To avoid this undesirable contribution to the pure nicotinic response, the experiments were performed in the presence of 100 µM niflumic acid and 100 µM fluflenamic acid, compounds that block the Ca^{2+}-activated Cl^- conductance (White and Aylwin, 1990).

Another striking feature of the α7 nAChR is the rapidity with which the response desensitises. It has been shown that increasing concentrations of agonists increase the rates of both the rise and desensitisation of the response (Revah *et al.*, 1991; Gerzanich *et al.*, 1994). In this study, the time course of recovery from desensitisation was estimated using a paired application protocol in experiments where the agonist was applied again at intervals after a control application. For saturating concentrations of (-)-nicotine (200 µM) the interval between applications was increased to a minimum of 5 min (Figure 2.6). Endogenously expressed ("native") α7 nAChR have also been reported to desensitise so rapidly that especially fast agonist application and fast electronics are required to measure channel opening accurately (Alkondon *et al.*, 1996; Frazier *et al.*, 1998a; Radcliffe and Dani, 1998). In oocytes (Couturier *et al.*, 1990; Revah *et al.*, 1991; Séguéla *et al.*, 1993; this study), the relative slowness with which the large cells can be perfused may prolong the response and be used to experimental advantage. Recently, Papke and Thinschmidt (1998) reported that rapid desensitisation of α7 nAChR combined with relative slow agonist application could potentially confound the interpretation of concentration-response relationships obtained for this nAChR when assayed using the TEVC technique in *Xenopus* oocytes. They suggested that estimates of EC_{50} derived from conventional analysis may overestimate the actual EC_{50} values by a factor of 10 and underestimate Hill slopes by a factor of 2-3. However, if these observations apply to this study, they do not affect the fact that pCDNA3α7, when injected in *Xenopus* oocytes, is capable of generating functional α-Bgt-sensitive nAChR (Figure 2.6).

Finally, by contrast with muscle nAChR, neuronal nAChR (including the α7 subtype) exhibit inward rectifying channel properties (Figure 2.7). Both the rapid desensitisation and the inward rectification combine to minimise sustained influx through these nAChR. These self-limiting features could be especially relevant when considering the possible functional roles of such nAChR (seen in 2.1.5).

2.4.2 Heterologous expression of rat α7 in mammalian cell lines

As seen in chapter 1, neuronal nAChR exist as multiple subtypes and display functional diversity (reviewed in Sargent, 1993; Albuquerque *et al.*, 1995; Lindstrom, 1996; Dani and Heinemann, 1996). As has been concluded from subunit expression studies in *Xenopus* oocytes and mammalian cell lines, functional neuronal nAChR are heteropentamers of α and β subunits (Elliott *et al.*, 1996; Ramirez-Latorre *et al.*, 1996; Colquhoun and Patrick, 1997), or homopentamers of α subunits (Couturier *et al.*, 1990; Séguéla *et al.*, 1993; Gerzanich *et al.*, 1994; Elgoyhen *et al.*, 1994). Because native neurones (e.g. Alkondon *et al.*, 1993; Yu and Role, 1998) and neuronal cell lines (e.g. Rogers *et al.*, 1992; Lukas *et al.*, 1993) usually coexpress several nAChR, the assignment of neuronal nicotinic responses to particular nAChR subtypes is progressing slowly. However, heterologous expression systems for individual nAChR subtypes offer an opportunity for investigating receptor structure and function. Transient expression using *Xenopus* oocytes or eukaryotic cells is particularly convenient for physiological studies (two-electrode voltage clamp and patch-clamp techniques). Injection of (transfection with) different nAChR subunit cDNA (and cRNA in *Xenopus* oocytes), either alone or in combination, has yielded information concerning receptor channel properties, agonists / antagonists interactions and desensitization (e.g. Revah *et al.*, 1991; Bertrand *et al.*, 1992; Galzi *et al.*, 1992; Gerzanich *et al.*, 1994; Palma *et al.*, 1996; Fucile *et al.*, 1997; Ragozzino *et al.*, 1997). Reconstitution of purified receptors in planar lipid bilayers is another approach that has helped identify receptor function (Gotti *et al.*, 1991, 1994). On the other hand, stable receptor expression in somatic cells has the advantage that large numbers of cells expressing the desired receptor are available, more readily allowing for receptor biochemical and pharmacological studies (e.g. drug screening). However, with a few notable exceptions (Whiting *et al.*, 1991; Gopalakrishnan *et al.*, 1995, 1996; Stetzer *et al.*, 1996; Quik *et al.*, 1996; Kassner and Berg, 1997), most ectopic expression systems for neuronal nAChR so far are based on transient expression (e.g. Fucile *et al.*, 1997; Ragozzino *et al.*, 1997). It is not absolutely clear, at present, why stable heterologous expression of nAChR, in particular the α7 subtype, is more difficult to achieve than for other ionotropic neuroreceptors.

Since 1990, the year in which the chick α7 nAChR subunit was first cloned and characterised (Schoepfer *et al.*, 1990; Couturier *et al.*, 1990), the α7 gene has also been cloned from rat (Séguéla *et al.*, 1993), human (Doucette-Stamm *et al.*, 1993; Peng *et al.*, 1994; Chini *et al.*, 1994) and mouse (Orr-Urtreger *et al.*, 1995). However, for five years, only two papers (Gopalakrishnan *et al.*, 1995; Quik *et al.*, 1996) were published reporting stable expression of the α7 nAChR subunit in cell lines that do not endogenously express this subunit: the HEK-293 and GH_4C_1 cell lines. At the time the studies presented in this thesis were initiated (January 1996) there was no major reason to doubt the ability of the α7 nAChR sequence to express in mammalian cell lines. Nevertheless, although the stable expression of

the α7 nAChR subunit has been the aim of several labs, none, including those that succeeded in expressing it, has conclusively explained the cause / s of so many failures.

In this study the rat α7 cDNA was used to stably transfect mammalian cell lines, because the rat nicotinic α-Bgt receptor has been extensively studied, and this would allow for direct comparisons between *in vitro* ("native" α7 nAChR on rat E18 hippocampal neurones, and heterologously expressed rat α7 nAChR) and *in vivo* work. The human SH-SY5Y and HEK-293 cell lines were transfected with pCDNA3α7, a plasmid construct that has been also used in this study for the successful expression of the rat α7 subunit by nuclear injection into *Xenopus* oocytes (see 2.3.2). Neuroblastoma derived SH-SY5Y cells endogenously express the nAChR α3, α5, α7, β2 and β4 subunits (Lukas *et al.*, 1993). On the other hand the HEK-293 cell line does not express endogenous nAChR and are well established heterologous expression systems (Wong *et al.*, 1995; Gopalakrishnan *et al.*, 1995, 1996; Stetzer *et al.*, 1996). HEK-293 cells also provide several advantages for the study of ligand gated ion channel expression. These cells exhibit fast exponential growth with a doubling time of about 24 hours (Graham *et al.*, 1977), show relatively high transfection efficiency and high levels of transient / stable expression compared with other suitable hosts. In this study, the ability of the α7 nAChR to bind α-Bgt was used to examine its expression in these mammalian cell lines.

Insight into cellular mechanisms involved in receptor expression and turnover comes from successful heterologous expression of the nAChR of the vertebrate neuromuscular junction and the analogous "muscle-like" nAChR that is expressed in the electric organ of the fish *Torpedo* or the electric eel *Electrophorus*. The high affinity of α-Bgt for the vertebrate muscle and *Torpedo* electric organ nAChR has proved to be an important tool for the investigation of nAChR subunit folding and assembly (Green and Millar, 1995). Moreover, the folding of the muscle or *Torpedo* nAChR can be monitored by following the formation of ligand binding sites (e.g. the α-Bgt binding site) and conformational epitopes for monoclonal antibodies. Studies in the early 80s demonstrated that the muscle α subunit (the nAChR ligand binding subunit) transits a precursor pool before acquiring α-Bgt binding activity (Merlie and Sebbane, 1981; Merlie and Lindstrom, 1983). Studies of each of the four cloned *Torpedo* subunits (α, β, γ and δ) expressed individually in mouse fibroblasts have shown that, in the absence of correct interactions with other subunits, misfolded aggregates were formed (Paulson *et al.*, 1991). In addition, all four peripheral nAChR subunits when expressed alone in fibroblast cells were degraded rapidly (Claudio *et al.*, 1989; Green *et al.*, 1991) as were unassembled nAChR subunits, when expressed in the presence of other subunits. These observations have suggested that many subunits (~70 % for the nAChR) misfold after their synthesis, causing aggregation and rapid degradation of nAChR subunits (Merlie and Lindstrom, 1983; Ross *et al.*, 1991). It is also clear that folding and oligomerization of the muscle nAChR subunits

are the rate-limiting steps in transport to the cell surface (Smith *et al.*, 1987; Ross *et al.*, 1991; Green and Claudio, 1993; Green and Wanamaker, 1998).

The neuronal nAChR α7 subunit, like the muscle and *Torpedo* nAChR (Barnard *et al.*, 1981; Mishina *et al.*, 1984), is capable of forming α-Bgt-sensitive functional ion channels when expressed in *Xenopus* oocytes (this study; Couturier *et al.*, 1990; Séguéla *et al.*, 1993). In 1994, the functional hyperexpression of the rat α7 subunit in the human neuroblastoma cell line SH-SY5Y was reported (Puchacz *et al.*, 1994). Interestingly, a comparison of transfected cell lines (Cooper and Millar, 1997) suggested that only cells expressing an endogenous α7 gene (namely SH-SY5Y and PC12 cells) could produce α-Bgt-binding protein from a transfected α7 gene. Other studies (Gopalakrishnan *et al.*, 1995; Quik *et al.*, 1996; Kassner and Berg, 1997) showed this not to be an absolute requirement, since HEK-293 (Gopalakrishnan isolates!!), GH_4C_1 and QT-6 transfectants could do so without expressing detectable levels of an endogenous α7 gene product.. Although this study corroborated the endogenous expression of human α7 in SH-SY5Y cells (see 2.3.3.1.), the hyperexpression of rat α7 in this cell line was not achieved (Puchacz *et al.*, 1994; Cooper and Millar, 1997). Probably the use of transfection conditions not fully optimised and the low number of colony forming units (cfu) isolated per condition, reduced the probability of picking up a cfu expressing high levels of surface α-Bgt-binding sites.

Peng *et al.* (1994) observed that, despite the high sequence identity between the cloned α7 sequences from different species (e.g. 91% identity between human and rat α7 nAChR mature peptides - Elliott *et al.*, 1996), there were large pharmacological differences between human and chicken α7 nAChR expressed in *Xenopus* oocytes. In 1995, Gopalakrishnan *et al.* transfected the human derived cell line HEK-293 with human α7 cDNA and successfully expressed α-Bgt binding sites. In this study, and although the same human cell line was transfected with rat α7 cDNA, no increase in α-Bgt binding sites was detected. Then, it was reasonable to think that the different outcomes observed with the human and rat α7 cDNAs when transfected in the HEK-293 cell line could be explained by sequence-specific differences. Cooper and Millar (1997) proved this hypothesis wrong by being unable to express human, rat or chicken α7 cDNA in the HEK-293 cell line.

The fact that the rat α7 cDNA is transcribed into α7 mRNA (as determined by RT-PCR in 2.3.4.1.2) and no α-Bgt binding sites were detected in HEK-293 cells transfected with pCDNA3α7 (2.3.4.1.2), points at the misfolding of the α7 subunit as the primary cause of the cell-dependent expression observed. The findings of Kassner and Berg (1997) support this view, since although high levels of α7 protein were produced by their HEK-293 transfectants, these cells were ineffective at assembling the protein into species capable of binding α-Bgt. Despite the inability of the HEK-293 cell line to fold correctly the α7 subunit

(this study; Cooper and Millar, 1997; Kassner and Berg, 1997), it has been demonstrated that it can express other subunits such as the 5-HT_{3A} receptor subunit (Cooper and Millar, 1997) and a chimaeric subunit (Eiselé *et al.*, 1993) containing the N-terminal region of the chick α7 and the C-terminal region of the 5-HT_{3A} subunit (α7/5-HT_{3A} Cooper and Millar, 1997). These cells, therefore, must contain all of the intracellular machinery required for the posttranslational processing, folding and assembly of these other homomeric neurotransmitter-gated ion channels. It is interesting to point out that the same source of HEK-293 cells used in this study, was exploited by Dr Andrew Davies (Nicotine Research Lab - Bath University) to successfully express the α7/5-HT_{3A} receptor (500-1000 fmol [^{3}H]-MLA binding sites / mg protein, personal communication). The successful expression of the chimaeric α7-5-HT_{3A} subunit in HEK-293 cells, also suggests that the C-terminal (putative transmembrane and intracellular) regions of α7 are responsible for cell-specific misfolding.

The hypothesis that the native α7 subunit may need to coassemble with other neuronal nAChR subunits to be "properly" expressed, has also been proposed. However, several lines of evidence suggest that the cell-specific phenomenon observed cannot be explained by a requirement for other nAChR subunits. These include the observation that the α7 subunit forms homomeric receptors in *Xenopus* oocytes in the absence of other subunits (Couturier *et al.*, 1990; Séguéla *et al.*, 1993). Also, after overexpression of correctly folded α7 in PC12 and SHSY5Y cells, there is no evidence for the coprecipitation of other endogenous subunits with antibodies against α7 (Anand *et al.*, 1993; Cooper and Millar, 1997). Moreover, Cooper and Millar have been unable to induce the "α7-nonpermissive" cells to fold correctly the α7 subunit by coexpressing this subunit with various combinations of all other cloned rat neuronal nAChR. The possible involvement of any, as yet, uncloned neuronal nAChR subunits is a possibility that cannot be rejected.

Changes in the activity of second messenger cascades can also modulate protein expression. It has been reported that the assembly efficiency of the cloned *Torpedo* electric organ, mouse muscle nAChR expressed in mouse fibroblast cells, α4β2 nAChR in M10 cells and α7 subunit in GH_4C_1 and SHSY5Y cells, is elevated by about twofold in response to increased levels of intracellular cyclic AMP (Green *et al.*, 1991; Ross *et al.*, 1991; Rothhut *et al.*, 1996; Quick *et al.*, 1997; Cooper and Millar, 1997). However, despite this effect on SH-SY5Y cells, Cooper and Millar (1997) could not detect specific [^{125}I]-α-Bgt binding when α7-transfected HEK-cells were grown in the presence of 8-bromo-cyclic AMP and isobutylmethylxantine (an inhibitor of phosphatases). An interesting link has also been recently established between the prolyl isomerase, cyclophilin, and the ability of oocytes to express homooligomeric ligand gated ion channels, such as the α7 and 5-HT_{3A} (Helekar *et al.*, 1994; Helekar and Patrick, 1997). Cooper and Millar (1997) studied the possible involvement of prolyl isomerases in the failure of cell lines like the HEK-293 to express correctly the α7 subunit.

They coexpressed this subunit in HEK-293 cells, together with a cloned ER-specific cyclophylin but could not detect specific [^{125}I]-α-Bgt binding under these experimental conditions. Similar negative results have been reported by Blumenthal *et al.* (1997), after coexpression of cyclophylin in an isolate of PC12 cells that failed to express correctly folded α7 subunit. The fact that it is possible to stably express the 5-HT$_{3A}$ receptor in HEK-293 cells in the absence of cyclophylin (Cooper and Millar, 1997) and that cyclosporin A treatment had no effect on expression of α-Bgt-binding sites either by QT-6 transfectants or by ciliary ganglion neurones in culture (Kassner and Berg, 1997), supports the idea that cyclophylin is not essential for the correct folding and assembly of homomeric receptors in mammalian cell lines like HEK-293.

The effect of protein glycosylation on α7 nAChR subunit heterologous expression has also been studied. Merlie *et al.* (1982) reported that, in muscle BC3H-1 cells treated with tunicamycin, nonglycosylated α1 failed to assemble into toxin-binding receptors on the cell surface. Recently and supporting this observation, Chen *et al.* (1998) showed that asparagine-linked glycosylation is required for the expression of functional α7 receptors in *Xenopus* oocytes. However, it seems unlikely that differences in glycosylation account for the lack of α-Bgt binding sites expression in HEK-293 cells reported in this thesis, since Cooper and Millar (1997) reported similar apparent molecular weights for the α7 protein expressed in permissive and nonpermissive cells lines. Moreover, these values closely agreed with those determined for α7 purified from brain (Dominguez Del Toro *et al.*, 1994), indicating glycosylation levels similar to those found for the endogenously expressed α7 subunit. Moreover, the functional expression of muscle nAChR, 5-HT$_{3A}$ and α7/5-HT$_{3A}$ receptors on the surface of cells that failed to correctly fold the α7 subunit (e.g. HEK-293), suggests that glycosylation alone is not responsible for the "abnormal" α7 nAChR subunit low expression levels reported in certain cell lines.

Difficulties in expressing ligand gated ion channels with high Ca^{2+}-conductances have been reported (Choi, 1988; Treinin and Chalfie, 1995; Grimwood *et al.*, 1996). These problems, mainly found with glutamate-gated ion channels, have been attributed to the spontaneous opening of the channel leading to calcium entry and cell death. The high Ca^{2+} permeability of α7 nAChR may place stringent requirements on the neurone to avoid errors in the assembly of nAChR with α7 subunits that might risk Ca^{2+}-mediated cytotoxicity (Choi, 1992). Recently, neurotoxicity associated with the expression of a mutated nAChR subunit (deg-3) was reported in the nematode *Caenorhabditis elegans* (Treinin and Chalfie, 1995). It is interesting to point out that the deg-3 gene encodes a nAChR α subunit, which in the transmembrane domain II is most close (~52% identity) to the neuronal α7 subunits from rat and chicken. Although it is possible that a similar "problem" may occur to some extent with the homomeric α7 receptor, it is unlikely that this can explain

the observations presented in this thesis. However, the above data could suggest that, expression of α7 nAChR may select (not kill) only those cells that express very low levels of "excitotoxic" receptors but also express the antibiotic-resistance gene to survive in selection medium. Apparently this is not true since Gopalakrishnan (1995), Quik (1996) and Kassner & Berg (1997) did not use nAChR antagonists to achieve their results. Moreover, in transient and stable transfections of HEK-293 cells with pCDNA3α7 (this study), the addition of dTC (10 μM) to the growth medium to block possible receptor activation, had no effect on the α-Bgt binding sites expression levels achieved.

The primary mechanism of regulating cell-specific expression of proteins appears to be at the level of mRNA synthesis, by cell-specific transcription factors. However, this thesis presents evidence that the transcription of the α7 sequence is not the limiting step in the heterologous expression of the α7 protein (at least in the HEK-293 cell line). This study reports the transcription of exogenous rat α7 gene in stably transfected HEK-293 (**Error! Unknown switch argument.**), but consistent with previous studies (Cooper and Millar, 1997; Kassner and Berg, 1997) failed to detect expression of specific [^{125}I]-α-Bgt-binding sites. It is important to remember that the same HEK-293 cells used in this study, heterologously expressed high levels of the chimeric α7/5-HT_{3A} receptor (A.Davies - personal communication). The results presented in this thesis, together with the reports reviewed above, suggest that the difficulties found in heterologously expressing α7 nAChR in mammalian cell lines, arise as consequence of cell-specific misfolding of the neuronal α7 nAChR subunit. A reasonable explanation for the differences between the results obtained by Cooper and Millar (1997), Kassner and Berg (1997) and those of Gopalakrishnan *et al.* (1995) is that the HEK-293 cell isolates used in different laboratories are different in some way that remains to be established. Perhaps, after extensive propagation under different conditions, the cell line diverged and produced subpopulations having different kinds of components for assembling complex membrane proteins. Recently, pertinent to this last point, it is interesting that Blumenthal *et al.* (1997) have reported that different isolates from the PC12 cell line differ in the extent to which they express correctly folded α7 protein.

Finally, it is possible that the cell-specific regulation of posttranscriptional events, such as protein folding, subunit assembly and receptor stabilisation (as suggested by Kassner and Berg, 1997), may constitute an additional mechanism for regulating the cell-specific expression of some neurotransmitter receptor subtypes.

3 KCl- and nicotine-evoked glutamate release in hippocampus

3.1 Introduction

As described in Section II, (-)-nicotine is thought to enhance cognition and the hippocampus is likely to be a locus of action for such effects. This brain region receives a rich cholinergic innervation (septohippocampal pathway) and displays a dense nicotinic expression especially of the α7-subtype (Séguéla *et al.*, 1993). Recent evidence supports the presence of α7-containing nAChR on GABAergic interneurones (Alkondon *et al.*, 1997; Frazier *et al.*, 1998a: first demonstration of a functional cholinergic synapse in the mammalian brain in which the primary postsynaptic receptors are α-Bgt-sensitive nAChR). However, most evidence supports a presynaptic role for α-Bgt-sensitive nAChR in the CNS.

Presynaptic nAChR are likely on the terminals of cholinergic hippocampal afferents since they have been shown to modulate acetylcholine release *in vitro* (e.g. Wilkie *et al.*, 1996). The α4β2-containing nAChR is a candidate for such modulatory action given the loss of this subtype as cholinergic projections degenerate in Alzheimers' disease (Nordberg, 1994; Maelicke and Alburquerque, 1996). Noradrenaline (Clarke and Reuben, 1996) and GABA (Lu *et al.*, 1998) release have been also shown to be modulated by presynaptic nAChR. Glutamate is the major excitatory neurotransmitter in hippocampus and glutamatergic excitatory synaptic transmission is also a likely target for modulation by nAChR. In fact, electrophysiological studies revealed that (-)-nicotine was able to enhance glutamatergic synaptic transmission by activation of presynaptic α-Bgt-sensitive nAChR (i.e. Gray *et al.*, 1996; Radcliffe and Dani, 1998). The aim of the present chapter was to examine this modulation using a neurochemical approach.

In this study, synaptosome preparations were used to study nicotinic agonist-evoked glutamate release in rat hippocampus. Synaptosomes, i.e. isolated nerve terminals, present distinct advantages for the investigation of the molecular mechanisms controlling the release of neurotransmitters. They are, at the same time, the simplest preparation in which Ca^{2+} -dependent release can be studied and the most complex preparation that is sufficiently homogeneous to be accessible to measurements of ion transport, membrane potentials, Ca^{2+} transients, bioenergetics, and intraterminal compartmentation.

To gain a better insight into how nicotinic agonists modulate neurotransmitter release in the CNS, this study intended to explore Ca^{2+} influx, $[Ca^{2+}]_i$ changes and release of labelled glutamate from rat hippocampal synaptosomes, as a consequence of presynaptic nAChR activation (hypothetically of a α-Bgt-sensitive subtype).

3.2 Experimental procedures

3.2.1 (-)-Nicotine-evoked [^{3}H]-glutamate release from Percoll-purified hippocampal synaptosomes

3.2.1.1 Materials

Sprague-Dawley rats were obtained from the University of Bath Animal House breeding colony. L-[3,4-^{3}H]-glutamic acid (L-[^{3}H]-Glu) and D-[2,3-^{3}H]-aspartic acid (D-[^{3}H]-Asp) (specific activities 1.8 TBq / mmol (49.4 Ci / mmol) and 403.3 GBq / mmol (10.9 Ci / mmol), respectively) were purchased from NEN DuPont (DuPont - Stevenage, Hertfordshire UK). Percoll was obtained from Pharmacia Biotech (Uppsala, Sweden) and (±)-anatoxin-a ((±)-AnTx-a) from Tocris Cookson (Bristol, UK). (-)-Nicotine, L-glutamate, D-aspartate and HEPES were purchased from Sigma (Poole, Dorset UK). All other chemicals used were of analytical grade and obtained from standard commercial sources.

3.2.1.2 Preparation of Percoll-purified hippocampal synaptosomes

Male Sprague-Dawley rats (weighing 240-250 g) were killed by cervical dislocation, decapitated, and brain hippocampi (200-215 mg of wet tissue weight per rat) were rapidly dissected. Percoll-purified synaptosomes were prepared according to the procedure of Dunkley *et al.* (1988) as previously described by Soliakov and Wonnacott (1996). Eight hippocampi (800-860 mg wet weight) were homogeneized (10% (w/v)) in 0.32 M sucrose 5 mM HEPES (pH 7.4) followed by centrifugation at 1000 g for 10 min. The resulting supernatant fraction was distributed between four centrifuge tubes containing discontinuous four-step Percoll gradients composed of 3, 10, 15 and 23% Percoll in 0.32 M sucrose (pH 7.4), respectively. After centrifugation at 29000 g for 5 min, five main fractions were obtained: functionally active synaptosomes are concentrated at the 15-23% Percoll gradient interface (Dunkley *et al.*, 1988; Thorne *et al.*, 1991; Taupin *et al.*, 1994). This synaptosomal fraction (fraction 4) was gently collected by Pasteur pipette and, after dilution with 2.5 volumes Krebs bicarbonate buffer (118 mM NaCl, 2.4 mM KCl, 2.4 mM $CaCl_2$, 1.2 mM $MgSO_4$, 1.2 mM K_2HPO_4, 25 mM $NaHCO_3$, and 10 mM glucose, buffered to pH 7.4 with 95% O_2 / 5% CO_2), was centrifuged at 20000 g for 20 min. The resulting pellet was washed once more, and the final synaptosomes were resuspended in 1.4 ml Krebs bicarbonate buffer (pH 7.4).

Synaptosomes were loaded with L-[^{3}H]-Glu (0.2 µM, 49.4 Ci / mmol) or D-[^{3}H]-Asp (0.9 µM, 10.9 Ci / mmol) at 37°C for 15 min. To increase L-[^{3}H]-Glu or D-[^{3}H]-Asp uptake, the incubations were performed in the presence of "cold" 10 µM L-glutamic acid or 10 µM D-aspartic acid, respectively (the plasma membrane glutamate uptake carrier apparent Km for binding extracellular glutamate is in the range 2-50 µM - Nicholls and Attwell, 1990). The experiments were performed in Krebs bicarbonate buffer supplemented with ascorbic acid (1 mM).

Superfusion of synaptosomes was performed as previously described (Soliakov *et al.*, 1995; Marshall *et al.*, 1996) in a Brandel Superfusion Apparatus Model SF-12 (Brandel - Gaithersburg, MD USA, see Figure 3.1) using Krebs bicarbonate buffer at a flow rate of 0.5 ml/min. Fractions were collected every 2 min. After 30 min washing with Krebs bicarbonate buffer, (-)-nicotine (1, 10 or 25 μM) or (±)-AnTx-a (1 μM) in buffer was applied for 40 s, separating the pulse of drug from the bulk buffer flow by 10 s air bubbles. For KCl depolarisation, a 40 s pulse of buffer with KCl increased to 23.5 mM was applied.

Fractions were counted in a Packard TRI-CARB Liquid Scintillation Analyzer Model 1500 (Packard Instrument Company - Downers Grove, IL USA - counting efficiency 48 %).

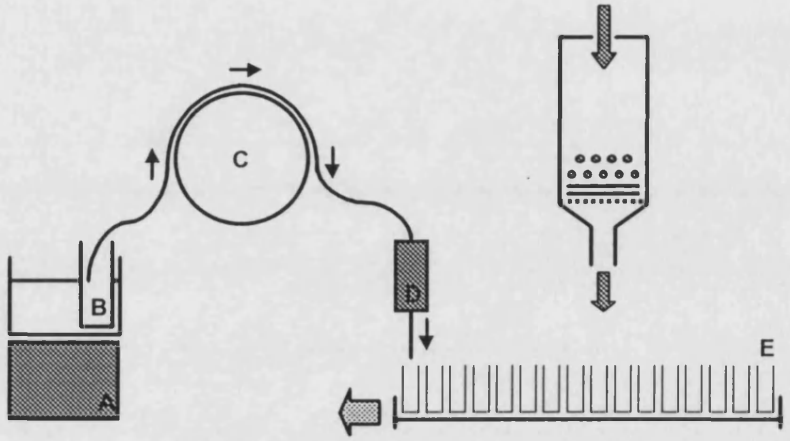

Figure 3.1 Schematic representation of the superfusion apparatus. Buffer and drug solutions (B) (maintained at 37°C by a thermostated water bath (A)) were collected using a stainless steel probe assembly and passed through the system by a 12-channel peristaltic pump (C). The superfusion block (D) contained 12 open superfusion chambers in parallel. Superfusate was collected by a second peristaltic pump (not shown), and delivered to an external fraction collector (E). The direction of buffer flow is indicated by small arrows. **Inset) Schematic representation of a superfusion chamber**. The walls and sintered support (horizontal dotted line) were made from the base of a BioRad disposable chromatography poly-prep column (BioRad - Hemel Hempstead, Herts UK). Krebs bicarbonate buffer was pumped into the chamber via a hypodermic needle (19G - upper arrow) to ensure delivery of small, regular drops of buffer. Synaptosomes (filled circles) were loaded into the chambers using the entry pump, to ensure that the points of sample and buffer delivery were the same. Retention of samples in the chambers was achieved using two Whatman GF/C filter discs (horizontal thick lines) placed on top of the sintered support.

3.2.1.3 Superfusion data analysis

The baseline was derived by fitting the data to the following double exponential decay equation:

$$y = ae^{-bx} + ce^{-dx}$$

(Equation 3.1)

where **a**, **b**, **c** and **d** are the curve parameters and **x** is the fraction number.

Evoked [^{3}H]-Glu or [^{3}H]-Asp release was calculated as the area under the peak after subtraction of the baseline. Responses are expressed as the percentage of radioactivity released from the total radioactivity loaded into the synaptosomes immediately before stimulation (Soliakov *et al.*, 1995). For comparison between different experiments, superfusion profiles were normalised as percentages of the fitted baselines (Figure 3.4).

3.2.2 KCl- and (-)-nicotine-evoked Ca^{2+} influx in Percoll-purified synaptosomes from rat hippocampus

3.2.2.1 Materials

A PTI dual-excitation spectrophotofluorimeter (PTI M-series instruments / PTI software v.2.060) manufactured by Photon Technology International Inc. (South Brunswick, NJ USA) was generously facilitated by Professor J. Westwick (University of Bath, Dept. of Pharmacy and Pharmacology). The acetoxymethyl derivative of fura-2 (fura-2/AM see Figure 3.2 - 1-[2-(5-carboxyoxazol-2-yl)-6-aminobenzofuran-5-oxyl-2-(2'-amino-5'-methylphenoxy) ethane N,N,N',N'- tetraacetic acid) was purchased from Molecular Probes (Eugene, OR USA). SDS and EGTA were purchased from Sigma (Poole, Dorset UK). All other chemicals used were of analytical grade and obtained from standard commercial sources.

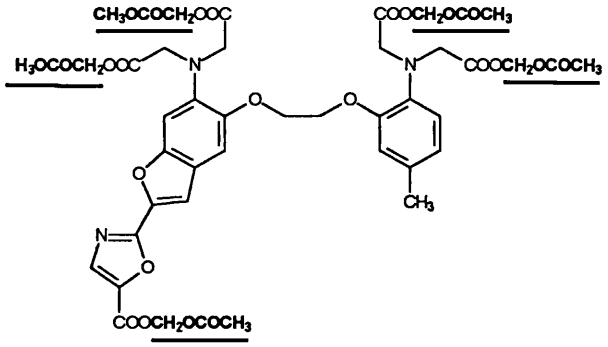

Figure 3.2 Chemical structure of fura-2/AM. This fluorescent Ca^{2+} chelator was developed by Tsien and colleagues (Grynkiewicz *et al.*, 1985) from the Ca^{2+} chelator BAPTA, which is the double aromatic analogue of EGTA. Hydrolysis of acetoxymethyl groups (underlined) by non-specific esterases traps the indicator in the nerve terminal cytosol.

3.2.2.2 Synaptosome loading with fura-2/AM

Percoll-purified hippocampal synaptosomes were prepared as described in 3.2.1.2. However, instead of normal Krebs buffer, low-Ca^{2+} Krebs bicarbonate buffer was used (118 mM NaCl, 2.4 mM KCl, 20 µM $CaCl_2$, 1.2 mM $MgSO_4$, 1.2 mM K_2HPO_4, 25 mM $NaHCO_3$, and 10 mM glucose, buffered to pH 7.4 with 95 % O_2 / 5 % CO_2). Percoll-purified hippocampal synaptosomes (fraction 4 - Percoll gradient 15-23% interface) were resuspended in 1 ml low-Ca^{2+} Krebs bicarbonate buffer before loading with fura-2/AM.

Fura-2/AM was prepared as a 1 mM stock solution in dimethyl sulfoxide (DMSO). Highly purified hippocampal synaptosomes (1.7±0.3 mg protein / ml - n=9) were incubated with 5 µM fura-2/AM in the dark at 37°C for 40 min, while gently shaking (Fontana and Blaustein, 1993). This incubation enabled the internalised fura-2/AM to be hydrolised by non-specific esterases to the non-cell permeable Ca^{2+}-sensitive fura-2 free acid (Figure 3.3). To remove remaining extrasynaptosomal fura-2/AM, the suspension was centrifuged at 500 g for 1.5 min and the supernatant was discarded. The pellet was then resuspended in 2 ml fresh low-Ca^{2+} Krebs bicarbonate buffer and stored on ice until use (within the following 2 h).

3.2.2.3 Calibration of $[Ca^{2+}]_i$ measurements

Ca^{2+} measurements rely on the change in the fluorescent properties of the indicator (fura-2) following Ca^{2+} binding. At equilibrium, the degree of Ca^{2+} saturation of the indicator is related to its free Ca^{2+}concentration according to the mass action equation:

$$Ca^{2+} = K_D ([CaX] / [X])$$

(Equation 3.2)

where **X** is the fluorescent indicator which binds Ca^{2+} with dissociation constant K_D.

With dyes such as fura-2 (K_D = 224 nM) which give a shift in fluorescence spectrum, measurements can be carried out at two excitation wavelengths to obtain signals that are proportional to Ca^{2+}-bound (λ=340 nm) and Ca^{2+}-free indicator (λ=380 nm). The $\lambda_{emission}$ for both excitation wavelengths is 510 nm. The ratio of fluorescence at the two wavelengths is directly related to the ratio of the two forms of the dye and therefore can be used to calculate $[Ca^{2+}]_i$. The equation (Grynkiewicz *et al.*, 1985) which relates the measured Ca^{2+}-bound / Ca^{2+}-free fluorescence ratio (R) to $[Ca^{2+}]_i$ is:

$$[Ca^{2+}]_i = K_D [(R - R_{min}) / (R_{max} - R)] (S_{f2} / S_{b2})$$

(Equation 3.3)

where R_{max} and R_{min} are the fluorescence ratio values under saturating and Ca^{2+}-free conditions respectively and S_{f2} / S_{b2} is the ratio of fluorescence values for Ca^{2+}-bound / Ca^{2+}-free indicator measured at the wavelength used to monitor the Ca^{2+}-free indicator. These are unitless values which depend on the chemical properties of the indicator. Calibration measurements at zero and saturating levels of Ca^{2+} are required to determine the constants R_{min}, R_{max} and S_{f2} / S_{b2}.

Overall, the objective of calibration is to determine the fluorescence levels under the conditions of maximum and minimum Ca^{2+} -binding. This can be achieved by using ionophores (e.g. detergents) which allow extracellular Ca^{2+} to go inside the synaptosome and in turn

saturate the indicator. Subsequently EGTA is added to the preparation to chelate the Ca^{2+} present in the cuvette, allowing the determination of the minimum fluorescence (Figure 3.7 a, c & e). $[Ca^{2+}]_i$ values derived from (Equation 3.3) can be plotted throughout the experiment (Figure 3.7 b, d & f).

In this study, to determine the apparent $[Ca^{2+}]_i$ in synaptosomes, an aliquot (200 µl) of the original suspension of fura-2-loaded nerve terminals, was diluted into 1.8 ml of low-Ca^{2+} Krebs bicarbonate buffer and warmed to 37°C for 5 min. The fluorescent emission of fura-2-loaded synaptosomes was recorded for at least 40 s before adding various reagents. A typical experiment involved the sequential addition of: first, 20 µl 240 mM $CaCl_2$ (final 2.4 mM), followed by 20 µl of either 2 M KCl (final 23.5 mM) or (-)-nicotine (1 mM or 5 mM (final 10 or 50 µM, respectively)). The measurements were made in a thermostated cuvette (37°C) with a PTI dual wavelength spectrophotofluorimeter by alternating the excitation wavelengths of 340±4 nm and 380±4 nm (340 nm / 380 nm fluorescence ratio): fluorescent emission was monitored at 510 nm (Figure 3.3). The samples were continuously mixed with a magnetic stirrer.

Calibration of the fluorescent signals was performed at the end of each experiment by adding 20 µl 20 % SDS (final concentration: 0.2% SDS) to obtain R_{max}, followed by 20 µl 0.5 M EGTA (final concentration: 5 mM EGTA) to obtain R_{min} (Equation 3.3).

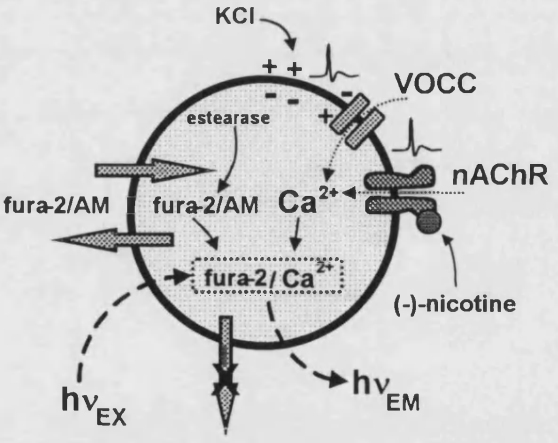

Figure 3.3 Determination of $[Ca^{2+}]_i$ in hippocampal synaptosomes using fura-2/AM. Percoll-purified synaptosomes from rat hippocampus are loaded with the cell-permeable acetoxymethyl derivative of fura-2 (fura-2/AM). During the incubation of synaptosomes with fura-2/AM, cytosolic non-specific esterases hydrolise the indicator to the non-cell permeable Ca^{2+}-sensitive fura-2 free acid. Depolarisation of the synaptosome membrane, either by an increase in the external concentration of KCl or by activation of neuronal nAChR (hypothesis), causes the opening of Voltage Operated Calcium Channels (VOCC) and subsequently an increase in $[Ca^{2+}]_i$. Ca^{2+} binding to the indicator fura-2 shifts its excitation ($h\nu_{EX}$) wavelength from λ=380 nm to λ=340 nm. Fluorescent emission ($h\nu_{EM}$) is monitored at λ=510 nm. Calibration is performed in each experiment by adding SDS (0.2%) and EGTA (5 mM). Intraterminal free Ca^{2+} is calculated using the Grynckiewicz equation (Equation 3.3).

3.2.3 Graphics and statistics

Results are expressed as mean±S.D. of several independent experiments and were analysed for statistical significance using Sigma Stat v.2.0 (Jandel Scientific, Germany). Graphics, plots and curve fittings were done using Sigma Plot for Windows v.2.0 (Jandel Scientific, Germany).

3.2.4 Protein determination

Synaptosome protein concentration was determined using a modification of the Lowry method as described by Markwell *et al.* (1978), using bovine serum albumin as standard.

3.3 Results

3.3.1 L-[^{3}H]-glutamate and D-[^{3}H]-aspartate release from rat hippocampal synaptosomes

Preliminary superfusion experiments intended to examine nicotinic agonist-evoked L-[^{3}H]-Glu and D-[^{3}H]-Asp release from Percoll-purified rat hippocampal synaptosomes. To test the functional status of the preparation, a general depolarising agent (23.5 mM KCl) was applied to evoke neurotransmitter release (Figure 3.4).

After 20 min perfusion with Krebs bicarbonate buffer, the basal release of L-[^{3}H]-Glu or D-[^{3}H]-Asp from hippocampal synaptosomes was constant for the duration of the experiment (following 26 min - Figure). Depolarisation with KCl (23.5 mM 40 s) in the presence of external Ca^{2+} (2.4 mM), caused a significant increase over basal values in L-[^{3}H]-Glu and D-[^{3}H]-Asp release. KCl stimulation (23.5 mM 40 s) evoked the release of 4.18±0.76% (n=4) and 3.06±0.47% (n=2) of the total radioactivity present in synaptosome preparations preloaded with L-[^{3}H]-Glu or D-[^{3}H]-Asp, respectively (Figure 3.5). On return to basal medium (Krebs bicarbonate buffer), the level of labelled amino acid released returned to prestimulation values within 1-2 min (Figure 3.4).

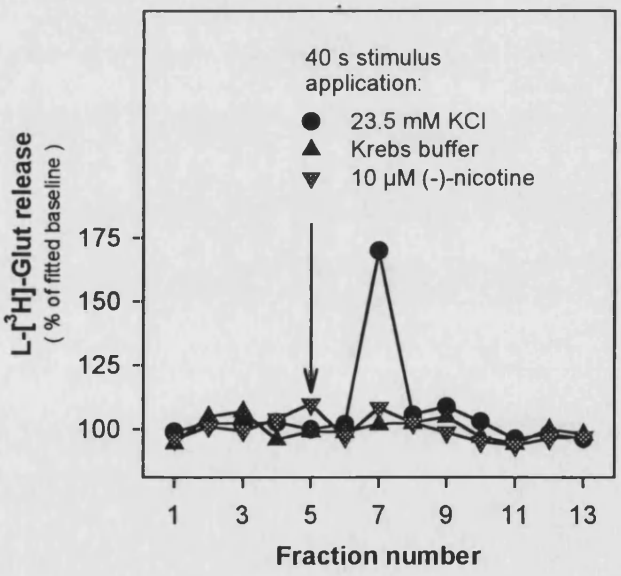

Figure 3.4 Representative superfusion profile for L-[^{3}H]-Glut release from purified rat hippocampal synaptosomes. Hippocampal synaptosomes were prepared and superfused as described in Experimental Procedures (3.2.1.2). Release of L-[^{3}H]-Glu was monitored by superfusion of Percoll-purified synaptosomes (fraction 4 - Percoll gradient 15-23% interface) with Krebs buffer, followed by stimulation (40 s) with KCl (23.5 mM), Krebs buffer or (-)-nicotine (10 µM). Fractions were collected every 2 min and counted for radioactivity. Superfusion profiles were normalised as percentages of the fitted baselines. In this particular experiment, KCl (23.5 mM) released 3.7% of total radioactivity present in the sample before stimulation.

(-)-Nicotine and (±)-AnTx-a were used to assess the nicotinic agonist-evoked release of labelled neurotransmitter from Percoll-purified hippocampal synaptosomes. (-)-Nicotine (1,10 & 25 μM) and (±)-AnTx-a (1 μM) failed to elicit significant release of L-[^{3}H]-Glu or D-[^{3}H]-Asp from this preparation (Figure 3.5- type IA current EC_{50} values for (-)-nicotine and Antx-a are 27 μM and 3.9 μM, respectively - Alkondon and Albuquerque, 1993). Differences between responses evoked by nicotinic agonists and Krebs buffer pulses were not significant (Figure 3.5 – $p>0.05$ - one way ANOVA).

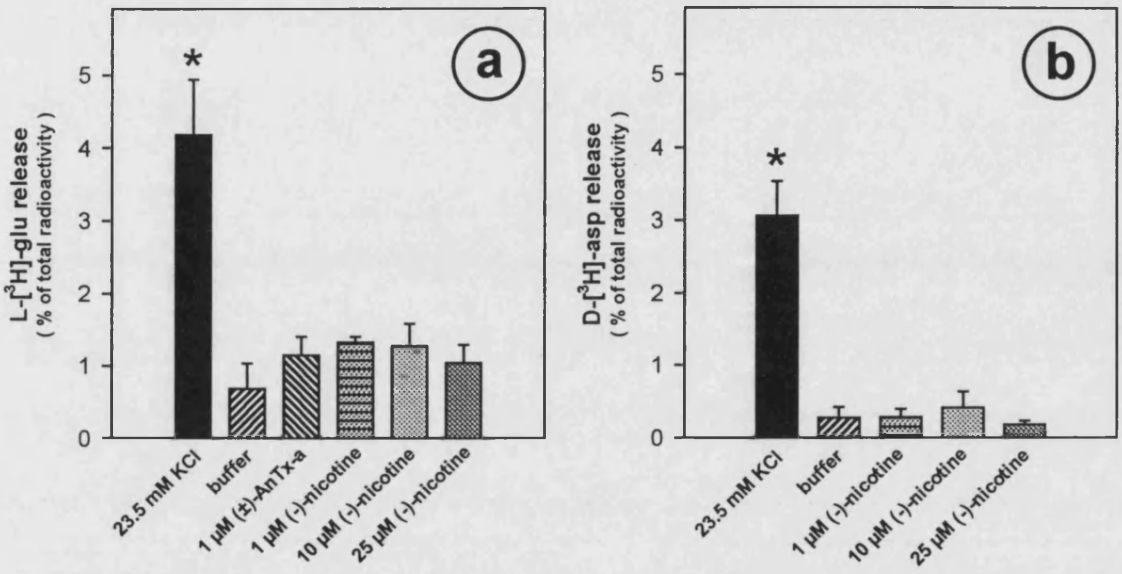

Figure 3.5 KCl- and nicotinic agonist-evoked release of (a) L-[^{3}H]-Glu and (b) D-[^{3}H]-Asp, from rat hippocampal synaptosomes. Percoll-purified hippocampal synaptosomes were prepared and perfused as described in 3.2.1.2. Release of L-[^{3}H]-Glu or D-[^{3}H]-Asp was monitored by superfusion of Percoll-purified synaptosomes (Percoll gradient 15-23% interface) with Krebs buffer followed by stimulation (40 s) with KCl (23.5 mM), Krebs buffer or nicotinic agonists. No significant differences were observed between the responses evoked by Krebs buffer and those elicited by nicotinic agonists (1, 10 & 25 μM (-)-nicotine and 1 μM (±)-AnTx-a). However, KCl (23.5 mM) significantly increased the release of labelled neurotransmitter. Responses were calculated as percentage of radioactivity released from total label present in the sample before stimulation. Results are expressed as mean±S.D. of several independent experiments (n=2-4).
(* $p<0.05$ significantly different from response evoked by a Krebs buffer pulse – Student *t* test)

3.3.2 Fluorescence Ca^{2+} studies using fura-2/AM

Hippocampal nerve terminal $[Ca^{2+}]_i$ values were determined before and after stimulation with KCl or nicotinic agonists, by fura-2 fluorescence analysis ($[Ca^{2+}]_o$ = 2.4 mM).

3.3.2.1 Effects of $[Ca^{2+}]_o$ and $[K^+]_o$ on hippocampal nerve terminals $[Ca^{2+}]_i$

The fluorescent calcium probe fura-2, have been extensively used to determine $[Ca^{2+}]_i$ in synaptosomes under resting and activated conditions (e.g. Budd *et al.*, 1996; Martinez Serrano *et al.*, 1996; Larsen *et al.*, 1998). These studies were performed with synaptosomes bathed in buffer containing a physiological external Ca^{2+} concentration of ~1-2 mM. To evaluate the effect of $[Ca^{2+}]_o$ on unstimulated hippocampal synaptosomes $[Ca^{2+}]_i$, they were resuspended in buffer containing a reduced $[Ca^{2+}]_o$ (0.02 mM) and later challenged with a higher $[Ca^{2+}]_o$ (2.4 mM).

In unstimulated synaptosomes incubated in low Ca^{2+} Krebs buffer containing 0.02 mM $CaCl_2$, the apparent resting $[Ca^{2+}]_i$ was 164±17 nM (n=9). This value was only modestly affected by changes in $[Ca^{2+}]_o$. When the Ca^{2+} in the buffer was increased 120 fold, to 2.4 mM, the apparent resting $[Ca^{2+}]_i$ increased only 27%, to 209±21 nM (n=9) (this difference was not statistically significant – $p>0.05$ one way ANOVA). The effect of increasing $[K^+]_o$ on $[Ca^{2+}]_i$ was determined in buffer containing 2.4 mM $CaCl_2$. High $[K^+]_o$ (23.5 mM) increased $[Ca^{2+}]_i$ by 268%, from 195±32 nM to 523±80 nM (n=3) (Figure a, b - difference statistically significant $p<0.05$ one way ANOVA – Bonferroni *t* test). When $[K^+]_o$ was increased to 23.5 mM, $[Ca^{2+}]_i$ reached a maximum within 1-2 s (Figure 3.6) and then remained constant, presumably because most of the voltage operated Ca^{2+} channels were then inactivated (Naschen and Blaustein, 1980).

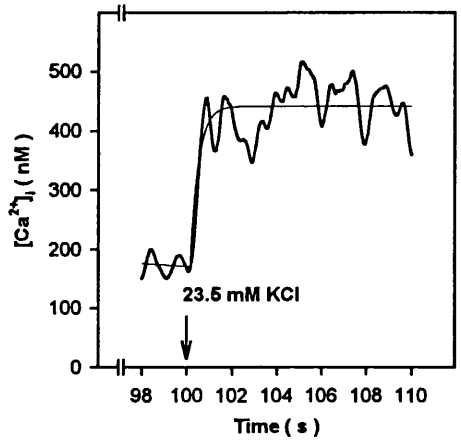

Figure 3.6 Representative time-course plot of 23.5 mM KCl-evoked changes in $[Ca^{2+}]_i$ of hippocampal synaptosomes at $[Ca^{2+}]_o$ = 2.4 mM. Percoll-purified hippocampal synaptosomes were prepared and loaded with fura-2/AM as described in 3.2.2. KCl-evoked depolarisation (arrow) of nerve terminals membrane, increased $[Ca^{2+}]_i$ to a maximum within 1-2 s. In this experiment, high $[K^+]_o$ (23.5 mM) increased $[Ca^{2+}]_i$ by 259%, from 170 nM to 441 nM. Raw data were fitted to an exponential function using Sigma Plot software (thin line plot).

3.3.2.2 (-)-Nicotine induced Ca^{2+} influx

To date there are no published studies related to (-)-nicotine-evoked Ca^{2+} influx in rat hippocampal synaptosomes loaded with fura-2. Preliminary trials (n=6) were carried out to evaluate putative (-)-nicotine-evoked $[Ca^{2+}]_i$ increases in Percoll-purified hippocampal synaptosomes loaded with fura-2.

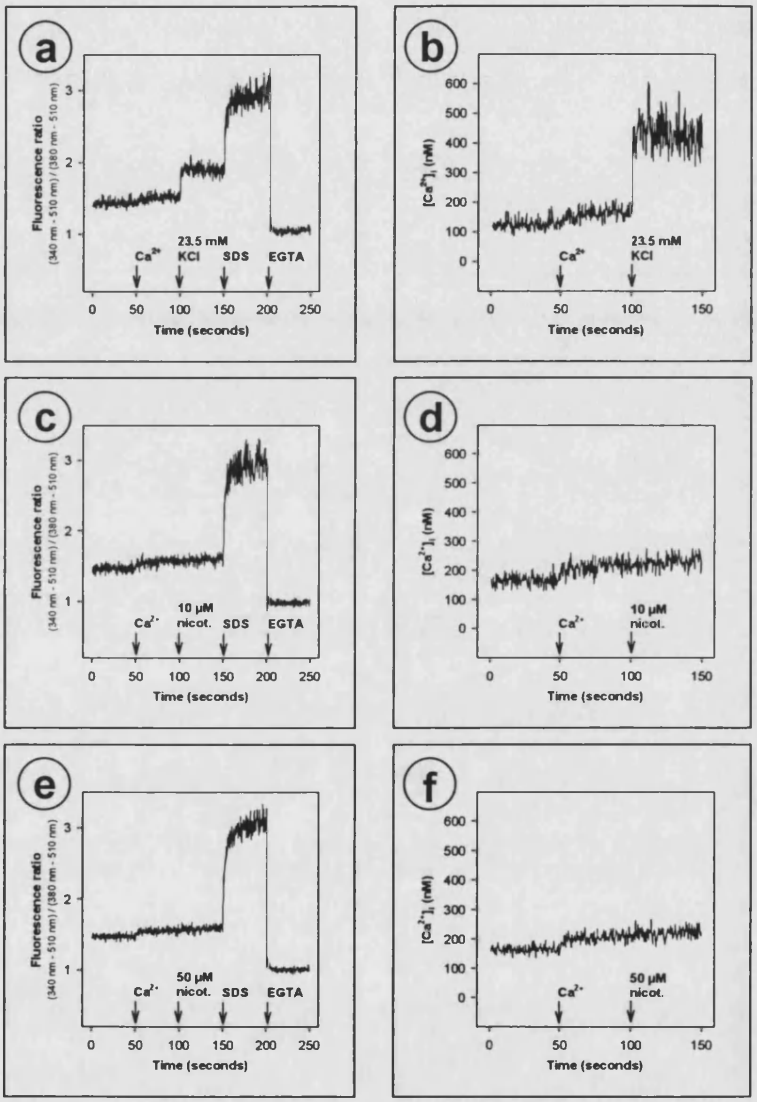

Figure 3.7 Effect of KCl and (-)-nicotine on hippocampal nerve terminals $[Ca^{2+}]_i$. Representative traces showing variations in synaptosome preparations fluorescence ratio and $[Ca^{2+}]_i$ in response to KCl (23.5 mM - **a** & **b**) and (-)-nicotine (10 µM (**c** & **d**) and 50 µM (**e** & **f**). Percoll-purified hippocampal synaptosomes were prepared and loaded with fura-2/AM as described in 3.2.2. Before increasing $[Ca^{2+}]_o$ to 2.4 mM (at 50 s), the effect of a lower $[Ca^{2+}]_o$ (0.02 mM) on the nerve terminal resting $[Ca^{2+}]_i$ was determined. Calibration was carried out with SDS (0.2%) and EGTA (5 mM) to determine maximum and minimum fluorescence, respectively (a, c & e). Corresponding $[Ca^{2+}]_i$ values, derived from the Grynkiewicz equation (Equation 3.3) are shown in b, d & f.

Two different concentrations of (-)-nicotine were chosen to stimulate the synaptosome preparations: 10 µM and 50 µM (Figure 3.7, c-f). The lower concentration was previously found to evoke maximum [^{3}H]-ACh release from Percoll-purified (fraction 4 - Percoll gradient 15-23% interface) rat hippocampal synaptosomes (EC_{50} = 0.99±0.23 µM - Wilkie *et al.*, 1996). The higher concentration of (-)-nicotine (50 µM) was chosen because in Ca^{2+} influx studies performed on rat E18 hippocampal neurones (monolayers) loaded with fura-2, it rendered the most reproducible and consistent responses (Barrantes *et al.*, 1995). Moreover, Type IA currents have an EC_{50} value for (-)-nicotine of 27 µM (Alkondon and Albuquerque, 1993) so 50 µM (-)-nicotine should give a near-maximum response.

Neither 10 µM nor 50 µM (-)-nicotine evoked detectable Ca^{2+} influx (Figure 3.7, c-f). The $[Ca^{2+}]_i$ increase after applying 10 µM and 50 µM (-)-nicotine was: from 218±3 nM to 226±7 nM (n=3); and from 214 ± 6 nM to 219 ± 4 nM (n=3), respectively (differences non statistically significant $p>0.05$ one way ANOVA). It is important to bear in mind that under the same experimental conditions, 23.5 mM KCl increased $[Ca^{2+}]_i$ by 268% above baseline (buffer containing ~ 3.5 mM $[K^+]_o$).

3.4 Discussion

The aim of these preliminary studies was to examine the role of α-Bgt-sensitive presynaptic nAChR in modulating glutamatergic neurotransmitter release in rat hippocampal preparations.

Experimental approaches other than electrophysiological techniques and Ca^{2+} imaging (Gray *et al.*, 1996; Radcliffe and Dani, 1998), have also been applied to the study of glutamate release in hippocampus. For instance, *in vivo* studies (Toth, 1996; Fedele *et al.*, 1998) showed that hippocampal microdialysis administration of (-)-nicotine specifically increased local extracellular levels of glutamate and aspartate, suggesting the involvement of nAChR in their release. On the other hand, *in vitro* assays using hippocampal slices (Keith *et al.*, 1995; Talke and Bickler, 1996) and nerve terminal preparations (Gannon *et al.*, 1992; Terrian *et al.*, 1993; Rodriguez *et al.*, 1997; Breukel *et al.*, 1997; HelmeGuizon *et al.*, 1998) have been extensively used to study the effect of different drugs (e.g. VOCC blockers, α2-adrenergic agonists, kappa opiod agonists, phorbol esters (PDBu), histamine, arachidonic acid) on general depolarising agent-evoked glutamate release or on the intraterminal mechanisms underlying it. *In vitro* studies on slices have also shown depolarisation-evoked aspartate release in rat hippocampus (Klancnik *et al.*, 1992; Keith *et al.*, 1994, 1995). However, attempts to demonstrate directly the nicotinic presynaptic modulation of hippocampal glutamate/aspartate release using a neurochemical approach have been largely unsuccessful (e.g. Wonnacott *et al.*, 1995).

In this study a perfusion system was used to examine labelled L-glutamate/D-aspartate release from synaptosomes prepared from rat hippocampi. The purity and viability of the synaptosomal preparation is crucial for the execution of this technique. To fulfil these criteria, hippocampal synaptosomes isolated by the discontinuous Percoll method were used (Dunkley *et al.*, 1988). When compared with conventional sucrose density fractionation (Rapier *et al.*, 1987), this procedure is faster, suitable for smaller amounts of tissue and employs an isotonic medium (Thorne *et al.*, 1991; Taupin *et al.*, 1994). The use of Percoll gradients for isolating hippocampal "nerve terminals" yields synaptosomes in four of the five fractions from the gradient (Thorne *et al.*, 1991). Previous reports have shown that hippocampal fraction 4 (Percoll gradient 15-23% interface) is enriched in intact viable synaptosomes that are relatively free with contamination from lysed synaptosomes and synaptic plasma membranes (Dunkley *et al.*, 1988; Thorne *et al.*, 1991). The highest uptake of [^{3}H]-GABA and [^{3}H]-choline in terms of mg of protein and the highest [^{3}H]-(-)-nicotine binding levels were also found in this fraction (Thorne *et al.*, 1991). Moreover, it has been demonstrated that hippocampal mossy fibre synaptosomal preparations obtained in the Percoll gradient 15-23% interface fraction, release glutamate in a Ca^{2+}-dependent manner when depolarised (Terrian *et al.*, 1988; Taupin *et al.*, 1994).

Although this preliminary study did not compare the Percoll gradient fractions obtained for L-[^{3}H]-Glu/D-[^{3}H]-Asp uptake, the results presented in this chapter demonstrate that Percoll-purified hippocampal synaptosomes from fraction 4 (15-23% interface), are capable of releasing labelled neurotransmitter (L-[^{3}H]-Glu or D-[^{3}H]-Asp) upon K^+ (23.5 mM) induced depolarisation, indicating the presence of viable glutamatergic nerve terminals in the preparation.

Previous studies (e.g. Verhage *et al.*, 1989) reported a steep increase in hippocampal synaptosome KCl-evoked glutamate release in the range 3-30 mM $[K^+]_o$ (maximal release at $[K^+]_o$ = ~50 mM - e.g. Taupin *et al.*, 1994; Rodriguez *et al.*, 1997). The effectiveness of K^+ depolarisation in inducing the release of L-[^{3}H]-Glu from preloaded hippocampal synaptosomes has been reported to change during rat post-natal development (Collard *et al.*, 1993), between PND4 (post-natal day 4) and PND15 the response was smaller than that seen in adult rats, the stage at which the sensitivity of the release reached a maximum level. On the other hand, Gray *et al.* (1996) used hippocampal slices from adult rats (PND 20- 63) to demonstrate that a puff of nicotine (~20 µM) elevates $[Ca^{2+}]_i$ in mossy-fibre presynaptic terminals (α-Bgt-sensitive response). In this study, L-[^{3}H]-Glu/D-[^{3}H]-Asp released by KCl (23.5 mM) from adult rat (PND>14) Percoll purified hippocampal synaptosomes, was used to test the functionality of the system (i.e. as positive control). Moreover, the values obtained in this study for KCl-evoked L-[^{3}H]-Glu/D-[^{3}H]-Asp release from hippocampal nerve terminals (Figure 3.5) are in perfect concordance with those reported by Taupin *et al.* (1994) for KCl-evoked release of the same neurotransmitters from a Percoll-purified (15-23% interface) mossy fibre nerve terminal preparation.

"Slow application" (seconds to minutes) of low micromolar (-)-nicotine concentrations enabled the neurochemical detection of ACh (Wilkie *et al.*, 1996), noradrenaline (Clarke and Reuben, 1996) and GABA (Lu *et al.*, 1998) release from hippocampal preparations, despite the pharmacological and kinetic properties of the nAChR involved (reviewed in the general introduction). Gray *et al.* (1996) demonstrated that the release of glutamate from mossy fibre nerve terminals is modulated by presynaptic α7-containing nAChR, equated with type IA responses in hippocampal neurones (EC_{50} values are 27 µM and 3.9 µM for (-)-nicotine and AnTx-a, respectively (Alkondon and Albuquerque, 1993)). Therefore, the (-)-nicotine (1, 10 & 25 µM) and (±)-AnTx-a (1µM) concentrations used in this study should have been sufficient to evoke responses. However, this study was unable to demonstrate nicotinic agonist-evoked L-[^{3}H]-glutamate release from hippocampal synaptosomes, probably because the superfusion technique is too slow given that α7 nAChR-mediated neurotransmitter release has been only detected with fast perfusion systems (msec) in electrophysiological studies.

Fluorescence studies using fura-2 were also carried out on the same biological preparation to explore changes in $[Ca^{2+}]_i$ as a consequence of KCl- and nicotinic agonist-induced nerve terminal depolarisation. A number of labs have previously used the fluorescent indicator fura-2 in hippocampal slices (Talke and Bickler, 1996) and synaptosomes (Bartschat and Rhodes, 1995; Martinez Serrano *et al.*, 1996) to study the effect of different chemical species (e.g. α2-adrenergic agonists, phorbol esters (PMA), okadaic acid, NO, arachidonic acid) on the apparent $[Ca^{2+}]_i$ before and after KCl-stimulation.

Studies correlating neurotransmitter release with increase in nerve terminal $[Ca^{2+}]_i$ have shown that an elevation of $[Ca^{2+}]_i$ <330 nM is ineffective in inducing release of transmitters and that a steep increase in release effectiveness is attained at a mean $[Ca^{2+}]_i$ between 350 and 400 nM (Adam-Vizi and Ashley, 1987; Knight, 1987; Verhage *et al.*, 1989). In this study elevation of $[K^+]_o$ to 23.5 mM, increased resting levels of $[Ca^{2+}]_i$ to ~520 nM and, consistent with the results of Verhage *et al.* (1989), 23.5 mM KCl evoked the release of labelled neurotransmitter by ~400% above baseline (see Figure 3.5).

In this thesis and consistent with previous values reported for the same Percoll purified hippocampal preparation (e.g. Verhage *et al.*, 1989), $[Ca^{2+}]_i$ resting levels fell in the range 150-250 nM. However, factors that may contribute to explain differences between results reported by different labs include the sequestration of fura-2 in intraterminal organelles and the presence of damaged terminals in the preparations (Fried and Blaustein, 1978). Fura-2 when loaded as the membrane-permeable acetoxymethyl ester, may not be confined to the cytosol, but may also be concentrated in intracellular organelles such as the ER (Goldman and Blaustein, 1990) and mitochondria (Miyata *et al.*, 1991) altering basal $[Ca^{2+}]_i$ level measurement. In addition, some damaged nerve terminals may be able to concentrate fura-2, but may nevertheless be relatively leaky to Ca^{2+} and have high $[Ca^{2+}]_i$ levels. The observed resting potentials represent the average $[Ca^{2+}]_i$ in the entire population of "normal" and damaged nerve terminals. The presence in the sample of damaged or non responding synaptosomes, could also affect the apparent $[Ca^{2+}]_i$ increase evoked by high $[K^+]_o$. In addition, KCl-evoked $[Ca^{2+}]_i$ increases may also have been underestimated because of the relatively slow time "resolution" of the recordings performed (seconds rather than milliseconds). It is possible that the increases in different nerve terminals within the preparation may be non-synchronous, so that $[Ca^{2+}]_i$ may be still increasing in some terminals while it is already decreasing in others.

The present work has shown that, in contrast to KCl, nicotinic agonists failed to evoke the release of labelled amino acids from Percoll-purified hippocampal synaptosomes. Fluorescence studies with fura-2 (this study) allowed the detection of KCl-evoked Ca^{2+} influx because the general depolarisation affected in a sustained way, if not all, a high percentage of the synaptosomes present in the preparation. When using (-)-nicotine as the stimulus, it was initially expected to detect some signal (increase in $[Ca^{2+}]_i$), at least due to the activation of non-α7-containing nAChR present on non-glutamatergic nerve terminals. However, no significant (-)-nicotine-evoked increase in intraterminal Ca^{2+} was detected.

As early as in 1993, Sargent suggested that the extremely rapid desensitisation of the α7-containing nAChR was making it considerably difficult to study. Recent studies have shown that some nAChR can be desensitised by concentrations of agonists that are too low to activate the receptor directly (Grady *et al.*, 1994; Marks *et al.*, 1996). Moreover, Frazier *et al.* (1998a) have shown that postsynaptic α7-containing nAChR located on CA1 interneurones, cannot be activated by bath superfusion with agonists and can be easily desensitised by the leakage of small amounts of agonist from drug-containing pipettes. These experiments suggested that successful nAChR activation requires techniques that permit both the rapid application and rapid removal of agonist (Alkondon and Albuquerque, 1993; Frazier *et al.*, 1998a; Radcliffe and Dani, 1998). Thus, from a functional point of view, the slow application of low concentrations of (-)-nicotine (100 nM - 1 μM) has an antagonistic rather than an agonistic effect on transmission at these synapses. Frazier *et al.* (1998a) also showed that α7-containing nAChR on interneurones can be desensitised completely by nanomolar concentrations of (-)-nicotine, and that this occurs under conditions in which the possibility of a presynaptic action of nicotine (e.g. release of neurotransmitters) is blocked. These results suggest an important determinant of the effects of (-)-nicotine in the brain may be the rate of desensitisation and that this can differ even for receptors that are thought to belong to the same receptor subclass. It has also been suggested e.g. Sargent, 1993; Anand *et al.*, 1993) that there may be multiple populations of α7-containing receptors (but see Chen and Patrick, 1997), each exhibiting similar sensitivity to MLA and α-Bgt but having different kinetics that arise as a result of the incorporation of other receptor subunits. In this respect, a recent study by Cuevas and Berg (1998) reported that a α7-containing receptor is responsible for the slowly desensitising, α-Bgt-reversible nicotinic response observed in rat intracardiac ganglia. Further experiments are needed to see if the differences in desensitisation are due to the presence of non-α7 subunits or the result of receptor localisation regulation within the neurone.

At the present time, neurochemical techniques appear to lack the temporal resolution to demonstrate α7-mediated transmitter release (but see Turner and Dunlap, 1995 for a fast superfusion system that measures neurotransmitter release on a sub-second timescale). However, it may be possible to detect such mechanisms indirectly (see chapter 5).

Section II: Basal ganglia: the neostriatum

A brief story of the basal ganglia

It was as early as 1664 when the first clear identification of distinct subcortical structures was published by the English anatomist Thomas Willis. What is now functionally known as the basal ganglia was then referred to as the corpus striatum. It held such a central position, striped with a wide range of cortical and brainstem fibres, that at the time it was thought to both receive all sensory modalities and initiate all motor acts. This idea appeared to be anatomically reinforced by its central position and clearly visible ascending and descending fibre systems.

Two subsequent events relegated the corpus striatum to an obscure and less defined position. The attractiveness of the histological organization of the cortex, and the possibility of localizing higher mental functions drew many neurologists of both the 18th and 19th centuries to cortical research. Amongst those that continued studying the corpus striatum, there was a sudden realisation that many of the functions originally assigned to it were in fact properties of neighbouring corticospinal paths.

At the beginning of the 20th century there were serious attempts to provide detailed comparative descriptions of the corpus striatum. It began to gain importance once again with the discoveries that lesions of these areas would often result in disorders of motor functions in humans. The corpus striatum came to be viewed as the major components of the "extrapyramidal motor system". This term loosely grouped the corpus striatum with an array of brain stem nuclei and reflected the assumption that this grouping constituted a complete and independent motor unit. The term "basal ganglia" has been generally used to refer to these major anatomical telencephalic subcortical nuclei at the base of the forebrain. More formally this definition groups the corpus striatum (**neostriatum** (putamen & caudate nucleus) and **globus pallidus**) with the **substantia nigra** and **subthalamic nucleus** (Figure IIa).

Motor control overview

Motor control occurs in a three-level hierarchy. The spinal cord is the "most primitive", controlling reflex and stereotypical actions. Integration of sensory and vestibular information occurs in the brain stem, which controls posture, eye, and head motions. The apex of the motor hierarchy is the cerebral cortex, in particular the primary motor cortex, the lateral premotor area, and the supplementary motor area.

It appears that the supplementary motor area is concerned with programming sequences of movements whereas the premotor area is concerned with the selection of movement plans based on external cues. Motor activity is also modified by the cerebellum and basal ganglia.

Both the cerebellum and the basal ganglia receive input from the cerebral cortex and send output to the cortex via the thalamus. The three major differences between the connections of the cerebellum and the basal ganglia are:

- the cerebellum receives input only from the sensorimotor parts of the cortex, whereas the basal ganglia receive input from the entire cerebral cortex.
- the cerebellum output goes only to the premotor and motor cortex, while the basal ganglia also project to the prefrontal association cortex.
- the cerebellum has direct ties with the spinal cord and the brain stem. The basal ganglia have little connection to the brainstem, and no direct connections with the spinal cord.

The cerebellum apparently modifies the output of motor systems to bring intention into line with performance; it acts as a "comparator". It has been suggested that the cerebellum is a very large associative memory. It is thought that the cerebellum regulates motion directly, whereas the **basal ganglia** have to do with the **planning and execution of complicated motor strategies.**

Basal ganglia components and pathways

The **neostriatum** serves as the **input centre for the basal ganglia.** The primary input comes from the cerebral cortex; there is a secondary input from the thalamus. Specific areas of the cortex map to specific parts of the striatum. These associations are maintained in projections throughout the basal ganglia.

The **globus pallidus** is divided into internal and external segments (Figure IIb). The internal section is one of two main output nuclei of the basal ganglia, along with the substantia nigra *pars reticulata.* The pallidal output is passed by the thalamus primarily to the supplementary motor area, and possibly also to the premotor cortex. The supplementary motor area is also a major input to the basal ganglia; therefore there is a loop between the supplementary motor area and the basal ganglia. As mentioned earlier, it appears that the supplementary motor area is involved with planning sequences of movements. The loop between the supplementary motor area and the basal ganglia therefore provides a clue to the function of the basal ganglia. The external section of the globulus pallidus passes information within the basal ganglia, in particular to the subthalamic nucleus (Figure IIb).

The **subthalamic nucleus** takes the output from the motor and premotor cortices, and from the external segment of the globus pallidus. The subthalamic nucleus projects to both segments of the globus pallidus and to the substantia nigra *pars reticulata.* The substantia nigra, along with the internal globus pallidus, is one of the two major output sections of the basal ganglia.

There are two major pathways through the basal ganglia, arising from different cellular populations of the neostriatum. The inhibitory **direct pathway** projects monosynaptically from the putamen to the motor regions of the internal globus pallidus and the substantia nigra *pars reticulata*. The **indirect pathway** is inhibitory from the putamen to the external globus pallidus, inhibitory from there to the subthalamic nucleus, and excitatory to the external globus pallidus or substantia nigra *pars reticulata*. It appears that the net effect of the direct pathway is to facilitate motion by exciting the supplementary motor area; the indirect pathway has the opposite effect.

In addition (and crucially for Parkinsons' disease), there is a loop from the neostriatum to the **substantia nigra *pars compacta*** and back to the striatum (Figure IIb). The return route is mediated by dopamine. Dopamine excites the direct pathway and inhibits the indirect pathway: since these two pathways have opposing effects, dopamine tends to facilitate motion. In effect, as it will be seen later, the dopamine terminals are in a position to influence information coming from cortex into the neostriatum. There are also reciprocal inhibitory connections between the internal and external segments of the globus pallidus.

The **major output of the basal ganglia**, from the **internal globus pallidus** and the **substantia nigra *pars reticulata***, project to three nuclei in the thalamus: the ventral lateral, ventral anterior and mediodorsal. These thalamic nuclei in turn project to the prefrontal cortex, the premotor cortex, the supplementary motor area, and the motor cortex.

From an input-output analysis, therefore, the basal ganglia do not appear to generate motions directly; they take input from the cortex, modify it in some way, and pass it back to the cortex (via the thalamus).

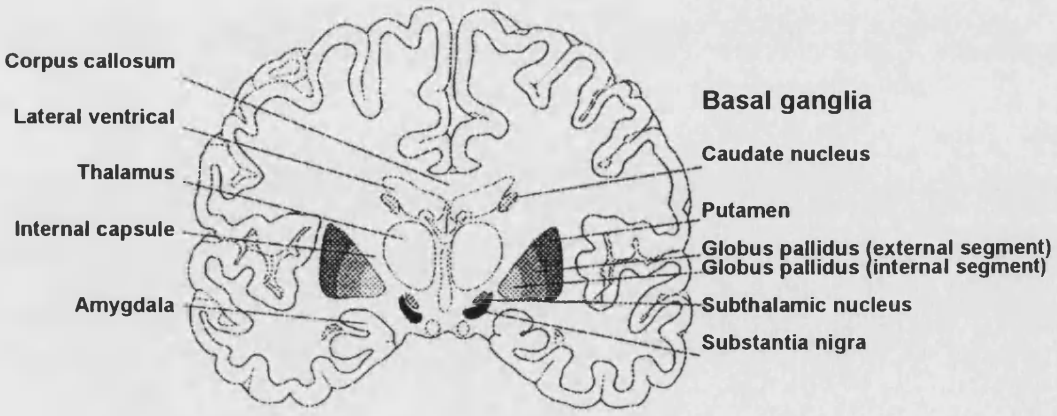

Figure IIa A coronal section of the cerebral hemispheres shows the basal ganglia in relation to surrounding brain structures. (From Kandel *et al.*, 1995)

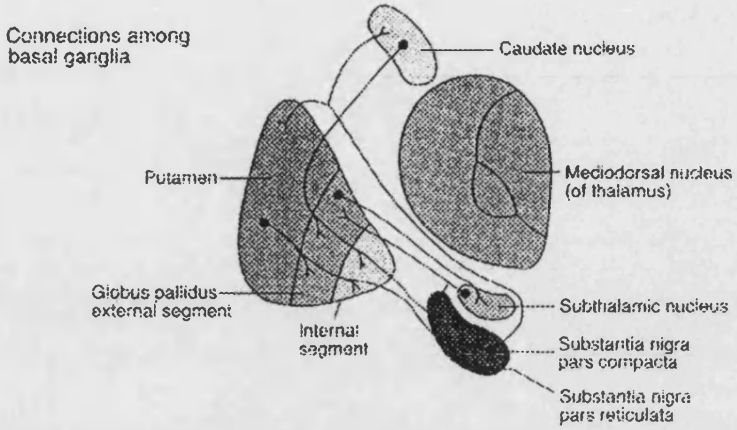

Figure IIb All of the basal ganglia are interconnected by topographically organised projections. Cells in different parts of the caudate and putamen project to specific areas of the globus pallidus and substantia nigra. Thus, because the pathways are all topographically organised, specific areas of the cortex act through the neostriatum on specific parts of the globus pallidus and substantia nigra. The subthalamic nucleus receives the output of the external segment of the globus pallidus and projects to both segments of the globus pallidus and the substantia nigra *pars reticulata*. It also receives inputs from the primary motor and premotor cortices (not shown). The neostriatum receives an important dopaminergic projection from the substantia nigra *pars compacta*. The major output pathways of the basal ganglia (not shown) arise from the internal segment of the globus pallidus and the substantia nigra *pars reticulata*. These pathways terminate in several nuclei in the thalamus; which in turn project to several areas of cortex: the prefrontal cortex, the premotor cortex, the supplementary motor area, and the primary motor cortex. (From Kandel *et al.*, 1995)

Diseases of the basal ganglia

As with brain research generally, much of what is known about the basal ganglia comes from studying diseases that affect them. This section briefly outlines the range of diseases that are caused by damage to the basal ganglia.

Damage to both the basal ganglia and the supplementary motor area are correlated with impaired performance on sequential tasks. The "theme" of diseases affecting the basal ganglia appears to be that the balance between the two major pathways is disturbed: the result is either **involuntary movements or impairments to motion**.

The impaired motions include: akinesia (lack of movement), bradykinesia (slowness of movement) and the shuffling gait of Parkinson's disease. The list of involuntary movements includes: tremors (rhythmic, involuntary, oscillatory movements), athetosis (slow, writhing movements of the fingers and hands, and sometimes of the toes), chorea (abrupt movements of the limbs and facial muscles), ballism (violent, flailing movements) and dystonia (a persistent posture of a body part which can result in grotesque movements and distorted positions of the body).

The major diseases of the basal ganglia are:

- **Parkinsons' disease** is related to a reduction of dopamine in the brain and damage to the dopaminergic pathway from the substantia nigra pars compacta to the neostriatum. The result is an increased output of the basal ganglia to the thalamus. The major symptoms are tremor, rigidity and akinesia.
- **Huntingtons' disease** is caused by a loss of specific striatal neurons. The result is a decreased output of the basal ganglia to the thalamus (as opposed to the increased output due to Parkinsons'). As one might expect from their opposing neural behaviour, Huntingtons' disease results in hyperkineticity, in opposite to the hypokineticity of Parkinsons' disease.
- **Ballism** is tied to damage to the subthalamic nucleus. It causes severe involuntary movements, which tend to slowly diminish.
- **Tardive dyskinesia** is related to changes in the dopaminergic receptors, causing hypersensitivity to dopamine. It causes abnormal involuntary movements, particularly of the face and tongue.

The facilitation of catecholamine release, particularly dopamine release, by nAChR is well documented, especially at the level of the terminal projections *in vitro* (Wonnacott, 1997; general introduction in this thesis). In **section II**, the superfusion technique was used to explore the following aspects of the nicotinic modulation of dopamine release in rat neostriatum:

1) identification of presynaptic and/or preterminal nAChR subtypes modulating striatal dopamine release (this thesis chapters 4 & 5)
2) functional crosstalk between striatal nerve terminals as a consequence of nAChR stimulation (this thesis chapter 5), and
3) second messenger mechanisms underlying nicotinic agonist-evoked striatal dopamine release (this thesis chapter 6)

4 A heterogeneous population of nAChR on dopaminergic nerve terminals directly modulates dopamine release in rat striatum

4.1 Introduction

Parkinsonism, as mentioned before, is linked to degeneration and loss of dopaminergic neurones, particularly those in the *pars compacta* of the substantia nigra. The etiology and mechanisms underlying this pathology are not well understood. Epidemiological evidence suggests that the incidence of Parkinsons' syndrome is lower in tobacco smokers than in non-smokers (Morens *et al.*, 1995), and in animals (-)-nicotine exerts a neuroprotective effect on lesions of the nigrostriatal dopamine system (Janson *et al.*, 1986). *In vitro* studies have demonstrated that (-)-nicotine can modulate dopamine (DA) release from striatal nerve terminals by acting on nAChR (Rapier *et al.*, 1990; Grady *et al.*, 1992; Soliakov *et al.*, 1995). Thus, nAChR represent candidate targets for the development of therapeutic agents (Williams *et al.*, 1994; Decker *et al.*, 1994; Holladay *et al.*, 1997).

The modulation of striatal DA release by nAChR is well documented, especially at the level of the terminal projections *in vitro* (Wonnacott, 1997). For example, nicotinic agonists evoke DA release from striatal synaptosomes (Rapier *et al.*, 1988; Grady *et al.*, 1992; El-Bizri and Clarke, 1994; Kaiser *et al.*, 1998) and slices (Sacaan *et al.*, 1995; Kaiser *et al.*, 1998). Nicotine elicits Ca^{2+}-dependent [^{3}H]-DA release from rat striatal synaptosomes in a concentration dependant, mecamylamine sensitive and stereospecific manner (Rapier *et al.*, 1988; El-Bizri and Clarke, 1994; Soliakov *et al.*, 1995), consistent with the activation of presynaptic nAChR (Wonnacott, 1997). However, the nAChR subtypes responsible have not been identified, largely reflecting a lack of subtype-selective pharmacological tools. Inhibition by n-Bgt has been interpreted in favour of α3-containing nAChR (Grady *et al.*, 1992), while the full (Grady *et al.*, 1992) or reduced but substantial efficacy of cytisine (El-Bizri and Clarke, 1994) could implicate the β4 subunit (Luetje and Patrick, 1991). On the other hand, nigrostriatal lesions produced a loss of striatal high affinity agonist binding sites, consistent with there being α4β2 nAChR on DA terminals (Clarke *et al.*, 1985).

Recently, a novel *Conus* toxin, α-conotoxin-MII (α-CTx-MII; see Figure 4.1) was described as a potent and selective antagonist at a nAChR subtype composed of α3 and β2 subunits (Cartier *et al.*, 1996; Harvey *et al.*, 1997). Here, this peptide was exploited to evaluate the contribution of the α3β2 subunit combination to the presynaptic modulation of striatal DA release. In this study the novel nicotinic agonist UB-165, an anatoxin-a/epibatidine hybrid (Wright *et al.*, 1997), was also assayed and used to evoke DA release from rat striatal synaptosomes.

This study reports:

1) the partial and differential inhibition by α-CTx-MII of the nicotinic stimulation by (±)-anatoxin-a of [^{3}H]-DA release from rat striatal synaptosomes and slices. These findings, which corroborate and extend the recent study by Kulak *et al.* (1997), have been published (Kaiser *et al.*, 1998).
2) the UB-165 selectivity for α3β2-containing nAChR when evoking DA release from rat striatal synaptosomes.

4.2 Experimental procedures

4.2.1 Materials

Male Sprague-Dawley rats were obtained from the University of Bath Animal House breeding colony. [7,8-^{3}H]-dopamine ([^{3}H]-DA - specific activity, 1.78 TBq / mmol) was purchased from Amersham International (Amersham, Bucks UK). α-Conotoxin-MII (α-CTx-MII Figure 4.1; Cartier *et al.*, 1996; Kaiser *et al.*, 1998) and (±)-UB-165 (Wright *et al.*, 1997) were synthesised as previously described. Tetrodotoxin (TTX) was obtained from Tocris Crookson (Bristol, UK). (±)-Epibatidine and methyllycaconitine (MLA) were purchased from RBI (Nateck, MA USA). (-)-Cytisine, mecamylamine, pargyline and nomifensine were purchased from Sigma (Poole, Dorset UK). All other chemicals used were of analytical grade and obtained from standard commercial sources.

4.2.2 α-CTx-MII synthesis

α-CTx-MII was synthesised at the University of Bath with correct disulphide bond formation exactly as described by Cartier *et al.* (1996). The linear peptide was produced using a Miligen 9050 peptide synthesiser. Because the peptide has two disulphide bonds (Figure), these were subsequently formed sequentially under controlled conditions, by incorporating acid-labile S-trityl cysteine in positions 3 and 16, and acid-stable S-acetamidomethyl cysteine in positions 2 and 8, as described (Cartier *et al.*, 1996). The peptide was isolated by solid phase extraction (recovery 68%) followed by reverse phase HPLC. The peak corresponding to the bicyclic peptide was confirmed by mass spectrometry. The concentration of α-CTx-MII in our stock solution was determined by quantitative amino acid analysis.

Figure 4.1 Amino acid sequence of α-conotoxin-MII. α-CTx-MII is a 16-amino acid peptide isolated from the venom of the marine snail *Conus magus* which potently antagonise α3β2-containing nAChR (Cartier *et al.*, 1996; Harvey *et al.*, 1997). The disulfide bond pattern of α-CTx-MII is also represented: C^3C^{16} and C^2C^8. This peptide was synthesised as previously described (Cartier *et al.*, 1996) by Sue Phillips and Richard Kinsman (University of Bath). The peptide in this figure has an amidated carboxyl-terminus as a consequence of the synthesis procedure.

4.2.3 Two electrode voltage clamp

The electrophysiological studies in this chapter were performed by Dr S.C. Harvey and Dr C.W. Luetje (Department of Molecular and Cellular Pharmacology, University of Miami, Miami, FL USA). See Kaiser *et al.* (1998) for details.

4.2.4 Superfusion experiments

Superfusion experiments involving the use of α-CTx-MII were performed in conjunction with Dr Lev Soliakov.

4.2.4.1 Superfusion of P2 striatal synaptosomes and striatal slices for [^{3}H]-DA release

Male Sprague-Dawley rats (240-250 g) were killed by cervical dislocation, decapitated and brain striata (180-240 mg of wet tissue weight / rat) rapidly dissected for the preparation of synaptosomes and / or slices. P2 synaptosomes were prepared by differential centrifugation as previously described (Soliakov *et al.*, 1995). Synaptosomes were loaded with [^{3}H]-DA (0.1 μM, 0.132 MBq / ml) for 15 min at 37°C and superfused in open chambers (Soliakov *et al.*, 1995). All superfusion experiments were performed in Krebs bicarbonate buffer of the following composition: 118 mM NaCl, 2.4 mM KCl, 2.4 mM $CaCl_2$, 1.2 mM $MgSO_4$, 1.2 mM KH_2PO_4, 25 mM $NaHCO_3$ and 10 mM glucose, buffered to pH 7.4 with 95% O_2 / 5% CO_2 and supplemented with 1mM ascorbic acid, 8 μM pargyline and 0.5 μM nomifensine to prevent DA degradation and DA re-uptake.

Striatal slices (0.25 mm) were prepared as previously described (Marshall *et al.*, 1996) using a McIlwain tissue chopper. In brief, striatal tissue prisms from two rats were washed twice with Krebs buffer (same composition as indicated above) and loaded with [^{3}H]-DA (0.1 μM, 0.132 MBq / ml) for 15 min at 37°C. After two washes, slices were resuspended in Krebs buffer and approximately 45 - 50 mg of slices / chamber were loaded into six closed superfusion chambers.

Superfusion of synaptosomes (open chambers) or slices (closed chambers) was performed as previously described (Soliakov *et al.*, 1995; Marshall *et al.*, 1996) in a Brandel apparatus using Krebs bicarbonate buffer at a flow rate of 0.5 ml / min; 2-min fractions were collected. After 30 min washing (20 min with normal buffer and a subsequent 10 min with buffer containing α-CTx-MII (1.1-112.0 nM) or 10 μM mecamylamine or no antagonist), (±)-AnTx-a (0.2-25.0 μM), (-)-nicotine (0.1-50.0 μM), cytisine (0.005-50.000 μM), UB-165 (0.01-1.00 μM) or (±)-epibatidine (0.1 μM) in buffer with or without antagonist was applied for 40 s. The pulse of drug was separated from the bulk buffer flow by 10s air bubbles. For KCl depolarisation, a 40 s pulse of buffer with KCl increased to 23.5 mM was applied.

Fractions were counted in a TRI-CARB 1500 liquid scintillation counter (counting efficiency 48%). Evoked tritium release above baseline was calculated as a percentage of the total radioactivity present in the synaptosomes immediately before stimulation (Soliakov *et al.*, 1995). To estimate the radioactivity remaining in slices at the end of the

experiment, superfusion was continued for 30 min with 10 mM HCl, to lyse the slices (Marshall *et al.*, 1996). Aliquots (1ml) of the lysates were counted for radioactivity. Total radioactivity in slices at the time of stimulation was calculated as the sum of subsequently released [^{3}H]-DA plus lysate.

4.2.4.2 Superfusion Data Analysis

The baseline was derived by fitting the following double exponential decay equation to the data, using Sigma Plot version 2.0 for Windows:

$$y = ae^{-bx} + ce^{-dx}$$

(Equation 4.1)

where **a**, **b**, **c** and **d** are the curve parameters and **x** is the fraction number.

Evoked [^{3}H]-DA release was calculated as the area under the peak after subtraction of the baseline. Data are represented as percentages of the corresponding controls, assayed in parallel in the absence of antagonist, and are mean±S.E.M. of several independent experiments, each consisting of two to three replicate chambers for each condition. One way ANOVA test was used to determine the significance of differences from control (Sigma Stat - Jandel Scientific, Germany).

For comparison between different experiments (Figure 4.3), superfusion profiles were normalised as percentages of the fitted baselines.

For analysis of agonist or antagonist dose-dependent relationships, the data (after subtraction of non-specific release determined in the presence of 10 µM mecamylamine) were fitted to the 4 parameter logistic equation:

$$y = (a - d) / [1 + (x / k)^n] + d$$

(Equation 4.2)

where **a** is the asymptotic maximum; **d** is the asymptotic minimum; **k** is the value at the inflection point and **n** is the slope parameter (Hill number).

4.3 Results

α-CTx-MII was synthesised as previously described (Cartier *et al.*, 1996). Its biological activity and specificity were examined by Harvey and Luetje by testing the ability of this synthetic peptide to antagonise nicotinic responses of defined rat nAChR subunit combinations expressed in *Xenopus* oocytes (Figure 4.2). ACh concentrations below the EC_{50} value for each of the subunit combinations were used to elicit responses (see Figure 4.2). Brief incubation (5 min) of the oocytes with α-CTx-MII inhibited ACh-evoked responses from the α3β2 subunit combination with an IC_{50} of 8.0±1.1nM. The α-CTx-MII concentration that produced complete inhibition (112 nM) showed no antagonism of ACh-elicited responses from α4β2, α2β2, and α3β4 nAChR subunit combinations (Figure 4.2). Therefore this synthetic peptide has the nAChR specificity predicted from previous work (Cartier *et al.*, 1996; Harvey *et al.*, 1997).

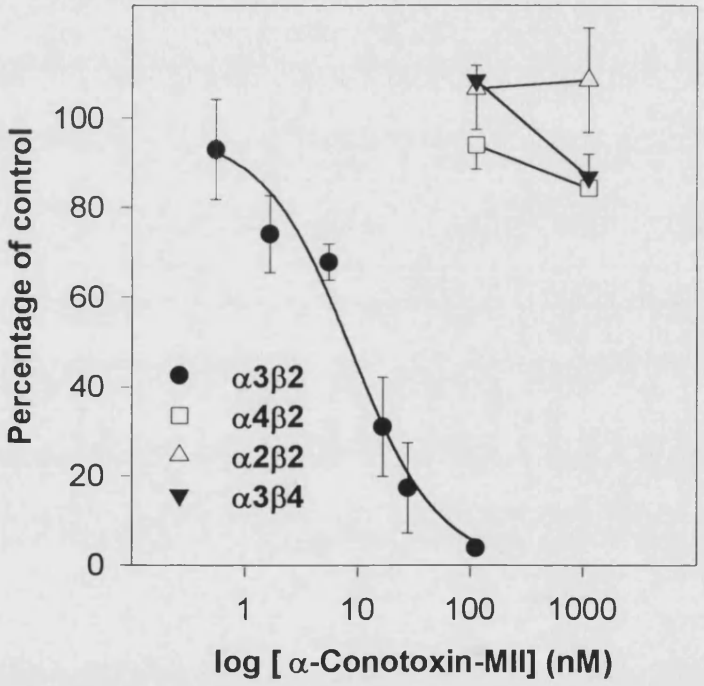

Figure 4.2 α-CTx-MII is selective for the rat α3β2 nAChR subunit combination. α-CTx-MII inhibition of α3β2 (●), α4β2 (■), α2β2 (❑) and α3β4 (○) neuronal nicotinic receptors expressed in *Xenopus* oocytes is shown. The response to an ACh concentration below the EC_{50} for each receptor after 5 min incubation with various concentrations of α-CTx-MII is presented as a percentage of the pre-incubation ACh response (mean±S.D. of 3-4 oocytes). The α3β2 data are fitted to a Hill equation (see (Equation 4.1), yielding an IC_{50} = 8.0±1.1nM; n=1.29.

To investigate the putative nAChR subtypes involved in the nicotinic modulation of DA release in rat striatum, the ability of α-CTx-MII to block this effect was examined. Using superfusion, the nicotinic stimulation of [^{3}H]-DA release from striatal synaptosomes and slices were compared, as models of presynaptic nAChR on dopamine terminals and of nAChR present in a more intact preparation, respectively. (±)-AnTx-a was the agonist of choice based on previous studies in the Wonnacott lab (Soliakov *et al.*, 1995; Soliakov and Wonnacott, 1996) in which (±)-AnTx-a evoked [^{3}H]-DA release from striatal synaptosomes was characterised and showed it to be a potent and efficacious agonist (EC_{50} = 0.11 μM Soliakov *et al.*, 1995). (±)-AnTx-a (1 μM) evoked a discrete peak of [^{3}H]-DA release over basal release, and this was higher in slices than in synaptosomes (Figure). The non-selective nicotinic antagonist mecamylamine (10 μM) inhibited (±)-AnTx-a evoked release by 77.9±3.7% (n=12) in synaptosomes and 88.0±2.1% (n=5) in slices, respectively. In contrast 112 nM α-CTx-MII produced a partial but significant decrease in the mecamylamine-sensitive (±)-AnTx-a evoked release: 56.0±5.5% (n=8) inhibition in synaptosomes and 28.4±4.1% (n=8) inhibition in slices, respectively (Figure 4.3). α-CTx-MII (112 nM) had no effect on basal release. In the presence of α-CTx-MII (112 nM), [^{3}H]-DA release elicited from striatal slices by stimulation with 23.5 mM KCl was 107.0±7.5% (n=3) of release evoked by 23.5 mM KCl in the absence of antagonist.

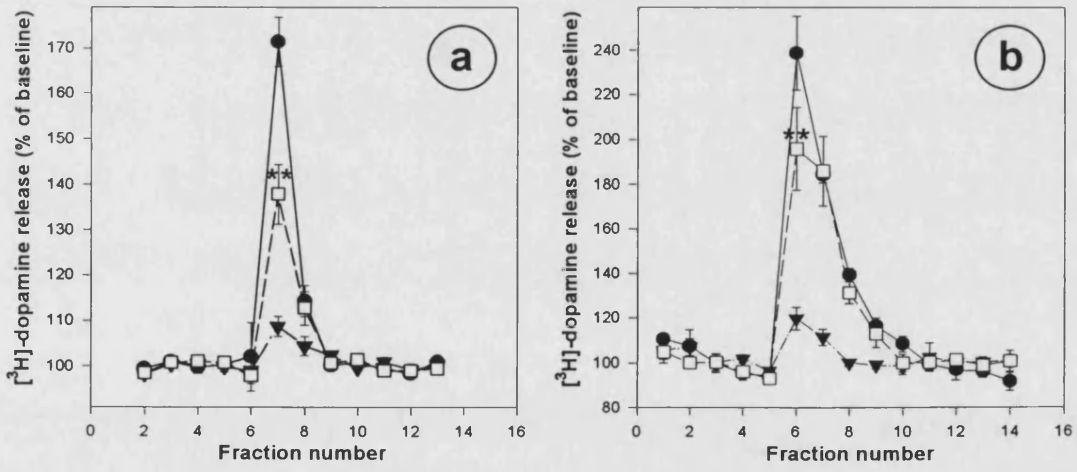

Figure 4.3 Superfusion profiles of [^{3}H]-DA release from (a) synaptosomes and (b) slices. Rat striatal synaptosomes (a) or slices (b) were prepared and superfused as described in **Error! Unknown switch argument.**. Antagonist (112 nM α-CTx-MII, □; 10 μM mecamylamine, ▼) was added to the perfusing buffer 10 min prior to stimulation with 1 μM (±)-AnTx-a for 40 s. Control responses (●) were determined in parallel in samples not exposed to antagonist. Release is calculated as a % of mean basal release. Vertical bars indicate the S.E.M. from 5 (slices) or 6 (synaptosomes) independent experiments, each consisting of two or more replicates. (** $p<0.01$ significantly different from control, one way ANOVA – Bonferroni *t* test)

To examine the inhibition by α-CTx-MII in more detail, dose-response curves were constructed for the inhibition of 1μM (±)-AnTx-a evoked [^{3}H]-DA release over a range of α-CTx-MII concentrations from 1 nM to 112 nM. The results are expressed as a percentage of mecamylamine-sensitive responses determined in parallel (Figure 4.4). The inhibition was dose-dependent; synaptosomes and slices gave similar IC_{50} values (24.3±2.9nM and 17.3±0.1nM, respectively). In both cases the inhibition was partial and was maximum at 112 nM αCTx-MII. (±)-AnTx-a-evoked [^{3}H]-DA release from synaptosomes was blocked to a greater extent than that from slices.

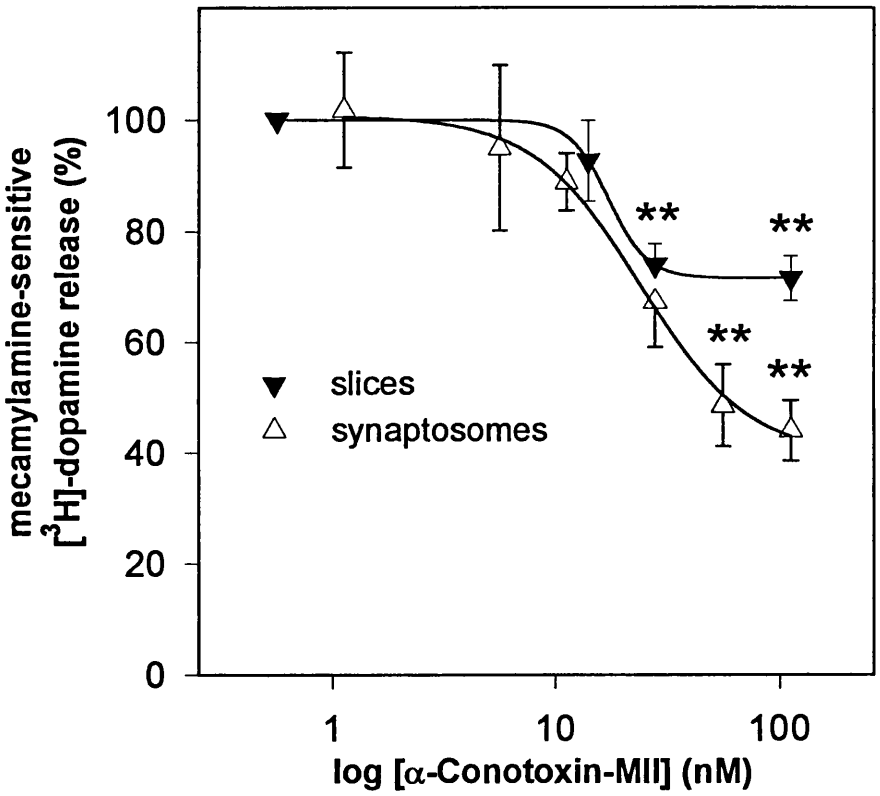

Figure 4.4 Dose-dependent inhibition of [^{3}H]-DA release by α-CTx-MII. Striatal synaptosomes (Δ) or slices (▼) were superfused in the presence or absence of increasing concentrations of α-CTx-MII prior to stimulation with 1 μM (±)-AnTx-a (control) for 40 s as described in 4.2.4.1. Evoked [^{3}H]-DA release in the presence of toxin is calculated as a % of the mecamylamine-sensitive fraction of the control response in the absence of α-CTx-MII. Vertical bars indicate the S.E.M. from 5 (slices) or 6 (synaptosomes) independent experiments each consisting of two or more replicates (** $p<0.01$ significantly different from control, one way ANOVA – Bonferroni *t* test). The data are fitted to a 4 parameter logistic equation (see 4.2.4.2 (Equation 4.2)), yielding IC_{50} = 24.3±2.9nM (synaptosomes) and IC_{50} = 17.3±0.1nM (slices).

The effect of increasing concentrations of peptide (1 nM - 112nM α-CTx-MII) was studied at different agonist concentrations (0.2, 1.0 and 25.0 μM (±)-AnTx-a) in synaptosome preparations (Figure 4.5). This experiment was conducted by Dr L.Soliakov in parallel with the other work in this chapter and is presented here to provide a more complete picture. As the agonist concentration was increased, the dose-response relationship of inhibition by α-CTx-MII was shifted to the right (IC_{50} values for α-CTx-MII were: 5.4±0.1nM, 24.3±2.9nM and 51.5±5.9nM at 0.2, 1.0 and 25.0 μM (±)-AnTx-a, respectively). However, at each agonist concentration the maximum inhibition of mecamylamine-sensitive responses achieved by α-CTx-MII was similar (48.2±4.9% (n=3) at 0.2 μM (±)-AnTx-a, 57.6±5.4% (n=8) at 1.0 μM (±)-AnTx-a, 46.4±3.5% (n=6) at 25.0 μM (±)-AnTx-a), confirming the partial inhibition described above.

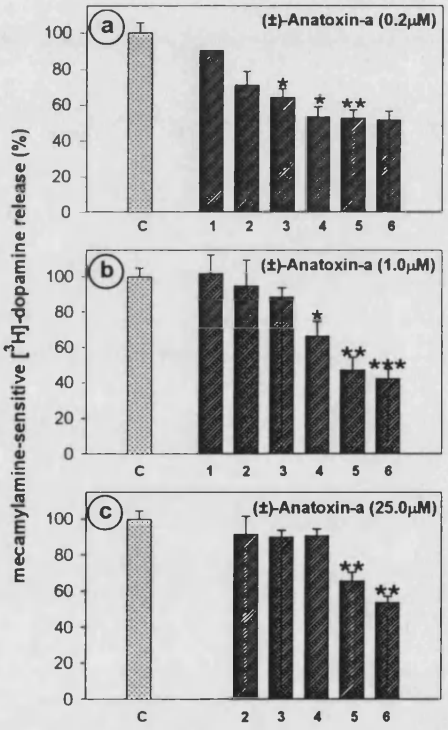

Figure 4.5 Dose-dependent inhibition of [^{3}H]-DA release from striatal synaptosomes by α-CTx-MII with increasing concentrations of (±)-AnTx-a. Striatal synaptosomes were superfused in the presence or absence of increasing concentrations of α-CTx-MII ((1) 1.0 nM, (2) 5.5 nM, (3) 11.0 nM, (4) 28.0 nM, (5) 56.0 nM, (6) 112.0 nM) prior to stimulation for 40 s with **(a)** 0.2 μM (±)-AnTx-a; **(b)** 1.0 μM (±)-AnTx-a; and **(c)** 25.0 μM (±)-AnTx-a. Under control conditions (C), these concentrations of agonist resulted in the release of 109.3±6.2 fmoles [^{3}H]-DA / mg synaptosomal protein, 160.7±9.8 fmoles [^{3}H]-DA / mg synaptosomal protein and 168.9±7.6 fmoles [^{3}H]-DA / mg synaptosomal protein respectively. Release in the presence of α-CTx-MII is presented as a % of control (mecamylamine-sensitive response) at each agonist concentration. Vertical bars indicate the S.E.M. from 3 to 8 synaptosome preparations. (* $p < 0.05$, ** $p < 0.01$ and *** $p < 0.001$ significantly different from control, one way ANOVA – Bonferroni *t* test)

The effect of TTX (1.5 μM) on the α-CTx-MII-sensitive response was also tested. As previously reported (Marshall *et al.*, 1996), 1.5 μM TTX partially (~50%) inhibited nicotinic evoked striatal DA release from synaptosomes. In this study, when a maximally effective concentration of α-CTx-MII (112 nM - see Figure 4.2 and Figure 4.4) was coapplied wit 1.5 μM TTX, the inhibition was not significantly different from that produced by each toxin applied alone (Figure 4.6).

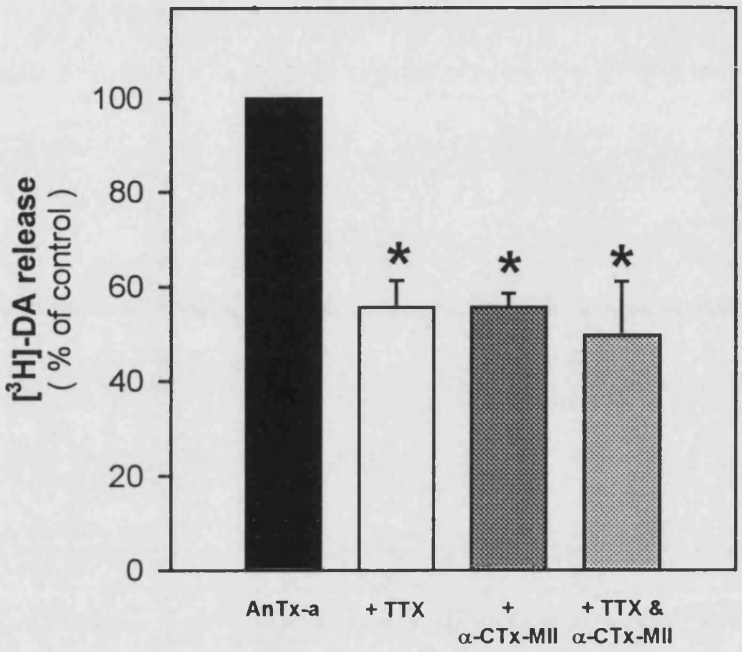

Figure 4.6 Effect of TTX on (±)-AnTx-a-evoked [^{3}H]-DA release from striatal synaptosomes. Results are expressed as percentage±S.D. of a control response ([^{3}H]-DA release evoked by 1 μM (±)-AnTx-a). In the presence of TTX (1.5 μM) or α-CTx-MII (112 nM) the response was inhibited by 44.4±5.7% and 44.4±3.0%, respectively (n=3). When both toxins were coapplied, the effects were not additive (50.4±11.4% inhibition - n=3).
(* $p<0.05$ significantly different from control, one way ANOVA – Bonferroni *t* test).

During the course of this work, the novel agonist UB-165 (Figure 4.7), an anatoxin-a/epibatidine hybrid was developed by our collaborator, Professor Gallagher (Wright *et al.*, 1997) and it was of interest to examine its agonist properties in the DA release assay. UB-165 was compared with (±)-AnTx-a, (-)-cytisine and (-)-nicotine (Figure 4.7) for their abilities to promote [^{3}H]-DA release from rat striatal synaptosomes (Figure 4.8). Of these four compounds, (-)-nicotine was the most efficacious and least potent, whereas (-)-cytisine and (±)-AnTx-a were similarly potent and equiefficacious, generating about 70% of the maximum response achieved by (-)-nicotine. Although UB-165 was slightly more potent than (±)-AnTx-a, it was much less efficacious then other agonists, achieving a maximum release of [^{3}H]-DA that was only 42% of that of (±)-AnTx-a.

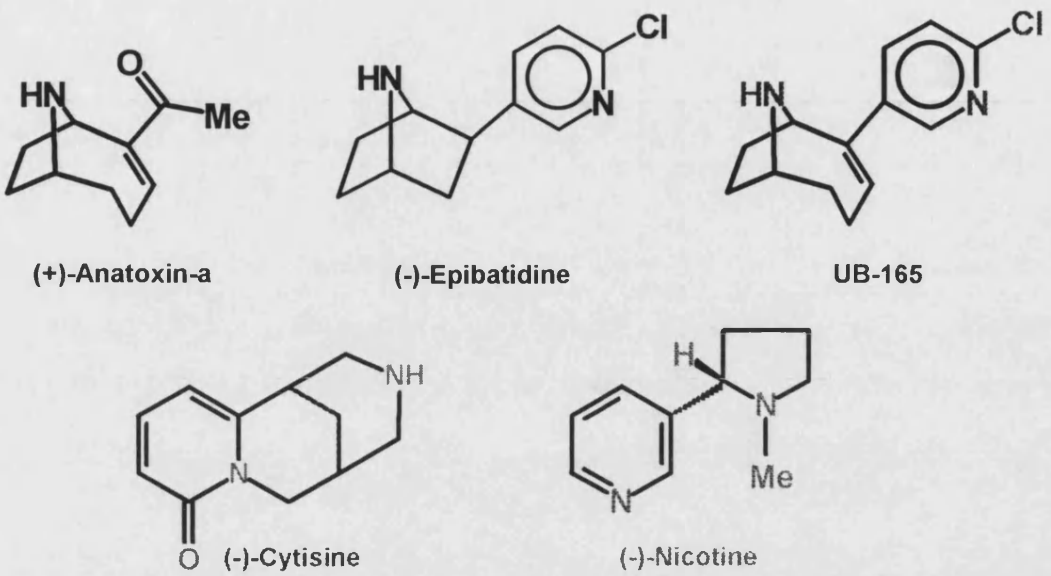

Figure 4.7 Molecular structures of (+)-AnTx-a, (-)-epibatidine, the enantiomer of UB-165 that corresponds to (+)-anatoxin-a, (-)-cytisine and (-)-nicotine.

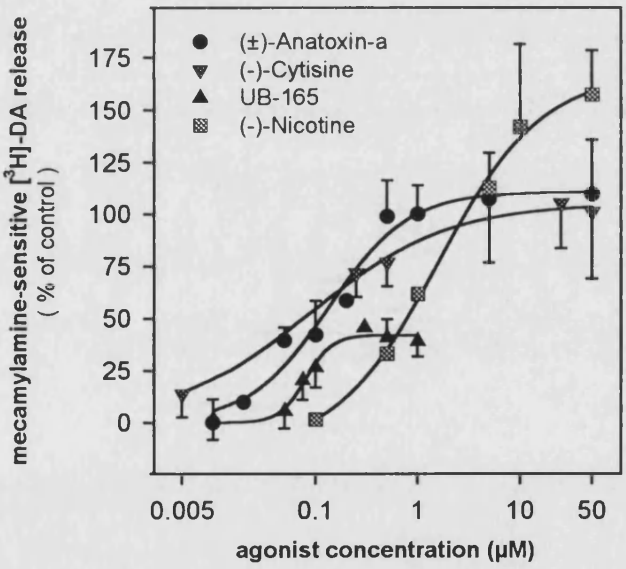

Figure 4.8 Dose-responses curves for the release of [^{3}H]-DA evoked by increasing concentrations of (-)-nicotine, (±)-AnTx-a, cytisine and UB-165. Each agonist concentration was tested in the presence and absence of mecamylamine (10 μM) to determine specific nAChR-mediated release. Responses were normalised to the response to 1 μM (±)-AnTx-a determined in parallel, and are percentage±S.E.M. (n≥3). The rank order of potencies (EC_{50}s) is cytisine (80±5nM) = UB-165 (88±18nM) ≈ (±)-AnTx-a (134±26nM) >> (-)-nicotine (1595±377nM).

nAChR mediating the presynaptic nicotinic stimulation of [^{3}H]-DA release from striatal terminals appear to be heterogeneous, based on the partial inhibition by the $\alpha 3\beta 2$-selective toxin α-CTx-MII (Figure 4.4 - Kulak *et al.*, 1997). A maximally effective concentration of this toxin (112 nM) was compared with mecamylamine (10 μM) for their abilities to inhibit [^{3}H]-DA release evoked by the four agonists above and by (±)-epibatidine (Figure 4.9). Concentrations of the agonists giving maximum [^{3}H]-DA release were compared: the results demonstrate the differences in efficacy noted above, and show that (±)-epibatidine is the most efficacious, eliciting a response that is 200% of that of (±)-AnTx-a. Whereas mecamylamine inhibited agonist-evoked [^{3}H]-DA release to the same extent in each case (the residual release being the non-specific component that is elicited by a buffer pulse without agonist), α-CTx-MII produced different degrees of inhibition. The mecamylamine-sensitive response to (±)-AnTx-a was reduced by 56.0% by the toxin, in agreement with the results showed in Figure 4.4, whereas the mecamylamine-sensitive [^{3}H]-DA release evoked by (±)-epibatidine, (-)-cytisine and (-)-nicotine was inhibited by 47.9%, 45.0% and 32.4%, respectively. However, the response to UB-165 was almost completely blocked by α-CTx-MII (87.8% inhibition).

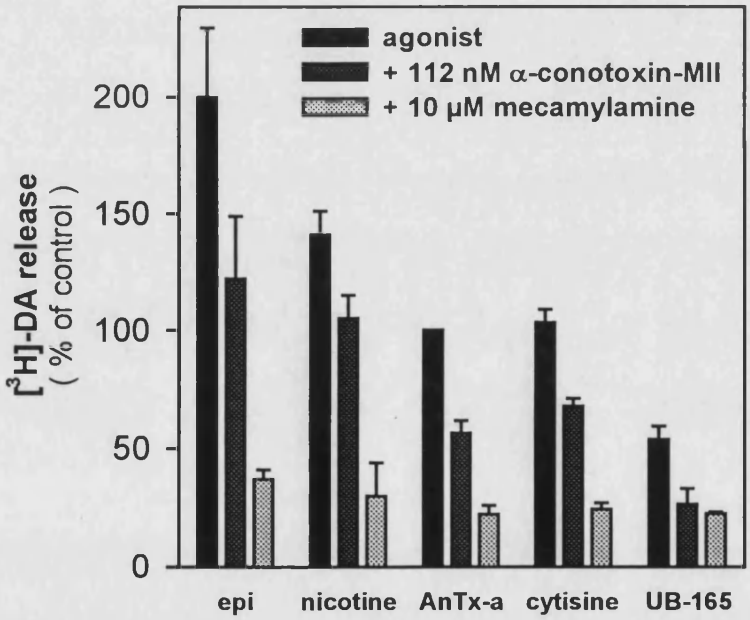

Figure 4.9 Comparison of the inhibition by α-conotoxin-MII (112 nM) and mecamylamine (10 μM) of [^{3}H]-DA release-evoked by maximally effective concentrations of agonists. Striatal synaptosomes were perfused with antagonist for 10 min before stimulation with (±)-epibatidine (0.1 μM), (-)-nicotine (10 μM), (±)-AnTx-a (1 μM), (-)-cytisine (50 μM) or UB-165 (1 μM). Responses were normalised to the response evoked by 1 μM (±)-AnTx-a determined in parallel. Values are expressed as percentage±S.D. of the control response (n=3).

In this study, the effect of α-CTx-MII on α7-containing nAChR expressed in *Xenopus* oocytes was not tested by Harvey and Luetje. In order to explore a putative contribution of MLA-sensitive nAChR to the response evoked by UB-165 in striatal synaptosomes, the effect of MLA on UB-165-evoked [^{3}H]-DA release was examined. MLA (50 nM) did not have any effect on 1 μM UB-165-evoked [^{3}H]-DA release from striatal synaptosomes (Figure 4.10). This result rules out α7-containing nAChR for the UB-165 component of the response.

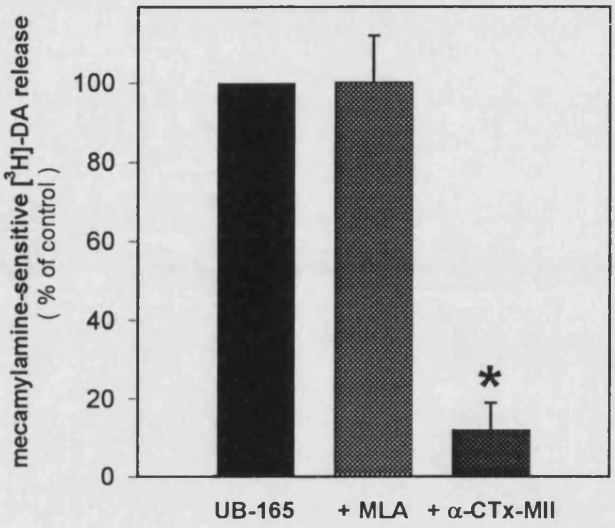

Figure 4.10 Effect of MLA (50 nM) on 1 μM UB-165-evoked [^{3}H]-DA release from striatal synaptosomes. Responses are expressed as percentage±S.D. of the 1 μM UB-165-evoked response (control - n=3-6). MLA (50 nM) had no significant effect on the response elicited by 1 μM UB-165 whereas α-CTx-MII (112 nM) inhibited it by 87.8±6.7%.
(* $p<0.05$ significantly different from control, one way ANOVA – Bonferroni *t* test)

4.4 Discussion

The ability of nicotinic agonists to stimulate DA release from rat striatal preparations *in vitro* is well documented (Rapier *et al.*, 1988; El-Bizri and Clarke, 1994; Sacaan *et al.*, 1995) but the particular nAChR subtypes mediating this effect have not been conclusively identified (Wonnacott, 1997; Kulak *et al.*, 1997). Involvement of nAChR comprising α3 nAChR subunits was suggested on the basis of sensitivity to n-Bgt in slices (Schulz and Zigmond, 1989) and synaptosomes (Grady *et al.*, 1992). In addition receptors that correlate with high affinity agonist binding sites comprising α4 and β2 subunits have been implicated by lesion studies (Clarke and Pert, 1985).

In this study, α-CTx-MII was exploited as an antagonist selective for the α3β2-interface of rat nAChR (Cartier *et al.*, 1996; Harvey *et al.*, 1997) to examine the subtype responsible for the nicotinic modulation of striatal [^{3}H]-DA release. To achieve this, the peptide was synthesised according to the previously documented method (Cartier *et al.*, 1996). Assessment of αCTx-MII on different putative nAChR expressed in *Xenopus* oocytes showed it to have specificity for the α3β2 subunit combination reported previously (Cartier *et al.*, 1996a; Harvey *et al.*, 1997). The IC_{50} (8.0±1.1nM) is approximately 2 fold less potent than found previously using the same static bath applied system (IC_{50} = 3.5 nM; Harvey *et al.*, 1997). These values are higher than the IC_{50} of 0.5 nM reported by Cartier *et al.* (1996) for rat α3β2 expressed in *Xenopus* oocytes, but this probably reflects a difference in the drug application technique, namely application of α-CTx-MII by continuous perfusion (see Harvey *et al.*, 1997). Despite these discrepancies it is clear that α-CTx-MII specifically antagonises responses of nAChR composed of α3 and β2 subunits at concentrations that have no effect on other nAChR subunit combinations tested (α4β2, α2β2, α3β4). Therefore this toxin could be used to distinguish α3β2-like nAChR from these combinations of nicotinic subunits.

In superfusion experiments (±)-AnTx-a-evoked DA release was sensitive to α-CTx-MII, consistent with the participation of α3β2-like nAChR. The IC_{50} values of 17.3 nM and 24.3 nM for slices and synaptosomes respectively **(Error! Unknown switch argument.)** are higher than the IC_{50} (8.0±1.1nM) found for the α3β2 combination of nAChR subunits expressed in *Xenopus* oocytes. Differences in experimental protocol and agonist concentration (relative to their respective EC_{50} values) provide a likely explanation of these differences in IC_{50}. The EC_{50} for (±)-AnTx-a evoked [^{3}H]-DA release from striatal synaptosomes was previously determined to be 0.11 μM (Soliakov *et al.*, 1995), with 1 μM (±)-AnTx-a giving almost maximum responses. Using an (±)-AnTx-a concentration closer to the EC_{50} (0.2 μM), the IC_{50} (5.4±0.1nM) for inhibition by α-CTx-MII in synaptosomes compares very well with the potency of α-CTx-MII determined in *Xenopus* oocytes. The shift of the IC_{50} values to the right with increasing

concentrations of (±)-AnTx-a indicates that antagonism by α-CTx-MII is surmountable, consistent with the competitive mode of action of α-CTx-MII proposed by Cartier *et al.* (1996b).

Despite the clear antagonism by α-CTx-MII, maximally effective concentrations failed to fully inhibit (±)-AnTx-a evoked DA release in synaptosomes and slices compared with the inhibition by mecamylamine. This partial blockade of mecamylamine sensitive responses shows that more than one nAChR must be involved in nicotinic evoked rat striatal DA release. This finding agrees with the recent study of Kulak *et al.* (1997) who used a more efficacious agonist, (-)-nicotine (Figure 4.8), to stimulate [^{3}H]-DA release from striatal synaptosomes. In the present study, α-CTx-MII inhibited by 56% the mecamylamine-sensitive (±)-AnTx-a-evoked [^{3}H]-DA release from synaptosomes. Although Kulak *et al.* (1997) found a slightly lower inhibition (34%-49%) of (-)-nicotine stimulated [^{3}H]-DA release by α-CTx-MII, their results match those reported in this chapter using (±)-AnTx-a. Because synaptosomes represent isolated nerve terminals, they provide a model for studying presynaptic receptors. Under the conditions of superfusion it can be assumed that only nAChR associated with DA terminals can promote [^{3}H]-DA release in the experiments described here. The present results indicate that these nAChR are heterogeneous but cannot distinguish between multiple receptor subtypes on a single nerve ending (Figure 4.11a1) or segregation of nAChR subtypes to different subpopulations of DA terminals (Figure 4.11a2). This finding of heterogeneity of presynaptic nAChR subtypes mediating striatal DA release confirms an earlier hypothesis from the Wonnacott lab (Wonnacott *et al.*, 1995).

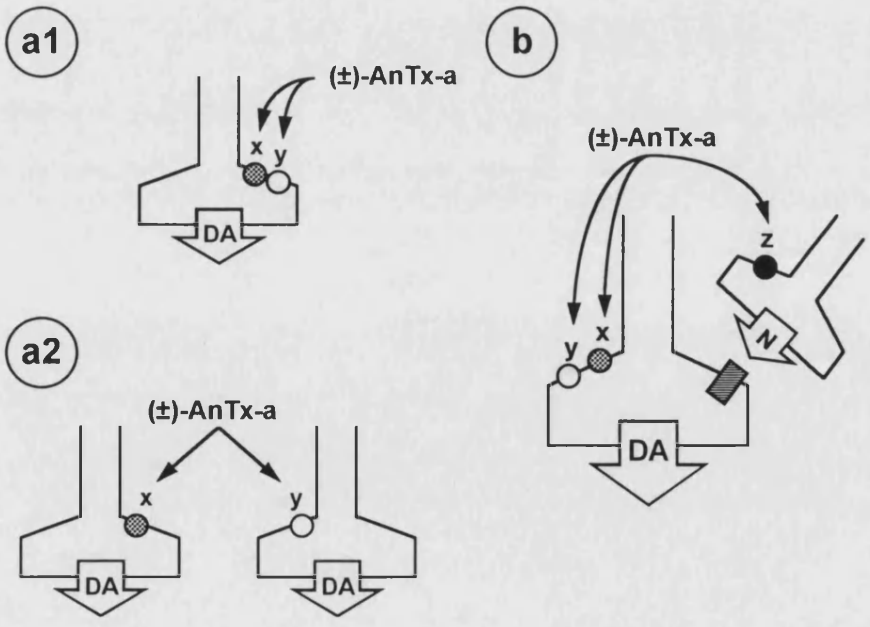

Figure 4.11 Schematic representation of nicotinic modulation of DA release based on (a) synaptosome studies and (b) slice experiments. In synaptosomes (a) (±)-AnTx-a can directly stimulate DA release, acting at presynaptic nAChR. α3β2-like nAChR (x) and αCTx-MII-insensitive nAChR (y) may be present on the same terminals **(a1)** or segregated on different

terminals **(a2)**. In more intact preparations, represented by slices **(b)**, (±)-AnTx-a may indirectly enhance DA release via presynaptic nAChR (z: α-CTx-MII-insensitive nAChR) located on non-DA terminals, in addition to presynaptic nAChR on DA terminals.

The tetrodotoxin (TTX) insensitivity of nicotinic agonist-elicited responses has been taken to define presynaptic nAChR in integrated preparations, such as brain slices and neuronal cultures. TTX sensitivity of nicotinic responses in the absence of nerve conduction has been interpreted in favour of a "preterminal" location, i.e. on the axon rather than the terminal bouton (Léna *et al.*, 1993). However, synaptosome preparations, in which nerve terminals should constitute the only functional elements, have given controversial results with various degrees of TTX sensitivity of nicotinic agonist-stimulated $^{86}Rb^+$ efflux or dopamine release (e.g. Marks *et al.*, 1995; Soliakov *et al.*, 1995). In accordance with a previous report from this lab (Marshall *et al.*, 1996), this study suggest that at least two populations of presynaptic nAChR (TTX-sensitive and TTX-insensitive) participate in nicotinic-evoked DA release from rat striatal synaptosomes (Figure). The nAChR that elicit TTX-insensitive release may be located close to the exocytotic machinery such that their activation produces sufficient Na^+ and / or Ca^{2+} influx to trigger release directly. Alternatively, the partial TTX-sensitivity observed in several studies (including this thesis) could suggest that nAChR segregate onto e.g. two types of nerve terminals, one expressing fewer voltage operated Na^+ channels (TTX-insensitive component of the response) than the other (TTX-sensitive component). In this chapter, it has been shown that the effects of maximally effective concentrations of TTX and α-CTx-MII on (±)-AnTx-a-evoked DA release from synaptosomes, were similar and not additive (Figure 4.6). This provokes the speculation that:

1. α-CTX-MII-sensitive nAChR may occur at some distance from the release sites, requiring the intervention of voltage operated Na^+ channels in order to elicit release, whereas the α-CTx-MII-insensitive nAChR may reside close to the release sites; or
2. α-CTX-MII-sensitive and α-CTx-MII-insensitive nAChR are segregated onto two different populations of nerve terminals (Figure 4.11a2) expressing different densities of voltage operated Na^+ channels.

However, the TTX-sensitivity of the response to activation of these nAChR may also depend upon various factors (such as the resting potential of the nerve terminals) which may contribute to the reports of variable TTX sensitivity.

Nicotinic agonists evoke dopamine release with different potencies and efficacies (Figure 4.8 - see Holladay *et al.*, 1997). In this study the natural and stereoselective alkaloid AnTx-a was used as the nicotinic agonist of reference. (±)-AnTx-a evokes DA release from rat striatal synaptosomes in a dose dependent-manner with an EC_{50} of 134 nM (Figure 4.8) in agreement with previous observations (EC_{50} = 110 nM - Soliakov *et al.*, 1995). As the nicotinic agonist activity resides mainly in the (+) enantiomer of AnTx-a, the true EC_{50} may be overestimated by a factor of 2. In this respect, Wonnacott *et al.* (1995) and Clarke and Reuben (1996) reported an EC_{50} value of 0.05 µM for (+)-AnTx-a-evoked [^{3}H]-DA release from rat striatal synaptosomes. (±)-AnTx-a is more potent than (-)-nicotine in evoking [^{3}H]-DA release from rat striatal synaptosomes: EC_{50} values for (-)-nicotine range from 3.8 µM (Rapier *et al.*, 1988) to 0.16 µM (Clarke and Reuben, 1996). Grady *et al.*, (1992) reported an EC_{50} value of 0.48 µM for nicotine-evoked [^{3}H]-DA release from mouse striatal synaptosomes.

The EC_{50} obtained in the present study for (-)-nicotine-evoked DA release from rat synaptosomes (1.60±0.38μM) is in good agreement with these previously published data. In this work (±)-AnTx-a and (-)-cytisine have been shown to be equipotent and equiefficacious (Figure 4.8), but the efficacies of (±)-AnTx-a and (-)-cytisine are clearly lower than that of (-)-nicotine (~70%). A previous study by Wonnacott *et al.* (1995) showed that (+)-AnTx-a attained only 54% of the maximum [^{3}H]-DA release from rat striatal synaptosomes elicited by (-)-nicotine (EC_{50} = 1.1 μM), whereas Clarke and Reuben (1996) reported for the same preparation that (+)-AnTx-a maximal effects were similar to those of (-)-nicotine. (±)-Epibatidine has been shown to potently (EC_{50} ≈ 0.4 nM - Sullivan *et al.*, 1994) evoke DA release from rat striatal slices (also Sacaan *et al.*, 1996). Consistent with Sullivan *et al.* (1994), it has been demonstrated in this chapter that (±)-epibatidine is the most efficacious of the nicotinic agonists used (**Error! Unknown switch argument.**) in eliciting DA release from rat striatal synaptosomes.

In this study the novel nicotinic agonist UB-165 (**Error! Unknown switch argument.** - Wright *et al.*, 1997) was also characterised for [^{3}H]-DA release from rat striatal synaptosomes. It only elicited ~40% of the maximum release evoked by 1 μM (±)-AnTx-a. This partial agonism of UB-165 was almost completely blocked by α-CTx-MII (112 nM) but unaffected by MLA (50 nM), suggesting that UB-165 only activates α3β2-containing nAChR on striatal DAergic nerve terminals (Figure 4.10).

Insight into the possible subunit composition of nAChR can be sought from pharmacological studies on the one hand and from approaches such as *in situ* hybridisation and immunoprecipitation on the other. Although α-CTx-MII sensitivity implicates α3β2-like nAChR, there is little pharmacological information on other subtypes that might also participate because of the lack of tools to discriminate nAChR subtypes. The α4β2 nAChR is a candidate for the α-CTx-MII insensitive presynaptic nAChR, based on evidence for [^{3}H]-nicotine binding sites on dopaminergic terminals from lesion studies (Clarke and Pert, 1985). The partial agonism of (-)-cytisine at rat β2-containing nAChR expressed in *Xenopus* oocytes (Luetje and Patrick, 1991) has been used to attempt to define native α4β2 nAChR, although partial versus full agonism by (-)-cytisine only distinguishes β2 from β4 subunits. The ability of (-)-cytisine to release [^{3}H]-DA from striatal synaptosomes has been inconsistent. (-)-Cytisine has been reported to be a full agonist with respect to [^{3}H]-DA release from mouse striatum (EC_{50} = 483 nM - Grady *et al.*, 1992) but was less efficacious than (-)-nicotine in rat studies (El-Bizri and Clarke, 1994 EC_{50} ≈ 0.1 μM; Wonnacott *et al.*, 1995 EC_{50} ≈ 0.1 μM; this study EC_{50} ≈ 0.08 μM), so species differences in nAChR properties or composition may be important. The almost total lack of response to (-)-cytisine predicted for β2-containing nAChR from oocyte experiments (Luetje and Patrick, 1991) has not been observed, although heterogeneity of nAChR subtypes mediating [^{3}H]-DA release could mask such differences.

However, β4 mRNA has not been detected in these DA neurones (see LeNovere *et al.*, 1996; Wonnacott, 1997).

For *in situ* hybridisation results pertinent to presynaptic nAChR on striatal dopamine terminals it is necessary to examine mRNA expression in the brain region containing the cell bodies, namely the substantia nigra *pars compacta*. In the rat this region expresses α3, α4, α5, α6, β2 and β3 mRNAs, but α2 and β4 mRNAs were not detected (see LeNovere *et al.*, 1996; Wonnacott, 1997). This pattern is compatible with α3β2 and α4β2 nAChR subunit combinations but clearly additional subunits could also contribute to form native receptors (and could influence the efficacy of (-)-cytisine, discussed above). In particular, high expression of α6 and β3 mRNA in catecholaminergic nuclei, including substantia nigra, has been noted (LeNovere *et al.*, 1996). Recent immunohistochemical studies (Goeldner *et al.*, 1997) demonstrated that the α6 nAChR protein is present on dopaminergic neurones of the midbrain (i.e. substantia nigra and ventral tegmental area).

Although α-CTx-MII specifically inhibits the α3β2 subunit combination expressed in *Xenopus* oocytes it should only be assumed to recognise the interface between α3 and β2 subunits (Harvey *et al.*, 1997; Kulak *et al.*, 1997). Indeed only one α3β2 pair of subunits may be sufficient for α-CTx-MII sensitivity (Kulak *et al.*, 1997). Therefore the presence of additional subunits in the pentamer cannot be excluded. There is precedent for neuronal nAChR composed of three or even four different types of subunits, including α5 (e.g. Conroy and Berg, 1995; see 2.1.1.1 and 2.1.1.2).

Striatal slices showed lower inhibition by α-CTx-MII of (±)-AnTx-a evoked [^{3}H]-DA. The IC_{50} value for α-CTx-MII (17.3±0.1nM) in striatal slices is very similar to that found in synaptosomes (24.3 ± 2.9 nM) at the same agonist concentration, suggesting that α-CTx-MII is interacting with the same class of nAChR in both preparations. As slices are more intact striatal preparations, the lower inhibition by α-CTx-MII might reflect additional nAChR (which are α-CTx-MII insensitive) on non-dopaminergic terminals, whose activation may indirectly enhance DA release (Figure 4.11b). For example local application of (-)-nicotine *in vivo* has been shown to release L-glutamate in the rat striatum (Toth *et al.*, 1993) and L-glutamate can stimulate DA release from striatal slices (Roberts and Anderson, 1979) and synaptosomes (Chéramy *et al.*, 1996). In chapter 5, the putative indirect nicotinic stimulation of striatal DA release via an increase in glutamate efflux will be examined.

This study has shown a) that α-CTx-MII partially and differentially blocks (±)-AnTx-a evoked [^{3}H]-DA release from striatal synaptosomes and slices, and b) that UB-165 selectively activates α-CTx-MII-sensitive nAChR on DAergic nerve terminals. From these results it can be concluded: 1) at least two populations of presynaptic nAChR (α-CTx-MII sensitive and α-CTx-MII insensitive) are involved in the direct modulation of DA release from rat striatal dopaminergic terminals; 2) the presynaptic α-CTx-MII sensitive nAChR comprises

α3 and β2 nAChR subunits but additional subunits cannot be excluded; 3) in slices, nAChR on non-dopaminergic terminals may enhance DA release by releasing other neurotransmitters that in turn act on DAergic terminals; and 4) α-CTx-MII sensitive nAChR are not involved, or play a minimum role, in this indirect effect.

5 Indirect nicotinic modulation of dopamine release in rat striatum by (±)-anatoxin-a-evoked glutamate release

5.1 Introduction

The interaction between brain neurotransmitters has been the focus of recent research (e.g. Di Chiara et al. 1994; Cheramy *et al.*, 1996; García-Muñoz *et al.*, 1996). In particular, the cross-talk between glutamatatergic (Glu) and cholinergic (ACh) with dopaminergic (DA) brain pathways have received much attention because of their implication in aging (Expósito *et al.*, 1995; Porras and Mora; 1995), in neurodegenerative disorders such as Parkinsons' disease and schizophrenia (Carlsson and Carlsson; 1990), as well as in drug addiction (tobacco consumption - Dani and Heinemann; 1996).

One of the most studied brain regions, in relation to neurotransmitter interactions, is the neostriatum (Carlsson and Carlsson, 1990; Di Chiara *et al.*, 1994; Lannes and Micheletti, 1994; Porras and Mora, 1994); due, in part at least, to the present knowledge of its connectivity and neurochemistry (Figure 5.1 and Figure 5.2 - Smith and Bolam, 1990; Kita, 1993; Smith *et al.*, 1998).

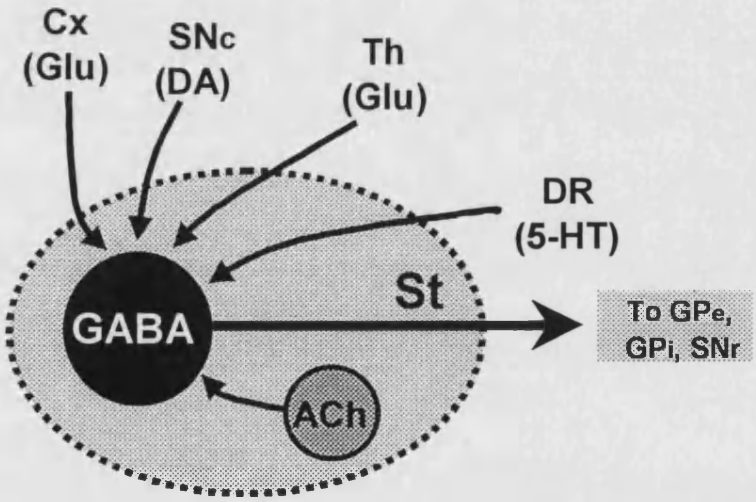

Figure 5.1 Diagram of the major afferent and efferent pathways and cholinergic interneurones in the striatum (St). Glutamatergic inputs from cortex (Cx) and thalamus (Th), dopaminergic inputs from the substantia nigra *pars compacta* (SN_c), and 5-HT inputs from the dorsal raphe nuclei (DR), synapse with the major efferent neurones, the GABAergic medium-sized spiny cells that project to the external segment of the globus pallidus (GP_e - globus pallidus in non-primates), internal segment of the globus pallidus (GP_i - entopeduncular nucleus in non-primates) and substantia nigra *pars reticulata* (SNr).

5.1.1 Anatomy of striatal DA-Glu interactions

The striatum regulates the activity of the GABAergic projection neurones of the substantia nigra *pars reticulata* (SNr) via two main functional opposing pathways, the direct and the indirect pathways (Figure 5.2 - Albin *et al.*, 1989; Alexander and Crutcher; 1990; Smith *et al.*, 1998). The former is represented by the striatonigral GABAergic projection and monosynaptically inhibits the nigrothalamic GABA pathway, leading to a thalamic disinhibition of the glutamatergic drive to the cortex and therefore leading to movement initiation, whereas the latter encompasses a trisynaptic link including 1) a GABAergic projection from the striatum to the external segment of the globus pallidus (GPe), 2) a GABAergic projection from the GPe to the subthalamic nucleus (STN), and 3) a glutamatergic projection from the STN to the SNr, which also innervates the GPe. Activation of the striatopallidal "link" in the indirect pathway is associated with an increase in STN glutamatergic input to the SNr and GP, and this results in changes in both thalamic activity and locomotor behaviour opposite to those elicited by activation of the direct pathway (Albin *et al.*, 1989; Alexander and Crutcher, 1990; Smith *et al.*, 1998).

The striatum receives dopaminergic input from the SNc (Figure 5.1 and Figure 5.2) and the main neostriatal targets of these projections are the GABAergic medium-sized spiny neurones (Freund *et al.*, 1984; Yung *et al.*, 1996) that innervate the SNr and the GP (Figure 5.2). It has been proposed that degeneration of the nigrostriatal dopaminergic pathway (e.g. in Parkinsons' disease) may differentially affect the two striatal GABAergic projections described above (Ingham *et al.*, 1998). Such a potential imbalance of activity in these two pathways is thought to be critical in generating the hyperkinesias or hypokinesias observed in basal ganglia disorders (Albin *et al.*, 1989; Alexander and Crutcher, 1990; De Long, 1990). Another main source of synaptic input to dendritic spines in the neostriatum is excitatory and is derived from cortex and thalamus (Figure 5.1 and Figure 5.2). In contrast to dopaminergic axons that form predominantly symmetric synapses on the necks of dendritic spines (Freund *et al.*, 1984; Groves *et al.*, 1994), the glutamatergic synaptic contacts are on the heads of spines, and exhibit asymmetric membrane specialisations (Somogyi *et al.*, 1981; Meshul and Casey, 1989; Chen and Hillman, 1990). Moreover, a proportion of cortical and nigral inputs converge on the same spines of medium spiny neurones (Bouyer *et al.*, 1984; Freund *et al.*, 1984; Smith *et al.*, 1994; Groves *et al.*, 1994; Kung *et al.*, 1998), suggesting that a major function of dopaminergic inputs to the striatum is the regulation of the glutamatergic corticostriatal pathway, or viceversa. Although the dopaminergic and glutamatergic striatal afferents form synapses in close proximity onto the dendritic spine, no direct synaptic connections between them have been shown (Bouyer *et al.*, 1984). Thus, endogenous neurotransmitters released into the extracellular space may diffuse short distances to reach appropriate presynaptic receptors and establish nonsynaptic (volumetric) interactions (Fuxe and Agnati, 1991; Lannes and Micheletti, 1994). A recent report by Scanziani *et al.* (1997), indicating that Glu released from synapses diffuses to perisynaptic zones to act on Glu receptors, is interesting in this regard.

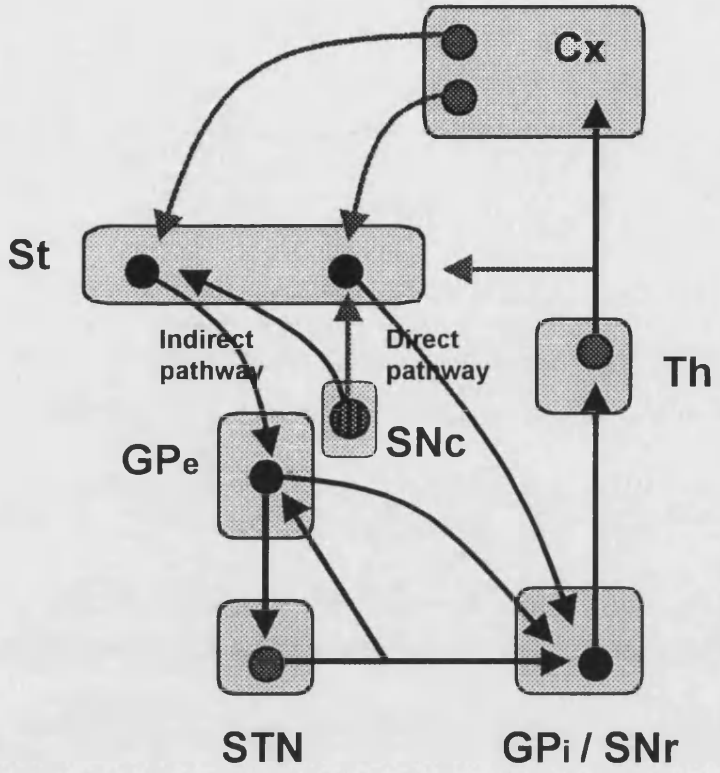

Figure 5.2 Simplified schematic representation of the basal ganglia-thalamocortical neuronal circuitry. Inhibitory projections are shown as black arrows, excitatory projections as blue arrows. According to this model, cortical information that reaches the striatum is conveyed to the basal output structures (GPi / SNr) via two pathways: a direct inhibitory projection from the striatum to the GPi / SNr and an indirect pathway, which involves an inhibitory projection from the striatum to the GPe, an inhibitory projection from the GPe to the STN and an excitatory projection from the STN to the GPi / SNr. The information is then transmitted back to the cortex via a relay in the thalamus or conveyed to various brain stem structures. The direct and indirect pathways largely arise from different populations of striatal medium-sized spiny neurones that contain different peptides and preferentially express different subclasses of dopamine receptors. The dopaminergic neurones of the substantia nigra *pars compacta* exert a net excitatory effect on spiny neurones giving rise to the direct pathway by the activation of D_1 receptors, whereas they exert a net inhibitory effect on spiny neurones giving rise to the indirect pathway by activation of D_2 receptors. GPe, external segment of the globus pallidus; GPi, internal segment of the globus pallidus; SNr, substantia nigra *pars reticulata*; SNc, substantia nigra *pars compacta*; STN, subthalamic nucleus; St, striatum; Th, thalamus; Cx, motor cortex. It should be noted that the diagram is a simplification, as many connections have not been indicated (Modified from Smith *et al.*, 1998).

5.1.2 Functional striatal DA-Glu cross-talk and nAChR

In striatum, *in vivo* infusion via a microdialysis probe of either NMDA (Keefe *et al.*, 1992; Morari *et al.*, 1993; Kendrick *et al.*, 1996) or AMPA (Kendrick *et al.*, 1996; Smolders *et al.*, 1996), increases the release of DA in this brain area. Using the same *in vivo* approach, local application of NMDA antagonists to the terminal regions of the mesolimbic (Museo and Pert, 1994) and nigrostriatal (Toth *et al.*, 1992) pathways markedly decreased the ability of locally applied nicotine to elicit DA release *in vivo*. Furthermore, locally applied

(-)-nicotine has been shown to increase levels of excitatory amino acids in the striatum and frontal cortex, predominantly glutamate (Toth *et al.*, 1993), and this effect was mecamylamine-sensitive. Thus, it has been proposed that (-)-nicotine can act at presynaptic nAChR on glutamatergic nerve terminals to release glutamate, which in turn stimulates the release of dopamine via presynaptic glutamate receptors on DA neurones, a conclusion consistent with recent electrophysiological recordings from striatum *in situ* (García-Muñoz *et al.*, 1996). A similar interaction between glutamate and dopamine is suggested in the frontal cortex (Jedema and Moghaddam, 1996).

In vitro, as long ago as 1979, glutamate was reported to stimulate [^{3}H]-DA release from rat striatal slices (Roberts and Anderson, 1979), interpreted as a reflection of presynaptic glutamate receptors on DAergic nerve terminals. This notion has been reinforced in subsequent studies, with evidence for the presence of both AMPA/kainate and NMDA receptors (e.g. Wang *et al.*, 1991; Desce *et al.*, 1992). Activation of AMPA/kainate receptors could relieve the physiological Mg^{2+} block of the NMDA receptors. In striatal synaptosomes, it has recently been proposed that ACh or (-)-nicotine, acting at presynaptic nAChR on DA terminals, can also relieve the Mg^{2+} block of the NMDA receptors, having a synergistic effect with NMDA itself (Chéramy *et al.*, 1996). The potential importance of presynaptic nAChR in modulating glutamate release was recently highlighted in electrophysiological studies (see chapter 2: e.g. McGehee *et al.*, 1995; Gray *et al.*, 1996). These studies are of considerable importance because it has been reported (Hunter *et al.*, 1994) that the highly Ca^{2+} permeable α7 nAChR may function in synapse formation and stabilisation i.e. a phenomena akin to LTP (long term potentiation) which could be pertinent to learnt behaviours underlying the addiction process. Clearly, a thorough examination of nicotine-evoked glutamate release in the striatum is timely and pertinent.

In the previous chapter it has been demonstrated that nAChR on DAergic nerve terminals are heterogeneous and those containing α3β2 subunits have been identified (Kulak *et al.*, 1997; Kaiser *et al.*, 1998). Although the IC_{50} value for α-CTx-MII in striatal slices was very similar to that found in synaptosomes at the same agonist concentration, striatal slices showed lower inhibition by α-CTx-MII of (±)-AnTx-a evoked [^{3}H]-DA (**Error! Unknown switch argument.**). As slices are more intact striatal preparations, the lower inhibition by α-CTx-MII might reflect additional nAChR (which are α-CTx-MII- insensitive) on non-dopaminergic terminals, whose activation may indirectly enhance DA release. The main objectives of the present study were:

1) to investigate in the striatum a possible indirect enhancement of nicotinic agonist-evoked DA release, via activation of nAChR on glutamatergic nerve terminals; and
2) to pharmacologically characterise the nAChR subtype/s involved.

Using the superfusion technique, the effects of nicotinic- and glutamate-related compounds on evoked striatal DA release, were addressed. Synaptosome preparations allow the study of ligand gated ion channels on dopaminergic nerve terminals and their functional cross-talk. However, studies performed on slices, a more intact preparation, provide evidence for functional interactions between striatal dopaminergic and glutamatergic nerve terminals as a consequence of presynaptic nAChR activation.

5.2 Experimental procedures

5.2.1 Materials

The following drugs were used in this study: 6,7-dinitroquinoxaline-2,3-dione (DNQX), kynurenic acid (KYNA - Tocris Crookson - Bristol, UK), α-conotoxin-Iml (α-CTx-Iml - Calbiochem - San Diego, CA USA), 4-amino pyridine (4-AP - RBI Natick, MA USA), L-glycine, N-methyl-D-aspartate (NMDA), strychnine (Sigma - Poole, Dorset U.K). All other chemicals used were of analytical grade and obtained from standard commercial sources.

5.2.2 Superfusion technique

P2 synaptosomes and slices (0.25 mm) were prepared from the striata of male Sprague-Dawley rats (250-280 g - University of Bath Animal House breeding colony), loaded with [^{3}H]-DA and perfused as previously described (Marshall *et al.*, 1996 - see 4.2.4.1) with Krebs bicarbonate buffer.

In brief, samples (synaptosomes or slices) were washed for 20 min with Krebs bicarbonate buffer and a further 10 min with normal buffer or buffer containing antagonist (112 nM α-Ctx-MII, 1 μM α-Ctx-Iml, 50 nM MLA, 10 μM mecamylamine, 500 μM KYNA, 100 μM DNQX). The pre-incubation time for α-Bgt (40 nM) was 1 h at 37°C. Then, the nicotinic agonists: (-)-nicotine or (±)-AnTx-a; or a non-specific chemical stimulus (KCl or 4-AP) was applied for 40s. Two min (0.5 ml / min) fractions were collected and counted for radioactivity.

Superfusion data analysis (see also 4.2.4.2)

The baseline was derived by fitting a double exponential decay equation (equation 4.1) to the data using Sigma Plot for Windows (Jandel Scientific, Germany). Evoked [^{3}H]-DA release was calculated as the area under the peak after subtraction of the baseline. Data are represented as percentages of the corresponding controls, assayed in parallel in the absence of antagonist, and are mean±S.D. of several independent experiments, each consisting of two to three replicate chambers for each condition. The one way ANOVA test was used to determine the significance of differences from control (Sigma Stat - Jandel Scientific).

For analysis of the (±)-AnTx-a dose-response curve in striatal slices, the data were fitted to the 2-sites model equation:

$$y = \{a / [1 + (k1 / x)^{n1}]\} + \{b / [1 + (k2 / x)^{n2}]\}$$

(Equation 5.1)

where **a** & **b** are the asymptotic maximums; **k1** & **k2** are the values at the inflection points (apparent EC_{50}s) and **n1** & **n2** are the slope parameters (Hill numbers).

5.3 Results

5.3.1 Permissive effect of (-)-nicotine for the NMDA-evoked release of [^{3}H]-DA from striatal slices

To evaluate the possible cross-talk between iGluR and nAChR on striatal dopaminergic nerve terminals, studies involving the application of NMDA and (-)-nicotine (applied alone or together) were performed. [^{3}H]-DA release from striatal slices was monitored using the superfusion technique. Initial studies were carried out in the presence and absence of the NMDA-R coagonist L-glycine (Gly, 1µM). Slices were perfused with Krebs buffer containing 1 µM strychnine to avoid any effect of glycine on glycine receptors (Gly-R). (-)-Nicotine (10 µM) stimulated the release of [^{3}H]-DA from rat striatal slices (Figure 5.3). Basal release was defined as the non-specific 10 µM (-)-nicotine-evoked response in the presence of 10 µM mecamylamine, a non-competitive nAChR blocker (Figure 5.3). In the absence of added L-glycine (Figure 5.3 left panel), 1 mM NMDA had no significant effect (17.9±3.2% - n=4) on basal (27.3±15.1% - n=4) or 10 µM (-)-nicotine-evoked [^{3}H]-DA release (106.9±17.9% - n=4). However, [^{3}H]-DA release from slices was significantly increased by 52.3±7.4% (n=4) following application of (-)-nicotine (10 µM) and NMDA (1 mM) in the presence of 1 µM L-glycine (Figure 5.3 right panel). NMDA (1 mM) plus L-glycine (1 µM) in the absence of (-)-nicotine (16.1±3.0% - n=4) still had no significant effect on basal release (25.4±8.0% - n=4).

In summary, presumably because of the Mg^{2+}-blockade of NMDA-receptors, NMDA alone (either in the presence or absence of added L-glycine) was without effect on [^{3}H]-DA release. However, (-)-nicotine exerted a "permissive effect" on the NMDA-evoked [^{3}H]-DA release, only in the presence of L-glycine. These results confirm previous observations by Desce *et al.* (1992) and Chéramy *et al.* (1996).

To correctly interpret the results it is necessary to consider the effect L-glycine and Mg^{2+} on the evoked responses. Chéramy *et al.* (1996) reported that NMDA-evoked release (in the absence of Mg^{2+}) was progressively reduced in the presence of increasing concentrations of Mg^{2+}, complete blockade being observed with 0.28 mM Mg^{2+}. In contrast, the marked stimulation of [^{3}H]-DA release induced by the combined application of NMDA and ACh (in the presence of L-glycine and absence of Mg^{2+}) was almost insensitive to increasing concentrations of Mg^{2+}. The response was not affected by the physiological concentration of Mg^{2+} (0.83 mM) and was only slightly reduced at a much higher concentration (7.48 mM) (Chéramy *et al.*, 1996). In this study, bearing in mind these previous data, a concentration of Mg^{2+} (1.2 mM) in the physiological range was used.

The system was also tested for a possible antagonistic effect of strychnine (1 µM) on nAChR. The effect of the Gly-R antagonist on 10 µM (-)-nicotine-evoked [^{3}H]-DA release was assessed in slices. In Krebs buffer without strychnine, [^{3}H]-DA-evoked by 10 µM (-)-nicotine represented 105.3%±7.4% (n=4) of control (10 µM (-)-nicotine-evoked response in buffer containing 1 µM strychnine). The difference was not significant ($p>0.05$ - one way ANOVA). In the following experiments, neither L-glycine nor strychnine was added to the Krebs bicarbonate buffer.

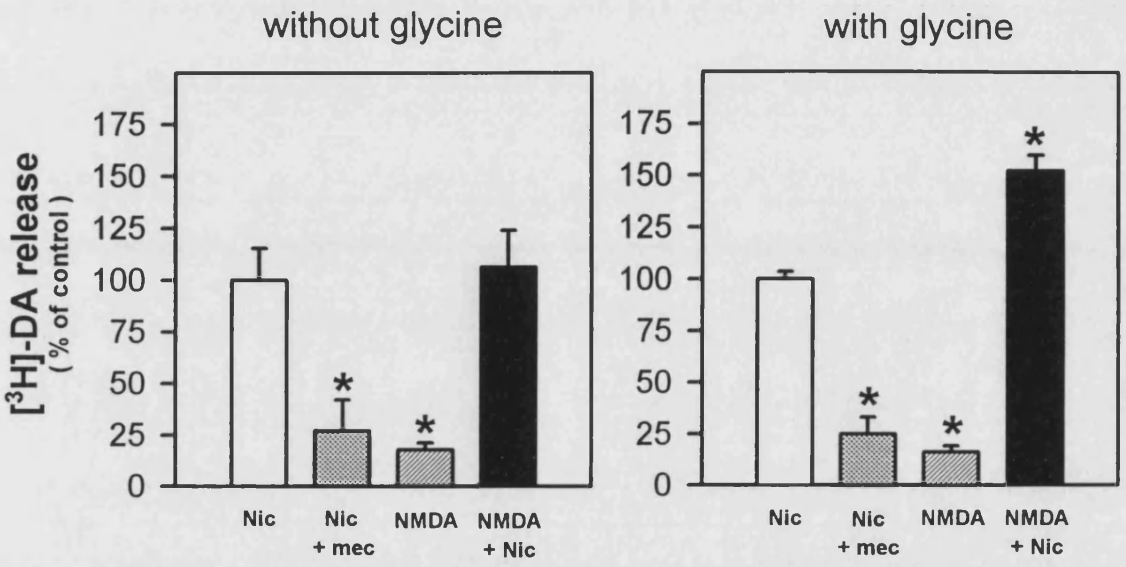

Figure 5.3 NMDA evokes [^{3}H]-DA release from rat striatal slices when coapplied with (-)-nicotine and L-glycine. Tissue prisms were continuously perfused with Krebs buffer containing strychnine (1 µM) to block striatal Gly-R. Basal release was defined as the non-specific 10 µM (-)-nicotine-evoked response in the presence of 10 µM mecamylamine. Responses are expressed as mean percentages±S.D. of control ([^{3}H]-DA-released by 10 µM (-)-nicotine). In the absence of added L-glycine (left panel), 1 mM NMDA had no significant effect on basal or 10 µM (-)-nicotine-evoked [^{3}H]-DA release. However, [^{3}H]-DA release from slices was significantly increased (~53%) following application of (-)-nicotine (10 µM) and NMDA (1 mM) in the presence of 1 µM L-glycine (right panel). NMDA (1 mM) plus L-glycine (1 µM) in the absence of (-)-nicotine still had no significant effect on basal release.
(* $p<0.05$ significantly different from control, one way ANOVA – Bonferroni *t* test)

5.3.2 Ionotropic glutamate receptor antagonists inhibit DA release from rat striatal slices

Further experiments were designed to establish the possible involvement of endogenous glutamate in the modulation of striatal DA release by presynaptic nAChR. Initially, the effect of the non-specific iGluR antagonist kynurenic acid (KYNA) on evoked striatal [^{3}H]-DA release from slices was examined. Addition of KYNA (500 µM and 800 µM) to the superfusion buffer caused a small but significant reduction of the [^{3}H]-DA released by KCl and 4-AP

(Figure 5.4 a & b). KYNA (500μM) inhibited 23.5 mM KCl- and 1 mM 4-AP-evoked DA release (controls) by 21.0±3.1% and 23.0±6.0% (n=3), respectively. A higher KYNA concentration (800 μM) did not increase the inhibition (18.0±5.0% and 21.0±4.0% (n=3) of the responses evoked by 23.5 mM KCl and 1 mM 4-AP, respectively. These results would suggest that L-glutamate, released by general depolarising agents, indirectly enhances DA release from striatal dopaminergic nerve terminals.

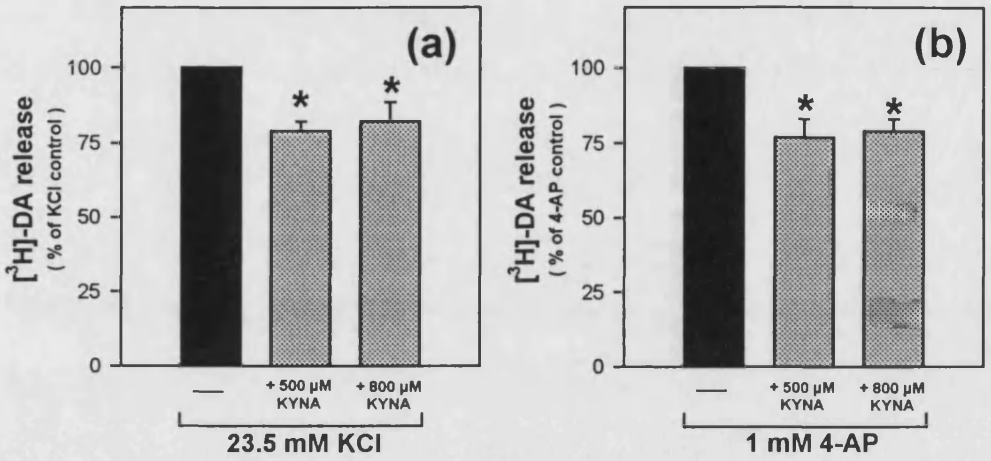

Figure 5.4 Effect of KYNA (500 μM and 800 μM) on (a) KCl-(23.5 mM) and (b) 4-AP-(1 mM) evoked [^{3}H]-DA release from rat striatal slices. Responses are expressed as mean percentages±S.D. of either 23.5 mM KCl- or 1 mM 4-AP-evoked [^{3}H]-DA-release (controls). KYNA (500μM) significantly inhibited 23.5 mM KCl- and 1 mM 4-AP-evoked DA release. A higher KYNA concentration (800 μM) did not increase the inhibition observed in the presence of 500 μM KYNA.
(* $p<0.05$ significantly different from control, one way ANOVA – Bonferroni *t* test)

In slices, KYNA (500 μM and 800 μM) also decreased the evoked response when, instead of depolarising agents, the nAChR agonist (±)-AnTx-a (1 μM) was used to elicit [^{3}H]-DA release (Figure 5.5 left panel). In slices, 500 and 800 μM KYNA inhibited 1 μM (±)-AnTx-a-evoked [^{3}H]-DA release (control) by 18.0±5.0% (n=4) and 18.0±2.0% (n=4), respectively. The effect of KYNA (500 μM and 800 μM) on 1 μM (±)-AnTx-a-evoked DA release was also studied in striatal synaptosomes (Figure 5.5 right panel). This set of experiments was designed to detect any possible non-specific effect of KYNA on nAChR. In synaptosomes, 1 μM (±)-AnTx-a-evoked DA release in the presence of 500 μM and 800 μM KYNA represented 98.0±2.0% (n=4) and 96.0±7.0% (n=4) of control (1 μM (±)-AnTx-a-evoked response in the absence of KYNA), respectively. Neither KYNA concentration (500 μM and 800 μM) had any significant effect on (±)-AnTx-a-evoked [^{3}H]-DA release from the nerve terminal preparation. These results would suggest that (±)-AnTx-a evokes DA release in striatum directly by acting on DA nerve terminals and indirectly by evoking the release of glutamate, than in turn acts on iGluR on dopaminergic terminals.

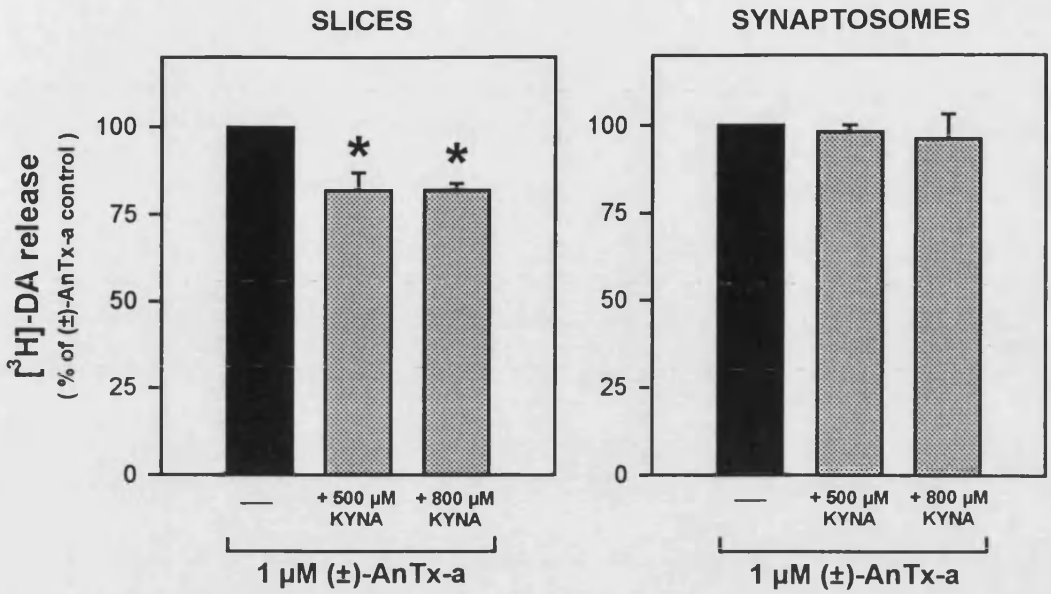

Figure 5.5 Effect of KYNA (500 µM and 800 µM) on 1 µM (±)-AnTx-a-evoked [^{3}H]-DA release from rat striatal slices and synaptosomes. Responses are expressed as mean percentages±S.D. of 1 µM (±)-AnTx-a-evoked [^{3}H]-DA-release. In slices, 500 and 800 µM KYNA inhibited (±)-AnTx-a-evoked [^{3}H]-DA release. However, at these concentrations, KYNA had no significant non-specific effects on nAChR when tested in synaptosomes.
(* $p<0.05$ significantly different from control, one way ANOVA – Bonferroni *t* test)

The (±)-AnTx-a concentration (1 µM) used in the above experiments was chosen bearing in mind the dose-response curve for (±)-AnTx-a-evoked DA release in striatal synaptosomes (EC_{50} = 134±26nM – Figure 4.8). To compare the potency of (±)-AnTx-a in evoking [^{3}H]-DA release from striatal slices, a dose-response curve was constructed. Unexpectedly, it had a reproducible and distinct biphasic overall shape with apparent EC_{50} values of 241.8±36.1nM and 5.1±0.3µM (n=8-26 – Figure 5.6).

As already stated, 500 µM KYNA had a small but significant effect on [^{3}H]-DA release from slices evoked by 1 µM (±)-AnTx-a (Figure 5.5 left panel). Testing 500 µM KYNA against higher concentrations of (±)-AnTx-a showed that the second phase of the dose-response curve was almost completely abolished in the presence of this antagonist (Figure 5.6), whereas mecamylamine (10 µM) decreased evoked release to ~20% of control across the entire dose-response curve. KYNA (500 µM) inhibited mecamylamine-sensitive responses to 1 µM, 10 µM and 25 µM (±)-AnTx-a by 23.0±2.4% (n=3), 53.0±1.8% (n=3) and 45.9±5.1% (n=4), respectively.

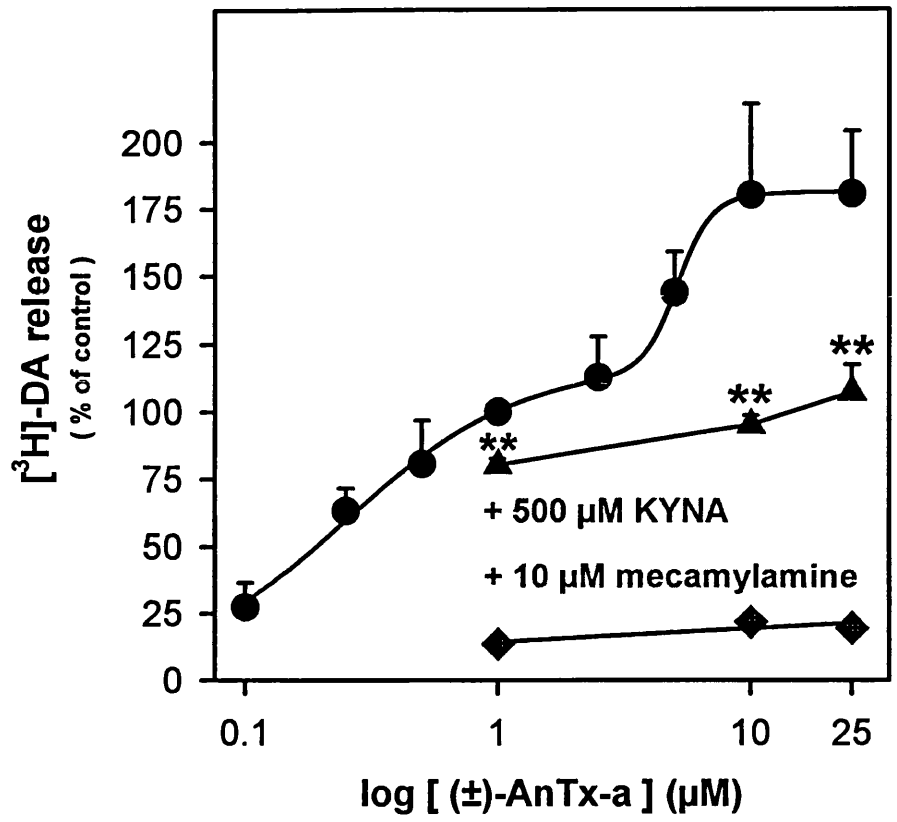

Figure 5.6 Dose-response curve for (±)-AnTx-a-evoked [^{3}H]-DA release from rat striatal slices. In slices, the dose-response curve for (±)-AnTx-a-evoked [^{3}H]-DA release was biphasic with apparent EC_{50} values of 241.8±36.1nM and 5.1±0.3μM (n=8-26). All the responses are expressed as mean percentages ± S.D. of the response evoked by 1 μM (±)-AnTx-a (control). KYNA (500 μM) almost abolished the second phase of the dose-response curve, whereas mecamylamine (10 μM) decreased evoked release to ~20% of control across the entire dose-response curve. Data were fitted to a 2-sites model using equation 5.1.
(** $p<0.01$ significantly different from 1 μM, 10 μM and 25 μM (±)-AnTx-a-evoked responses in the absence of KYNA, one way ANOVA – Dunnett test)

5.3.3 iGluR involved in [^{3}H]-DA release from striatal slices

In addition to KYNA, the non-NMDA-R antagonist 6,7-dinitroquinoxaline-2,3-dione (DNQX), was also examined on responses elicited by 25 μM (±)-AnTx-a. In slices, DNQX (100 μM) inhibited 25 μM (±)-AnTx-a-evoked [^{3}H]-DA release by 42.6±8.0% (n=5 – Figure 5.7 right panel). The magnitude of this inhibition was similar to that seen, under the same experimental conditions, with 500 μM KYNA (Figure 5.7 right panel). However, when KYNA (500 μM) and DNQX (100μM) were coapplied, they decreased mecamylamine-sensitive 25 μM (±)-AnTx-a-evoked response by 42.5±10.0% (n=4 – Figure 5.7 right panel). The fact that no additive effect was observed, would indicate that both antagonists were acting predominantly on the same iGluR (in nominally glycine-free conditions and in the presence of 1.2 mM Mg^{2+}). As previously described (see Figure 4.8), 1 μM and 25 μM (±)-AnTx-a evoked maximum

dopamine release from striatal synaptosomes (Figure 5.7 left panel). In the same preparation, neither 500 µM KYNA (88.1±12.0% - n=4) nor 100 µM DNQX (88.0±10.5% - n=4) had significant effect on 25 µM (±)-AnTx-a-evoked [^{3}H]-DA release (105.2±13.3% n=4 – Figure 5.7 left panel). This result suggests that neither KYNA nor DNQX (at the concentrations used) exert non-specific effects on nAChR present on dopaminergic nerve terminals.

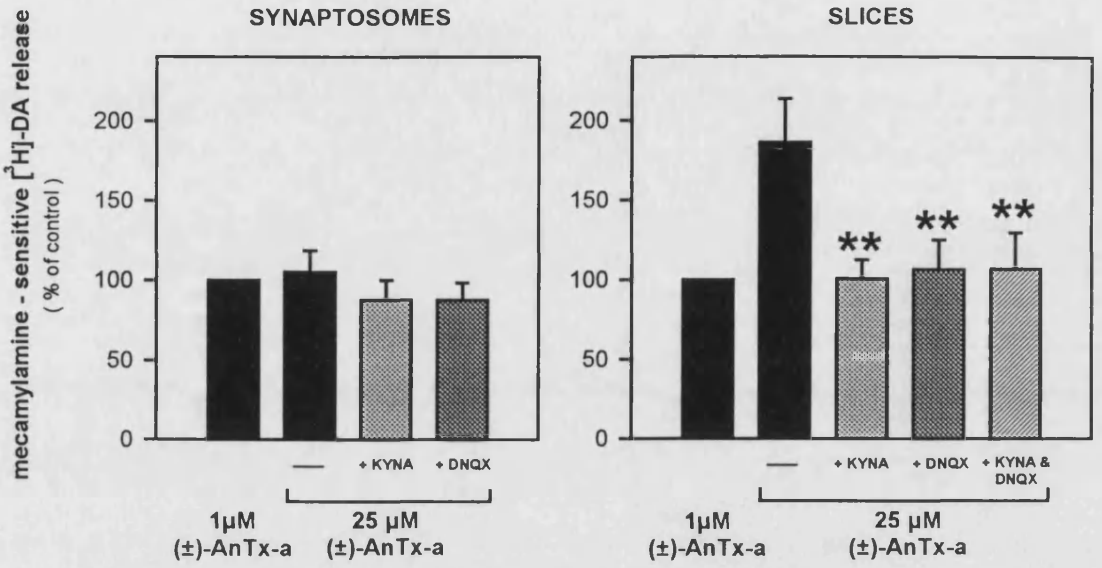

Figure 5.7 Comparison of the effects of DNQX and KYNA on 25 µM (±)-AnTx-a-evoked [^{3}H]-DA release from rat striatal synaptosomes and slices. Results are expressed as mean percentages±S.D. of mecamylamine-sensitive 1 µM (±)-AnTx-a-evoked responses (control). In slices, DNQX (100 µM) significantly inhibited 25 µM (±)-AnTx-a-evoked [^{3}H]-DA release. However, when KYNA (500 µM) and DNQX (100µM) were coapplied, no additive effect was observed (right panel). In synaptosomes, 1 µM and 25 µM (±)-AnTx-a evoked maximum dopamine release, whereas neither 500 µM KYNA nor 100 µM DNQX had significant effect on 25 µM (±)-AnTx-a-evoked [^{3}H]-DA release (left panel).
(** $p<0.01$ significantly different from 25 µM (±)-AnTx-a-evoked response, one way ANOVA – Bonferroni *t* test)

5.3.4 Pharmacology of nAChR modulating DA release in striatal slices

To characterise the nAChR modulating striatal DA release, several nAChR antagonists were assayed on the responses evoked by 1µM and 25 µM (±)-AnTx-a in synaptosomes and slices. MLA (50 nM) and α-CTx-Iml (1 µM) were applied as selective antagonists of α7-containing nAChR whereas α-CTx-MII (112 nM) was used to competitively antagonise nAChR containing α3β2 interfaces. Figure 5.8 summarises the results obtained for (±)-AnTx-a-evoked DA release in the presence and absence of these nAChR antagonists.

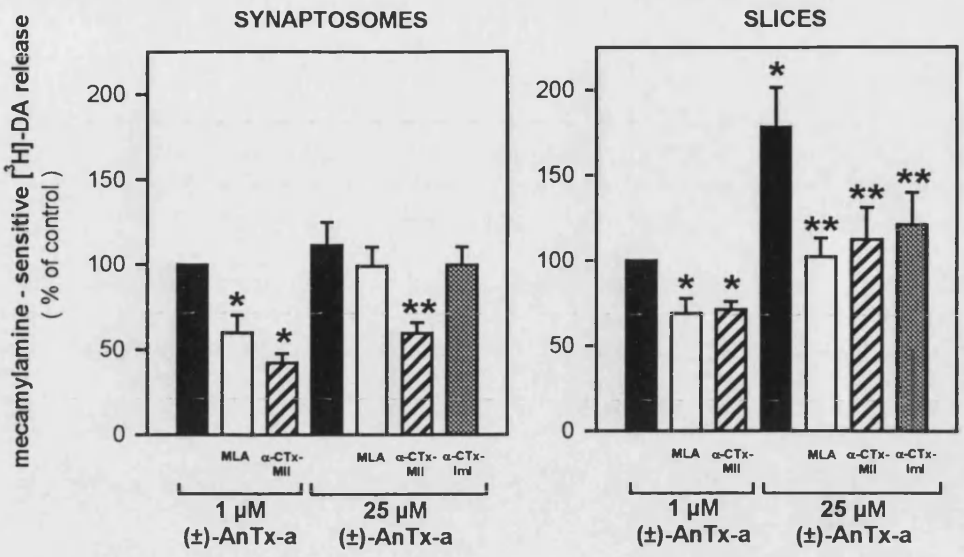

Figure 5.8 Pharmacology of (±)-AnTx-a-evoked [^{3}H]-DA release in rat striatal synaptosomes and slices. Results are expressed as mean percentages±S.D. of mecamylamine-sensitive 1 μM (±)-AnTx-a-evoked responses (control). In **synaptosomes**, 1 μM and 25 μM (±)-AnTx-a elicited maximum dopamine release. α-CTx-MII (112 nM) significantly diminished 1 μM and 25 μM (±)-AnTx-a-evoked DA release. Although MLA (50 nM) significantly inhibited the 1 μM (±)-AnTx-a-evoked response, it had no significant effect on the 25 μM (±)-AnTx-a-evoked response. α-Ctx-Iml (1 μM) had no significant effect on the response evoked by 25 μM (±)-AnTx-a. In **slices**, the response elicited by 25 μM (±)-AnTx-a was significantly higher than control. MLA (50 nM) and α-CTx-MII (112 nM) significantly diminished 1 μM and 25 μM (±)-AnTx-a-evoked DA release. α-CTx-Iml also had significant effect on 25 μM (±)-AnTx-a-evoked DA release.
(* $p<0.05$ significantly different from control; ** $p<0.01$ significantly different from 25 μM (±)-AnTx-a-evoked response, one way ANOVA – Bonferroni *t* test)

In **synaptosomes**, the response elicited by 25 μM (±)-AnTx-a (111.3±13.9% - n=9) was not significantly different from control (1 μM (±)-AnTx-a-evoked mecamylamine-sensitive response). MLA (50 nM) and α-CTx-MII (112 nM) decreased 1 μM (±)-AnTx-a-evoked DA release by 39.1±10.2% (n=5) and 57.6±5.4% (n=8), respectively. α-CTx-MII (112nM) diminished 25 μM (±)-AnTx-a-evoked DA release by 46.4%±5.4% (n=6). However, MLA (50 nM) and α-Ctx-Iml (1 μM) had no significant effect on the response evoked by 25 μM (±)-AnTx-a in synaptosomes. Responses in the presence of MLA and α-CTx-Iml were 88.8±10.2% (n=6) and 89.4±9.7% (n=3) of the 25 μM (±)-AnTx-a-evoked response, respectively.

In **slices**, the response elicited by 25 μM (±)-AnTx-a was significantly higher (178.2±23.23% - n=26) than control (1 μM (±)-AnTx-a-evoked mecamylamine-sensitive response). MLA (50 nM) and α-CTx-MII (112 nM) reduced 1 μM (±)-AnTx-a-evoked DA release by 31.3±9.0% (n=7) and 29.1±4.8% (n=4), respectively. Moreover, MLA (50 nM), α-CTx-MII (112 nM) and α-CTx-Iml (1 μM) decreased the 25 μM (±)-AnTx-a-evoked response by 42.7±6.2% (n=4), 36.8±10.5% (n=4) and 31.9±10.4% (n=5), respectively.

As previously described in chapter 4, 112 nM α-CTx-MII partially inhibited the (±)-AnTx-a-evoked response in slices and synaptosomes (Figure 5.8 and Figure 4.4). Interestingly, the slice preparation also showed partial sensitivity to α7-containing nAChR antagonists (MLA and α-CTx-Iml – Figure 5.8 right panel). As will be discussed in section 5.4, striatal dopaminergic nerve terminals are not thought to possess α7-containing nAChR. However, in this study, MLA (50 nM) unexpectedly inhibited (±)-AnTx-a-evoked DA release from synaptosomes. In an attempt to shed some light on this result, the effects of a lower (10 nM) and a higher (500 nM) MLA concentration were also tested (Figure 5.9). The results obtained showed that 10 nM and 50 nM MLA inhibited mecamylamine-sensitive 1 μM (±)-AnTx-a-evoked DA release from synaptosomes by 37.1±9.9% (n=6) and 39.1±10.2% (n=5), and are not significantly different ($p>0.01$, one way ANOVA). However, 500 nM MLA produced significantly more inhibition of 60.6±7.0% (n=5).

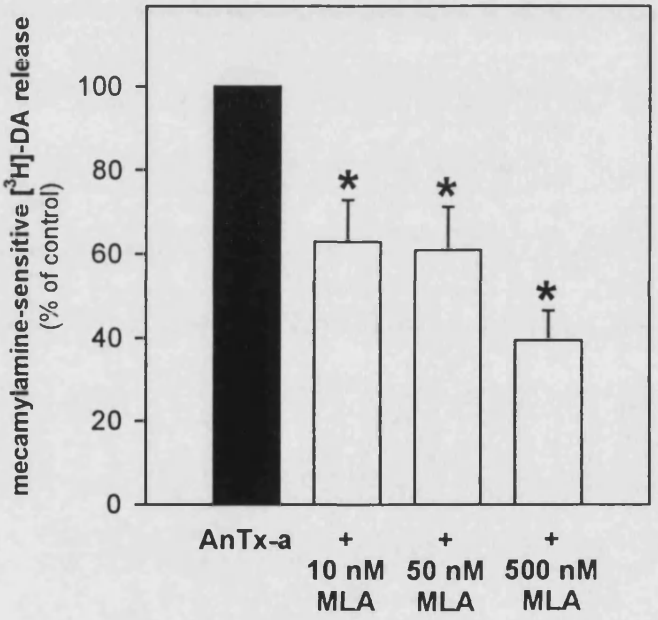

Figure 5.9 Effect of MLA on (±)-AnTx-a-evoked [^{3}H]-DA release from rat striatal synaptosomes. Results are expressed as mean percentages±S.D. of the mecamylamine-sensitive 1 μM (±)-AnTx-a-evoked response (control). Low nanomolar concentrations of MLA, 10 nM and 50 nM, inhibited 1 μM (±)-AnTx-a-evoked responses. The effects of 10 nM and 50 nM MLA were not statistically different. However, 500 nM MLA produced significantly more inhibition than 10 or 50 nM MLA.
(* $p<0.05$ significantly different from control, one way ANOVA – Bonferroni *t* test)

5.3.5 α-Bgt-sensitive nAChR modulate glutamate release in rat striatal slices

The sensitivity of (±)-AnTx-a-evoked [^{3}H]-DA release from slices to MLA and α-CTx-Iml hinted at the possible participation in the response of α7-containing nAChR. In order to test this hypothesis, another α7-selective antagonist, α-Bgt, was examined. Striatal slices were preincubated in 40 nM α-Bgt for 1 h at 37°C, before stimulation with 25 µM (±)-AnTx-a. This treatment decreased the response by 39.8±15.6% (n=8 Figure 5.11), i.e. to the same extent as 50 nM MLA and 1 µM α-CTx-Iml (Figure 9 and Figure 5.10). The similar sensitivity of the response evoked in slices by (±)-AnTx-a to maximally effective concentrations of three α7-selective antagonists (MLA, α-CTx-Iml & α-Bgt) strongly suggests the involvement of α7-containing nAChR.

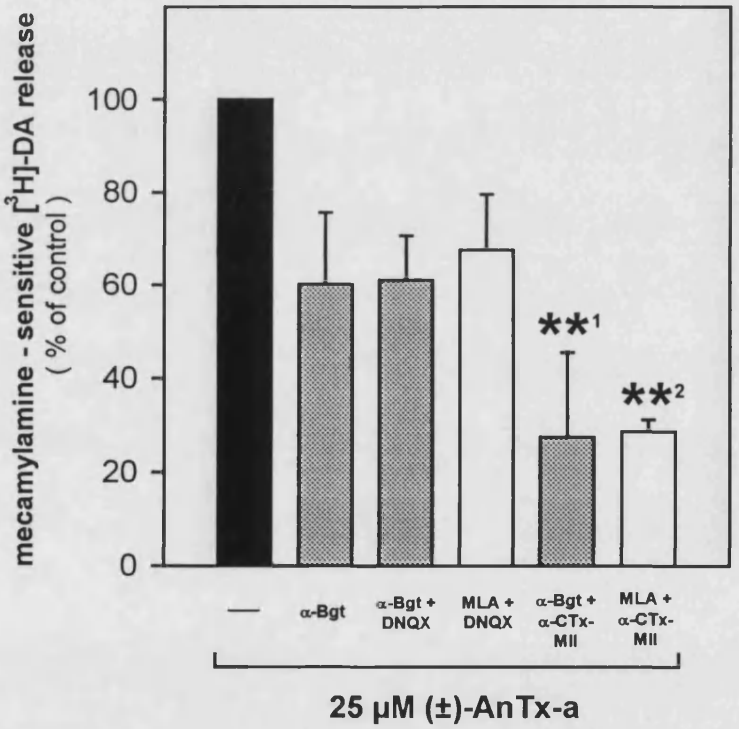

Figure 5.11 Combined effect of α7-selective antagonists and DNQX or α-CTx-MII on 25 µM (±)-AnTx-a evoked [^{3}H]-DA release in rat striatal slices. Results are expressed as mean percentages±S.D. of mecamylamine sensitive 25 µM (±)-AnTx-a-evoked responses (control). In slices, α-Bgt (40 nM) significantly decreased DA release. This inhibition was not significantly different from that achieved during coapplication of DNQX (100 µM) with either α-Bgt (40 M) or MLA (50 nM). When α-CTx-MII (112 nM) was coapplied with either α-Bgt (40 nM) or MLA (50 nM) the effects were additive.
(**^{1} $p<0.01$ significantly different from response in the presence of α-Bgt and DNQX; **^{2} $p<0.01$ significantly different from response in the presence of MLA and DNQX, one way ANOVA – Bonferroni *t* test)

Additional experiments were carried out to elucidate if the α-Bgt-sensitive nAChR were responsible for the indirect glutamate enhancement of DA release. The inhibition achieved with α-Bgt alone (39.8±15.6% n=8) was not significantly different from that observed during coapplication of DNQX (100 μM) with either 40 nM α-Bgt (38.9±9.6% - n=5) or 50 nM MLA (32.7±11.9% - n=3). However, when α-CTx-MII (112 nM) was coapplied with either α-Bgt (40 nM) or MLA (50 nM) the inhibition increased to 72.6±18.0% (n=5) and 71.3±2.5% (n=3), respectively (Figure 5.11).

5.4 Discussion

In this study, the superfusion technique was used to investigate possible striatal interactions that could lead to DA release enhancement as a consequence of presynaptic nAChR activation on non-dopaminergic nerve terminals. In particular, assays were designed and performed in an attempt to describe a putative involvement of presynaptic nAChR in striatal glutamate release.

5.4.1 "Permissive effect" of nAChR-activation on NMDA-evoked DA striatal release

It is well known that neostriatal neurones receive direct excitatory innervation from cortex and thalamus (review: see Di Chiara, 1994). Presynaptic modulation of DA release in striatum by excitatory afferents occurs at different levels. Released glutamate, e.g. from corticostriatal nerve terminals, would be expected to interact with postsynaptic NMDA- and / or non-NMDA-(AMPA/kainate) receptors. Moreover, both glutamate release and the excitability of glutamate-containing corticostriatal terminals are increased by activation of glutamate autoreceptors (Biziere and Coyle, 1978; Greenamyre and Young, 1989; García-Muñoz *et al.*, 1991). Indirect modulation of the excitatory input may also occur as a consequence of local changes in the extracellular concentration of endogenous compounds capable of altering the performance of ionotropic excitatory amino acid receptors. L-Glycine, the coagonist of NMDA-receptors, is known to exert such a modulatory effect on NMDA-R (Johnson and Asher, 1987). Then, subtle changes in extracelullar concentrations of L-glycine or endogenous antagonists of strychnine insensitive-glycine sites (e.g. D-serine) may indirectly regulate the excitatory effects of NMDA-activated ion conductances. Local generation in astrocytes of kynurenic acid (KYNA) may also indirectly modify the effects of glutamatergic agonists. KYNA is a "broad spectrum" excitatory amino acid receptor antagonist that competitively antagonises NMDA- and AMPA/kainate- receptors.

It is important to highlight at this point two features of the NMDA-R. First, in the absence of L-glycine, NMDA completely fails to activate the NMDA-receptor (Kleckner and Dingledine, 1988; Vyklicky *et al.*, 1990). Second, although the potentiating effect of L-glycine is seen even at low concentrations of this amino acid, it has been reported that the NMDA response desensitises at low L-glycine concentrations (i.e. 0.1 µM). Only an increase of the glycine concentration in the medium (e.g. to 3 µM), suppresses the NMDA-R desensitisation (Vyklicky *et al.*, 1990; Benveniste *et al.*, 1990).

Under physiological conditions, the Mg^{2+}-induced blockade of the NMDA ionophore is sufficient to hide the L-glycine potentiation of NMDA excitation. However, this study shows that, in the presence of magnesium (1.2 mM) and L-glycine (1 µM), NMDA stimulated DA release when coapplied with (-)-nicotine. On the other hand, the absence of response when slices were stimulated with NMDA alone, revealed the permissive effect of (-)-nicotine on the NMDA-evoked DA release, an effect previously reported in striatal synaptosomes by Chéramy *et al.* (1996).

The same permissive role observed for nAChR, was also reported by Desce *et al.* (1992) for the AMPA-R. The synergism between NMDA-R and nAChR presumably results from removal of the magnesium block of NMDA receptors after nicotinic depolarisation of the nerve terminal membrane (Chéramy *et al.*, 1996). These results would suggest that nAChR and NMDA-R are located relatively close to each other on DAergic nerve terminals.

In this chapter, it has been also demonstrated that L-glycine, under standard experimental conditions (Krebs buffer as extracelullar medium), is not present at saturating concentrations. This observation is evident since addition of exogenous L-glycine potentiated [^{3}H]-DA release from striatal slices evoked by (-)-nicotine and NMDA applied together. When L-glycine was not added to the buffer (nominally L-glycine-free conditions), the synergism was not observed.

5.4.2 (±)-AnTx-a-evoked striatal glutamate release

Although axoaxonic synapses between dopaminergic and cortical afferents are not present, these inputs to the striatum form synapses in close proximity to each other onto the dendrites and dendritic spines of medium-sized spiny neurones. Thus, endogenous neurotransmitter released from one nerve terminal may diffuse short distances to stimulate heteroreceptors and thereby indirectly affect the release in another neurotransmitter pathway. It appears that neurotransmitter release can be modulated not only by changes in the frequency of incoming action potentials, but also by changes in transmitter levels in the local presynaptic environment. Modification of the local concentration of one neurotransmitter can produce subsequent changes in stimulation of presynaptic heteroreceptors on the axons or nerve terminals of another transmitter system. Most D1 dopaminergic receptors are located on striatal dendrites outside symmetric synapses formed by dopaminergic terminal fibres (Levey *et al.*, 1993; Gonon, 1998). As mentioned in the introduction, these receptors are often located in the proximity of asymmetric synapses formed by glutamatergic terminals on the head of dendritic spines (Levey *et al.* 1993; Ingham *et al.*, 1998). Recent studies (Ingham *et al.*, 1998) have made evident the complexity of these synaptic interactions. Unilateral lesion of the nigrostriatal pathway using 6-OHDA, showed that loss of dendritic spines on striatal medium-sized spiny neurones is accompanied by a loss of asymmetric synapses, rather than by the movement of excitatory synapses from spines to other postsynaptic targets.

When striatal slices are stimulated with general depolarising agents such as 4-aminopyridine (4-AP) or KCl, a major percentage of the transmitters present in the sample are probably released. These compounds exert their effect through different mechanisms. The former by blocking a particular type of K^+ channels, and the latter by perturbing the electrochemical equilibrium across the nerve terminal membrane. In 1994, Jin and Fredholm showed that, in the presence of 4-AP, endogenous glutamate contributes to dopamine release from striatal slices. Later, in 1997, the same lab reported that glutamate, by acting on NMDA -R in the absence of Mg^{2+}, regulates electrically-evoked DA release from the same brain preparation.

In the present study, DA release from striatal slices was initially evoked, in the presence of Mg^{2+}, by acute application of 4-AP or KCl (see Figure 5.4). The broad spectrum iGluR antagonist KYNA (500 µM), reduced striatal 4-AP- and KCl-evoked DA release by 23.0% and 21.0%, respectively. A higher KYNA concentration (800 µM) did not increase the inhibition: 21.0% and 18.0% for 4-AP and KCl, respectively. Therefore, these results suggested that part of the 4-AP- and KCl-evoked DA release was mediated by glutamate. Although Jin and Fredholm (1997), using similar KYNA concentrations (400 µM), reported a higher degree of inhibition (>50%), the present results qualitatively reproduce theirs. Quantitative mismatch between this study and their observations probably reflects differences in experimental design, such as the addition of Mg^{2+} to the buffer and the nature (chemical vs. electrical) and the duration (40 s vs. 3 min) of the evoking-stimulus.

In striatal slices, 1 µM (±)-AnTx-a-evoked [^{3}H]-DA release was also partially blocked by 500 µM (18.0%) and 800 µM (18.0%) KYNA (see Figure 5.6). However, in striatal synaptosomes and in the presence of Mg^{2+}, KYNA (500 µM and 800 µM) had no significant effect on the response elicited by 1 µM (±)-AnTx-a. Therefore, KYNA (at the concentrations used) had not non-specific effects on DAergic nerve terminal nAChR. It is important to consider that (±)-AnTx-a probably releases only a small percentage of the neurotransmitters released by general depolarising agents (e.g. 1 µM (±)-AnTx-a gives a response that is 46% of the [^{3H}]-DA released by 25 mM KCl in striatal synaptosomes - Soliakov *et al.*, 1995). In absolute numbers (±)-AnTx-a (1µM) and KCl/4-AP (at the concentrations used in this study) evoked 1.5-2.0% and 5.0-6.0% of the total [^{3}H]-DA loaded into the striatal slices, respectively. Thus, although in relative terms the degree of inhibition found for the nicotinic agonist is close to that found for 4-AP/KCl (~20% of controls), in absolute numbers it was significantly lower (~0.35% vs. ~1.10% of total slice cpm). These results have also indicated that (±)-AnTx-a can evoke at least the release of one neurotransmitter, glutamate, that in turn modifies (±)-AnTx-a-evoked DA release.

(±)-AnTx-a dose-dependently evokes striatal DA release from synaptosomes (Soliakov *et al.*, 1995 - Figure 4.8) and slices (see Figure 5.7). In striatal synaptosomes, the dose-response curve was monophasic with an apparent EC_{50} of 134 nM. This observation and the nAChR heterogeneity on DAergic nerve terminals previously reported (Kaiser *et al.*, 1998), suggest that (±)-AnTx-a has similar potencies at α-Ctx-MII-sensitive and α-Ctx-MII-insensitive nAChR. In slices, (±)-AnTx-a-evoked DA release was biphasic with apparent EC_{50} values of 241.8±36.1nM and 5.1±0.3µM suggesting the contribution of additional nAChR with low affinity for (-)-AnTx-a and absent from DA-containing synaptosomes. As seen in Figure 5.7, the fact that the second phase of the dose-response curve was almost completely abolished in the presence of KYNA (500 µM) suggests that the low affinity nAChR mediates [^{3}H]-DA release via the mediation of glutamate release. Thus, in addition to its direct effect on dopaminergic nerve terminals, striatal administration of a nicotinic agonist generate other striatal interactions (as reported above) that indirectly modify nigrostriatal neurotransmission.

The overall shape of the dose-response curve obtained in this study for (±)-AnTx-a-evoked DA release from striatal slices, could be described as the apparent summation of at least two curves (equation 5.1) corresponding to nAChR with different sensitivities to (±)-AnTx-a. Similarities between the EC_{50}s defined in this lab for (±)-AnTx-a-evoked DA release from synaptosomes (EC_{50} = 110 nM Soliakov *et al.,* 1995; EC_{50} = 134 nM Figure 4.8) and slices (EC_{50} = 241 nM - first phase of the dose-response curve Figure 5.7) support this view. The suppression of the second phase in the presence of KYNA is consistent with the presence of nAChR on striatal glutamatergic terminals. An apparent EC_{50} for the second phase in the low micromolar range could reflect that nAChR on the glutamatergic terminal have lower affinity for (±)-AnTx-a than those nAChR present on the DAergic terminal. Consistent with the pharmacological profile (Figure 5.9 - also see below) and the apparent low micromolar EC_{50} (EC_{50} = 5.1 µM - second phase of the dose-response curve Figure 5.7) observed in this study for nAChR on glutamatergic terminals, Alkondon and Albuquerque (1993) reported an AnTx-a EC_{50} of 3.9±0.6µM for Type IA currents (α-Bgt-sensitive) recorded from rat foetal hippocampal neurones. In this chapter, it has been demonstrated *in vitro* that (±)-AnTx-a-evoked glutamate release indirectly enhances DA release in rat striatum. However, it can not be excluded the possibility that additional modulation of striatal DA release by nicotinic agonists could involve the release of neurotransmitters other than glutamate. For example, previous studies have reported nicotine-evoked 5-hydroxytryptamine (5-HT) release (Westfall *et al.*, 1983; Takahashi *et al.*, 1998), and 5-HT-evoked DA release in striatum (Blandina *et al.*, 1989; De Deurwaerdere *et al.*, 1997).

As mentioned before in this chapter, it is well established that non-NMDA- and NMDA-receptors are present on DAergic nerve terminals (Desce *et al.*, 1992; Chéramy *et al.*, 1996). However, although DNQX (100 µM) blocked the 25 µM (±)-AnTx-a response to the same extent as KYNA (500 µM), both iGluR antagonists when applied together did not show an additive effect in slices (see Figure 5.7 right panel). Probably, under the experimental conditions chosen (nominally glycine-free conditions) and despite of the permissive effect of nAChR and non-NMDA-R activation on DAergic terminals, NMDA-R were not activated or at least rapidly desensitised.

To summarise, these results suggest that the second phase of the dose-response curve is, at least partially and under this studys' experimental conditions, a consequence of (±)-AnTx-a-evoked glutamate release that in turn enhances DA release via activation of non-NMDA-R on the DAergic nerve terminal.

Before analysing the pharmacology of (±)-AnTx-a-evoked DA release from striatal slices, it is necessary to discuss the non-significant, but observable, effect of KYNA and DNQX on the 25 µM (±)-AnTx-a-evoked response in striatal synaptosomes (see Figure 5.7 left panel). A "mild" and non-specific effect of commonly used KYNA and DNQX concentrations (Jin and Fredholm, 1997; Sulzer *et al.*, 1998) on nAChR could explain this observation. These compounds act as competitive antagonists of iGluR. To my best knowledge,

there are no studies reporting non-specific effects of KYNA or DNQX on nAChR. These antagonists undoubtedly had not significant effect on the 1 μM (±)-AnTx-a-evoked response in synaptosomes (not shown). Although having different chemical structures, KYNA (500 μM) and DNQX (100 μM) inhibited 25 μM (±)-AnTx-a-evoked DA release to the same extent (~12% Figure 5.8 left panel). Assuming that they could act in a competitive way on nAChR, the opposite trend should have been observed.

To test whether (±)-AnTx-a-evoked glutamate release might affect DA release from DAergic terminals in perfused synaptosome preparation, the following experiment was designed. Striatal synaptosomes and a 1:4 dilution, were assayed for [^{3}H]-DA release evoked by 25 μM (±)-AnTx-a in the absence (control) and presence of KYNA (500 μM). When compared with controls, the low-density synaptosome sample showed the same decrease of DA release as the undiluted preparation (~15%). This result suggests that the observed effect of KYNA on 25 μM (±)-AnTx-a-evoked DA release from striatal synaptosomes could not be merely explained by the proximity of DAergic and glutamatergic terminals, as a consequence of the sample synaptosome density.

On the other hand, several lines of evidence have suggested that the ventral midbrain dopamine neurones that give rise to the major CNS dopaminergic projections may also be glutamatergic (Hattori *et al.*, 1991; Plenz and Kitai, 1996). Recently (1998), Sulzer *et al.* reported that most DA neurones in the intact brain, as well as postnatal ventral tegmental area (VTA) cell cultures, immunostain for Glu (neurotransmitter, neither GABA precursor nor metabolic Glu). Moreover, ultrastructural studies have shown that single DA neurones are capable of forming synapses with both DAergic symmetric and glutamatergic asymmetric synaptic specialisations. Therefore, the observed effects of KYNA in synaptosomes could be a consequence of this iGluR antagonist acting on DAergic nerve terminal iGlu-autoreceptors. However, similar KYNA effects might be obtained if, during the preparation of synaptosomes, the mechanical disruption (homogenisation procedure) of the striatum does not yield totally independent nerve terminals. Then, nigrostriatal DAergic and corticostriatal glutamatergic nerve terminals would remain closely attached to postsynaptic membranes (spines), preserving the original structural and functional relationship.

5.4.3 Striatal nAChR subtypes

Although the pre-synaptic nicotinic modulation of dopamine release from striatal nerve terminals is well established, the nAChR subtypes underlying this response are far from being completely identified (Wonnacott et al., 1990; Wonnacott, 1997; Kaiser and Wonnacott, 1998). In striatal synaptosomes, the nicotinic stimulation of DA release is blocked by mecamylamine, DHβE and n-Bgt and is insensitive to α-Bgt (Rapier *et al.*, 1990) and α-CTx-Iml (Kulak *et al.*, 1997). The sensitivity of (-)-nicotine-evoked [^{3}H]-DA release to n-Bgt has been interpreted in favour of α3-type nAChR (Schulz and Zigmond, 1989; Grady et al., 1992).

However, loss of [^{3}H]-(-)-nicotine binding sites following lesion of the nigrostriatal tract (Clarke and Pert, 1985) favours presynaptic nAChR composed of α4 and β2 subunits on striatal DAergic nerve terminals.

In the present study, the effects of MLA (Alkondon *et al.*, 1992), α-CTx-Iml (Johnson et al., 1995; Pereira et al., 1996) and α-CTx-MII (Cartier et al., 1996; Harvey et al., 1997) on striatal (±)-AnTx-a-evoked DA release from both synaptosomes and slices, were compared (see Figure 5.8). Previous studies have excluded the presence of the α7 subunit on DAergic terminals, as (-)-nicotine-evoked [^{3}H]-DA release was found to be insensitive to α-Bgt (Rapier et al., 1990; Grady et al., 1992; Wonnacott et al., 1995) and α-CTx-Iml (Kulak et al., 1997). However, [^{125}I]-α-Bgt binding sites (Clarke et al., 1985; Rapier et al., 1990; Davies et al., 1999) as well as [^{3}H]-MLA binding sites (Davies et al., 1999) are present in rat striatum.

In slices (this study), MLA (50 nM), α-CTx-Iml (1 μM), α-Bgt (40 nM) and α-CTx-MII (112 nM) decreased the 25 μM (±)-AnTx-a-evoked response by 42.7%, 31.9%, 39.8% and 36.8%, respectively (see Figure 5.8 and Figure 5.10). In striatal synaptosomes, (±)-AnTx-a-evoked DA release was partially sensitive to α-CTx-MII (Figure 4.4 and Figure 5.8; Kulak *et al.*, 1997; Kaiser *et al.*, 1998) but clearly insensitive to α-CTx-Iml (this study Figure 5.8; Kulak *et al.*, 1997). The observed sensitivity to α-Bgt, α-CTx-Iml and MLA of the (±)-AnTx-a-evoked response in slices, together with the insensitivity to these antagonists reported in striatal synaptosomes for nicotinic agonist-evoked responses, support the presence of α7-containing nAChR on striatal non-DAergic nerve terminals. Moreover, when α-Bgt (40 nM) and MLA (50 nM) where applied together with α-CTx-MII (112 nM), the effects were additive (Figure 5.11). These results suggest that αCtx-MII- and α-Bgt-sensitive nAChR are segregated onto different striatal nerve terminals. Interestingly, iGlu-R and α7-nAChR antagonists inhibited the second phase of release in a non-additive manner (Figure 5.11), observations consistent with α7-containing nAChR modulating the release of glutamate that in turn enhances striatal DA release (Figure 5.12).

The nicotinic facilitation of glutamate release from habenular, olfactory bulb and hippocampal neurones involves a presynaptic nAChR that contains the α7 subunit, based on sensitivity of evoked currents to α-Bgt and MLA (McGehee *et al.*, 1995; Alkondon *et al.*, 1996; Gray *et al.*, 1996; Radcliffe and Dani, 1998) and antisense knockout experiments (McGehee *et al.*, 1995). This study has demonstrated using a neurochemical approach, the involvement of presynaptic α-Bgt-sensitive nAChR in striatal glutamate release.

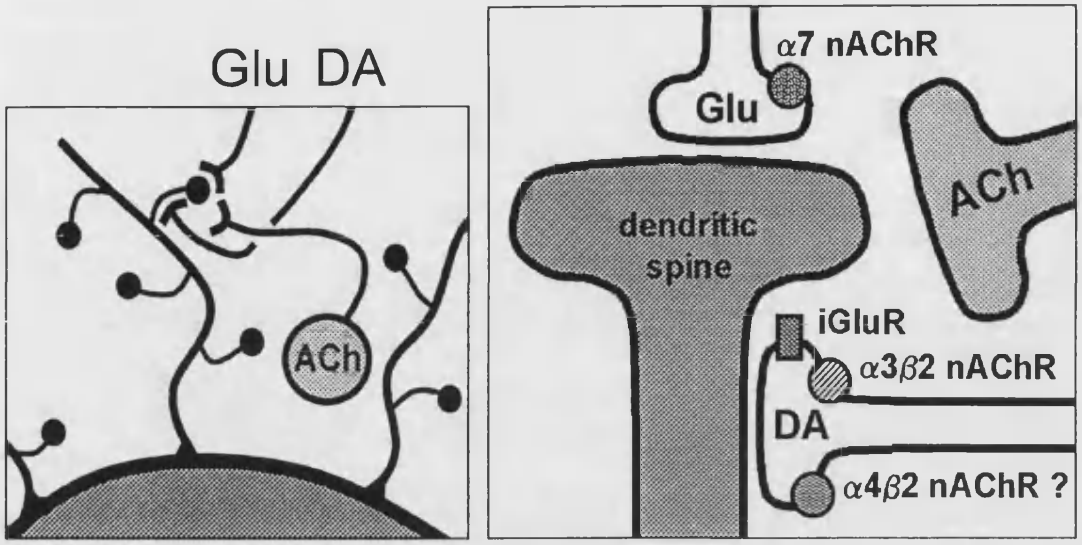

Figure 5.12 Possible physiological relationship between DA and Glu terminals in the striatum. Left panel) Synapses onto the dendritic spine of a medium-sized spiny neurone. Glutamatergic and dopaminergic terminals make synapses onto the head and neck of a medium-sized spiny GABAergic neurone, respectively. **Right panel**) Schematic representation of the proposed segregation of particular nAChR subtypes on different afferent nerve terminals.

MLA is known to be a potent and selective antagonist of α7-containing nAChR (Alkondon *et al.*, 1992). Unexpectedly, 10 nM, 50 nM and 500 nM MLA inhibited 1 μM (±)-AnTx-a-evoked DA release from synaptosomes by 37.1%, 39.1% and 60.6%, respectively (see Figure 5.9). There are few published data supporting a low nanomolar MLA (10-50 nM) inhibition of striatal DA release evoked by nicotinic agonists. In 1996, Clarke and Reuben reported that MLA blocks DA release evoked from striatal synaptosomes by (-)-nicotine with an IC_{50} of 38±1nM. The observed low nanomolar MLA-sensitivity for (±)-AnTx-a evoked DA release in synaptosomes, together with the results presented for the novel nicotinic agonist UB-165 (see Figure 4.10), could suggest that striatal α-Bgt-insensitive MLA binding sites on DAergic nerve terminals, at least do not contain either α3β2 interfaces or α7 nAChR subunits. In the rat, the substantia nigra expresses α3, α4, α5, α6, β2 and β3 mRNAs, but α2 and β4 mRNAs were not detected (see LeNovere *et al.*, 1996; Wonnacott, 1997). This pattern is compatible with α3β2 and α4β2 nAChR subunit combinations but clearly additional subunits could also contribute to form native receptors (and could explain the MLA-sensitivity observed above). In particular, high expression of α6 and β3 mRNA in catecholaminergic nuclei, including substantia nigra, has been noted (LeNovere *et al.*, 1996) but the pharmacology conferred by these subunits is unknown.

This chapter, using the superfusion technique and a more holistic preparation (tissue slices), presented evidence for the involvement of further subtypes of nAChR in striatal DA release. This may be the first neurochemical demonstration of α-Bgt-sensitive nAChR (α7-containing nAChR) mediating glutamate release in the rat striatum. The diversity of nAChR involved in striatal DA release reported in this thesis, increases the range of potential presynaptic nicotinic modulatory effects on neurotransmitter release in this brain area. Second-messenger-mediated mechanisms underlying this modulation are briefly considered in the next chapter.

6 Second messenger-mediated mechanisms involved in (±)-anatoxin-a-evoked dopamine release in rat striatum: phosphorylation of synapsin I

6.1 Introduction

Presynaptic nAChR probably have more subtle modulatory functions than simply triggering transmitter release: e.g. nAChR are proposed to increase the probability of release (Gray *et al.*, 1996), to modulate the frequency of EPSP (Frazier *et al.*, 1998) and to sustain release through the mobilisation of a reserve pool of neurotransmitter (Bowman *et al.*, 1990). Such actions are likely to be mediated by second messengers, and phosphorylation / dephosphorylation events offer a plausible regulatory mechanism. The high relative permeability to Ca^{2+} of neuronal nAChR advocates the potential involvement of Ca^{2+}-dependent kinases (such as Ca^{2+}-calmodulin dependent kinase II (Ca^{2+}/CaM kinase II) and protein kinase C (PKC)), as well as Ca^{2+}-activatable phosphatases.

Synapsin I, composed of 86 kDa synapsin Ia and 80 kDa synapsin Ib, is a basic phosphoprotein expressed specifically in neurones and located preferentially in presynaptic nerve terminals (De Camilli *et al.*, 1990; Hilfiker *et al.*, 1998). Previous studies indicated that synapsin I binds to actin, tubulin, neurofilaments, and is associated with synaptic vesicles (Benfenati *et al.*, 1992). Quick freeze-deep etch electron microscopy analysis strongly suggested that synapsin I forms cross-bridges among synaptic vesicles and the nerve terminal cytoskeleton, mainly with actin filaments (Hirokawa *et al.*, 1989). The binding of synapsin I and cytoskeletal elements or membranes has been reported to be regulated by phosphorylation of synapsin I via Ca^{2+}/calmodulin kinase II (Ca^{2+}/CaM kinase II - Benfenati *et al.*, 1992). In addition, physiological studies have also proposed that phosphorylation of synapsin I could regulate the release of neurotransmitter by making the vesicles readily available for release (Llinás *et al.*, 1991; Greengard *et al.*, 1993). A recent link between presynaptic nAChR stimulation, protein kinase activation and transmitter release, relevant to the mobilisation of a reserve pool of neurotransmitter, comes from the study of Ochoa and O'Shea (1994). These authors reported that the nicotinic stimulation of ACh release from cortical synaptosomes was accompanied by a Ca^{2+}-dependent increase in the phosphorylation of a 80 kDa band, proposed to correspond to synapsin I. Further analysis indicated that nicotine (50 μM) resulted in phosphorylation of site 3 on the synapsin I molecule (Ochoa and O'Shea, 1994). This site is known to be phosphorylated by vesicle-associated Ca^{2+}/CaM kinase II (Benfenati *et al.*, 1992), and Ca^{2+} entry accompanying nAChR activation might provide the stimulus. Recently, an increase in the level of site 3-phospho-synapsin I, together with an increase in Ca^{2+}/CaM kinase II activity, has been proposed to play a role in the enhancement of dopamine release from striatal synaptosomes provoked by amphetamine (Iwata *et al.*, 1997).

PKC has been also implicated in the modulation of exocytosis and PKC activators such as phorbol esters enhance neurotransmitter release evoked by electrical stimulation or KCl depolarisation (Dekker *et al.*, 1991). Evidence for a PKC enhancement of the nicotinic stimulation of transmitter release comes from studies on chromaffin cells (Terbush *et al.*, 1988; Cox and Parsons, 1997). Here, the nicotine-induced secretion of catecholamines is associated with entry of extracellular Ca^{2+} (Wakade *et al.*, 1986), rapid translocation of PKC from cytosol to membrane (Terbush *et al.*, 1988) and concomitant activation of PKC (Brocklehurst *et al.*, 1985). There has been little work published on any interaction between nAChR and PKC in neurones. Chéramy *al.* (1996) reported that the synergism between (-)-nicotine and NMDA in stimulating [^{3}H]-DA release from striatal synaptosomes (attributed to the nicotinic depolarisation relieving the Mg^{2+} block of NMDA receptors - see 5.3.1) was sensitive to blockade by the PKC inhibitors staurosporine and chelerythrine. Recently, Soliakov and Wonnacott (in preparation) found that (±)-AnTx-a activation of presynaptic nAChR on striatal DAergic nerve terminals elicits a contribution from PKC in promoting [^{3}H]-DA release, and that independent activation of PKC can greatly enhance the response to nicotinic stimulation. It has also been proposed that PKC can influence transmitter release by phosphorylating ion channels (Smart , 1997) or acting on proteins that participate in vesicle docking and fusion events (Gillis *et al.*, 1996). The presynaptic nAChR may itself be a target for PKC: phosphorylation of the $\alpha 4$ subunit by PKC has been hypothesised to be necessary for maintaining the $\alpha 4\beta 2$ nAChR in an activatable state (Eilers *et al.*, 1997), although phosphorylation of muscle and ganglionic nAChR has been found to enhance desensitisation (Hoffmann *et al.*, 1994). Transmitter release or $^{86}Rb^+$ efflux stimulated by presynaptic nAChR is subject to short term (desensitisation) and long term (functional inactivation) reduction, in response to sub-stimulating and stimulatory agonist concentrations, respectively (Rowell and Hillebrand, 1994; Marks *et al.*, 1996). Any contribution of kinase or phosphatase activities in mediating these responses is not known, but such mechanisms are very plausible.

This brief chapter presents preliminary functional (superfusion experiments) and biochemical (immunoblots) evidence for the involvement of Ca^{2+}/CaM kinase II and PKC in (±)-AnTx-a evoked DA release from rat striatal synaptosomes.

6.2 Experimental procedures

6.2.1 Materials

The following reagents were used in this study: monoclonal mouse antibody anti-synapsin I (mAb 355 concentration: 1 µg/µl - Chemicon International, Temecula, CA USA), Ro-31-8220, KN-62 (Calbiochem, Nottingham, UK - Figure 6.1), KN-04 (Seikagaku Corporation, Tokyo, Japan - Figure 6.1) pepstatin, leupeptin, aprotinin, antipain and chimostatin (Sigma, Pooie, Dorset UK). Enhanced chemiluminescence (ECL) immunoblotting reagents and Hyperfilm-ECL were purchased from Amersham International (Amersham International, Bucks UK). Immobilon-P polyvinylidine difluoride (PVDF) membranes and Centricon-50 membrane concentrators were obtained from Millipore (Watford, Herts UK). All other chemicals used were of analytical grade and purchased from standard commercial sources.

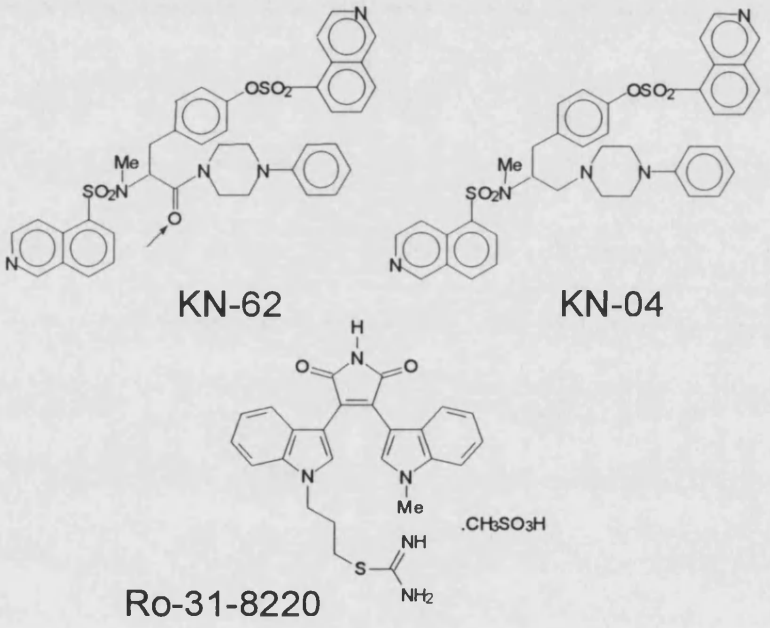

Figure 6.1 Molecular structures of the Ca^{2+}/CaM-kinase II inhibitor KN-62, its inactive analogue KN-04 and the PKC inhibitor Ro-31-8220 (the arrow indicates the chemical group that converts KN-04 in the active compound KN-62).

6.2.2 Superfusion technique

P2 synaptosomes were prepared from the striata of male Sprague-Dawley rats (250-280 g - University of Bath Animal House breeding colony), loaded with [^{3}H]-DA and perfused as previously described (see 4.2.4.1 - Soliakov *et al.*, 1995) with Krebs bicarbonate buffer.

In brief, synaptosomes were washed for 20 min with Krebs bicarbonate buffer and a further 10 min with normal buffer or buffer containing antagonist (5 μM KN-62, 5 μM KN-04, 1 μM Ro-31-8220 or 10 μM mecamylamine). Then, (±)-AnTx-a (1 μM) was applied for 40s. Two min (0.5 ml / min) fractions were collected and counted for radioactivity. Data were analysed (see 4.2.4.2) using Sigma Plot for Windows version 2.0 (Jandel Scientific - Germany), and responses were compared using the one way ANOVA test (Sigma Stat - Jandel Scientific).

6.2.3 Preparation of cytosolic and membrane fractions from Percoll gradient purified synaptosomes for western blotting

Percoll purified synaptosomes were prepared from striata dissected from 4 male Sprague Dawley rats as described previously (see section 3.2; Dunkley *et al.*, 1988; Thorne *et al.*, 1991). Functionally active synaptosomes were collected from the 15-23% Percoll gradient interface and washed once with Krebs-bicarbonate buffer. Then, they were resuspended in the same buffer to a final volume of 0.5 ml (protein concentration 3.6-4.2 mg/ml). Aliquots (90μl) were preincubated for 10 min at 37°C in the presence or absence of antagonists (KN-62, KN-04, mecamylamine); then (±)-AnTx (1μM) or buffer (in control and antagonist/s-exposed preparations) was applied (5s-40s). The stimulation was stopped by adding 20 volumes of ice-cold hypotonic lysis buffer composed of 20mM Tris-HCl, pH 7.4, 1mM EGTA, 1mM EDTA, 100μM PMSF and supplemented with 1μg/ml pepstatin, 2.5μg/ml leupeptin, 2.5μg/ml aprotinin, 2.5μg/ml antipain and 1μg/ml chimostatin. After 15 min on ice, samples were homogenised in a glass-teflon homogeniser by 10 up and down strokes at maximum speed. After another 20 min on ice, the homogenisation procedure was repeated. Following an additional 10 min on ice, the samples were centrifuged for 45 min at 100,000g, and pellets containing the membrane fraction, were separated from the cytosolic supernatant fraction. Pellets were resuspended in Laemmli SDS sample buffer (Laemmli, 1970) by shaking for 40 min in a total volume of 90 μl. Supernatant fractions were concentrated on a Centricon 50 membrane concentrator to about 45 μl and mixed with an equal volume of 2x Laemmli SDS sample buffer, to give a final volume of 90 μl. All samples were heated for 5 min at 95°C and run using 7.5% SDS PAGE. Blotting onto PDVF (Millipore) membranes was carried out in a semi-dry apparatus. Monoclonal mouse anti-synapsin I antibodies (mAb 355 diluted 1:2000) were used as first antibodies and HRP-conjugated monoclonal anti-mouse immunoglobulins (diluted 1:3000) were used as secondary antibodies. ECL western blotting reagents were used for detection of synapsin I according to the manufacturer's instructions. Protein bands were quantified using an AGFA Arcus II scanner and Scanalytics Zero-Dscan v.1.0 software. The values were within the linear range of the protein dependence of band density.

6.3 Results

6.3.1 Effect of Ca^{2+}/calmodulin-dependent protein kinase II and PKC inhibitors on (±)-AnTx-evoked striatal [^{3}H]-DA release

To start studying the cytoplasmic mechanisms underlying nicotinic modulation of striatal [^{3}H]-DA release from synaptosomes, the system was stimulated with the nicotinic agonist (±)-AnTx-a (this study; Soliakov *et al.*, 1995; Soliakov and Wonnacott, 1996) in the presence and absence of Ca^{2+}/calmodulin-dependent protein kinase II and PKC inhibitors. Application of (±)-AnTx-a (1 μM) for 40 s evoked a clear response over basal efflux in striatal synaptosomes (see Figure 4.3).

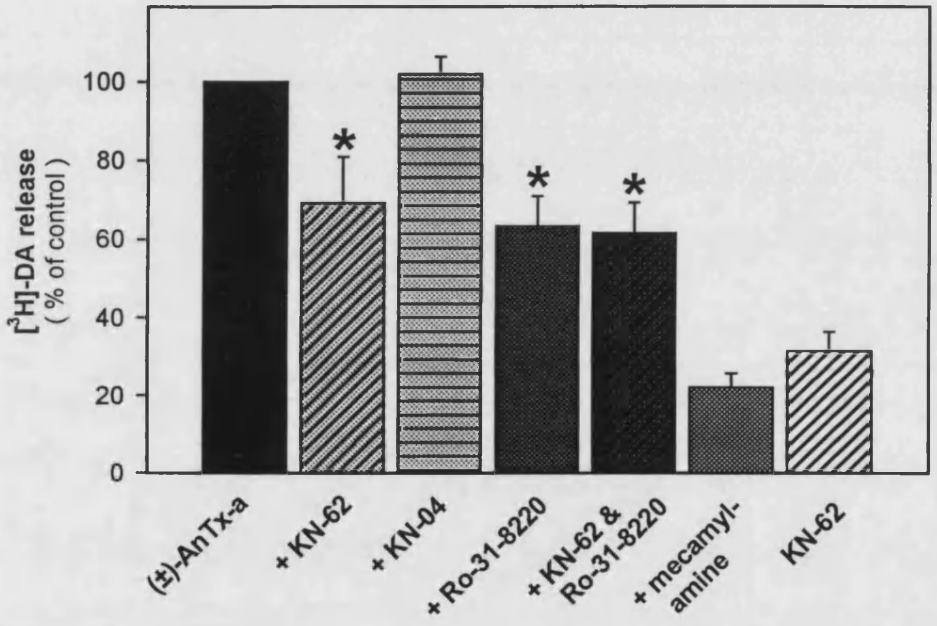

Figure 6.2 Effect of KN-62, KN-04 and Ro-31-8220 on (±)-AnTx-a-evoked [^{3}H]-DA release from striatal synaptosomes. Responses are expressed as percentage±S.D. of control (1 μM (±)-AnTx-a-evoked response). The Ca^{2+}/CaM-kinase II inhibitor KN-62 (5 μM) and the PKC inhibitor Ro-31-8220 (1 μM) significantly decreased the control response. When KN-62 and Ro-31-8220 were applied together, no additive effect was observed. The control response was not significantly affected by 5 μM KN04, the KN-62 inactive analogue. KN-62 (5μM) did not evoke a response significantly different from that elicited by 1 μM (±)-AnTx-a in the presence of 10 μM mecamylamine.
(* $p<0.05$ significantly different from control, one way ANOVA – Bonferroni *t* test)

To define the residual nonspecific release of [^{3}H]-DA from striatal synaptosomes, 1 μM (±)-AnTx-a was applied in the presence of 10 μM mecamylamine (22.1±3.7% of control n=3 Figure 6.2). To determine if Ca^{2+}/calmodulin-dependent protein kinase II (Ca^{2+}/CaM kinase II) is involved in nAChR-mediated [^{3}H]-DA release from striatal synaptosomes the effect of KN-62, an inhibitor of Ca^{2+}/CaM kinase II

(Tokumitsu *et al.*, 1990 - Figure 6.1), was examined (Figure 6.2). KN-62 (5μM) alone did not evoke a response significantly different from that elicited by 1 μM (±)-AnTx-a in the presence of 10 μM mecamylamine (31.5±4.9% of control n=3 - Figure 6.2). Synaptosomes were also exposed to KN-62 (5 μM) for 10 min prior to stimulation with (±)-AnTx-a (1 μM). KN-62 (5 μM) significantly decreased 1 μM (±)-AnTx-a-evoked [^{3}H]-DA release by 30.8±11.7% (n=8 - Figure 6.2). This concentration of KN-62 should be maximally effective (Ki = 0.9 μM; Tokumitsu *et al.*, 1990), while retaining specificity for Ca^{2+}/CaM kinase II. In contrast KN-04 (5μM - Figure 6.1), the inactive structural analogue of KN-62, had no significant effect on (±)-AnTx-evoked [^{3}H]-DA release (101.9±4.4% of control n=3 - Figure 6.2). Taken together, these results suggest that nAChR-evoked [^{3}H]-DA release from rat striatal synaptosomes involves, at least partially, the activation of Ca^{2+}/CaM kinase II.

Having determined that a Ca^{2+}/CaM kinase II inhibitor (5 μM KN-62) can attenuate (±)-AnTx-a-evoked [^{3}H]-DA release, the effect of a PKC inhibitor (Ro-31-8220 Figure 6.1) on (±)-AnTx-a-evoked [^{3}H]-DA release from striatal synaptosomes was examined. Synaptosome pretreatment with 1 μM Ro-31-8220 (10 min) decreased the 1 μM (±)-AnTx-a-evoked response by 36.7±7.6% (n=4 - Figure 6.2). This concentration of Ro-31-8220 should be maximally effective (IC_{50} = 10 nM; Davis *et al.*, 1992), while retaining specificity for PKC. This observation agrees well with previous studies in this lab which also showed that the maximum effect by Ro-31-8220 was achieved after 7 min preincubation with 1 μM Ro-31-8220 (Soliakov and Wonnacott, 1998). Interestingly, when KN-62 and Ro-31-8220 were coapplied, their individual effects were not additive (38.5±7.8% inhibition n=3 - Figure 6.2). This observation suggests that both second messenger cascades are related at some point.

6.3.2 Translocation of synapsin I in response to (±)-AnTx-a stimulation of isolated nerve terminals

Experiments were performed to examine the distribution of the Ca^{2+}/CaM kinase II substrate synapsin I, in cytosolic (soluble) and particulate fractions of synaptosomes after stimulation with (±)-AnTx-a (1 μM) for varying times (5-40s). Phosphorylation of synapsin I results in its translocation from the particulate to the cytosolic fraction (Sihra *et al.*, 1989). The subcellular localisation of synapsin I was determined by using hypotonic lysis to disrupt the highly purified striatal synaptosomes after stimulation with (±)-AnTx-a. The separated fractions were then subjected to SDS/PAGE, electrotransferred onto PVDF membranes, and probed with a mouse monoclonal antibody anti-synapsin I (mAb 355). Initial results showed that (±)-AnTx-a stimulation of synaptosomes causes a rapid (within 2-5 s) increase of synapsin I in the soluble fraction (Figure 6.3).

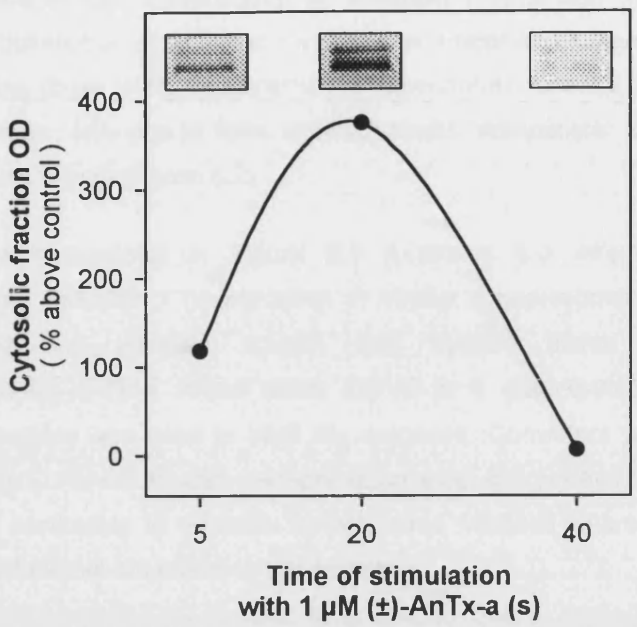

Figure 6.3 Time course of translocation of synapsin I into the cytosolic (soluble) fraction following 1 µM (±)-AnTx-a stimulation. Striatal Percoll purified synaptosomes were stimulated for the indicated times, hypotonically lysed, and fractioned as described in **Error! Unknown switch argument.**. Synapsin I bands were identified by Western blot analysis using mouse anti-sinapsin I mAb 355 and the ECL technique (insets). Curve values are expressed as percentage above control:
synapsin I translocated by a 40 s buffer pulse (n=1).

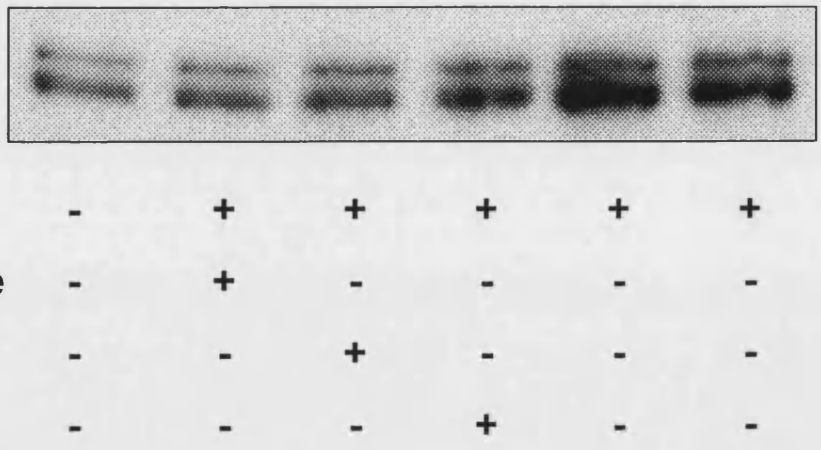

Figure 6.4 Effect of KN-62, KN-04 and mecamylamine on 1 µM (±)-AnTx-a evoked synapsin I translocation in striatal synaptosome preparations. Percoll purified synaptosomes were pretreated for 10 min with KN-62 (5 µM), KN-04 (5 µM) or mecamylamine (10 µM) before stimulation with (±)-AnTx-a (1µM, 20 s). After hypotonic lysis and separation of soluble and particulate factions, synapsin I bands were identified by Western blot analysis using mAb 355 and the ECL technique. A control response was obtained by stimulating the synaptosomes just with Krebs buffer for 20 s.

Further experiments were designed to study the effect of the Ca^{2+}/CaM-kinase II inhibitor KN-62 on the (±)-AnTx-a-evoked translocation of synapsin I in striatal synaptomes (Figure 6.4). The subcellular distribution of synapsin I was studied under experimental conditions (see 6.2.3) closely resembling those used for superfusion experiments (see 6.2.2). Six experiments were performed. However, only one of them showed results "compatible" with those obtained using the superfusion technique (Figure 6.2).

The preliminary immunoblot in Figure 6.4 illustrates the effect of 5 µM KN-62 on (±)-AnTx-a-evoked synapsin I transiocation in striatal synaptosomes. The translocation was maximum when the nicotinic agonist was applied alone; and minimum when, instead of 1 µM (±)-AnTx-a, Krebs buffer (20 s) or 1 µM (±)-AnTx-a in the presence of 10 µM mecamylamine was used to elicit the response. Consistent with the superfusion data presented in 6.3.1, KN-62 (5 µM) partially decreased the (±)-AnTx-a-evoked movement of synapsin I from particulate to cytosolic synaptosome fractions whereas its inactive analogue KN-04 (5 µM) had almost not effect on the response.

6.4 Discussion

Brain nAChR may serve a predominantly modulatory role, exemplified by the facilitation of neurotransmitter release by presynaptic nAChR (Wonnacott, 1997). The interaction between a nicotinic agonist and nAChR may be the first step in a series of events that culminate in exocytosis of e.g. DA-filled vesicles. (-)-Nicotine, by acting on presynaptic nAChR, depolarises the nerve terminal membrane and promotes the influx of Ca^{2+} into synaptosomes (Grady *et al.*, 1992; Soliakov *et al.*, 1995; Marshall *et al.*, 1996; Soliakov and Wonnacott, 1996). This ionic influx may trigger many intracellular mechanisms that depend on this divalent cation, among them the phosphorylation of specific proteins such as synapsin I (Greengard *et al.*, 1993) and calpacitins such as GAP-43 and MARCKS. Both, Ca^{2+}/CaM kinase II-mediated phosphorylation of synapsin I (Llinás *et al.*, 1991; Greengard *et al.*, 1993) and PKC-mediated phosphorylation of GAP-43 and MARCKS, have been postulated to enhance Ca^{2+}-dependent neurotransmitter release (Dekker *et al.*, 1989; Hens *et al.*, 1995). However, whether these phosphorylated proteins contribute to the nicotinic agonist-mediated DA release from striatal synaptosomes has been scarcely studied. The fact that striatal DA release evoked by nicotinic agonists is highly dependant on extracelullar Ca^{2+} suggests that these proteins could potentially participate in the nicotinic-evoked response.

In vitro, synapsin I binds reversibly to synaptic vesicles, promotes G-actin nucleation and polymerisation and induces the formation of thick bundles of actin filaments (Valtorta *et al.*, 1992; Greengard *et al.*, 1993). Phosphorylation (i.e. by Ca^{2+}/CaM kinase II) at sites 2 and 3 abolishes the interactions of synapsin I with synaptic vesicles and actin filaments (Pieribone at al., 1995; Rosahl *et al.*, 1995), therefore increasing the cytoplasmic and vesicular pool of neurotransmitter available for release. Superfusion and immunoblot preliminary data, obtained in this study using the Ca^{2+}/CaM kinase II selective inhibitor KN-62 (Tokumitsu *et al.*, 1989) and its inactive analogue KN-04, support synapsin I phosphorylation by Ca^{2+}/CaM kinase II in response to (±)-AnTx-a stimulation of striatal synaptosomes (Figure 6.2 and Figure 6.4). Moreover, as previously reported for KCl depolarisation of striatal synaptosomes (Sihra *et al.*, 1989), synapsin I translocation after stimulation with 1 μM (±)-AnTx-a showed a critical time dependence, reaching a maximum when the system was stimulated for ~20s (Figure 6.3).

On the other hand and according to previous studies performed by Soliakov and Wonnacott (1998), the PKC inhibitor Ro-31-8220 (1μM) significantly inhibited the release of [^{3}H]-DA evoked by (±)-AnTx-a (Figure 6.2). Although, an involvement of PKC in striatal (±)-AnTx-a-evoked DA release is evident, the source of diacylglycerol following nAChR stimulation is not clear. There is considerable documentation that depolarising conditions elicit the generation of inositol phosphates (presumably in concert with the formation of diacylglycerol; see Dekker *et al.*, 1991), and nicotinic stimulation may fall into this category. Indeed, in chromaffin cells, KCl depolarisation or nAChR stimulation by DMPP increased the

accumulation of inositol phosphates (Eberhand and Holz, 1987), and a mechanism based on the activation of PLC by the increase in intracellular Ca^{2+} was advocated. That PKC activation contributes to the release of neurotransmitters from nerve terminals is clear, but the mechanisms by which it do so remain obscure. As mentioned before, a correlation between PKC-mediated phosphorylation of GAP-43 and neurotransmitter release has been reported (Dekker *et al.*, 1989; 1991). Although it is unclear which property of GAP-43 is essential for transmitter release, the phosphorylation state of GAP-43 rather than PKC activity *per se* may be important for Ca^{2+}-dependant release (Hens *et al.*, 1995). Because PKC-mediated phosphorylation of GAP-43 leads to dissociation of calmodulin (CaM), there could be more CaM available in the synaptosomal cytosol to contribute to Ca^{2+} -dependent processes (e.g. activation of Ca^{2+}/CaM kinase II). However, an understanding of how kinases (e.g Ca^{2+}/CaM kinase II and PKC) modulate exocytosis will not be complete until the physiological substrates are identified and functionally characterised. Recently, it has been reported that PKC also acts on proteins that participate in vesicle docking and fusion events (Gillis *et al.*, 1996). This observation could help to explain the lack of additive effects on (±)-AnTx-a evoked DA release observed in this study when KN-62 and Ro-31-8220 were coapplied (Figure 6.2). This outcome suggests that both kinases act on the same exocytotic pathway, with PKC controlling at least one of its later steps. These results would also propose:

1. the existence of other, undetermined mechanisms/pathways not related with the activation of Ca^{2+}/CaM kinase II or PKC, involved in striatal (±)-AnTx-a evoked [^{3}H]-DA release; or
2. the inhibition by KN-62/Ro-31-8220 of the intraterminal cascades activated by one population of nAChR mediating DA release.

Both synapsin I and calpacitins (e.g. GAP-43) are widely distributed in the brain, and virtually all nerve terminals have both protein types (Walaas *et al.*, 1988; Skene, 1989). However, functional superfusion experiments performed in synaptosomes (this study; Sokiakov and Wonnacott, 1998) have linked for the very first time stimulation of presynaptic nAChR with activation of Ca^{2+}/CaM kinase II / PKC and subsequent release of DA from rat striatal nerve terminals.

7 Conclusions: unanswered questions and future prospects

This thesis has considered the evidence for presynaptic nAChR in the mammalian CNS and discussed the possible mechanisms and physiological relevance of these receptors. It is evident from the information presented in section 1.2 that presynaptic nAChR are widespread in the brain, and are associated with many different transmitters. The pharmacological characteristics of nAChR in different preparations vary, consistent with several different nAChR subtypes fulfilling a presynaptic role. Despite this wealth of documentation, we are still far from understanding their contribution to normal synaptic transmission and brain function. Some of the questions that have already been alluded to in this thesis are:

- What is the subunit composition of presynaptic nAChR associated with particular transmitters? Incomplete pharmacological profiles and, more importantly, the dearth of definitive subtype-selective tools have obstructed the identification of subtypes. Elucidation of the full complement of constituent subunits is even more challenging, and this task has not been accomplished for any particular nAChR yet. Antisense strategies (McGehee *et al.*, 1995) or metabolic labelling / immunoisolation of nAChR in synaptosome preparations are plausible approaches.

- Where on nerve terminals are nAChR localised with respect to (i) release sites; (ii) cholinergic innervation to provide the endogenous agonist for activation? Does a single nerve terminal have more than one subtype of nAChR, and if so are they spatially segregated? These are crucial questions that can only be addressed by microscopic techniques such as immunogold labelling of nAChR subunits and colabelling of transmitter markers for visualisation at the electron microscope level. This approach has proved very illuminating in the case of $GABA_A$ and glutamate receptors (Nusser *et al.*, 1996). In addition to establishing the proximity to release sites, electron microscopy can also demonstrate the co-localisation of different receptor subunits. However, microscopy does not necessarily reflect functional receptors.

- What is the purpose of presynaptic nAChR? At the neuronal level, electrophysiological studies are perhaps the best means of assessing receptor function in a physiological context (e.g. Gray *et al.*, 1996). However, such experiments are technically demanding and measurements are indirect because terminals are too small to impale. Recourse to cultured neurones for this purpose imposes the limitation that the culture system may provide a developmental snapshot, the cultured neurones generally being of perinatal origin. Biochemical studies are also needed, to investigate the down stream events that follow nAChR activation. It will be important to elucidate changes produced in the nerve terminal (e.g. phosphorylation events, intraterminal Ca^{2+} dynamics, vesicle recruitment), in addition to the release of transmitter. To evaluate the contribution of presynaptic nAChR on a broader scale, i.e. in terms of brain function, *in vivo* antisense or transgenic knockout

strategies but neither of these approaches is selective for presynaptic nAChR: subunit deletion will affect nAChR on soma and dendrites as well as terminals. If it emerges that certain subtypes are only localised to terminals, the deletion approaches would have considerable merit, although interpretation of results can be confounded by compensatory or plastic adaptations (McGehee *et al.*, 1995).

- Are presynaptic nAChR valid therapeutic targets? Given our poverty of understanding of the significance of these receptors in normal brain function, this question is difficult to answer. Putative presynaptic nAChR are lost in Alzheimers' and Parkinsons' disease and offer a rational site of drug action to boost residual activity, especially in the earlier stages of degeneration. Indeed presynaptic nAChR may become more effective under sub-optimal conditions (Marchi *et al.*, 1996). Moreover, the modulatory actions of presynaptic nAChR make them attractive therapeutic targets, as modulation is preferable to direct manipulation of on/off signals.

There is much more still to be learnt about nAChR in the brain and this, I am sure, will be a fascinating and illuminating voyage of discovery !

8 References

Adam-Vizi V and Ashley RH (1987) Relation of acetylcholine release to Ca^{2+} uptake and intra-terminal Ca^{2+} concentration in guinea-pig cortex synaptosomes. *J Neurochem* **49**:1013-1021.

Aigner TG and Mishkin M (1986) The effects of physostigmine and scopolamine on recognition memory in monkeys. *Behav Neural Biol* **45**:81-87.

Akabas MH, Kaufmann C, Archdeacon P and Karlin A (1994) Identification of acetylcholine receptor channel-lining residues in the entire M2 segment of the α subunit. *Neuron* **13**:919-927.

Albin RL, Young AB and Penney JB (1989) The functional anatomy of basal ganglia disorders. *Trends Neurosci* **12**:366-375.

Albuquerque EX, Pereira EF, Castro NG, Alkondon M, Reinhardt S, Schroder H and Maelicke A (1995) Nicotinic receptor function in the mammalian central nervous system. *Ann N Y Acad Sci* **757**:48-72.

Albuquerque EX, Pereira EF, Alkondon M, Schrattenholz A and Maelicke A (1997) Nicotinic acetylcholine receptors on hippocampal neurons: distribution on the neuronal surface and modulation of receptor activity. *J Recept Signal Transduct Res* **17**:243-266.

Albuquerque EX, Alkondon M, Pereira EF, Castro NG, Schrattenholz A, Barbosa CT, Bonfante-Cabarcas R, Aracava Y, Eisenberg HM and Maelicke A (1997) Properties of neuronal nicotinic acetylcholine receptors: pharmacological characterization and modulation of synaptic function. *J Pharmacol Exp Ther* **280**:1117-1136.

Alexander GE and Crutcher ME (1990) Functional architecture of basal ganglia circuits: neural substrates of parallel processing. *Trends Neurosci* **13**:266-271.

Alkondon M, Pereira EF, Wonnacott S and Albuquerque EX (1992) Blockade of nicotinic currents in hippocampal neurons defines methyllycaconitine as a potent and specific receptor antagonist. *Mol Pharmacol* **41**:802-808.

Alkondon M and Albuquerque EX (1993) Diversity of nicotinic acetylcholine receptors in rat hippocampal neurons. I. Pharmacological and functional evidence for distinct structural subtypes. *J Pharmacol Exp Ther* **265**:1455-1473.

Alkondon M, Rocha ES, Maelicke A and Albuquerque EX (1996) Diversity of nicotinic acetylcholine receptors in rat brain. V. α-Bungarotoxin-sensitive nicotinic receptors in olfactory bulb neurons and presynaptic modulation of glutamate release. *J Pharmacol Exp Ther* **278**:1460-1471.

Alkondon M, Pereira EF, Cortes WS, Maelicke A and Albuquerque EX (1997) Choline is a selective agonist of α7 nicotinic acetylcholine receptors in the rat brain neurons. *Eur J Neurosci* **9**:2734-2742.

Alkondon M, Pereira EF, Barbosa CT and Albuquerque EX (1997) Neuronal nicotinic acetylcholine receptor activation modulates γ-aminobutyric acid release from CA1 neurons of rat hippocampal slices. *J Pharmacol Exp Ther* **283**:1396-1411.

Allen CM, Ely CM, Juaneza MA and Parsons LH (1996) Activation of Fyn tyrosine kinase upon secretagogue stimulation of bovine chromaffin cells. *J Neurosci Res* **44**:421-429.

Amaral DG (1987) The Nervous System (V). *In: Handbook of Physiology (eds. Brookhard,J.M. and Mountcastle,V.B.).Bethesda: Am Physiol Soc.*

Anand R, Conroy WG, Schoepfer R, Whiting P and Lindstrom J (1991) Neuronal nicotinic acetylcholine receptors expressed in *Xenopus* oocytes have a pentameric quaternary structure. *J Biol Chem* **266**:11192-11198.

Anand R, Peng X and Lindstrom J (1993) Homomeric and native α7 acetylcholine receptors exhibit remarkably similar but non-identical pharmacological properties, suggesting that the native receptor is a heteromeric protein complex. *FEBS Lett* **327**:241-246.

Anderson DJ and Arneric SP (1994) Nicotinic receptor binding of [^{3}H]cytisine, [^{3}H]nicotine and [^{3}H]methylcarbamylcholine in rat brain. *Eur J Pharmacol* **253**:261-267.

Araujo DM, Lapchak PA, Collier B and Quirion R (1988) Characterization of N-[^{3}H]methylcarbamylcholine binding sites and effect of N-methylcarbamylcholine on acetylcholine release in rat brain. *J Neurochem* **51**:292-299.

Barish ME (1983) A transient calcium-dependent chloride current in the immature *Xenopus* oocyte. *J Physiol* **342**:309-325.

Barrantes GE, Rogers AT, Lindstrom J and Wonnacott S (1995) α-Bungarotoxin binding sites in rat hippocampal and cortical cultures: initial characterisation, colocalisation with α7 subunits and up-regulation by chronic nicotine treatment. *Brain Res* **672**:228-236.

Barrantes GE, Murphy CT, Westwick J and Wonnacott S (1995) Nicotine increases intracellular calcium in rat hippocampal neurons via voltage-gated calcium channels. *Neurosci Lett* **196**:101-104.

Bartschat DK and Rhodes TE (1995) Protein kinase C modulates calcium channels in isolated presynaptic nerve terminals of rat hippocampus. *J Neurochem* **64**:2064-2072.

Benfenati F, Valtorta F, Rubenstein JL, Gorelick FS, Greengard P and Czernik AJ (1992) Synaptic vesicle-associated Ca^{2+}/calmodulin-dependent protein kinase II is a binding protein for synapsin I. *Nature* **359**:417-420.

Bennett JA and Dingledine R (1999) Topology profile for a glutamate receptor: three transmembrane domains and a channel lining-reentrant membrane loop. *Neuron* **14**:373-384.

Benveniste M, Clements J, Vyklicky L and Asher P (1990) A kinetic analysis of the modulation of NMDA receptors by glycine in mouse cultured hippocampal neurons. *J Physiol* **428**:333

Bernard C (1857) Leçons sur les effets des substances toxiques et médicamenteuses. *Paris: Baillière*

Bertrand D, Bertrand S and Ballivet M (1992) Pharmacological properties of the homomeric α7 receptor. *Neurosci Lett* **146**:87-90.

Bertrand D, Galzi JL, Devillers-Thiery A, Bertrand S and Changeux JP (1993) Mutations at two distinct sites within the channel domain M2 alter calcium permeability of neuronal α7 nicotinic receptor. *Proc Natl Acad Sci U S A* **90**:6971-6975.

Betz H (1992) Structure and function of inhibitory glycine receptors. *Q Rev Biophys* **25**:381-394.

Biedler JL, Helson L and Spengler BA (1973) Morphology and growth, tumorigenicity, and cytogenetics of human neuroblastoma cells in continuous cell culture. *Cancer Res* **33**:2643-2652.

Biziere K and Coyle JT (1978) Influence of cortico-striatal afferents on striatal kainic acid neurotoxicity. *Neurosci Lett* **8**:303-310.

Blandina P, Goldfarb J, Craddock-Royal B and Green JP (1989) Release of endogenous dopamine by stimulation of 5-hydroxytryptamine3 receptors in rat striatum. *J Pharmacol Exp Ther* **251**:803-809.

Blumenthal EM, Conroy WG, Romano SJ, Kassner PD and Berg DK (1997) Detection of functional nicotinic receptors blocked by α- bungarotoxin on PC12 cells and dependence of their expression on post- translational events. *J Neurosci* **17**:6094-6104.

Blumenthal EM, Shoop RD and Berg DK (1999) Developmental changes in the nicotinic responses of ciliary ganglion neurons. *J Neurophysiol* **81**:111-120.

Bonfante-Cabarcas R, Swanson KL, Alkondon M and Albuquerque EX (1996) Diversity of nicotinic acetylcholine receptors in rat hippocampal neurons. IV. Regulation by external Ca^{2+} of α-bungarotoxin- sensitive receptor function and of rectification induced by internal Mg^{2+}. *J Pharmacol Exp Ther* **277**:432-444.

Bouyer JJ, Park DH, Joh TH and Pickel VM (1984) Chemical and structural analysis of the relationship between cortical inputs and tyrosine hydroxylase-containing terminals in rat neostriatum. *Brain Res* **302**:276-275.

Bowman WC, Prior C and Marshall IG (1990) Presynaptic receptors in the neuromuscular junction. *Ann N Y Acad Sci* **604**:69-81.

Breukel AI, Besselsen E, Lopes DSF and Ghijsen WE (1997) Arachidonic acid inhibits uptake of amino acids and potentiates PKC effects on glutamate, but not GABA, exocytosis in isolated hippocampal nerve terminals. *Brain Res* **773**:90-97.

Briggs CA and Cooper JR (1982) Cholinergic modulation of the release of [^{3}H]acetylcholine from synaptosomes of the myenteric plexus. *J Neurochem* **38**:501-508.

Britto LR, Keyser KT, Lindstrom JM and Karten HJ (1992) Immunohistochemical localization of nicotinic acetylcholine receptor subunits in the mesencephalon and diencephalon of the chick (*Gallus gallus*). *J Comp Neurol* **317**:325-340.

Brocklehurst KW, Morita K and Pollard HB (1985) Characterization of protein kinase C and its role in catecholamine secretion from bovine adrenal-medullary cells. *Biochem J* **228**:35-42.

Broide RS, O'Connor LT, Smith MA, Smith JA and Leslie FM (1995) Developmental expression of α7 neuronal nicotinic receptor messenger RNA in rat sensory cortex and thalamus. *Neuroscience* **67**:83-94.

Budd DC, May GR, Nicholls DG and McCormack JG (1996) Inhibition by lifarizine of intracellular Ca^{2+} rises and glutamate exocytosis in depolarized rat cerebrocortical synaptosomes and cultured neurones. *Br J Pharmacol* **118**:162-166.

Buller AL and White MM (1990) Functional acetylcholine receptors expressed in *Xenopus* oocytes after injection of Torpedo β, γ, and δ subunit RNAs are a consequence of endogenous oocyte gene expression. *Mol Pharmacol* **37**:423-428.

Bunsey M and Eichenbaum H (1996) Conservation of hippocampal memory function in rats and humans. *Nature* **379**:255-257.

Carlsson M and Carlsson A (1990) Interactions between glutamatergic and monoaminergic systems within the basal ganglia-implications in schizophrenia and Parkinsons' disease. *Trends Neurosci* **13**:272-276.

Carneiro RC and Markus RP (1990) Presynaptic nicotinic receptors involved in release of noradrenaline and ATP from the prostatic portion of the rat vas deferens. *J Pharmacol Exp Ther* **255**:95-100.

Cartier GE, Yoshikami D, Gray WR, Luo S, Olivera BM and McIntosh JM (1996) A new α-conotoxin which targets α3β2 nicotinic acetylcholine receptors. *J Biol Chem* **271**:7522-7528.

Cartier GE, Yoshikami D, Gray WR, Luo SQ, Olivera BM and McIntosh JM (1996b) α-Conotoxin-MII (α-CTx-MII) interaction with nicotinic acetylcholine receptors. *Soc Neurosci Abs* **22**:268

Chakravarthy BR, Whitfield JF and Durkin JP (1994) Inactive membrane protein kinase Cs: a possible target for receptor signalling. *Biochem J* **304**:809-816.

Changeux JP, Kasai M and Lee CY (1970) Use of a snake venom toxin to characterize the cholinergic receptor protein. *Proc Natl Acad Sci U S A* **67**:1241-1247.

Chen D and Patrick JW (1997) The α-bungarotoxin-binding nicotinic acetylcholine receptor from rat brain contains only the α7 subunit. *J Biol Chem* **272**:24024-24029.

Chen D, Dang H and Patrick JW (1998) Contributions of N-linked glycosylation to the expression of a functional α7-nicotinic receptor in *Xenopus* oocytes. *J Neurochem* **70**:349-357.

Chen S and Hillman DE (1990) Robust synaptic plasticity of striatal cells following partial deafferentation. *Brain Res* **520**:103-114.

Cheramy A, Godeheu G, L'Hirondel M and Glowinski J (1996) Cooperative contributions of cholinergic and NMDA receptors in the presynaptic control of dopamine release from synaptosomes of the rat striatum. *J Pharmacol Exp Ther* **276**:616-625.

Chini B, Raimond E, Elgoyhen AB, Moralli D, Balzaretti M and Heinemann S (1994) Molecular cloning and chromosomal localization of the human α7- nicotinic receptor subunit gene (CHRNA7). *Genomics* **19**:379-381.

Choi DW (1988) Glutamate neurotoxicity and diseases of the nervous system. *Neuron* **1**:623-634.

Choi DW (1992) Excitotoxic cell death. *J Neurobiol* **23**:1261-1276.

Clarke PB, Schwartz RD, Paul SM, Pert CB and Pert A (1985) Nicotinic binding in rat brain: autoradiographic comparison of [^{3}H]acetylcholine, [^{3}H]nicotine, and [^{125}I]-α-bungarotoxin. *J Neurosci* **5**:1307-1315.

Clarke PB and Pert A (1985) Autoradiographic evidence for nicotine receptors on nigrostriatal and mesolimbic dopaminergic neurons. *Brain Res* **348**:355-358.

Clarke PB and Reuben M (1996) Release of [^{3}H]-noradrenaline from rat hippocampal synaptosomes by nicotine: mediation by different nicotinic receptor subtypes from striatal [3H]-dopamine release. *Br J Pharmacol* **117**:595-606.

Claudio T, Paulson HL, Green WN, Ross AF, Hartman DS and Hayden D (1989) Fibroblasts transfected with Torpedo acetylcholine receptor β-, γ-, and δ-subunit cDNAs express functional receptors when infected with a retroviral alpha recombinant. *J Cell Biol* **108**:2277-2290.

Collard KJ, Edwards R and Liu Y (1993) Changes in synaptosomal glutamate release during postnatal development in the rat hippocampus and cortex. *Brain Res Dev Brain Res* **71**:37-43.

Colquhoun LM and Patrick JW (1997) α3, β2, and β4 form heterotrimeric neuronal nicotinic acetylcholine receptors in *Xenopus* oocytes. *J Neurochem* **69**:2355-2362.

Conroy WG, Vernallis AB and Berg DK (1992) The α5 gene product assembles with multiple acetylcholine receptor subunits to form distinctive receptor subtypes in brain. *Neuron* **9**:679-691.

Conroy WG and Berg DK (1995) Neurons can maintain multiple classes of nicotinic acetylcholine receptors distinguished by different subunit compositions. *J Biol Chem* **270**:4424-4431.

Conti-Tronconi BM, Dunn SM, Barnard EA, Dolly JO, Lai FA, Ray N and Raftery MA (1985) Brain and muscle nicotinic acetylcholine receptors are different but homologous proteins. *Proc Natl Acad Sci U S A* **82**:5208-5212.

Cooper E, Couturier S and Ballivet M (1991) Pentameric structure and subunit stoichiometry of a neuronal nicotinic acetylcholine receptor. *Nature* **350**:235-238.

Cooper ST and Millar NS (1997) Host cell-specific folding and assembly of the neuronal nicotinic acetylcholine receptor α7 subunit. *J Neurochem* **68**:2140-2151.

Couturier S, Bertrand D, Matter JM, Hernandez MC, Bertrand S, Millar N, Valera S, Barkas T and Ballivet M (1990) A neuronal nicotinic acetylcholine receptor subunit (α7) is developmentally regulated and forms a homo-oligomeric channel blocked by α-BTX. *Neuron* **5**:847-856.

Cox ME, Ely CM, Catling AD, Weber MJ and Parsons LH (1996) Tyrosine kinase are required for catecholamine secretion and mitogen-activated protein kinase activation in bovine adrenal chromaffin cells. *J Neurochem* **66**:1103-1112.

Cox ME and Parsons SJ (1997) Roles for protein kinase C and mitogen-activated protein kinase in nicotine-induced secretion from bovine adrenal chromaffin cells. *J Neurochem* **69**:1119-1130.

Cuevas J and Berg DK (1998) Mammalian nicotinic receptors with α7 subunits that slowly desensitize and rapidly recover from α-bungarotoxin blockade. *J Neurosci* **18**:10335-10344.

Dani JA and Heinemann S (1996) Molecular and cellular aspects of nicotine abuse. *Neuron* **16**:905-908.

Davies ARL, Hardick DJ, Blagbrough IS, Potter BVL, Wolstenholme AJ and Wonnacott S (1999) Characterization of the binding of [^{3}H]methyllycaconitine: a new radioligand for labelling α7-type neuronal nicotinic acetylcholine receptors. *Neuropharmacology* **(in press)**:

Davis P, Elliot I, Harris W, Hill C, Hurst S, Keech E, Kumar MKH, Lawton G, Nixon J and Wilkinson S (1992) Inhibitors of Protein kinase C. II. Substituted Bisindolylmaleimides with improved potency and selectivity. *J Med Chem* **35**:994-1001.

De Camilli P, Benfenati F, Valtorta F and Greengard P (1990) The synapsins. *Ann Rev Cell Biol* **6**:433-460.

De Deurwaerdere P, L'Hirondel M, Bonhomme N, Lucas G, Cheramy A and Spampinato U (1997) Serotonin stimulation of 5-HT_4 receptors indirectly enhances *in vivo* dopamine release in the rat striatum. *J Neurochem* **68**:195-203.

Dekker LV, De Graan PNE, Versteeg DHG, Oestreicher AB and Gispen WH (1989) Phosphorylation of B-50 (GAP 43) is correlated with neurotransmitter release in rat hippocampal slices. *J Neurochem* **52**:24-30.

Dekker LV, DeGraan PNE and Gispen WH (1991) Transmitter release: target of regulation by protein kinase C?. *Progr Brain Res* **89**:209-233.

Delbono O, Gopalakrishnan M, Renganathan M, Monteggia LM, Messi ML and Sullivan JP (1997) Activation of the recombinant human α7 nicotinic acetylcholine receptor significantly raises intracellular free calcium. *J Pharmacol Exp Ther* **280**:428-438.

DeLong MR (1990) Primate models of movement disorders of basal ganglia origin. *Trends Neurosci* **13**:281-285.

Deneris ES, Boulter J, Swanson LW, Patrick J and Heinemann S (1989) β3: a new member of nicotinic acetylcholine receptor gene family is expressed in brain. *J Biol Chem* **264**:6268-6272.

Deneris ES, Connolly J, Rogers SW and Duvoisin R (1991) Pharmacological and functional diversity of neuronal nicotinic acetylcholine receptors. *Trends Pharmacol Sci* **12**:34-40.

Descarries L, Gisiger V and Steriade M (1997) Diffuse transmission by acetylcholine in the CNS. *Prog Neurobiol* **53**:603-625.

Desce JM, Godeheu G, Galli T, Artaud F, Cheramy A and Glowinski J (1992) L-glutamate-evoked release of dopamine from synaptosomes from synaptosomes of the rat striatum: involvement of AMPA and NMDA receptors. *Neurosci* **47**:333-339.

Di Chiara G, Morelli M and Consolo S (1994) Modulatory functions of neurotransmitters in the striatum: ACh / dopamine / NMDA interactions. *Trends Neurosci* **17**:228-233.

Dineley-Miller K and Patrick J (1992) Gene transcripts for the nicotinic acetylcholine receptor subunit, β4, are distributed in multiple areas of the rat central nervous system. *Brain Res Mol Brain Res* **16**:339-344.

Dolezal V, Lee K, Schobert A and Hertting G (1996) The influx of Ca^{2}+ and the release of noradrenaline evoked by the stimulation of presynaptic nicotinic receptors of chick sympathetic neurons in culture are not mediated via L-, N-, or P-type calcium channels. *Brain Res* **740**:75-80.

Domet MA, Webb CE and Wilson DF (1995) Impact of α-bungarotoxin on transmitter release at the neuromuscular junction of the rat. *Neurosci Lett* **199**:49-52.

Dominguez del Toro, Juiz JM, Peng X, Lindstrom J and Criado M (1994) Immunocytochemical localization of the α7 subunit of the nicotinic acetylcholine receptor in the rat central nervous system. *J Comp Neurol* **349**:325-342.

Doucette-Stamm L, Monteggia LM, Donnelly-Roberts D, Tai Wang M, Lee J, Tian J and Giordano T (1993) Cloning and sequence of the human α7 nicotinic acetylcholine receptor. *Drug Dev Res* **30**:252-256.

Downing JE and Role LW (1987) Activators of protein kinase C enhance acetylcholine receptor desensitization in sympathetic ganglion neurons. *Proc Natl Acad Sci U S A* **84**:7739-7743.

Dunkley PR, Heath MJ, Harrison SM, Jarvie PE, Glenfiel PJ and Rostas JAP (1988) A rapid Percoll gradient procedure for isolation of synaptosomes directly from an S1 fraction: homogeneity and morphology of subcellular fractions. *Brain Res* **441**:72-80.

Dunnet SB and Fibiger HC (1993) Role of forebrain cholinergic systems in learning and memory: relevance to the cognitive deficits of aging and Alzheimers' dementia. *Progr Brain Res* **98**:413-420.

Duvoisin RM, Deneris ES, Patrick J and Heinemann S (1989) The functional diversity of the neuronal nicotinic acetylcholine receptors is increased by a novel subunit: β4. *Neuron* **3**:487-496.

Eberhard DA and Holz RW (1987) Cholinergic stimulation of inositol phosphate formation in bovine adrenal chromaffin cells: distinct nicotinic and muscarinic mechanisms. *J Neurochem* **49**:1634-1643.

Ehrlich P (1865) Das Sauerstoff Bedürfnis des Organismus, eine farbenanalytishe Studie. *Berlin*

Eilers H, Schaeffer E, Bickler PE and Forsayeth JP (1997) Functional deactivation of the major neuronal nicotinic receptor caused by nicotine and protein kinase C-dependent mechanism. *Mol Pharmacol* **52**:1105-1112.

Eisele JL, Bertrand S, Galzi JL, Devillers-Thiery A, Changeux JP and Bertrand D (1993) Chimaeric nicotinic-serotonergic receptor combines distinct ligand binding and channel specificities. *Nature* **366**:479-483.

El-Bizri H and Clarke PB (1994) Blockade of nicotinic receptor-mediated release of dopamine from striatal synaptosomes by chlorisondamine administered in vivo. *Br J Pharmacol* **111**:414-418.

Elgoyhen AB, Johnson DS, Boulter J, Vetter DE and Heinemann S (1994) α9: an acetylcholine receptor with novel pharmacological properties expressed in rat cochlear hair cells. *Cell* **79**:705-715.

Elliott KJ, Ellis SB, Berckhan KJ, Urrutia A, Chavez-Noriega LE, Johnson EC, Velicelebi G and Harpold MM (1996) Comparative structure of human neuronal α2-α7 and β2-β4 nicotinic acetylcholine receptor subunits and functional expression of the α2, α3, α4, α7, β2, and β4 subunits. *J Mol Neurosci* **7**:217-228.

Elmslie FV, Rees M, Williamson MP, Kerr M, Kjeldsen MJ, Pang KA, Sundqvist A, Friis ML, Chadwick D, Richens A, Covanis A, Santos M, Arzimanoglou A, Panayiotopoulos CP, Curtis D, Whitehouse WP and Gardiner RM (1997) Genetic mapping of a major susceptibility locus for juvenile myoclonic epilepsy on chromosome 15q. *Hum Mol Genet* **6**:1329-1334.

Ely CM, Oddie KM, Litz JS, Rossomando AJ, Kanner SB, Sturgill TW and Parsons SJ (1990) A 42-kd tyrosine kinase substrate linked to chromaffin cell secretion exhibits an associated MAP kinase activity and is highly related to 42-kd mitogen-stimulated protein in fibroblasts. *J Cell Biol* **110**:731-742.

Exposito I, Mora F, Zisapel N and Oaknin S (1995) The modulatory effect of melatonin on the dopamine-glutamate interaction in the anterior hypothalamus during ageing. *Neuroreport* **6**:2399-2403.

Fedele E, Varnier G, Ansaldo MA and Raiteri M (1998) Nicotine administration stimulates the in vivo N-methyl-D-aspartate receptor/nitric oxide/cyclic GMP pathway in rat hippocampus through glutamate release. *Br J Pharmacol* **125**:1042-1048.

Flores CM, Rogers SW, Pabreza LA, Wolfe BB and Kellar KJ (1992) A subtype of nicotinic cholinergic receptor in rat brain is composed of α4 and β2 subunits and is up-regulated by chronic nicotine treatment. *Mol Pharmacol* **41**:31-37.

Fontana G and Blaustein MP (1993) Calcium buffering and free Ca^{2+} in rat brain synaptosomes. *J Neurochem* **60**:843-850.

Forsayeth JR and Kobrin E (1997) Formation of oligomers containing the β3 and β4 subunits of the rat nicotinic receptor. *J Neurosci* **17**:1531-1538.

Frazier CJ, Buhler AV, Weiner JL and Dunwiddie TV (1998) Synaptic potentials mediated via α-bungarotoxin-sensitive nicotinic acetylcholine receptors in rat hippocampal interneurons. *J Neurosci* **18**:8228-8235.

Frazier CJ, Rollins YD, Breese CR, Leonard S, Freedman R and Dunwiddie TV (1998b) Acetylcholine activates an α-bungarotoxin-sensitive nicotinic current in rat hippocampal interneurons, but not pyramidal cells. *J Neurosci* **18**:1187-1195.

Freedman R, Coon H, Myles-Worsley M, Orr-Urtreger A, Olincy A, Davis A, Polymeropoulos M, Holik J, Hopkins J, Hoff M, Rosenthal J, Waldo MC, Reimherr F, Wender P, Yaw J, Young DA, Breese CR, Adams C, Patterson D, Adler LE, Kruglyak L, Leonard S and Byerley W (1997) Linkage of a neurophysiological deficit in schizophrenia to a chromosome 15 locus. *Proc Natl Acad Sci U S A* **94**:587-592.

Freund TF, Powell JF and Smith AD (1984) Tyrosine hydroxylase-immunoreactive boutons in synaptic contact with identified striatonigral neurons, with particular reference to dendritic spines. *Neurosci* **13**:1189-1215.

Fried RC and Blaustein MP (1978) Retrieval and recycling of synaptic vesicle membrane in pinched-off nerve terminals (synaptosomes). *J Cell Biol* **78**:685-700.

Fu WM and Liu JJ (1997) Regulation of acetylcholine release by presynaptic nicotinic receptors at developing neuromuscular synapses. *Mol Pharmacol* **51**:390-398.

Fuchs JL (1989) [^{125}I]-α-Bungarotoxin binding marks primary sensory areas of developing rat neocortex. *Brain Res* **501**:223-234.

Fucile S, Barabino B, Palma E, Grassi F, Limatola C, Mileo AM, Alema S, Ballivet M and Eusebi F (1997) α5 subunit forms functional α3β4 α5 nAChRs in transfected human cells. *Neuroreport* **8**:2433-2436.

Fucile S, Matter JM, Erkman L, Ragozzino D, Barabino B, Grassi F, Alema S, Ballivet M and Eusebi F (1998) The neuronal α6 subunit forms functional heteromeric acetylcholine receptors in human transfected cells. *Eur J Neurosci* **10**:172-178.

Fuxe K and Agnati LF (1991) Volume transmission in the brain: novel mechanisms for neural transmission. *New York: Raven Press*

Galzi JL, Bertrand D, Devillers-Thiery A, Revah F, Bertrand S and Changeux JP (1991) Functional significance of aromatic amino acids from three peptide loops of the α7 neuronal nicotinic receptor site investigated by site-directed mutagenesis. *FEBS Lett* **294**:198-202.

Galzi JL, Devillers-Thiery A, Hussy N, Bertrand S, Changeux JP and Bertrand D (1992) Mutations in the channel domain of a neuronal nicotinic receptor convert ion selectivity from cationic to anionic. *Nature* **359**:500-505.

Galzi JL and Changeux JP (1995) Neuronal nicotinic receptors: molecular organization and regulations. *Neuropharmacology* **34**:563-582.

Gannon RL and Terrian DM (1992) Kappa opioid agonists inhibit transmitter release from guinea pig hippocampal mossy fibre synaptosomes. *Neurochem Res* **17**:741-747.

Garcia-Muñoz M, Young SJ and Groves PM (1991) Terminal excitability of the corticostriatal pathway. II. Regulation by glutamate receptor stimulation. *Brain Res* **551**:207-215.

Garcia-Muñoz M, Patino P, Young SJ and Groves PM (1996) Effects of nicotine on dopaminergic nigrostriatal axons requires stimulation of presynaptic glutamatergic receptors. *J Pharmacol Exp Ther* **277**:1685-1693.

Gerzanich V, Anand R and Lindstrom J (1994) Homomers of α8 and α7 subunits of nicotinic receptors exhibit similar channel but contrasting binding site properties. *Mol Pharmacol* **45**:212-220.

Gerzanich V, Kuryatov A, Anand R and Lindstrom J (1997) "Orphan" α6 nicotinic AChR subunit can form a functional heteromeric acetylcholine receptor. *Mol Pharmacol* **51**:320-327.

Gerzanich V, Wang F, Kuryatov A and Lindstrom J (1998) α5 Subunit alters desensitization, pharmacology, Ca^{2+} permeability and Ca^{2+} modulation of human neuronal α3 nicotinic receptors. *J Pharmacol Exp Ther* **286**:311-320.

Gillis KD, Mössner R and Neher E (1996) Protein kinase C enhances exocytosis from chromaffin cells by increasing the size of the readily releasable pool of secretory granules. *Neuron* **16**:1209-1220.

Giorguieff-Chesselet MF, Kemel ML, Wandscheer D and Glowinski J (1979) Regulation of dopamine release by presynaptic nicotinic receptors in rat striatal slices: effect of nicotine in a low concentration. *Life Sci* **25**:1257-1262.

Goeldner FM, Dineley KT and Patrick JW (1997) Immunohistochemical localization of the nicotinic acetylcholine receptor subunit α6 to dopaminergic neurons in the substantia nigra and ventral tegmental area. *Neuroreport* **8**:2739-2742.

Goldman WF and Blaustein MP (1990) Non-homogeneous Mn^{2+} quench of fura-2 signals in cultured arterial myocytes visualized by digital imaging. *Biophys J* **57**:162a

Gonon F (1998) Prolonged and extrasynaptic excitatory action of dopamine mediated by D1 receptors in the rat striatum *in vivo*. *J Neurosci* **17**:5972-5978.

Gopalakrishnan M, Buisson B, Touma E, Giordano T, Campbell JE, Hu IC, Donnelly-Roberts D, Arneric SP, Bertrand D and Sullivan JP (1995) Stable expression and pharmacological properties of the human α7 nicotinic acetylcholine receptor. *Eur J Pharmacol* **290**:237-246.

Gopalakrishnan M, Monteggia LM, Anderson DJ, Molinari EJ, Piattoni-Kaplan M, Donnelly-Roberts D, Arneric SP and Sullivan JP (1996) Stable expression, pharmacologic properties and regulation of the human neuronal nicotinic acetylcholine α4β2 receptor. *J Pharmacol Exp Ther* **276**:289-297.

Gopalakrishnan M, Molinari EJ and Sullivan JP (1997) Regulation of human α4β2 neuronal nicotinic acetylcholine receptors by cholinergic channel ligands and second messenger pathways. *Mol Pharmacol* **52**:524-534.

Goslin K and Banker G (1991) Rat hippocampal neurons in low-density culture. *In: Culturing nerve cells (eds. Banker,G. and Goslin,K.).Cambridge MA: MIT Press.* 251-281.

Gotti C, Ogando AE, Hanke W, Schlue R, Moretti M and Clementi F (1991) Purification and characterization of an α-bungarotoxin receptor that forms a functional nicotinic channel. *Proc Natl Acad Sci U S A* **88**:3258-3262.

Gotti C, Hanke W, Maury K, Moretti M, Ballivet M, Clementi F and Bertrand D (1994) Pharmacology and biophysical properties of α7 and α7-α8 α-bungarotoxin receptor subtypes immunopurified from the chick optic lobe. *Eur J Neurosci* **6**:1281-1291.

Grady S, Marks MJ, Wonnacott S and Collins AC (1992) Characterization of nicotinic receptor-mediated [^{3}H]dopamine release from synaptosomes prepared from mouse striatum. *J Neurochem* **59**:848-856.

Grady SR, Marks MJ AND Collins AC (1994) Desensitization of nicotine-stimulated [^{3}H]dopamine release from mouse striatal synaptosomes. *J Neurochem* **62**:1390-1398.

Graham F, Smiley J, Russell WC and Nairn R (1977) Characteristics of a human cell line transformed by DNA from human Adenovirus type 5. *J Gen Virol* **36**:59-74.

Gray R, Rajan AS, Radcliffe KA, Yakehiro M and Dani JA (1996) Hippocampal synaptic transmission enhanced by low concentrations of nicotine. *Nature* **383**:713-716.

Green WN, Ross AF and Claudio T (1991) cAMP stimulation of acetylcholine receptor expression is mediated through posttranslational mechanism. *Proc Natl Acad Sci U S A* **88**:854-858.

Green WN and Claudio T (1993) Acetylcholine receptor assembly: subunit folding and oligomerization occur sequentially. *Cell* **74**:57-69.

Green WN and Millar NS (1995) Ion-channel assembly. *Trends Neurosci* **18**:280-287.

Green WN and Wanamaker CP (1998) Formation of the nicotinic acetylcholine receptor binding sites. *J Neurosci* **18**:5555-5564.

Greenberg ME, Ziff EB and Greene LA (1986) Stimulation of neuronal acetylcholine receptors induces rapid gene transcription. *Science* **234**:80-83.

Greengard P, Valtorta F, Czernik AJ and Benfenati F (1993) Synaptic vesicle phosphoproteins and regulation of synaptic function. *Science* **259**:780-785.

Greenmamyre JT and Young AB (1989) Synaptic localization of striatal NMDA, quisqualate and kainate receptors. *Neurosci Lett* **101**:133-137.

Grimwood S, Le Bourdelles B, Atack JR, Barton C, Cockett W, Cook SM, Gilbert E, Hutson PH, McKernan RM, Myers J, Ragan CI, Wingrove PB and Whiting PJ (1996) Generation and characterisation of stable cell lines expressing recombinant human N-methyl-D-aspartate receptor subtypes. *J Neurochem* **66**:2239-2247.

Groves PM, Linder JC and Young SJ (1994) 5-Hydroxydopamine-labeled dopaminergic axons: three dimensional reconstructions of axons, synapses and postsynaptic targets in rat neostriatum. *Neurosci* **58**:593-604.

Grynkiewicz G, Poenie M and Tsien RY (1985) A new generation of Ca^{2+} indicators with greatly improved fluorescence properties. *J Biol Chem* **260**:3440-3450.

Guo JZ, Tredway TL and Chiappinelli VA (1998) Glutamate and GABA release are enhanced by different subtypes of presynaptic nicotinic receptors in the lateral geniculate nucleus. *J Neurosci* **18**:1963-1969.

Gurd JW (1997) Protein tyrosine phosphorylation: implications for synaptic function. *Neurochem Int* **31**:635-649.

Harrison T, Graham F and Williams J (1977) Host-range mutants of Adenovirus type 5 defective for growth in HeLa cells. *Virology* **77**:319-329.

Harsing LGJ, Sershen H, Vizi SE and Lajtha A (1992) N-type calcium channels are involved in the dopamine releasing effect of nicotine. *Neurochem Res* **17**:729-734.

Hartman DS and Claudio T (1990) Coexpression of two distinct muscle acetylcholine receptor α- subunits during development. *Nature* **343**:372-375.

Harvey SC, McIntosh JM, Cartier GE, Maddox FN and Luetje CW (1997) Determinants of specificity for α-conotoxin MII on α3β2 neuronal nicotinic receptors. *Mol Pharmacol* **51**:336-342.

Hattori T, Takada M, Moriizumi T and Van der Kooy D (1991) Single dopaminergic nigrostriatal neurons form two chemically distinct synaptic types: possible transmitter segregation within neurons. *J Comp Neurol* **309**:391-401.

Helekar SA, Char D, Neff S and Patrick J (1994) Prolyl isomerase requirement for the expression of functional homo- oligomeric ligand-gated ion channels. *Neuron* **12**:179-189.

Helekar SA and Patrick J (1997) Peptidyl prolyl cis-trans isomerase activity of cyclophilin A in functional homo-oligomeric receptor expression. *Proc Natl Acad Sci U S A* **94**:5432-5437.

Helme-Guizon A, Davis S, Israel M, Lesbats B, Mallet J, Laroche S and Hicks A (1998) Increase in syntaxin 1B and glutamate release in mossy fibre terminals following induction of LTP in the dentate gyrus: a candidate molecular mechanism underlying transsynaptic plasticity. *Eur J Neurosci* **10**:2231-2237.

Hens JJH, De Wit M, Boomsma F, Mercken M, Oestreicher AB, Gispen WH and De Graan PNE (1995) N-Terminal-specific anti B-50 (GAP-43) antibodies inhibit Ca^{2+}-induced noradrenaline release, B-50 phosphorylation and dephosphorylation, and calmodulin binding. *J Neurochem* **64**:1127-1136.

Hilfiker S, Schweizer FE, Kao HT, Czernik AJ, Greengard P and Augustine G (1998) Two sites of action for synapsin domain E in regulating neurotransmitter release. *Nature Neurosci* **1**:29-35.

Hillard CJ (1992) Nicotine-induced depolarization of cerebral cortical synaptosomes is dependent upon sodium. *Neuropharmacology* **31**:909-914.

Hirokawa N, Sobue K, Kanda K, Harada A and Yorifuyi H (1989) The cytoscheletal architecture of the presynaptic terminal and molecular structure of synapsin I. *J Cell Biol* **108**:111-126.

Hoffman PW, Ravindran A and Huganir RL (1994) Role of phosphorylation in desensitization of acetylcholine receptors expressed in *Xenopus* oocytes. *J Neurosci* **14**:4185-4195.

Holladay MW, Dart MJ and Lynch JK (1997) Neuronal nicotinic acetylcholine receptors as targets for drug discovery. *J Med Chem* **40**:4169-4194.

Hollmann M, Maron C and Heinemann SF (1994) N-glycosylation site tagging suggests a three transmembrane domain topology for the glutamate receptor GluR1. *Neuron* **13**:1331-1343.

Hunter BE, de Fiebre CM, Papke RL, Kem WR and Meyer EM (1994) A novel nicotinic agonist facilitates induction of long-term potentiation in the rat hippocampus. *Neurosci Lett* **168**:130-134.

Imoto K, Busch C, Sakmann B, Mishina M, Konno T, Nakai J, Bujo H, Mori Y, Fukuda K and Numa S (1988) Rings of negatively charged amino acids determine the acetylcholine receptor channel conductance. *Nature* **335**:645-648.

Imoto K, Konno T, Nakai J, Wang F, Mishina M and Numa S (1991) A ring of uncharged polar amino acids as a component of channel constriction in the nicotinic acetylcholine receptor. *FEBS Lett* **289**:193-200.

Ingham CA, Hood SH, Taggart P and Arbuthnott GW (1998) Plasticity of synapses in the rat neostriatum after unilateral lesion of the nigrostriatal dopaminergic pathway. *J Neurosci* **18**:4732-4743.

Iwata SI, Keikilani GH, Ferrell ST, Kantor L and Gnegy ME (1997) Enhanced dopamine release and phosphorylation of synapsin I and neuromodulin in striatal synaptosomes after repeated amphetamine. *J Pharmacol Exp Ther* **283**:1445-1452.

Janson AM, Fuxe K, Kitayama I, Harfstand A and Agnati LF (1986) Morphometric studies on the protective action of nicotine on the substantia nigra dopamine nerve cells after partial hemitransection in the male rat. *Neurosci Lett* **26**:S88

Jedema HP and Moghaddam B (1996) Characterization of excitatory amino acid modulation of dopamine release in the prefrontal cortex of conscious rats. *J Neurochem* **66**:1448-1453.

Jin S and Fredholm BB (1994) Role of NMDA, AMPA and kainate in mediating glutamate- and 4-AP-induced dopamine and acetylcholine release from rat striatal slices. *Neuropharmacology* **33**:1039-1048.

Jin S and Fredholm BB (1997) Electrically-evoked dopamine and acetylcholine release from rat striatal slices perfused without magnesium: regulation by glutamate acting on NMDA receptors. *Br J Pharmacol* **121**:1269-1276.

Johnson DS, Martinez J, Elgoyhen AB, Heinemann SF and McIntosh JM (1995) α-Conotoxin ImI exhibits subtype-specific nicotinic acetylcholine receptor blockade: preferential inhibition of homomeric α7 and α9 receptors. *Mol Pharmacol* **48**:194-199.

Johnson JW and Asher P (1987) Glycine potentiates the NMDA response in cultured mouse brain neurons. *Nature* **325**:529

Kaiser SA, Soliakov L, Harvey SC, Luetje CW and Wonnacott S (1998) Differential inhibition by α-conotoxin-MII of the nicotinic stimulation of [^{3}H]dopamine release from rat striatal synaptosomes and slices. *J Neurochem* **70**:1069-1076.

Kaiser SA and Wonnacott S (1999) Nicotinic Receptor Modulation of Neurotransmitter Release. *In: Neuronal Nicotinic Receptors: Pharmacology and Therapeutic Opportunities (eds. Arneric,S. and Brioni,D.). New York: John Wiley and Sons.* 141-159.

Kandel ER, Schwartz JH and Jessell M (1995) Voluntary movement (29). *In: Essentials of Neural Science and Behaviour.Prentice Hall International, Inc.* 529-550.

Karlin A (1993) Structure of nicotinic acetylcholine receptors. *Curr Opin Neurobiol* **3**:299-309.

Kassner PD and Berg DK (1997) Differences in the fate of neuronal acetylcholine receptor protein expressed in neurons and stably transfected cells. *J Neurobiol* **33**:968-982.

Katz B (1969) The release of Neural Transmitter Substances. *Liverpool: Liverpool University Press*

Keefe KA, Zigmond MJ and Abercrombie ED (1992) Extracellular dopamine in striatum: influence of nerve impulse activity in medial forebrain bundle and local glutamatergic input. *Neurosci* **47**:325-332.

Keith RA, Mangano TJ, DeFeo PA, Ernst GE and Warawa EJ (1994) Differential inhibition of neuronal calcium entry and [^{3}H]-D-aspartate release by the quaternary derivatives of verapamil and emopamil. *Br J Pharmacol* **113**:379-384.

Keith RA, Mangano TJ, Lampe RA, DeFeo PA, Hyde MJ and Donzanti BA (1995) Comparative actions of synthetic omega-grammotoxin SIA and synthetic omega-Aga-IVA on neuronal calcium entry and evoked release of neurotransmitters *in vitro* and *in vivo*. *Neuropharmacology* **34**:1515-1528.

Kellar KJ and Wonnacott S (1990) Nicotinic cholinergic receptors in Alzheimers' disease. *In: Nicotine Psycopharmacology. Molecular, cellular and behavioural aspects (eds. Wonnacott,S. Russell,M.A.H. and Stolerman,I.P.).Oxford: Oxford University Press.* 341-373.

Kendrick KM, Guevara-Guzman R, De la Riva C, Christensen J, Ostergaard K and Emson PC (1996) NMDA and kainate-evoked release of nitric oxide and classical transmitters in the rat striatum: *in vivo* evidence that nitric oxide may play a neuroprotective role. *Eur J Neurosci* **8**:2619-2634.

Kennedy MB (1989) Regulation of synaptic transmission in the CNS. *Cell* **59**:777-787.

Keyser KT, Britto LR, Schoepfer R, Whiting P, Cooper J, Conroy W, Brozozowska-Prechtl A, Karten HJ and Lindstrom J (1993) Three subtypes of α-bungarotoxin-sensitive nicotinic acetylcholine receptors are expressed in chick retina. *J Neurosci* **13**:442-454.

Kita H (1993) GABAergic circuits of the striatum. *In: Progress in Brain Research (eds. Arbuthnott,G.W. and Emson,P.C.).Amsterdam: Elsevier Science.* 51-72.

Klancnik JM, Cuenod M, Gahwiler BH, Jiang ZP and Do KQ (1992) Release of endogenous amino acids, including homocysteic acid and cysteine sulphinic acid, from rat hippocampal slices evoked by electrical stimulation of Schaffer collateral-commissural fibres. *Neuroscience* **49**:557-570.

Kleckner NW and Dingledine R (1988) Requirements for glycine in activation of NMDA-receptors expressed in *Xenopus* oocytes. *Science* **241**:835

Knight DE (1987) Calcium and diacylglycerol control of secretion. *Biosci Rep* **7**:355-367.

Koelle GB (1961) A proposed dual neurohumoral role of acetylcholine: its functions at the pre- and post-synaptic sites. *Nature* **190**:208-211.

Konno T, Busch C, von Kitzing E, Imoto K, Wang F, Nakai J, Mishina M, Numa S and Sakmann B (1991) Rings of anionic amino acids as structural determinants of ion selectivity in the acetylcholine receptor channel. *Proc R Soc Lond B Biol Sci* **244** :69-79.

Kölliker A (1862) Untersuchungen über die letzten Endigungen der Nerven. *Leipzig: Engelmann*

Kulak JM, Nguyen TA, Olivera BM and McIntosh JM (1997) α-Conotoxin MII blocks nicotine-stimulated dopamine release in rat striatal synaptosomes. *J Neurosci* **17**:5263-5270.

Kung L, Force M, Chute DJ and Roberts RC (1998) Immunocytochemical localization of tyrosine hydroxylase in the human striatum: a postmortem ultrastructural study. *J Comp Neurol* **390**:52-62.

Kusano K, Miledi R and Stinnakre J (1977) Acetylcholine receptors in the oocyte membrane. *Nature* **328**:143-170.

Kühne W (1862) Über der peripherishen Endorgane der motorishen Nerven. *Leipzig: Engelmann.*

Laemmli UK (1970) Cleavage of structural proteins during the assembly of the head of bacteriophage T4. *Nature* **227**:680-685.

Langer SZ (1997) 25 years since the discovery of presynaptic receptors: present knowledge and future perspectives [see comments]. *Trends Pharmacol Sci* **18**:95-99.

Langley JN (1905) On the reaction of cells and of nerve-endings to certain poisons, chiefly as regards the reaction of striated muscle to nicotine and to curare. *J.Physiol.(London)* **33**:374-413.

Langley JN (1907) On the contraction of muscle, chiefly in relation to the presence of receptive substances: Part I. *J.Physiol.(London)* **36**:347-384.

Langley JN (1914) The antagonism of curare and nicotine in skeletal muscles. *J.Physiol.(London)* **48**:73-108.

Lannes B and Micheletti G (1994) Glutamate-dopamine balance in the striatum: pre- and post-synaptic interactions. *In: The Basal Ganglia IV.New ideas and data on structure and function (eds. Percheron,G. McKenzie,J.S. and Feger,J.).New York: Plenum Press.* 475-489.

Lapchak PA, Araujo DM, Quirion R and Collier B (1989) Presynaptic cholinergic mechanisms in the rat cerebellum: evidence for nicotinic, but not muscarinic autoreceptors. *J Neurochem* **53**:1843-1851.

Larsen M, Valo ET, Berg-Johnsen J and Langmoen IA (1998) Isoflurane reduces synaptic glutamate release without changing cytosolic free calcium in isolated nerve terminals. *Eur J Anaesthesiol* **15**:224-229.

Le Novere N, Zoli M and Changeux JP (1996) Neuronal nicotinic receptor $\alpha 6$ subunit mRNA is selectively concentrated in catecholaminergic nuclei of the rat brain. *Eur J Neurosci* **8**:2428-2439.

Lee CY and Chang CC (1966) Modes of actions of purified toxins from elapid venoms on neuromuscular transmission. *Mem Inst Butantan* **33**:555-572.

Lena C, Changeux JP and Mulle C (1993) Evidence for "preterminal" nicotinic receptors on GABAergic axons in the rat interpeduncular nucleus. *J Neurosci* **13**:2680-2688.

Lena C and Changeux JP (1997) Role of Ca^{2}+ ions in nicotinic facilitation of GABA release in mouse thalamus. *J Neurosci* **17**:576-585.

Lendvai B, Sershen H, Lajtha A, Santha E, Baranyi M and Vizi ES (1996) Differential mechanisms involved in the effect of nicotinic agonists DMPP and lobeline to release [^{3}H]5-HT from rat hippocampal slices. *Neuropharmacology* **35**:1769-1777.

Levey AI, Hersh SM, Rye DB, Sunahara RK, Niznik HB, Kitt C, Price DL, Maggiou R, Brann MR and Ciliax BJ (1993) Localization of D1 and D2 dopamine receptors in brain with subtype-specific antibodies. *Proc Natl Acad Sci U S A* **90**:8861-8865.

Levin ED (1992) Nicotinic systems and cognitive function. *Psychopharmacology* **108**:417-431.

Li X, Rainnie DG, McCarley RW and Greene RW (1998) Presynaptic nicotinic receptors facilitate monoaminergic transmission. *J Neurosci* **18**:1904-1912.

Liang SD and Vizi ES (1997) Positive feedback modulation of acetylcholine release from isolated rat superior cervical ganglion. *J Pharmacol Exp Ther* **280**:650-655.

Lindstrom J, Anand R, Peng X, Gerzanich V, Wang F and Li Y (1995) Neuronal nicotinic receptor subtypes. *Ann N Y Acad Sci* **757**:100-116.

Lindstrom J (1996) Neuronal nicotinic acetylcholine receptors. *In: Ion Channels (ed.Toshio Narahashi).New York: Plenum Press* **4**:377-450.

Llinás R, Gruner JA, Sugimori M, McGuinness TL and Greengard P (1991) Regulation by synapsin I and Ca^{2+} -calmodulin-dependent protein kinase II of transmitter release in squid giant synapse. *J.Physiol.(London)* **436**:257-282.

Lu Y, Grady S, Marks MJ, Picciotto M, Changeux JP and Collins AC (1998) Pharmacological characterization of nicotinic receptor-stimulated GABA release from mouse brain synaptosomes. *J Pharmacol Exp Ther* **287**:648-657.

Luetje CW, Wada K, Rogers S, Abramson SN, Tsuji K, Heinemann S and Patrick J (1990) Neurotoxins distinguish between different neuronal nicotinic acetylcholine receptor subunit combinations. *J Neurochem* **55**:632-640.

Luetje CW and Patrick J (1991) Both α- and β-subunits contribute to the agonist sensitivity of neuronal nicotinic acetylcholine receptors. *J Neurosci* **11**:837-845.

Luetje CW, Piattoni M and Patrick J (1993) Mapping of ligand binding sites of neuronal nicotinic acetylcholine receptors using chimeric α subunits. *Mol Pharmacol* **44**:657-666.

Lukas RJ, Norman SA and Lucero L (1993) Characterization of nicotinic acetylcholine receptors expressed by cells of the SH-SY5Y human neuroblastoma clonal line. *Mol and Cel Neurosci* **4**:1-12.

Luo S, Kulak JM, Cartier GE, Jacobsen RB, Yoshikami D, Olivera BM and McIntosh JM (1998) α-Conotoxin AuIB selectively blocks α3β4 nicotinic acetylcholine receptors and nicotine-evoked norepinephrine release. *J Neurosci* **18**:8571-8579.

Maelicke A and Albuquerque EX (1996) New approach to drug therapy in Alzheimers' dementia. *Discovery Drugs Today* **1**:53-59.

Marchi M, Raiteri M (1996) Nicotinic autoreceptors mediating enhancement of acetylcholine release become operative in conditions of "impaired" cholinergic presynaptic function. *J Neurochem* **67**:1974-1981.

Marks MJ, Bullock AE and Collins AC (1995) Sodium channel blockers partially inhibit nicotine-stimulated ^{86}Rb+ efflux from mouse brain synaptosomes. *J Pharmacol Exp Ther* **274**:833-841.

Marks MJ, Robinson SF and Collins AC (1996) Nicotinic agonists differ in activation and desensitization of ^{86} Rb+ efflux from mouse thalamic synaptosomes. *J Pharmacol Exp Ther* **277**:1383-1396.

Markus RP, Zago WM and Carneiro RC (1996) Melatonin modulation of presynaptic nicotinic acetylcholine receptors in the rat vas deferens. *J Pharmacol Exp Ther* **279**:18-22.

Markwell M, Haas SM, Bieber L and Tolbert N (1978) A modification of the Lowry procedure to simplify protein determination in membrane and lipoprotein samples. *Anal Biochem* **87**:206-210.

Marshall D, Soliakov L, Redfern P and Wonnacott S (1996) Tetrodotoxin-sensitivity of nicotine-evoked dopamine release from rat striatum. *Neuropharmacology* **35**:1531-1536.

Martinez-Serrano A, Borner C, Pereira R, Villalba M and Satrustegui J (1996) Modulation of presynaptic calcium homeostasis by nitric oxide. *Cell Calcium* **20**:293-302.

McConahey PJ and Dixon FJ (1980) Radioiodination of proteins by the use of the chloramine-T method. *Methods in Enzymology* **70**:210-213.

McGehee DS, Heath MJ, Gelber S, Devay P and Role LW (1995) Nicotine enhancement of fast excitatory synaptic transmission in CNS by presynaptic receptors. *Science* **269** :1692-1696.

McGehee DS and Role LW (1995) Physiological diversity of nicotinic acetylcholine receptors expressed by vertebrate neurons. *Annu Rev Physiol* **57**:521-546.

McGehee DS and Role LW (1996) Neurobiology: memories of nicotine. *Nature* **383**:670-671.

McKernan RM and Whiting PJ (1996) Which $GABA_A$-receptor subtypes really occur in the brain? *Trends Neurosci* **19**:139-143.

McMahon LL, Yoon KW and Chiappinelli VA (1994) Electrophysiological evidence for presynaptic nicotinic receptors in the avian ventral lateral geniculate nucleus. *J Neurophysiol* **71**:826-829.

McMahon LL, Yoon KW and Chiappinelli VA (1994b) Nicotinic receptor activation facilitates GABAergic neurotransmission in the avian lateral spiriform nucleus. *Neuroscience* **59**:689-698.

Merlie JP and Sebbane R (1981) Acetylcholine receptor subunits transit a precursor pool before acquiring α-bungarotoxin binding activity. *J Biol Chem* **256**:-3605

Merlie JP, Sebbane R, Tzartos S and Lindstrom J (1982) Inhibition of glycosylation with tunicamycin blocks assembly of newly synthesised acetylcholine receptor subunits in muscle cells. *J Biol Chem* **257**:2694-2701.

Merlie JP and Lindstrom J (1983) Assembly *in vivo* of mouse acetylcholine receptor: identification of an α subunit species that may be an assembly intermediate. *Cell* **34**:747-757.

Meshul CK and Casey DE (1989) Regional, reversible ultrastructural changes in rat brain with chronic neuroleptic treatment. *Brain Res* **489**:338-346.

Messing RO, Stevens AM, Kiyasu E and Sneade AB (1989) Nicotinic and muscarinic agonists stimulate rapid protein kinase C translocation in PC12 cells. *J Neurosci* **9**:507-512.

Miledi R (1982) A calcium-dependent transient outward current in *Xenopus laevis* oocytes. *Proc R Soc Lond* **B215**:491-497.

Miledi R and Parker I (1984) Chloride current induced by injection of calcium into *Xenopus* oocytes. *J Physiol (Lond)* **357**:173-183.

Miner LL and Collins AC (1989) Strain comparison of nicotine-induced seizure sensitivity and nicotinic receptors. *Pharmacol Biochem Behav* **33**:469-475.

Miyata H, Silverman HS, Sollott SJ, Lakatta EG, Stern MD and Hansford RG (1991) Measurement of mitochondrial free Ca^{2+} concentration in living single rat cardiac myocytes. *Am J Physiol* **261**:H1123-H1134

Morari M, O'Connor WT, Ungerstedt U and Fuxe K (1993) NMDA differentially regulates extracellular doapmine, GABA and glutamate levels in the dorsolateral neostriatum of the halothane-anesthetized rat: an *in vivo* microdialysis study. *J Neurochem* **60**:1884-1893.

Morens DM, Grandinetti A, Reed D, White LR and Ross GW (1995) Cigarette smoking and protection from Parkinsons' disease. *Neurology* **45**:1041-1051.

Museo E and Pert A (1994) Nicotine-induced dopamine overflow in the nucleus accumbens: evaluation of possible mechanisms of action. *In: Effects of nicotine on biological systems II (eds. Clarke,P.B.S. Quick,M. Adlkofer,F. and Thurau, K.).Basel: Birkhauser Verlag* 65

Nachmanson D (1959) Chemical and molecular basis of nerve activity. *New York: Academic Press.*

Nashen DA and Blaustein MP (1980) Some properties of potassium-stimulated calcium influx in presynaptic nerve endings. *J Gen Physiol* **76**:709-728.

Nicholls D and Attwell D (1990) The release and uptake of excitatory amino acids. *Trends Pharmacol Sci* **11**:462-468.

Nordberg A (1994) Human nicotinic receptors: their role in aging and dementia. *Neurochem Int* **25**:93-97.

Nusser Z, Sieghart W, Benke D, Fritschy JM and Somogyi P (1996) Differential synaptic localization of 2 major γ-aminobutyric-acid type-A receptor-alpha subunits on hippocampal pyramidal cells. *Proc Natl Acad Sci U S A* **93**:11939-11944.

O'Hara PJ, Sheppard PO, Thørgesen H, Venezia D, Haldeman BA, McGrane V, Houamed KM, Thomsen C, Gilbert TL and Mulvihill ER (1993) The ligand-binding domain in metabotropic glutamate receptors is related to bacterial periplasmic binding proteins. *Neuron* **11**:41-52.

Ochoa EL and O'Shea SM (1994) Concomitant protein phosphorylation and endogenous acetylcholine release induced by nicotine: dependency on neuronal nicotinic receptors and desensitization. *Cell Mol Neurobiol* **14**:315-340.

Ohno M, Yamamoto T and Watanabe S (1993) Blockade of hippocampal nicotinic receptors impairs working memory but not reference memory in rats. *Pharmacol Biochem Behav* **45**:89-93.

Orr-Urtreger A, Seldin MF, Baldini A and Beaudet AL (1995) Cloning and mapping of the mouse α7-neuronal nicotinic acetylcholine receptor. *Genomics* **26**:399-402.

Orr-Urtreger A, Goldner FM, Saeki M, Lorenzo I, Goldberg L, De Biasi M, Dani JA, Patrick JW and Beaudet AL (1997) Mice deficient in the α7 neuronal nicotinic acetylcholine receptor lack α-bungarotoxin binding sites and hippocampal fast nicotinic currents. *J Neurosci* **17**:9165-9171.

Ortells MO and Lunt GG (1995) Evolutionary history of the ligand-gated ion-channel superfamily of receptors. *Trends Neurosci* **18**:121-127.

Palma E, Bertrand S, Binzoni T and Bertrand D (1996) Neuronal nicotinic α7 receptor expressed in *Xenopus* oocytes presents five putative binding sites for methyllycaconitine. *J Physiol (Lond)* **491 (Pt 1)**:151-161.

Papke RL and Heinemann SF (1991) The role of the β4-subunit in determining the kinetic properties of rat neuronal nicotinic acetylcholine α3-receptors. *J Physiol (Lond)* **440**:95-112.

Papke RL, Duvoisin RM and Heinemann SF (1993) The amino terminal half of the nicotinic β-subunit extracellular domain regulates the kinetics of inhibition by neuronal-bungarotoxin. *Proc R Soc Lond B Biol Sci* **252**:141-148.

Papke RL and Heinemann SF (1994) Partial agonist properties of cytisine on neuronal nicotinic receptors containing the β2 subunit. *Mol Pharmacol* **45**:142-149.

Papke RL and Thinschmidt JS (1998) The correction of α7 nicotinic acetylcholine receptor concentration-response relationships in *Xenopus* oocytes. *Neurosci Lett* **256**:163-166.

Parsons LH, Weiss F and Koob GF (1996) Serotonin 1b receptor stimulation enhances dopamine-mediated reinforcement. *Psychopharmacol* **128**:150-160.

Paulson HL, Ross AF, Green WN and Claudio T (1991) Analysis of early events in acetylcholine receptor assembly. *J Cell Biol* **113**:1371-1384.

Peng X, Katz M, Gerzanich V, Anand R and Lindstrom J (1994) Human α7 acetylcholine receptor: cloning of the α7 subunit from the SH-SY5Y cell line and determination of pharmacological properties of native receptors and functional α7 homomers expressed in *Xenopus* oocytes. *Mol Pharmacol* **45**:546-554.

Pereira EF, Alkondon M, McIntosh JM and Albuquerque EX (1996) α-Conotoxin-Iml: a competitive antagonist at α-bungarotoxin- sensitive neuronal nicotinic receptors in hippocampal neurons. *J Pharmacol Exp Ther* **278**:1472-1483.

Picciotto MR, Zoli M, Lena C, Bessis A, Lallemand Y, LeNovere N, Vincent P, Pich EM, Brulet P and Changeux JP (1995) Abnormal avoidance learning in mice lacking functional high-affinity nicotine receptor in the brain. *Nature* **374**:65-67.

Pieribone VA, Shupliakov O, Brodin L, Hilfiker S, Czernik AJ and Greengard P (1995) Distinct pools of synaptic vesicles in neurotransmitter release. *Nature* **375**:493-497.

Plenz D and Kitai ST (1996) Organotypic cortex-striatum-mesencephalon cultures: the nigrostriatal pathway. *Neurosci Lett* **209**:177-180.

Popot JL and Changeux JP (1984) Nicotinic receptor of acetylcholine: structure of an oligomeric integral membrane protein. *Physiol Rev* **64**:1162-1239.

Porras A and Mora F (1995) Dopamine--glutamate--GABA interactions and ageing: studies in the striatum of the conscious rat. *Eur J Neurosci* **7**:2183-2188.

Prince RJ, Fernandes KG, Gregory JC, Martyn ID and Lippiello PM (1996) Modulation of nicotine-evoked [^{3}H]dopamine release from rat striatal synaptosomes by voltage-sensitive calcium channel ligands. *Biochem Pharmacol* **52**:613-618.

Puchacz E, Buisson B, Bertrand D and Lukas RJ (1994) Functional expression of nicotinic acetylcholine receptors containing rat α7 subunits in human SH-SY5Y neuroblastoma cells. *FEBS Lett* **354**:155-159.

Pugh PC and Berg DK (1994) Neuronal acetylcholine receptors that bind α-bungarotoxin mediate neurite retraction in a calcium-dependent manner. *J Neurosci* **14**:889-896.

Quik M, Choremis J, Komourian J, Lukas RJ and Puchacz E (1996) Similarity between rat brain nicotinic α-bungarotoxin receptors and stably expressed α-bungarotoxin binding sites. *J Neurochem* **67**:145-154.

Quik M, Philie J and Choremis J (1997) Modulation of α7 nicotinic receptor-mediated calcium influx by nicotinic agonists. *Mol Pharmacol* **51** :499-506.

Radcliffe KA and Dani JA (1998) Nicotinic stimulation produces multiple forms of increased glutamatergic synaptic transmission. *J Neurosci* **18**:7075-7083.

Ragozzino D, Fucile S, Giovannelli A, Grassi F, Mileo AM, Ballivet M, Alema S and Eusebi F (1997) Functional properties of neuronal nicotinic acetylcholine receptor channels expressed in transfected human cells. *Eur J Neurosci* **9**:480-488.

Ramirez-Latorre J, Yu CR, Qu X, Perin F, Karlin A and Role L (1996) Functional contributions of α5 subunit to neuronal acetylcholine receptor channels. *Nature* **380**:347-351.

Rao TS, Correa LD and Lloyd GK (1997) Effects of lobeline and dimethylphenylpiperazinium iodide (DMPP) on N- methyl-D-aspartate (NMDA)-evoked acetylcholine release *in vitro*: evidence for a lack of involvement of classical neuronal nicotinic acetylcholine receptors. *Neuropharmacology* **36**:39-50.

Rapier C, Wonnacott S, Lunt GG and Albuquerque EX (1987) The neurotoxin histrionicotoxin interacts with the putative ion channel of the nicotinic acetylcholine receptors in the central nervous system. *FEBS Lett* **212**:292-296.

Rapier C, Lunt GG and Wonnacott S (1988) Stereoselective nicotine-induced release of dopamine from striatal synaptosomes: concentration dependence and repetitive stimulation. *J Neurochem* **50**:1123-1130.

Rapier C, Lunt GG and Wonnacott S (1990) Nicotinic modulation of [^{3}H]dopamine release from striatal synaptosomes: pharmacological characterisation. *J Neurochem* **54**:937-945.

Rathouz MM, Vijayaraghavan S and Berg DK (1996) Elevation of intracellular calcium levels in neurons by nicotinic acetylcholine receptors. *Mol Neurobiol* **12**:117-131.

Ravdin PM and Berg DK (1979) Inhibition of neuronal acetylcholine sensitivity by α-toxins from *Bungarus multicinctus*. *Proc Natl Acad Sci U S A* **76**:2072-2076.

Revah F, Bertrand D, Galzi JL, Devillers-Thiery A, Mulle C, Hussy N, Bertrand S, Ballivet M and Changeux JP (1991) Mutations in the channel domain alter desensitization of a neuronal nicotinic receptor. *Nature* **353**:846-849.

Roberts PJ and Anderson SD (1979) Stimulatory effect of L-glutamate and related amino acids on [^{3}H]dopamine release from rat striatum: an *in vitro* model for glutamate actions. *J Neurochem* **32**:1539-1545.

Rodriguez FJ, Lluch M, Dot J, Blanco I and Rodriguez-Alvarez J (1997) Histamine modulation of glutamate release from hippocampal synaptosomes. *Eur J Pharmacol* **323**:283-286.

Rogers SW, Mandelzys A, Deneris ES, Cooper E and Heinemann S (1992) The expression of nicotinic acetylcholine receptors by PC12 cells treated with NGF. *J Neurosci* **12**:4611-4623.

Role LW (1992) Diversity in primary structure and function of neuronal nicotinic acetylcholine receptor channels. *Curr Opin Neurobiol* **2**:254-262.

Role LW and Berg DK (1996) Nicotinic receptors in the development and modulation of CNS synapses. *Neuron* **16**:1077-1085.

Rosahl TW, Spillane D, Missler M, Herz J, Selig DK, Wolff JR, Hammer RE, Malenka RC and Südhof TC (1995) Essential functions of synapsins I and II in synaptic vesicle regulation. *Nature* **375**:488-493.

Ross AF, Green WN, Hartman DS and Claudio T (1991) Efficiency of acetylcholine receptor subunit assembly and its regulation by cAMP. *J Cell Biol* **113**:623-636.

Ross RA, Spengler BA and Biedler JL (1983) Coordinate morphological and biochemical interconversion of human neuroblastoma cells. *J Natl Cancer Inst* **71**:741-749.

Rothhut B, Romano SJ, Vijayaraghavan S and Berg DK (1996) Post-translational regulation of neuronal acetylcholine receptors stably expressed in a mouse fibroblast cell line. *J Neurobiol* **29**:115-125.

Rowell PP and Winkler DL (1984) Nicotinic stimulation of [^{3}H]acetylcholine release from mouse cerebral cortical synaptosomes. *J Neurochem* **43**:1593-1598.

Rowell PP, Carr LA and Garner AC (1987) Stimulation of [^{3}H]dopamine release by nicotine in rat nucleus accumbens. *J Neurochem* **49**:1449-1454.

Rowell PP and Hillebrand JA (1994) Characterization of nicotine-induced desensitization of evoked dopamine release from rat striatal synaptosomes. *J Neurochem* **63**:561-569.

Sacaan AI, Dunlop JL and Lloyd GK (1995) Pharmacological characterization of neuronal acetylcholine gated ion channel receptor-mediated hippocampal norepinephrine and striatal dopamine release from rat brain slices. *J Pharmacol Exp Ther* **274**:224-230.

Sacaan AI, Menzaghi F, Dunlop JL, Correa LD, Whelan KT and Lloyd GK (1996) Epibatidine: a nicotinic acetylcholine receptor agonist releases monoaminergic neurotransmitters: *in vitro* and *in vivo* evidence in rats. *J Pharmacol Exp Ther* **276**:509-515.

Sargent PB (1993) The diversity of neuronal nicotinic acetylcholine receptors. *Annu Rev Neurosci* **16**:403-443.

Scanziani M, Salin PA, Vogt KE, Malenka RC and Nicoll RA (1997) Use-dependent increases in glutamate concentration activate presynaptic metabotropic glutamate receptors. *Nature* **385**:630-634.

Schoepfer R, Conroy WG, Whiting P, Gore M and Lindstrom J (1990) Brain α-bungarotoxin binding protein cDNAs and MAbs reveal subtypes of this branch of the ligand-gated ion channel gene superfamily. *Neuron* **5**:35-48.

Schröder H, Giacobini E, Struble RG, Zilles K and Maelicke A (1991) Nicotinic cholinoceptive neurons of the frontal cortex are reduced in Alzheimers' disease. *Neurobiol aging* **12**:259-262.

Schulz DW and Zigmond RE (1989) Neuronal bungarotoxin blocks the nicotinic stimulation of endogenous dopamine release from rat striatum. *Neurosci Lett* **98**:310-316.

Schulz DW, Loring RH, Aizenman E and Zigmond RE (1991) Autoradiographic localization of putative nicotinic receptors in the rat brain using ^{125}I-neuronal bungarotoxin. *J Neurosci* **11**:287-297.

Schwartz RD, Lehmann J and Kellar KJ (1984) Presynaptic nicotinic cholinergic receptors labeled by [^{3}H]acetylcholine on catecholamine and serotonin axons in brain. *J Neurochem* **42**:1495-1498.

Seeburg PH (1993) The TINS/TiPS Lecture. The molecular biology of mammalian glutamate receptor channels. *Trends Neurosci* **16**:359-365.

Seguela P, Wadiche J, Dineley-Miller K, Dani JA and Patrick JW (1993) Molecular cloning, functional properties, and distribution of rat brain α7: a nicotinic cation channel highly permeable to calcium. *J Neurosci* **13**:596-604.

Sershen H, Balla A, Lajtha A and Vizi ES (1997) Characterization of nicotinic receptors involved in the release of noradrenaline from the hippocampus. *Neuroscience* **77**:121-130.

Sheng Z, Rettig J, Takahashi M and Catterall WA (1994) Identification of a syntaxin-binding site on N-type calcium channels. *Neuron* **13**:1303-1313.

Shoop RD, Martone ME, Yamada N, Ellisman MH and Berg DK (1999) Neuronal acetylcholine receptors with α7 subunits are concentrated on somatic spines for synaptic signaling in embryonic chick ciliary ganglia. *J Neurosci* **19**:692-704.

Sihra TS, Wang JKT, Gorelick FS and Greengard P (1989) Translocation of synapsin I in response to depolarization of isolated nerve terminals. *Proc Natl Acad Sci U S A* **86**:8108-8112.

Skene JHP (1989) Axonal growth-associated proteins. *Annu Rev Neurosci* **12**:127-156.

Smart T (1997) Regulation of excitatory and inhibitory neurotransmitter-gated ion channels by protein phosphorylation. *Curr Opin Neurobiol* **7**:358-367.

Smith M., Lindstrom J and Merlie JP (1987) Formation of the α-bungarotoxin binding site and assembly of the nicotinic acetylcholine receptor subunits occur in the endoplasmic reticulum. *J Biol Chem* **262**:4367-4376.

Smith AD and Bolam JP (1990) The neural network of the basal ganglia as revealed by the study of synaptic connections of identified neurons. TINS 13: 259-265. *Trends Neurosci* **13**:259-265.

Smith Y, Bennett BD, Bolam JP, Parent A and Sadikot AF (1994) Synaptic relationships between dopaminergic afferents and cortical or thalamic input in the sensorimotor territory of the striatum in monkey. *J Comp Neurol* **344**:1-19.

Smith Y, Bevan MD, Shink E and Bolam JP (1998) Microcircuitry of the direct and indirect pathways of the basal ganglia. *Neurosci* **86**:353-387.

Smolders I, Sarre S, Vanhaesendonck C, Ebinger G and Michotte Y (1996) Extracellular striatal dopamine and glutamate after decortication and kainate receptor stimulation, as measured by microdialysis. *J Neurochem* **66**:2373-2380.

Soliakov L, Gallagher T and Wonnacott S (1995) Anatoxin-a-evoked [^{3}H]dopamine release from rat striatal synaptosomes. *Neuropharmacology* **34**:1535-1541.

Soliakov L and Wonnacott S (1996) Voltage-sensitive Ca^2+ channels involved in nicotinic receptor-mediated [^{3}H]dopamine release from rat striatal synaptosomes. *J Neurochem* **67**:163-170.

Soliakov L and Wonnacott S (1998) Nicotinic modulation of [^{3}H]dopamine release in rat striatum: involvement of PKC subtypes. *European Society for Neurochemistry Abstract* **12**:S52A.

Somogyi P, Bolam JP and Smith AD (1981) Moosynaptic cortical input and local axon collaterals of identified striatonigral neurons. A light and electron microscopic study using Golgi-peroxidase transport-degeneration procedure. *J Comp Neurol* **195**:567-584.

Squire LR (1992) Memory and the hippocampus: a synthesis from findings with rats, monkeys and humans. *Psychol Rev* **99**:195-231.

Steinlein OK, Mulley JC, Propping P, Wallace RH, Phillips HA, Sutherland GR, Scheffer IE and Berkovic SF (1995) A missense mutation in the neuronal nicotinic acetylcholine receptor α4 subunit is associated with autosomal dominant nocturnal frontal lobe epilepsy. *Nat Genet* **11**:201-203.

Stern-Bach Y, Better B, Hartley M, Sheppard PO, O'Hara PJ and Heinemann SF (1994) Agonist selectivity of glutamate receptor is specified by two domains structurally related to bacterial amino acid-binding proteins. *Neuron* **13**:1345-1357.

Stetzer E, Ebbinghaus U, Storch A, Poteur L, Schrattenholz A, Kramer G, Methfessel C and Maelicke A (1996) Stable expression in HEK-293 cells of the rat α3/β4 subtype of neuronal nicotinic acetylcholine receptor. *FEBS Lett* **397**:39-44.

Stitzel JA, Robinson SF, Marks MJ and Collins AC (1997) Differences in response to nicotine are determined by genetic factors. *Adv Pharmacol Sci* 279-284.

Stolerman IP, Garcha HS and Mirza NR (1995) Dissociations between the locomotor stimulant and depressant effects of nicotinic agonists in rats. *Psychopharmacology (Berl)* **117**:430-437.

Sullivan JP, Decker MW, Brioni JD, Donnelly-Roberts D, Anderson DJ, Bannon AW, Kang CH, Adams P, Piattoni-Kaplan M and Buckley MJ (1994) (+/-)-Epibatidine elicits a diversity of *in vitro* and *in vivo* effects mediated by nicotinic acetylcholine receptors. *J Pharmacol Exp Ther* **271**:624-631.

Sulzer D, Joyce MP, Lin L, Geldwert D, Haber SN, Hattori T and Rayport S (1998) Dopamine neurons make glutamatergic synapses *in vitro. J Neurosci* **18**:4588-4602.

Südhof TC (1995) The synaptic vesicle cycle: a cascade of protein-protein interactions. *Nature* **375**:645-653.

Takahashi H, Takada Y, Nagai N, Urano T and Takada A (1998) Nicotine increases stress-induced serotonin release by stimulating nicotinic acetylcholine receptor in rat striatum. *Synapse* **28**:212-219.

Takahashi T, Tsunoda Y, Lu Y, Wiley J and Owyang C (1992) Nicotinic receptor-evoked release of acetylcholine and somatostatin in the myenteric plexus is coupled to calcium influx via N-type calcium channels. *J Pharmacol Exp Ther* **263**:1-5.

Talke P and Bickler PE (1996) Effects of dexmedetomidine on hypoxia-evoked glutamate release and glutamate receptor activity in hippocampal slices. *Anesthesiology* **85** :551-557.

Taupin P, Ben-Ari Y and Roisin MP (1994) Subcellular fractionation on Percoll gradient of mossy fiber synaptosomes: evoked release of glutamate, GABA, aspartate and glutamate decarboxylase activity in control and degranulated rat hippocampus. *Brain Res* **644**:313-321.

Terbush DR, Bittner MA and Holz RW (1988) Ca^{2+} influx causes rapid translocation of protein kinase C to membranes. *J Biol Chem* **263**:18873-18879.

Terrian DM, Johnston D, Claiborne BJ, Ansah-Yiadom R, Strittmatter WJ and Rea MA (1988) Glutamate and dynorphin release from a subcellular fraction enriched in hippocampal mossy fibre synaptosomes. *Brain Res Bull* **21**:343-351.

Terrian DM, Ways DK, Gannon RL and Zetts DA (1993) Transduction of a protein kinase C-generated signal into the long- lasting facilitation of glutamate release. *Hippocampus* **3**:205-220.

Thomas P (1995) Structure-activity studies of ligands for brain nicotinic acetylcholine receptors. *PhD Thesis - Bath University – UK.*

Thorne B, Wonnacott S and Dunkley PR (1991) Isolation of hippocampal synaptosomes on Percoll gradients: cholinergic markers and ligand binding sites. *J Neurochem* **56**:479-484.

Tian L, Prior C, Dempster J and Marshall IG (1994) Nicotinic antagonist-produced frequency-dependent changes in acetylcholine release from rat motor nerve terminals. *J Physiol (Lond)* **476**:517-529.

Tian L, Prior C, Dempster J and Marshall IG (1997) Hexamethonium- and methyllycaconitine-induced changes in acetylcholine release from rat motor nerve terminals. *Br J Pharmacol* **122**:1025-1034.

Todorov L, Windisch K, Shersen H, Lajtha A, Papasova M and Vizi ES (1991) Prejunctional nicotinic receptors involved in facilitation of stimulation-evoked noradrenaline release from the vas deferens of the guinea-pig. *Br J Pharmacol* **102**:186-190.

Tokumitsu H, Chijiwa T, Hagiwara M, Mizutani A, Terasawa M and Hidaka H (1990) KN-62, 1-[N,O-Bis(5-isoquinolinesulfonyl0-N-methyl-L-tyrosyl]-4-phenylpiperazine, a specific inhibitor of Ca^{2+} /calmodulin-dependent protein kinase II. *J Biol Chem* **265**:4315-4320.

Toth E, Sershen H, Hashim A, Vizi ES and Lajtha A (1992) Effect of nicotine on extracellular levels of neurotransmitters assessed by microdialysis in various brain regions: role of glutamic acid. *Neurochem Res* **17**:265-271.

Toth E, Vizi ES and Lajtha A (1993) Effect of nicotine on levels of extracellular amino acids in regions of the rat brain *in vivo*. *Neuropharmacology* **32**:827-832.

Toth E (1996) Effect of nicotine on the level of extracellular amino acids in the hippocampus of rat. *Neurochem Res* **21**:903-907.

Treinin M and Chalfie M (1995) A mutated acetylcholine receptor subunit causes neuronal degeneration in *C. elegans*. *Neuron* **14**:871-877.

Turner TJ and Dunlap K (1995) Pharmacological characterization of presynaptic calcium channels using subsecond biochemical measurements of synaptosomal neurosecretion. *Neuropharmacology* **34**:1469-1478.

Umemori H, Wanaka A, Kato H, Tohyama M and Yamamoto T (1992) Specific expression of Fyn and Lyn, lymphocyte antigen receptor-associated tyrosine kinases, in the central nervous system. *Mol Brain Res* **16**:303-310.

Unwin N (1993) Nicotinic acetylcholine receptor at 9 A resolution. *J Mol Biol* **229**:1101-1124.

Unwin N (1995) Acetylcholine receptor channel imaged in the open state. *Nature* **373** :37-43.

Valtorta F, Benfenati F and Greengard P (1992) Structure and function of the synapsins. *J Biol Chem* **267**:7195-7198.

Verhage M, Besselsen E, Lopes DSF and Ghijsen WE (1989) Ca^{2+}-dependent regulation of presynaptic stimulus-secretion coupling. *J Neurochem* **53**:1188-1194.

Vernino S, Amador M, Luetje CW, Patrick J and Dani JA (1992) Calcium modulation and high calcium permeability of neuronal nicotinic acetylcholine receptors. *Neuron* **8** :127-134.

Vijayaraghavan S, Pugh PC, Zhang ZW, Rathouz MM and Berg DK (1992) Nicotinic receptors that bind α-bungarotoxin on neurons raise intracellular free Ca^{2}+. *Neuron* **8**:353-362.

Vijayaraghavan S, Huang B, Blumenthal EM and Berg DK (1995) Arachidonic acid as a possible negative feedback inhibitor of nicotinic acetylcholine receptors on neurons. *J Neurosci* **15**:3679-3687.

Villarroel A, Herlitze S, Witzemann V, Koenen M and Sakmann B (1992) Asymmetry of the rat acetylcholine receptor subunits in the narrow region of the pore. *Proc R Soc Lond B Biol Sci* **249**:317-324.

Vyklicky L, Benveniste M and Mayer ML (1990) Modulation of NMDA receptor desensitization by glycine in mouse cultured hippocampal neurons. *J Physiol* **428**:313

Wada E, Wada K, Boulter J, Deneris E, Heinemann S, Patrick J and Swanson LW (1989) Distribution of α2, α3, α4, and β2 neuronal nicotinic receptor subunit mRNAs in the central nervous system: a hybridization histochemical study in the rat. *J Comp Neurol* **284**:314-335.

Wakade AR, Malhotra RK and Wakade TD (1986) Phorbol ester facilitates ^{45}Ca accumulation and catecholamine secretion by nicotine and excess K^{+} but not by muscarine in rat adrenal medulla. *Nature* **321**:698-700.

Walaas SI, Jahn R and Greengard P (1988) Quantitation of nerve terminals populations: synaptic vesicle-associated proteins as markers for synaptic density in the rat neostriatum. *Synapse* **2**:516-520.

Walmsley B, Alvarez FJ and Fyffe REW (1998) Diversity of structure and function at mammalian central synapses. *Trends Neurosci* **21**:81-88.

Wang F, Gerzanich V, Wells GB, Anand R, Peng X, Keyser K and Lindstrom J (1996) Assembly of human neuronal nicotinic receptor α5 subunits with α3, β2, and β4 subunits. *J Biol Chem* **271**:17656-17665.

Wang JKT (1991) Presynaptic glutamate receptors modulate dopamine release from striatal synaptosomes. *J Neurochem* **57**:819-822.

Wecker ML, Brioni JD, Bannon AW and Arneric SP (1995) Diversity of neuronal nicotinic acetylcholine receptors: lessons from behaviour and implications for CNS therapeutics. *Life Sci* **56**:545-570.

Wessler I (1989) Control of transmitter release from the motor nerve by presynaptic nicotinic and muscarinic autoreceptors. *Trends Pharmacol Sci* **10**:110-114.

Wessler I, Apel C, Garmsen M and Klein A (1992) Effects of nicotine receptor agonists on acetylcholine release from the isolated motor nerve, small intestine and trachea of rats and guinea- pigs. *Clin Investig* **70**:182-189.

Westfall TC (1974) Effect of nicotine and other drugs on the release of ^{3}H-norepinephrine and ^{3}H-dopamine from rat brain slices. *Neuropharmacology* **13**:693-700.

Westfall TC and Tittermary V (1982) Inhibition of the electrically induced release of [^{3}H]dopamine by serotonin from superfused rat striatal slices. *Neurosci Lett* **28**:205-209.

Westfall TC, Grant H and Perry H (1983) Release of dopamine and 5-hydroxytryptamine from rat striatal slices following activation of nicotinic cholinergic receptors. *Gen Pharmacol* **14**:321-325.

White MM and Aylwin M (1990) Niflumic and flufenamic acids are potent reversible blockers of Ca^{2+}-activated Cl^{-} channels in *Xenopus* oocytes. *Mol Pharmacol* **37**:720-724.

White TD and Al-Hummayyd (1983) Acetylcholine releases ATP from varicosities isolated from guinea pig myenteric plexus. *J Neurochem* **40**:1069-1075.

Whiteaker P, Garcha HS, Wonnacott S and Stolerman IP (1995) Locomotor activation and dopamine release produced by nicotine and isoarecolone in rats. *Br J Pharmacol* **116**:2097-2105.

Whiting P, Schoepfer R, Lindstrom J and Priestley T (1991) Structural and pharmacological characterization of the major brain nicotinic acetylcholine receptor subtype stably expressed in mouse fibroblasts. *Mol Pharmacol* **40**:463-472.

Whiting PJ and Lindstrom JM (1986) Purification and characterization of a nicotinic acetylcholine receptor from chick brain. *Biochemistry* **25**:2082-2093.

Wilkie GI, Hutson P, Sullivan JP and Wonnacott S (1996) Pharmacological characterization of a nicotinic autoreceptor in rat hippocampal synaptosomes. *Neurochem Res* **21**:1141-1148.

Wilkie GI, Hutson P, Sullivan JP and Wonnacott S (1996) Pharmacological characterization of a nicotinic autoreceptor in rat hippocampal synaptosomes. *Neurochem Res* **21**:1141-1148.

Williams M, Sullivan JP and Arneric SP (1994) Neuronal nicotinic acetylcholine receptors. *Drug News and Perspectives* **4**:205-223.

Wong ET, Holstad SG, Mennerick SJ, Hong SE, Zorumski CF and Isenberg KE (1995) Pharmacological and physiological properties of a putative ganglionic nicotinic receptor, α3β4, expressed in transfected eucaryotic cells. *Brain Res Mol Brain Res* **28**:101-109.

Wonnacott S, Harrison R and Lunt GG (1980) Interrelationship of carbohydrate and the α-toxin binding site on the acetylcholine receptor from *Torpedo marmorata*. *Life Sci* **19**:1769-1775.

Wonnacott S (1987) Brain nicotine binding sites. *Hum Toxicol* **6**:343-353.

Wonnacott S (1990) Characterisation of nicotine receptor sites in the brain. *In: Nicotine psychopharmacology: molecular, cellular and behavioural aspects (eds. Wonnacott,S. Russell, M.A.H. and Stolerman,I.P.).Oxford: Oxford University Press* 226-277.

Wonnacott S and Drasdo A (1991) Presynaptic actions of nicotine in the CNS. *In: Effects of nicotine on biological systems (ed. Adlkofer,F.).Basel: Birkhauser Verlag.* 295-306.

Wonnacott S, Wilkie GI, Soliakov L and Whiteaker P (1995) Presynaptic nicotinic autoreceptors and heteroreceptors in the CNS. *In: Effects of nicotine on biological systems II (eds. Clarke,P.B.S. Quick,M. Adlkofer,F. and Thurau, K.).Basel: Birkhauser Verlag.* 87-94.

Wonnacott S (1997) Presynaptic nicotinic ACh receptors. *Trends Neurosci* **20**:92-98.

Wright E, Gallagher T, Sharples CGV and Wonnacott S (1997) Synthesis of UB-165: a novel nicotinic ligand and anatoxin-a/epibatidine hybrid. *Biorganic & Medicinal Chemistry Letters* **7**:2867-2870.

Yang X, Criswell HE and Breese GR (1996) Nicotine-induced inhibition in medial septum involves activation of presynaptic nicotinic cholinergic receptors on γ-aminobutyric acid-containing neurons. *J Pharmacol Exp Ther* **276**:482-489.

Yu CR and Role LW (1998) Functional contribution of the α7 subunit to multiple subtypes of nicotinic receptors in embryonic chick sympathetic neurones. *J Physiol (Lond)* **509**:651-665.

Yu CR and Role LW (1998b) Functional contribution of the α5 subunit to neuronal nicotinic channels expressed by chick sympathetic ganglion neurones. *J Physiol (Lond)* **509**:667-681.

Yu ZJ and Wecker L (1994) Chronic nicotine administration differentially affects neurotransmitter release from rat striatal slices. *J Neurochem* **63**:186-194.

Yung KKL, Smith AD, Levey AI and Bolam JP (1996) Synaptic connections between spiny neurons of the direct and indirect pathways in the neostriatum of the rat: evidence from dopamine receptor and neuropeptide immunostaining. *Eur J Neurosci* **8**:861-869.

Zoli M, Lena C, Picciotto MR and Changeux JP (1998) Identification of four classes of brain nicotinic receptors using β2 mutant mice. *J Neurosci* **18**:4461-4472.